



# The University of Tasmania

IN SITU INVESTIGATIONS OF THE ADSORPTION  
OF FLOTATION COLLECTORS ON CASSITERITE  
BY FTIR-ATR SPECTROSCOPY

by

Kelvin J. Kuys B.Sc.(Hons.)

A thesis submitted in fulfilment  
of the requirements for the degree  
of Master of Science.

Chemistry Department  
University of Tasmania  
January 1986



Controlling the flotation process.

To the best of my knowledge this thesis contains no material which has been accepted for the award of any other degree or diploma in any University and contains no copy or paraphrase of material previously published or written by another person, except where due reference is made in the text.

## Abstract

Flotation is used industrially to recover fine cassiterite which cannot effectively be treated by gravity concentration methods. The adsorption of cassiterite collectors on cassiterite and the accompanying mineral rutile was investigated using a Fourier transform infrared attenuated total reflection technique. The FTIR-ATR technique has considerable advantages over previously used *ex situ* methods since it allows real time investigation of adsorption of the flotation reagents *in situ*. The collectors investigated were the industrially used collectors styrene phosphonic acid and the sulphosuccinamates and some novel polycarboxylic acid and phosphonocarboxylic acid collectors.

The nature of the species present when the collectors adsorb on the mineral surface was determined by comparison of the infrared spectra of the collectors, their tin and titanium complexes and the adsorbates on cassiterite and rutile. The infrared band positions for phosphonic, sulphonic, and carboxylic acid groups when adsorbed on cassiterite and rutile were found to be similar to those in their tin and titanium complexes. This indicates that these reagents adsorb by a chemisorption mechanism in which a metal-collector complex is formed at the mineral surface. Possible structures for the surface complexes involving bidentate co-ordination of phosphonate groups

and monodentate co-ordination of carboxylate groups are postulated from the fine structure of the spectra of the adsorbates.

The nature of the surface species was found to be strongly dependent on pH. At low pH values higher concentrations of protonated acid groups are present at the mineral surface. With increasing pH the number of undissociated acid groups decreases. The presence of these groups may be due to undissociated groups on the chemisorbed collector molecules or physisorbed free acid molecules.

The presence of iron in the cassiterite lattice or adsorbed on the cassiterite surface was found not to be necessary for collector adsorption and adsorption occurred on pure tin oxide in the same manner as on natural cassiterite.

The kinetics of adsorption of the collectors was also studied by the FTIR-ATR method.

## Acknowledgements

I wish to offer my sincere thanks to my supervisors Dr. N.K. Roberts and Dr. P.W. Smith for their advice, guidance, patience and encouragement throughout the duration of this work.

I would also like to thank Greg Lane and Dr. J.B. Bremner for their advice and assistance.

I am also very grateful to Kevin Foo, Simon Meik, Nick Moony and Tony Choo of Aberfoyle Ltd. who initiated this project and offered guidance and assistance.

Greg Lane also synthesised the new flotation collectors used in this study. Noel Davies introduced me to the operation of the FTIR spectrometer, Mr W. Jablonski produced the tin oxide coatings and carried out the electron microprobe work, and Dr. R.J. Ford gave assistance with the x-ray diffraction work. Their help is greatly appreciated.

I also gratefully acknowledge the help of the members of staff of the Chemistry Department who offered their assistance throughout the course of my study.

I wish to offer my grateful thanks to Aberfoyle Ltd. who provided the funding for this project in the form of a research scholarship.

Thanks are also due to Debbie Slevin for her patient and skilful typing of this thesis.

My thanks also go to my friends who helped and encouraged me throughout the study.

## Contents

		page
Chapter 1.	<b>Introduction</b>	1
Chapter 2.	<b>Mineral Flotation</b>	4
Chapter 3.	<b>Cassiterite Flotation</b>	10
3.1	Introduction	10
3.2	Collectors for Cassiterite Flotation	13
Chapter 4.	<b>The Cassiterite Surface and the Cassiterite - Aqueous Interface</b>	17
Chapter 5.	<b>Investigations of the Mode of Action of Cassiterite Collectors</b>	22
5.1	Phosphonic and Arsonic Acids	22
5.2	Sulphosuccinamates	38
5.3	Carboxylic Acids	43
Chapter 6.	<b>Spectroscopic Investigations of Collector Adsorption in Oxide Flotation Systems</b>	52
6.1	Introduction	52
6.2	Adsorption of Flotation Collectors on Oxide Minerals	54

6.3	Discussion	66
Chapter 7.	<b>Fourier Transform Infrared Attenuated Total Reflection Spectroscopy</b>	67
7.1	Introduction	67
7.2	Fourier Transform Infrared Spectroscopy	69
7.3	Attenuated Total Reflection Spectroscopy	75
Chapter 8.	<b>Experimental Techniques</b>	82
8.1	Reagents and Materials	82
8.2	Apparatus and Experimental Procedure	84
Chapter 9	<b>Adsorption of Styrene Phosphonic Acid on Cassiterite and Rutile</b>	92
9.1	Introduction	92
9.2	Infrared Spectra of Styrene Phosphonic Acid and its Tin, Titanium and Iron Complexes	92
9.3	Infrared Spectra of Styrene Phosphonic Acid Adsorbed on Cassiterite	96
9.4	Effect of Iron on Adsorption of Styrene Phosphonic Acid on Cassiterite	100
9.5	Effect of pH on Adsorption of Styrene Phosphonic Acid on Cassiterite	101
9.6	Kinetics of Adsorption of Styrene Phosphonic Acid on Cassiterite	103

9.7	Infrared Spectra of Styrene Phosphonic Acid Adsorbed on Rutile	105
9.8	Discussion	105
Chapter 10	<b>Adsorption of Sulphosuccinamate Flotation Collectors on Cassiterite</b>	110
10.1	Introduction	110
10.2	Infrared Spectra of Sulphosuccinamates and their Tin Complexes	111
10.3	Infrared Spectra of Sulphosuccinamates Adsorbed on Cassiterite	113
10.4	Discussion	115
Chapter 11	<b>Adsorption of Polycarboxylic Acid Collectors on Cassiterite and Rutile</b>	116
11.1	Introduction	116
11.2	Infrared Spectra of Carboxylic Acids and their Tin Complexes	120
11.3	Infrared Spectra of Carboxylic Acids Adsorbed on Cassiterite and Rutile	134
11.4	Discussion	137
Chapter 12	<b>Conclusion</b>	141
Chapter 13	<b>Suggestions for Further Work</b>	143
	<b>References</b>	146

Appendix 1	<b>Spectroscopic Investigations of Collector Adsorption in Flotation Systems other than those used to recover Oxides.</b>	155
1.1	Adsorption of Flotation Collectors on Sulphide Minerals	155
1.2	Adsorption of Flotation Collectors on Silicate Minerals	180
1.3	Adsorption of Flotation Collectors on Semi-soluble Salt Minerals	184
1.4	Adsorption of Flotation Collectors on Carbonate Minerals	190
	References	194

Appendix 2	<b>Calculations of Depth of Penetration of the IR beam and Concentration of Adsorbate on the Surface of the ATR Element and in the Adjacent Solution.</b>	199
------------	---	-----

## 1. Introduction

Since the commercial introduction of the flotation process for mineral concentration early this century its mode of operation has been the subject of much interest. Like many other methods used to process raw materials flotation has developed by the continued application of empirical methods rather than as the result of intensive fundamental research. Hence the chemistry of the flotation process is still not completely understood. In 1982 Aberfoyle Ltd., owners of the Cleveland Tin mine in Western Tasmania and the Ardlethan tin mine in New South Wales initiated this project in order to develop a better understanding of the cassiterite flotation process. Cassiterite flotation, although developed over forty years ago, remains only as a secondary process in the treatment of tin ores. The lack of progress in the development of cassiterite flotation has largely been hampered by a poor understanding of its chemistry. Although considerable research has been carried out on the chemistry of cassiterite flotation many of the proposed theories of reagent action are based on indirect evidence or on data which may be interpreted in other ways.

Surface chemistry must play an important part in the flotation process since different reagents react with the mineral surface in an aqueous medium. Spectroscopic techniques provide a direct method of observing such interactions. Over the last thirty years numerous

spectroscopic methods have been applied to the study of the surface chemistry of flotation in order to identify and characterise the adsorbed species at the mineral-aqueous interface. However most of these observations have been conducted *ex situ* (ie. after reaction of the reagents with the mineral surface and the removal of the aqueous phase). In these cases the system studied is only an approximation to the actual adsorption system since the removal of the aqueous phase may lead to changes in the bonding of the adsorbate molecules to the mineral surface.

Infrared spectroscopy has been the most frequently used method to study the adsorption of flotation collectors on mineral surfaces. However most infrared investigations have been conducted *ex situ* due to the high absorbance of water in the infrared region. The commonly used flotation collectors for cassiterite are based on arsonic, phosphonic, sulphonic or carboxylic acid groups, all of which are amenable to investigation by infrared spectroscopy. *Ex situ* methods have been used previously to record the infrared spectra of these flotation collectors adsorbed on the cassiterite surface. The mode of adsorption of flotation collectors on cassiterite has largely been proposed as the result of the application of these *ex situ* infrared spectroscopic methods. However the results of these investigations have remained the subject of considerable debate. Hence this investigation was conducted in order to develop a method

capable of giving information on the adsorption of flotation collectors on cassiterite *in situ* (ie.to study the structure of the adsorbate actually at the interface between the mineral and the aqueous phase).

This was achieved by the use of Fourier transform infrared attenuated total reflection spectroscopy. This is a sensitive technique which allows real time observation of the spectra of adsorbates on surfaces *in situ*. This method was used to study the adsorption behaviour of the most common industrially used cassiterite collectors, styrene phosphonic acid and sulphosuccinamates, as well as some novel cassiterite collectors based on carboxylic and phosphonic acid groups synthesised by Mr Greg Lane. The adsorption of these collectors was studied on natural cassiterite as well as on pure tin (IV) oxide which served as a model compound for cassiterite. The adsorption behaviour of some of these collectors was also studied on pure rutile-type titanium (IV) oxide as this mineral has the same crystal structure as cassiterite and rutile is also recovered by the industrially used flotation collectors.

## 2. Mineral Flotation

The froth flotation process was originally used in its present day form in 1906 at Broken Hill in New South Wales. It is now the most important and versatile mineral processing technique available. This is because this sensitive technique is capable of facilitating very specific separations of minerals since it utilises differences in physico-chemical surface properties between specific minerals.

In practice flotation works by agitating a mineral pulp (5-35 % solids by volume) and blowing air bubbles through it so that certain minerals attach themselves to the bubbles and are floated out in a froth for recovery. Gangue minerals remain in the pulp. This is shown diagrammatically in Figure 1. Minerals prepared for flotation must be ground below about 300 $\mu$ m with slimes (<30 $\mu$ m) held to a minimum. Depending on density material coarser than 300 $\mu$ m is generally too heavy to be carried out of the pulp by the air bubbles. Slimes are also difficult to collect, usually because they fail to attach to the bubbles. Slimes may also be lost by spontaneous flocculation to a size too heavy to float.

With flotation it is possible to obtain highly pure mineral components from low low grade (< 1% useful component) and complex ore bodies which would otherwise be regarded as uneconomic.

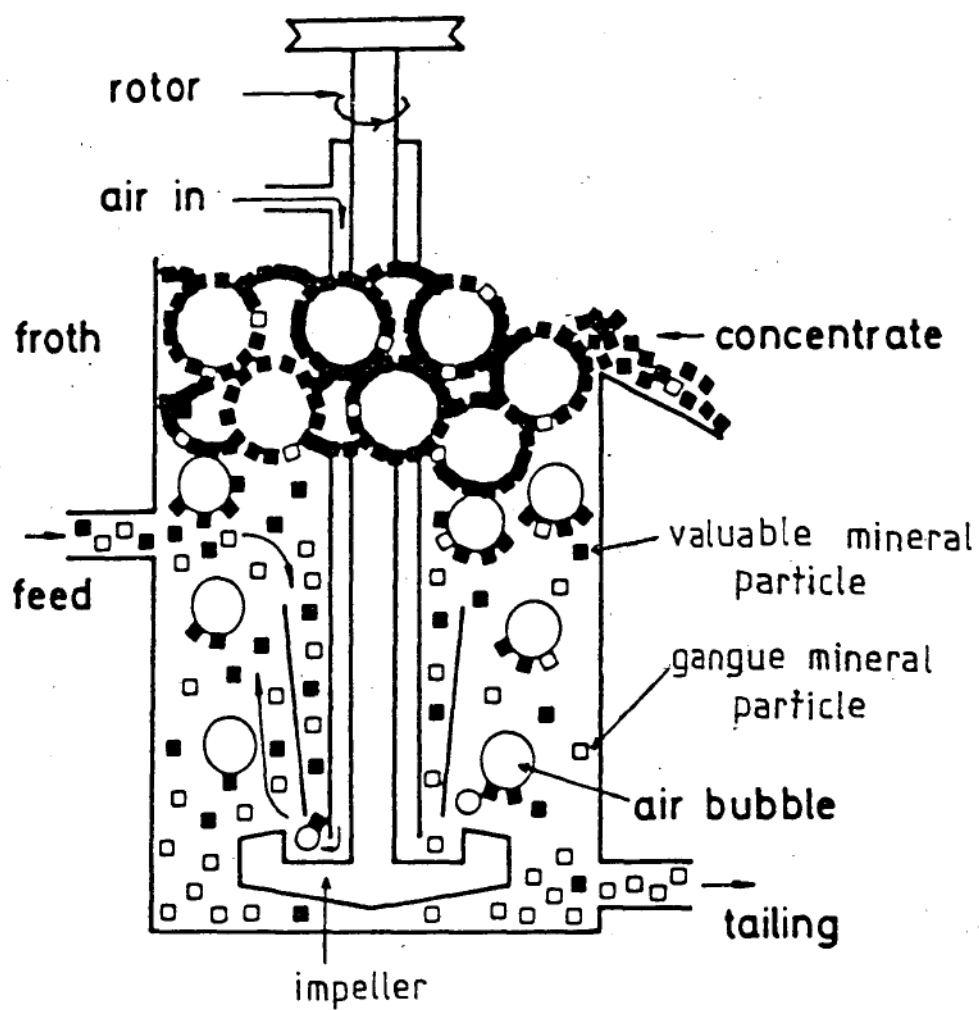
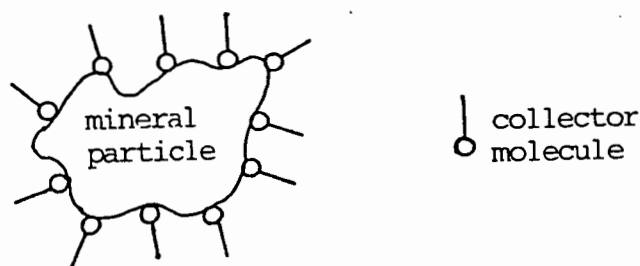


Fig.1 Diagrammatic representation of the flotation process.

The theory of flotation is complex and is not yet completely understood. The surface chemical aspects of flotation have been recently reviewed by Leja (1982). For flotation to occur an air bubble must attach itself to the mineral particles and lift it to the water surface. The air bubbles can only attach to mineral particles if they can displace water from the mineral surface. This can only happen if the mineral is to some extent hydrophobic. Most minerals are naturally hydrophilic and their surfaces must be rendered hydrophobic by treatment with suitable surfactants known as collectors. Surface properties of ore and gangue minerals vary within too narrow a range to be useful for effecting separations directly. Such differences as do exist must be exaggerated by bringing about selective adsorption of the collector on to the mineral it is desired to float.

Collectors used in mineral flotation are of three types - nonionic, anionic, and cationic. They are generally heteropolar, ie; the molecule contains both a non-polar group and a polar group. The non-polar group, generally an alkyl chain, has pronounced hydrophobic properties. The polar group, generally based on pentavalent nitrogen in the case of cationic collectors or divalent oxygen or sulphur in the anionic collectors, can attach itself to an ion of opposite sign on the mineral surface. Attachment of the polar group of collectors can occur by chemical, physical or electrical attraction between them and the surface sites. The collectors adsorb

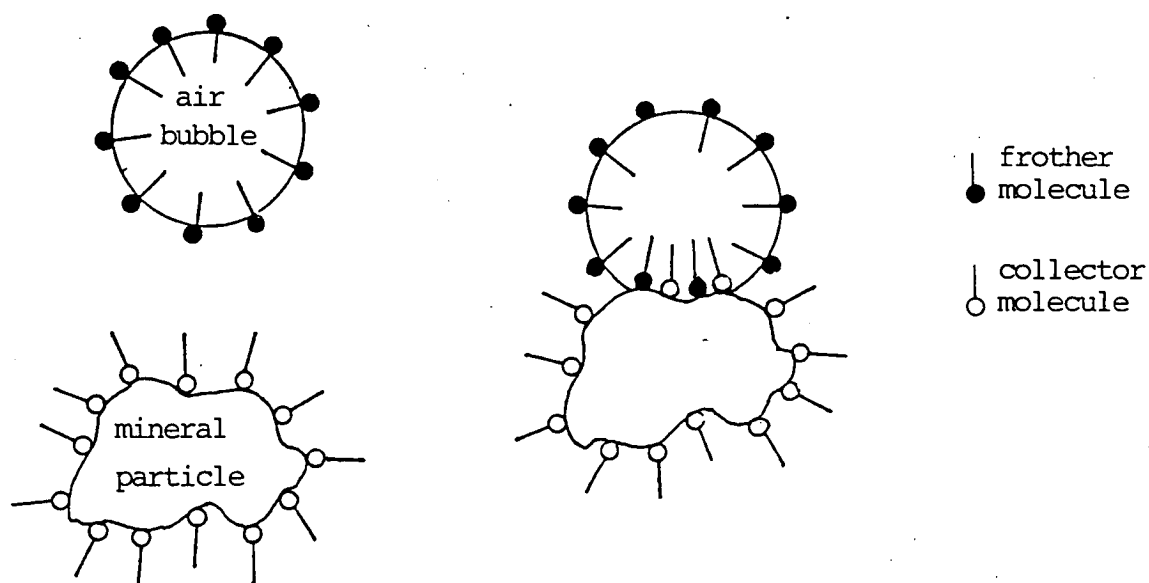
on the mineral particles with their hydrophobic ends oriented towards the bulk solution thereby imparting hydrophobicity to the particles, viz



Collectors are generally designed so that the polar group will adsorb selectively onto specific minerals. Sulphydryl type collectors, where the polar group contains bivalent sulphur, such as xanthates and dithiophosphate, are generally used in the selective flotation of sulphide minerals. Oxhydryl type collectors, where the polar group contains bivalent oxygen, such as carboxylic, sulphonic, phosphonic and arsonic acids and their salts are generally used in selective flotation of oxide and semi-soluble salt type minerals. Cationic collectors generally based on pentavalent nitrogen, such as amines and quaternary ammonium salts are mainly used in the flotation of silicates and semi-soluble salt minerals.

Non-anionic surfactants are usually used in flotation as frothers - reagents which ensure the formation of a stable froth with sufficient buoyancy to carry the load of floatable mineral out of the pulp. Frothers adsorb strongly at the air-water interface rather than at the

mineral-aqueous interface, with the polar groups towards the water. When two bubbles come together their surface films meet with the non-polar groups facing each other and they tend to repel each other rather than coalesce. This gives the froth stability. Frother molecules may also adsorb on the mineral surface when a bubble attaches to a mineral particle. In this situation frother-collector interaction may occur by the adhesion of their hydrophobic groups by van der Waal forces viz.



Additional reagents called regulators, modifiers or conditioners are also added to the flotation pulp to modify the action of the collector by intensifying or reducing its hydrophobic effect on the mineral surface. They thus make the collector more selective towards certain minerals. Regulators are generally of three types - activators, depressants and pH modifiers. Activators

are reagents which alter the chemical nature of mineral surfaces so that the collector can attach itself. They are generally soluble salts which ionise in solution, the ions then reacting with the mineral surface. Depressants, increase the selectivity of flotation by rendering certain minerals hydrophilic thus preventing their flotation. pH modifiers are used to maintain the flotation pulp at the correct pH for collector attachment.

### 3. Cassiterite Flotation

#### 3.1 Introduction

Up till 1938 gravity concentration was the only method used to concentrate tin ores. Today this is still the case for secondary ores since their mineralogy and particle size distribution make them suitable for the use of gravity concentration processes (sluices, jigs, shaking tables, spirals, cones etc.). Over 60% of the world's tin is recovered from the alluvial deposits of Malaysia, Indonesia and Thailand by simple gravity methods. However a significant and increasing amount of tin is removed from hardrock sources mainly in Bolivia, Australia, South Africa and Britain.

The exclusive use of gravity processing for primary ores has met with only poor recoveries due to the small particle sizes of the cassiterite and complex mineralogy. Some upgrading of such ores has been accomplished by the flotation to separate sulphides, cleaning of the concentration by magnetic separation and leaching of the concentrates to remove carbonate minerals. Improvements in recoveries have been produced by the refinement of gravity methods such as vanners and the Bartles-Mozley concentrator, but cassiterite particles finer than 20-40  $\mu\text{m}$  must be regarded as non-recoverable by gravity concentration. Since many primary deposits have such fine intergrowths the tin content of the fines can be quite

substantial in economic terms. Hence much research has been devoted to developing methods for the recovery of fine cassiterite. The cassiterite flotation process was first put into industrial use in 1938. Since then it has remained the only process to supplement gravity concentration on an industrial scale. At present most hardrock tin concentrators use a combined flowsheet with gravity concentration of cassiterite coarser than 20-40  $\mu\text{m}$  and flotation of cassiterite in the size range 2-20  $\mu\text{m}$  after desliming. The advantages of cassiterite flotation over gravity concentration methods and its limitations are shown in Fig.2.

The main problems which have hampered the development of cassiterite flotation are the narrow size range of operation, the need for rigid desliming and the high cost of flotation reagents. With presently used cassiterite collectors and depressants for silicate gangue the reagent costs can account for up to 55 % of total flotation costs. Generally the use of lower cost collectors results in lower grade concentrates. Hence, much research has been devoted to the development of low cost collectors which can produce acceptable recoveries and concentrate grades.

<u>ADVANTAGES</u>	<u>LIMITATIONS</u>
<ul style="list-style-type: none"> <li>• Good recovery of tin into medium grade concentrates</li> <li>• Circuits easier to control than gravity, OSA, and auto-control can be used</li> <li>• Higher unit throughput than most gravity devices. Takes up less floorspace</li> <li>• Low maintenance and labour costs</li> <li>• Recovery into rougher (low grade) concentrates is usually &gt;90% Sn</li> <li>• Wide range of reagents can be used</li> </ul>	<ul style="list-style-type: none"> <li>• Size range limited to 2-20<math>\mu</math>m into final concentrates</li> <li>• Grade of concentrates rarely exceed 25% Sn and upgrading magnetically or by leaching is often needed</li> <li>• Rigid desliming to -6<math>\mu</math>m or 2<math>\mu</math>m is required</li> <li>• Slimes consume reagent and downgrade concentrate</li> <li>• Prior removal of sulphides is necessary before oxide flotation stage</li> <li>• High operating costs (usually) because of expensive collectors needed</li> <li>• Recovery reduced in cleaning stages. Up to 4 stages of cleaning required to produce acceptable grade concentrates</li> <li>• Soluble ions in pulp such as <math>Fe^{3+}</math>, <math>Ca^{+}</math> and <math>Cu^{+}</math> can create major problems.</li> </ul>

Fig.2 Advantages of cassiterite flotation over gravity concentration methods and its limitations.  
(From Foo and Enraght-Moony, 1982 )

### 3.2 Collectors for Cassiterite Flotation

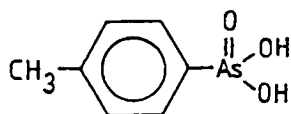
The first industrial cassiterite flotation plant was operated at the Altenberg mine in East Germany from 1938 to 1945. The process used oleic acid,



as the cassiterite collector and sodium silicate and hydrofluorosilicic acid as depressants for gangue minerals. As it was not possible to stabilise this process it was discontinued after World War II. The flotation of cassiterite ores with oleic acid or oleates and carboxylic acids obtained as by-products from the processing of animal and vegetable materials is still used in the USSR today. The use of these collectors is confined to ores of simple mineralogy (mainly those with quartz gangue) since oleic acid has very poor selectivity and the only effective control of the flotation process is achieved by depression of silicate minerals with sodium silicate or sodium fluorosilicate.

The first investigations to produce cassiterite collectors with greater selectivity were conducted at the Research Institute for Mineral Processing at Freiberg, East Germany. As early as 1943 the suitability of arsonic acids as cassiterite collectors was being investigated. The investigation of arsonic acids arose from their use as specific complexing agents in the gravimetric analysis of

tin (a method which was first used in the mid 1920's). On a laboratory scale these proved to be considerably more effective than oleic acid as tin collectors. In 1958 tin flotation was resumed at the Altenberg plant using p tolyl arsonic acid

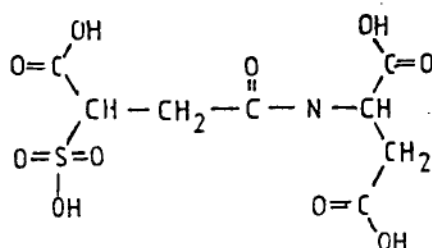


as the collector. This provided a considerable improvement in selectivity over oleic acid but has a much higher toxicity.

Following the success of arsonic acids as flotation collectors for cassiterite, researchers at the Freiberg Institute investigated phosphonic and stibonic acids as cassiterite collectors (Kirchberg and Wottgen, 1963). Phosphonic acids were found to be almost as effective as arsonic acids in laboratory trials but stibonic acids were found to be ineffective as collectors. Wottgen and co-workers determined that of the phosphonic acids they developed n-hexyl, n-heptyl and p-ethyl benzyl phosphonic acids were the best collectors but their cost of manufacture precluded their use on an industrial scale.

Professor N. Arbiter of the Henry Krumb School of Mines, Columbia University began independent investigations into tin flotation collectors in 1964. In 1965 he proposed the use of the commercial surfactant Cyanamid Aerosol 22 as a cassiterite collector. The active constituent of Aerosol 22 is N-octadecyl (1,2,

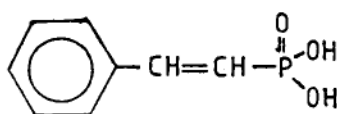
dicarboxyethyl) sulphosuccinamate.



A cassiterite flotation plant using sulphosuccinamate as a collector was commissioned at Catavi in Bolivia in 1968.

Between 1970 and 1972 five cassiterite flotation plants were commissioned by mines of the Consolidated Gold Fields Group and Cleveland Tin N.L. The plants at Rooiberg and Union Tin in South Africa and Renison and Cleveland mines in Tasmania used p-tolyl arsonic acid as the collector while that at Wheal Jane in Cornwall used a sulphosuccinamate collector.

Wottgen, with the aid of workers from VEB Fettchemie Karl-Marx-Stadt, developed a process for producing the cassiterite collector styrene phosphonic acid



economically on an industrial scale. This collector proved to have collector properties similar to p tolyl arsonic acid without having its toxic properties. In 1971 styrene phosphonic acid was successfully used to replace p-tolyl arsonic acid at the Altenberg plant. Conversion of the South African and Australian plants to styrene phosphonic acid soon followed.

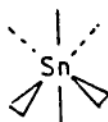
Researchers at the Freiberg Institute together with workers from VEB Fettchemie Karl-Marx-Stadt also investigated the use of carboxylic acids as collectors. They developed alkane dicarboxylic acids which proved to be very effective cassiterite collectors, although they displayed some selectivity problems. It is not known if these reagents have gone into industrial use.

Since the early 1970's considerable work on cassiterite flotation reagents has been carried out by D.N.Collins and co-workers at the Warren Spring Laboratories, Hertfordshire, U.K. Recently, Collins has developed a series of N-alkyl imino-N,N- di methylene phosphonic acids for use as cassiterite collectors (Collins, Wright and Watson, 1984) These reagents have proved to be effective collectors in Cornish tin flotation plants.

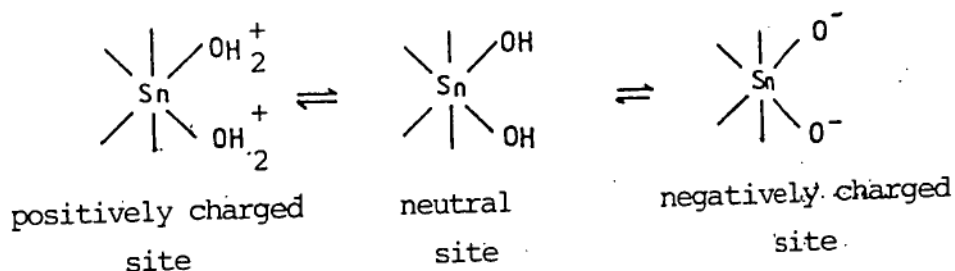
At present work is being carried out at the University of Tasmania by Mr Greg Lane on the development of improved cassiterite collectors based on phosphonic and carboxylic acids. The adsorption of some of these collectors, as well as styrene phosphonic acid and sulphosuccinamate, on cassiterite is examined in this investigation.

#### 4. The Cassiterite Surface and the Cassiterite - Aqueous Interface

Cassiterite ( $\text{SnO}_2$ ) has a tetragonal (+) crystal lattice (a.4.73, c.3.18, Z=2) with each tin ion being surrounded by six oxygen anions arranged in an octahedron and each oxygen having three tin ions surrounding it in an equilateral triangle. It has the same crystal structure as rutile ( $\text{TiO}_2$ ). Cassiterite typically contains appreciable amount of ferrous or ferric iron with smaller amounts of titanium, tantalum, niobium and scandium. It is almost chemically inert and is highly insoluble. In aqueous solution the surface tin ions complete their co-ordination shells with hydroxyl groups forming an amphoteric surface structure as shown below.



As for other insoluble oxide minerals the potential determining ions are  $\text{H}^+$  and  $\text{OH}^-$ . The surface charge of the mineral is generally thought to result from the adsorption - dissociation of  $\text{H}^+$  from the surface hydroxyls viz.



However Wottgen (1969) considered that in acid media the hydroxyl ions dissociate to give the structures shown below.



These structures are unlikely due to the chemical instability of the four or five co-ordinated tin (IV) ion. Six co-ordinated tin (IV) is the favoured state for tin (IV) in aqueous solution.

The isoelectric point and the point of zero charge of cassiterite and stannic oxide have been determined by numerous workers resulting in a wide range of results (Figs.3,4). The wide variation in results has been attributed to impurities and lattice substitution in natural cassiterite and sample pre-treatment. For example, the presence of iron in cassiterite has been reported to shift the PZC to higher pH values (O'Connor and Buchanan, 1953.) with the magnitude of the shift depending on the iron content.

In industrial flotation systems the presence of trace metal ions (such as  $\text{Fe}^{3+}$ ,  $\text{Ca}^{2+}$  and  $\text{Cu}^{2+}$ ) in the flotation pulp is often detrimental to flotation. The presence of hydrolysable ions in the flotation pulp may change the surface charge on the cassiterite. Of particular importance is the ferric ion which is often present at high levels in tin flotation plants and increases the PZC

SOURCE OF SnO <sub>2</sub>	IEP or PZC		MEASUREMENT TECHNIQUE	REFERENCE
	ELECTROLYTE			
Stannic Oxide: Aldrich 99.9999%	KNO <sub>3</sub>	IEP 4.5 PZC 4.3	Electrophoresis Potentiometric Titration	Houchin & Warren (1984)
Stannic Oxide: Sn + HNO <sub>3</sub> , Above, ignited		IEP 4.5, 5.4 IEP 5.6, 6.5	Electrophoresis Electrophoresis	Johansen & Buch- anan (1957)
Stannic Oxide	KNO <sub>3</sub>	PZC 5.5		Huang (1971)
Stannic Oxide	NaNO <sub>3</sub>	PZC 5.7		Kokarev et al. (1982)
Cassiterite: Australia	-	IEP 7.3, 7.7	Electrophoresis	Johansen & Buch- anan (1957)
Cassiterite: Rhodesia	KCl	IEP 3.4	Streaming Potential	Blazy, Degoul & Houot (1969)
Congo, D.R.	KCl	IEP 3.9	Streaming Potential	
France	KCl	IEP 4.5	Streaming Potential	
Cassiterite: Germany		IEP 5.6		Wottgen (1969)
Cassiterite: Potasi (Bolivia)	KCl	IEP 4.0	Potentiometric Titration	Gutierrez & Pom- mier (1969)
Catair (Bolivia)	KCl	IEP 4.0	Potentiometric Titration	
Cassiterite: British Columbia (Canada)	KNO <sub>3</sub>	PZC 5.4, 5.5	Potentiometric Titration	Ahmed & Maksimov (1969)
Cassiterite: Potasi (Bolivia)	KCl	PZC 4.0	Potentiometric Titration	Bellot (1970)
Cassiterite: Altenberg (DDR)		PZC 3.0	Electrophoresis	de Cuyper & Salas (1977)
Cassiterite: Bolivia	-	IEP 4.5	Streaming Potential	Doren, van Lierde & de Cuyper (1979)
Cassiterite	-	IEP 4.2	Electrophoresis	Gochin & Solari (1983)
Cassiterite: Renison (Aust.)	KCl	IEP 4.0	Electrophoresis	Senior (1985)

Fig.3 Values of the isoelectric point and point of zero charge for various samples of stannic oxide and cassiterite. (From Senior and Poling, 1985 and references quoted therein.)

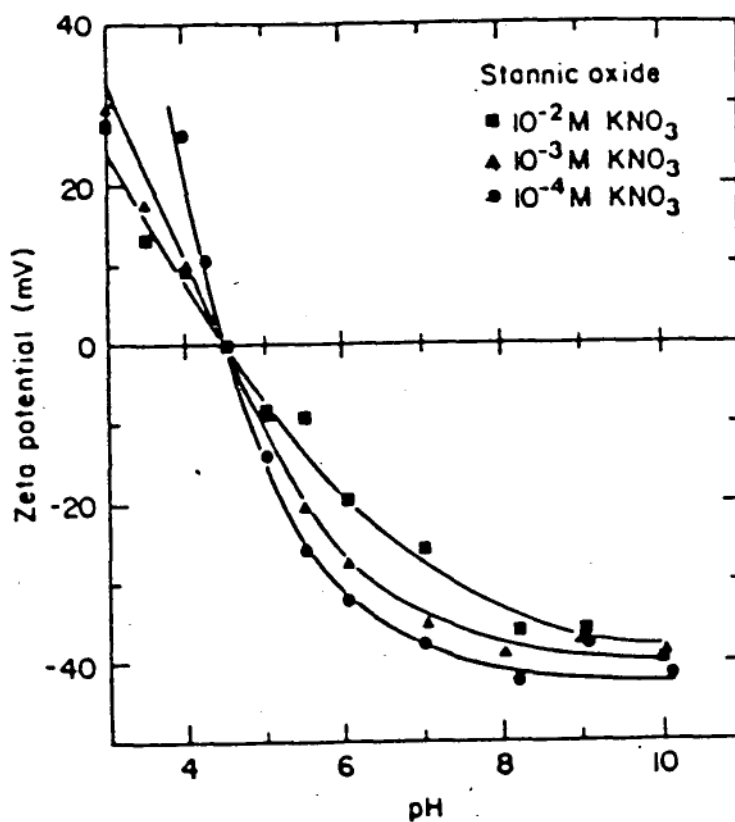


Fig.4 Zeta potential of SnO<sub>2</sub> as a function of pH.  
(From Houchin and Warren, 1984.)

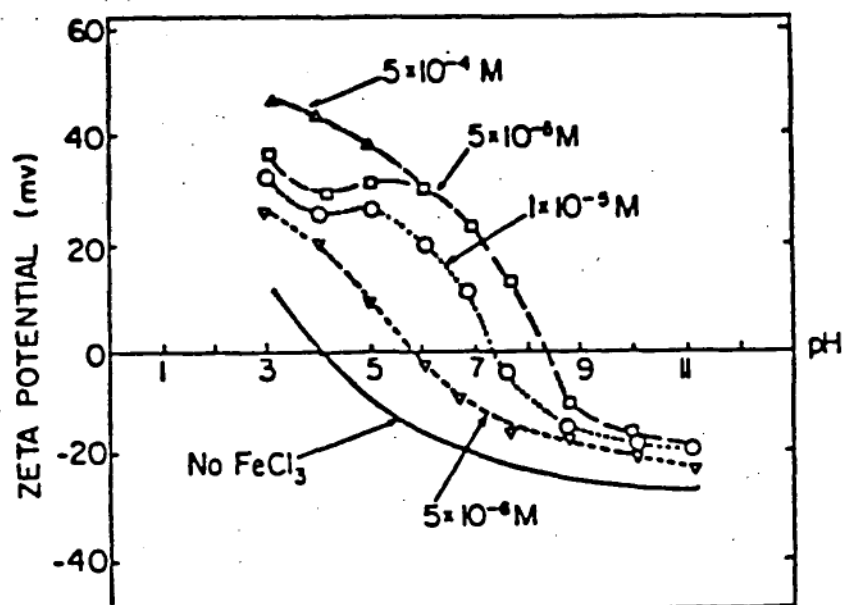


Fig.5 Zeta potential of cassiterite in the presence of increasing concentrations of ferric chloride.  
(From Senior and Poling, 1985.)

of the mineral. Measurements of the PZC of cassiterite in the presence of ferric chloride (Fig.5) have shown that the positively charged ferric hydroxy species adsorbs strongly on the cassiterite surface in the pH range of tin flotation (pH 3.0 to 7.0).

## 5. Investigations of the Mode of Action of Cassiterite Collectors

### 5.1 Phosphonic and Arsonic Acids

Extensive research has been carried out by investigators at the Freiberg Institute, East Germany to determine the mode of action of the arsonic and phosphonic acids they developed as cassiterite collectors. Kirchberg and Wottgen (1963) considered that phosphonic and arsonic acids imparted floatability to cassiterite by forming a sparingly soluble salt with tin (II) at the surface. Accordingly they determined the solubility products of the arsonic, phosphonic and stibonic acids they had prepared. However they could not correlate the solubilities with flotation performance of the acids and concluded that the solubility products of the tin (II) salts were not important in determining flotation properties.

Wottgen (1969) used n-heptyl phosphonic acid labelled with  $^{32}\text{P}$  to study its adsorption on cassiterite and associated minerals using a radiotracer technique. He examined the effects of time, pH and collector concentration on adsorption density. In the pH range 4 to 10 he found that collector adsorption had reached a plateau after approximately 100 minutes. (Fig.6). The adsorption isotherms he measured showed that at low pH values (1, 2) an adsorption plateau is not

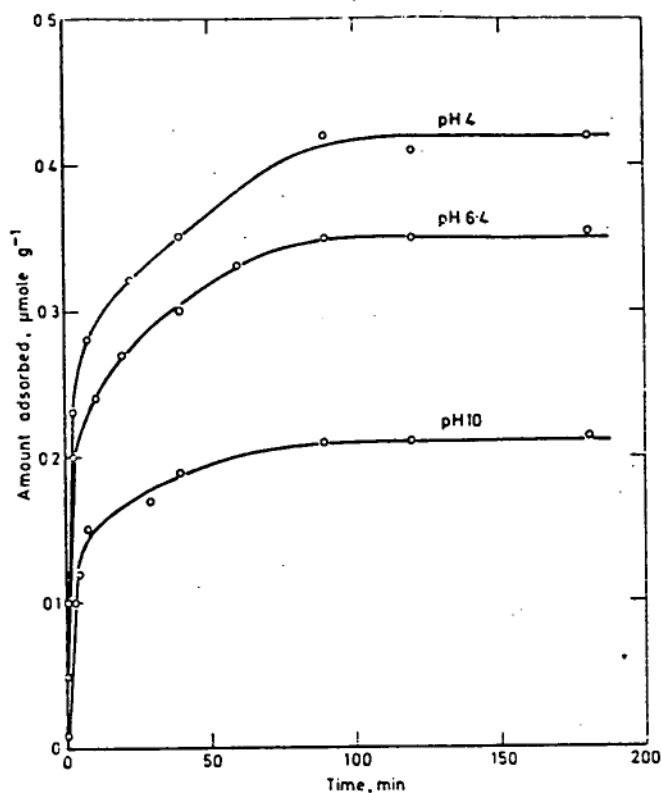


Fig.6 Kinetics of adsorption of n-heptyl phosphonic acid on cassiterite ( $C = 2.5 \times 10^{-3} \text{ mol l}^{-1}$ ).  
(From Wottgen, 1969.)

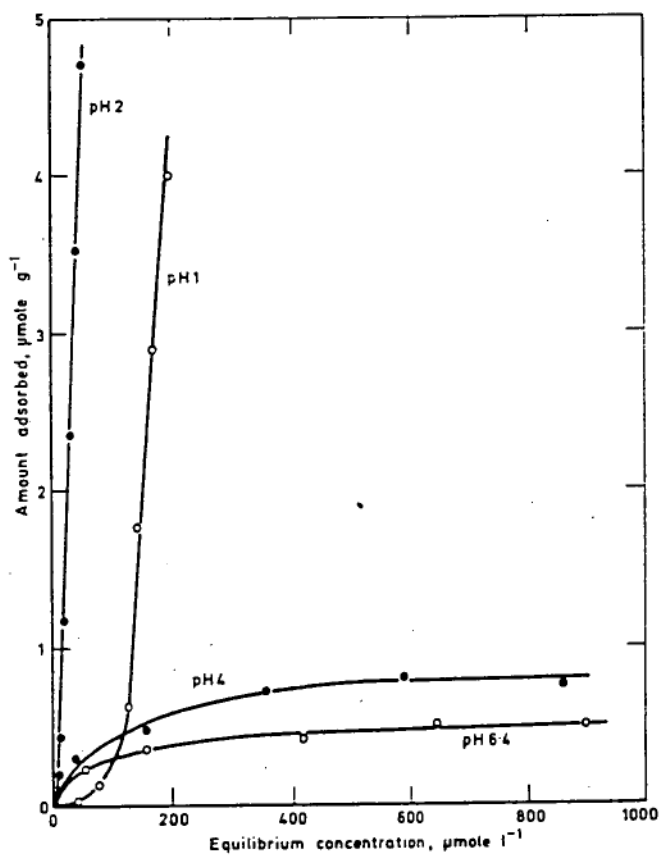


Fig.7 Adsorption isotherms for n-heptyl phosphonic acid on cassiterite. (From Wottgen, 1969.)

reached (Fig.7) and this occurs only when the pH is greater (4, 6.4). From low pH values the amount of acid adsorbed on cassiterite (with an isoelectric point of 5.6) increases with a rise in pH up to a maximum at pH 2, then with a further increase in pH there is a sharp drop in the amount adsorbed until pH 4 is reached (Fig.8). Above pH 4 there is a gradual decrease in the amount adsorbed. Wottgen's studies of the effect of concentration on adsorption found that for a given pH the amount adsorbed on the cassiterite surface increased with concentration of collector in the range of concentrations he studied ( $5 \times 10^{-5}$  -  $10^{-3} \text{ mol l}^{-1}$ ) (Fig.9). Wottgen considered the maximum adsorption at pH 2 as being due to the maximum amount of surface phosphonate compound being present at this pH. This view was based on his measurements of the solubility of tin (IV) phosphonate at different pH values (which showed minimum phosphonate solubility at pH 2). The decrease in adsorption below pH 2 he ascribed to a decrease in ionisation of the phosphonic acid and an increase in the solubility of the Sn(IV) phosphonate species formed at the surface.

Wottgen also studied the adsorption of n-heptyl phosphonic acid on the gangue minerals found with cassiterite using the radiotracer technique. He found that n-heptyl phosphonic acid had an adsorption behaviour on topaz, muscovite, fluorite and zinnwaldite similar to that on cassiterite with adsorption maxima generally

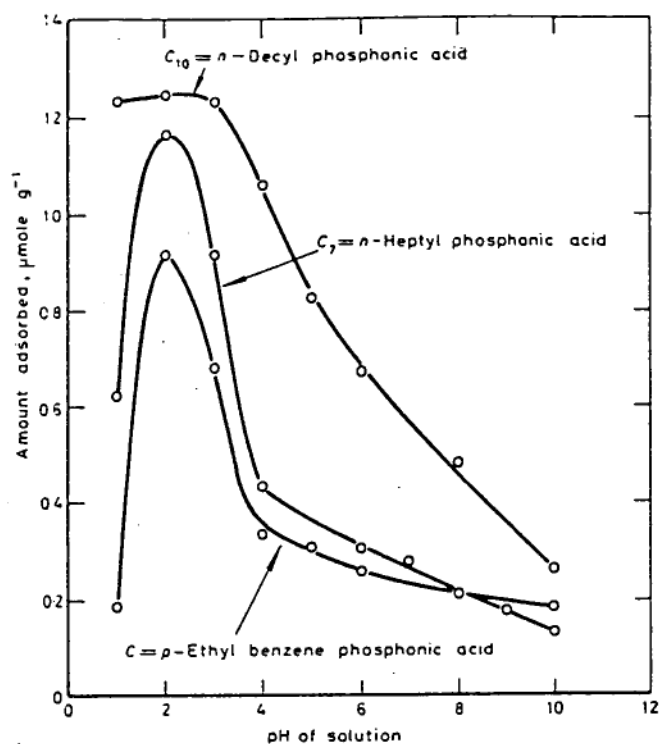


Fig. 8 Change in adsorption density with pH for various phosphonic acids on cassiterite ( $C = 2.5 \times 10^{-3} \text{ mol l}^{-1}$ ) (From Wottgen, 1969.)

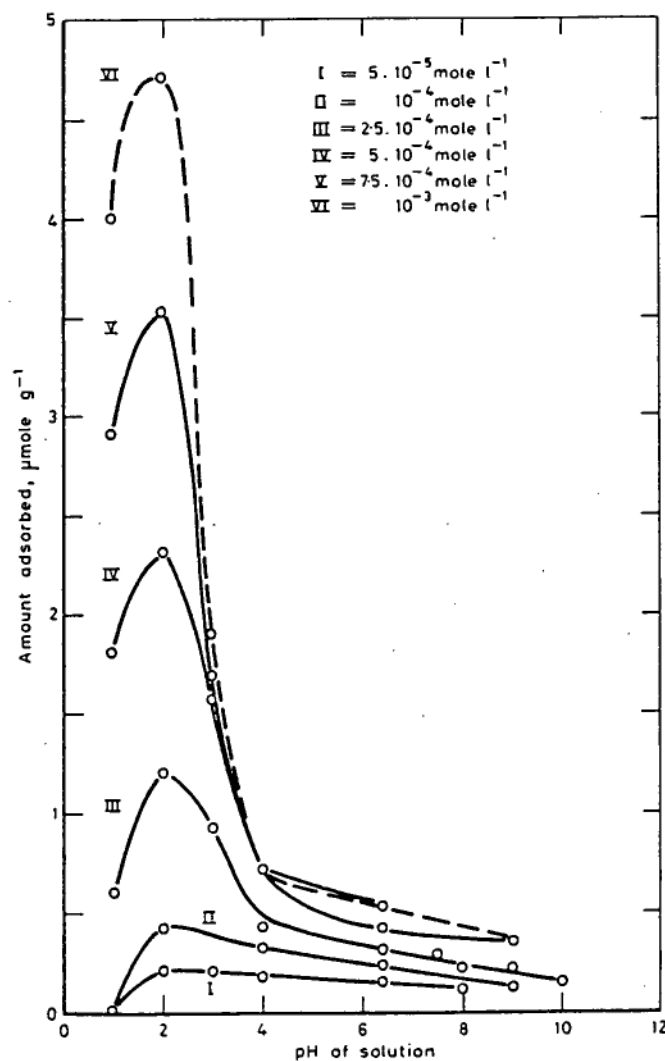


Fig. 9 Change in adsorption density of n-heptyl phosphonic acid adsorbed on cassiterite with pH and concentration. (From Wottgen, 1969.)

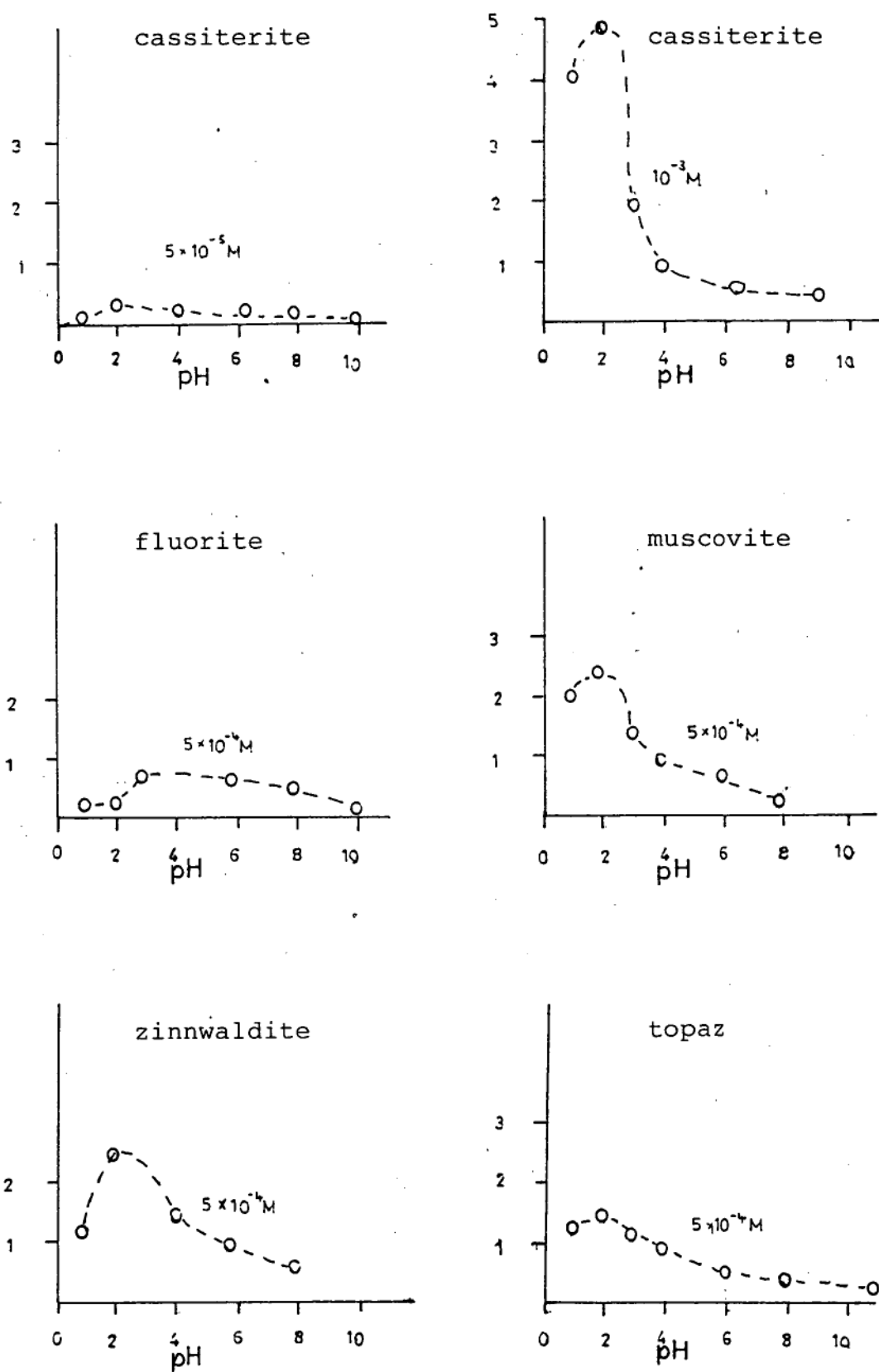


Fig.10 Adsorption of n-heptyl phosphonic acid on cassiterite and associated minerals as a function of pH. (From Wottgen, 1980.)

occurring around pH 2 (Fig. 10). Hematite had an adsorption maximum around pH 1.5 whereas no adsorption could be determined on pure quartz. However the radiotracer technique cannot be used to determine if the surface coverage is due to chemisorbed acid or undissociated acid physisorbed on the minerals (possibly by hydrogen bonding or hydrophobic interaction).

Wottgen (1969) and Wottgen and Dietze (1969) studied the mechanism of adsorption of phosphonic acids on cassiterite using infrared spectroscopy. After the  $-5 \mu\text{m}$  cassiterite used in the radiotracer studies had been treated with phosphonic acid solution the sample was filtered, dried then washed with acetone to remove any physically adsorbed phosphonic acid. The infrared spectrum of the adsorbate was then examined using the KBr disc method. In the free heptyl phosphonic acid there are infrared bands at  $940 - 1052 \text{ cm}^{-1}$  due to the  $\nu_{\text{as,s}} \text{P-O}$  vibrations,  $1040 - 1095 \text{ cm}^{-1}$  due to  $\nu \text{P=O}$  vibrations,  $2260 - 2320 \text{ cm}^{-1}$  due to  $\delta \text{O-H}$  vibrations and  $2750 - 2880 \text{ cm}^{-1}$  due to  $\nu \text{O-H}$  (Figs. 11, 12, 13). In the tin (II) and tin (IV) complexes these bands are absent and a single band due to the resonance stabilised phosphonate group is present at  $1025 - 1060 \text{ cm}^{-1}$  (Figs. 12, 13.). In the spectrum of heptyl phosphonic acid adsorbed on cassiterite a single band is present similar to that found in the tin complexes indicating the formation of a surface phosphonate compound (Figs. 12, 13.). Wottgen and Dietze (1975) also studied

n-heptyl phosphonic acid	n-heptyl arsonic acid	Assignment
2965 vs	2962 vs	$\nu_{as} CH_3$
2930 vs	2935 vs	$\nu_{as} CH_2$
2875 Sh	2872 vs	$\nu_s CH_3$
2862 vs	2854 vs	$\nu_s CH_2$
2850 s (b)	2820 s (b)	$\nu OH$
2330 m(b)	2345 m(b)	$2x \delta OH$
1710 vw(b)	1670 Sh(b)	combination?
1468 m	1473 m	$\delta CH_2$ and $\delta_{as} CH_3$
1410 w	1414 w	$\delta CH_2$
1380 w	1386 w	$\delta_s CH_3$
1330 w		$\omega CH_2$
1310 m	1318 Sh	} $\delta OH$ $\gamma CH_2$
1274 s	1269 Sh	
1235 m	1215 m	
	1210 m	
1185 s		$\nu P=O$
1155 s		$\delta OH$
	1125 vw	$\rho CH_2$
1110 s		} $\nu P=O$
1078 s		
	1080 Sh	} $\nu C-C$
	1025 w	
1010 s		$\nu_{as} P-O$
952 s		$\nu_s P-O$
	942 vs	} $\nu As=O$
	874 m	
788 m		$\nu P-C$ and $\gamma OH$
	778 vs	$\nu_{as}$ and $\nu_s As-O$
720 m	715 m	$\rho CH_2$
620 vw	607 vw	} $\delta CCC$
	445 Sh	
560 Sh		} $\delta PO$
540 m		
518 w		
497 m		
460 s		

vs-very strong, s-strong, m-medium, w-weak

vw-very weak, Sh-shoulder, b-broad

$\nu$ -stretching,  $\delta$ -bending,  $\rho$ -rocking

$\omega$ -wagging,  $\tau$ -twisting

Fig.11 Infrared spectral bands and their assignments for n-heptyl phosphonic acid and n-heptyl arsonic acid. (From Dietze, 1975.)

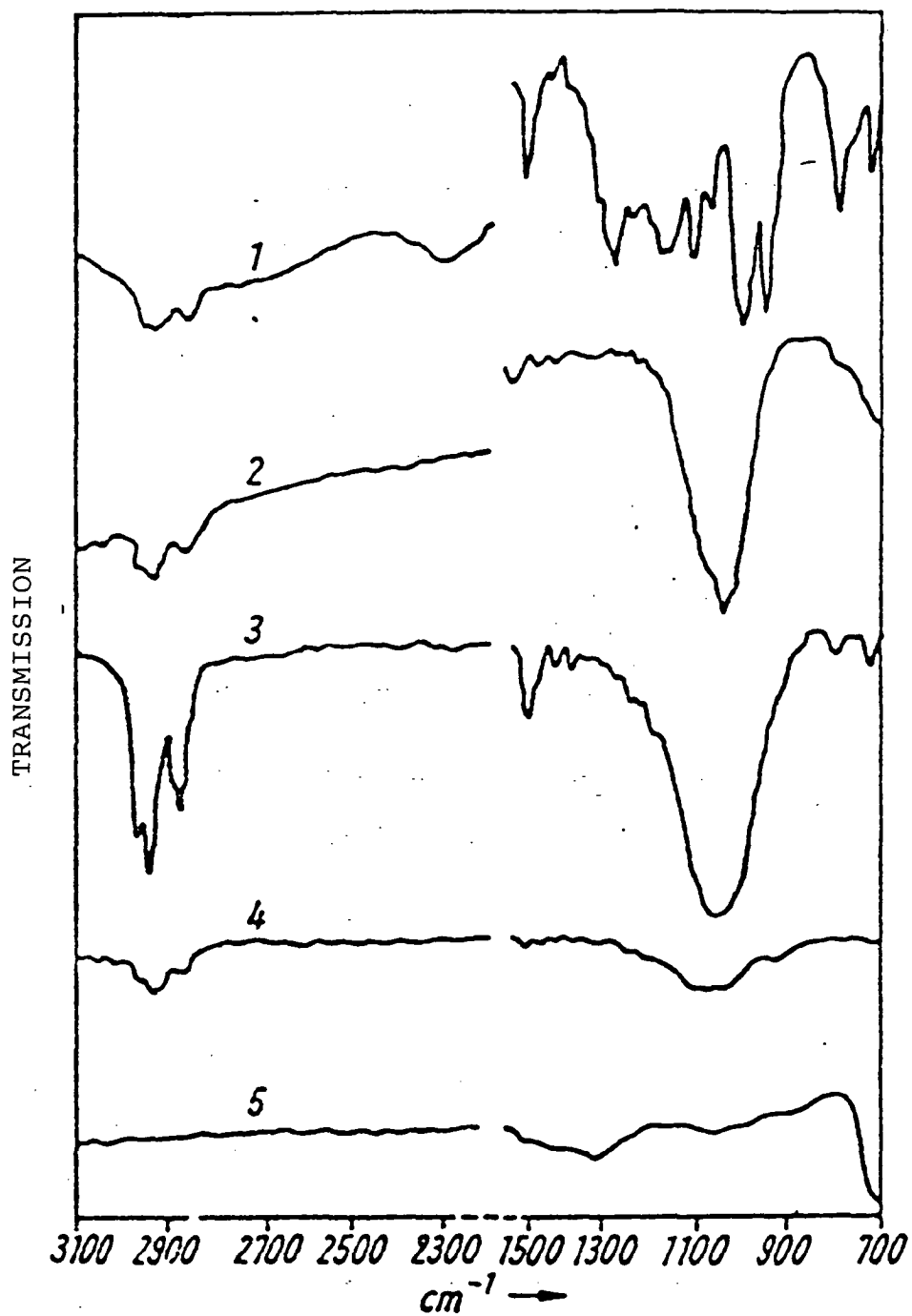


Fig.12 Infrared spectra of:

- 1 - n-heptyl phosphonic acid
- 2 - tin (II) heptyl phosphonate
- 3 - tin (IV) heptyl phosphonate
- 4 - heptyl phosphonic acid adsorbed on cassiterite
- 5 - cassiterite

(From Wottgen and Dietze, 1969.)

substance	$\Delta O-H$	$\Delta PO_3$
butyl phosphonic acid  Sn(II) butyl phosphonate Sn(IV) butyl phosphonate cassiterite + butyl phosphonic acid	$\sim 2800$ m $\sim 2312$ m	1185 Sh 1150 s 1110 s 1060 s 1005 vs $\sim 1040$ vs $\sim 1055$ vs $\sim 1060$ vw
heptyl phosphonic acid  Sn(II) heptyl phosphonate Sn(IV) heptyl phosphonate cassiterite + heptyl phosphonic acid	$\sim 2800$ m $\sim 2300$ m	1180 s 1160 Sh 1110 s 1075 m 1007 vs $\sim 1035$ vs $\sim 1070$ vs $\sim 1100$ m
benzyl phosphonic acid  Sn(II) benzyl phosphonate  Sn(IV) benzyl phosphonate  cassiterite + benzyl phosphonic acid	$\sim 2800$ m $\sim 2300$ m	1150 vs 1085 vs 1020 vs 1005 vs 1145 s 1125 m 1105 m 1055 vs 1035 vs 1005 s 980 s 1150 s 1060 vs 1040 vs 1025 vs 1000 s 1118 w 1060 w 1020 vw
p-ethylbenzyl phosphonic acid  Sn(II) ethylbenzyl phosphonate  Sn(IV) ethylbenzyl phosphonate  cassiterite + p-ethylbenzyl phosphonate	$\sim 2900$ m $\sim 2300$ m	1145 s 1100 Sh 1060 vs 1025 vs 1145 vs 1105 Sh 1065 vs 1020 vs 990 s 1150 vs 1105 Sh 1065 vs 1020 vs 1140 w 1075 w
phenylethylene phosphonic acid  Sn(II) phenylethylene phosphonate  Sn(IV) phenylethylene phosphonate  cassiterite + phenylethylene phosphonic acid	$\sim 2850$ m $\sim 2260$ m	1200 m 1180 Sh 1130 vs 1015 s 1005 vs 1200 m 1180 m $\sim 1050$ vs 1205 m 1180 Sh $\sim 1050$ vs 1000 Sh $\sim 1060$ w

vs-very strong, s-strong, m-medium, w-weak, vw-very weak, Sh-shoulder

Fig.13 Infrared spectral band assignments for phosphonic acids, their tin (II) and tin (IV) complexes and adsorbates on cassiterite.

( From Wottgen and Dietze, 1975 )

the adsorption of butyl, benzyl, p-ethyl benzyl and phenyl ethylene phosphonic acids on cassiterite using the KBr disc method to record infrared spectra and reached similar conclusions (Fig.13.)

Goold (1973) criticised Wottgens conclusions that the infrared studies indicated the formation of an adsorbed tin phosphonate compound. Goold pointed out that the spectra of tin (IV) and iron (III) complexes were identical and since cassiterite is known to contain small amounts of iron, the surface compound may be an iron (III) phosphonate complex. Goold, however, did not put forward any supporting evidence for his theory.

Dietze ( 1971, 1974a, 1974b ) undertook detailed studies of the infrared spectra of arsonic and phosphonic acids in order to gain a better understanding of the chemical information which could be deduced from the spectra. Dietze (1975) gave further infrared spectral evidence for the mechanism of adsorption of phosphonic and arsonic acids on cassiterite and associated minerals. Dietze prepared the arsonic and phosphonic acid complexes with Sn (II), Sn (IV), Ti (IV), Zr (IV), Fe (III), Fe (II), Al (III), Mn (II) and Ca (II) . He found that the complexes had different structures depending on the metal ion. For Sn (IV), Sn (II), Ti (IV), Zr (IV), and Fe (III) he found that simple neutral complexes were formed (Fig.14.), whilst for Al (III), Mn (II) and Ca (II) the complexes contained hydrogen bonded free acid groups. Iron (II) was found to form an acid

complex with one free phosphonic acid group. The infrared spectral band assignments for the phosphonic and arsonic acids are shown in Fig.14. Full infrared spectral band assignments are shown for heptyl phosphonic and heptyl arsonic acid in Fig.11.

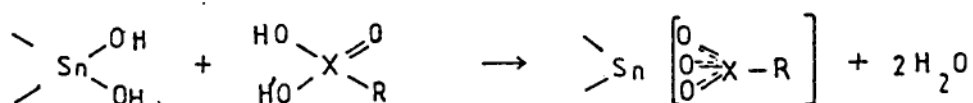
Dietze used the KBr pressed disc method to record the infrared spectra of heptyl phosphonic acids adsorbed on synthetic  $\text{SnO}_2$ ,  $\text{Fe}_2\text{O}_3$ ,  $\text{SiO}_2$ ,  $\text{SnO}_2$  doped with  $\text{Fe}_2\text{O}_3$  and  $\text{SnO}_2$  doped with  $\text{Al}_2\text{O}_3$  as models for cassiterite, hematite, corundum and quartz. He also studied the adsorption of the acids on cassiterite, apatite, topaz, tourmaline, hematite, muscovite and zinnwaldite. Dietze claims that the infrared spectra of heptyl phosphonic acid adsorbed on cassiterite,  $\text{SnO}_2$ ,  $\text{Fe}_2\text{O}_3$ ,  $\text{SnO}_2$  doped with  $\text{Fe}_2\text{O}_3$  and  $\text{SnO}_2$  doped with  $\text{Al}_2\text{O}_3$  show bands characteristic of the Sn (IV), Fe(II) and Al(III) phosphonate complexes. However from the published spectra it is not possible to distinguish differences between the bands that Dietze purports to be due to the Sn(IV), Fe(II) and Al (III) complexes.

Dietze only recorded the spectra of the adsorbed heptyl phosphonic acid on the gangue minerals from 3500 to  $2000\text{cm}^{-1}$  ( in the region where the  $\nu$  O-H band is present but where there is no information on the  $\nu$  P=O and  $\nu$  P-O vibrations ). In each case there is a band present due to  $\nu$  O-H vibrations but the band intensities vary markedly from mineral to mineral. Dietze views the presence of the  $\nu$  O-H band as evidence that heptyl

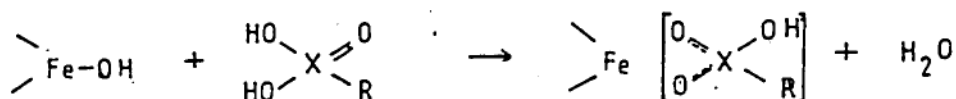
structure X = P, As R = alkyl, aryl	band assignment	band position (cm )	
		P	As
$\begin{array}{c} \text{R}-\text{X}-\text{O}-\text{H} \\ \quad \diagdown \quad \diagup \\ \quad \text{O} \quad \text{O}-\text{H} \end{array}$	$\downarrow \text{X}=\text{O}$ $\downarrow \text{X}-\text{O}_{\text{as},\text{s}}$ $\downarrow \text{X}-\text{C}_{\text{ar}}$ $\downarrow \text{X}-\text{C}_{\text{al}}$ $\downarrow \text{O}-\text{H}$	1040 - 1195 940 - 1052 1150 767 - 805 2750 - 2880	845 - 944 770 - 810 1100 - 1134 - 2750 - 2820
$\left[ \begin{array}{c} \text{O} \\ \diagup \quad \diagdown \\ \text{R}-\text{X} \\ \diagdown \quad \diagup \\ \text{O} \end{array} \right]_{\text{m}}^{2-}$ <p>M=Sn(II), Sn(IV) Ti(IV), Zr(IV) Fe(III)</p>	$\downarrow \text{XO}_3_{\text{as},\text{s}}$	1025 - 1060	815 - 855
$\left[ \begin{array}{c} \text{O} \\ \diagup \quad \diagdown \\ \text{R}-\text{X} \\ \diagdown \quad \diagup \\ \text{HO} \end{array} \right]_{\text{m}}^{2-}$ <p>M=Fe(II)</p>	$\downarrow \text{XO}_2_{\text{as},\text{s}}$ $\downarrow \text{X}-\text{O}_{\text{as},\text{s}}$ $\downarrow \text{O}-\text{H}$	1060 - 1080 920 - 995 3150 - 3250	855 745 3200
$\left[ \begin{array}{c} \text{O} \\ \diagup \quad \diagdown \\ \text{R}-\text{X} \\ \diagdown \quad \diagup \\ \text{O} \end{array} \right]_{\text{m}}^{2-}$ <p>M=Ca(II), Mn(II) Al(III)</p>	$\downarrow \text{XO}_3_{\text{as},\text{s}}$ $\downarrow \text{X}=\text{O}_{\text{as},\text{s}}$ $\downarrow \text{X}-\text{O}_{\text{as},\text{s}}$ $\downarrow \text{O}-\text{H}$	985 - 1090 1120 - 1185 920 - 995 2800 - 3200	805 - 875 905 750 3200

Fig.14 Infrared spectral band assignments for phosphonic and arsonic acids and their complexes.  
(From Dietze, 1975.)

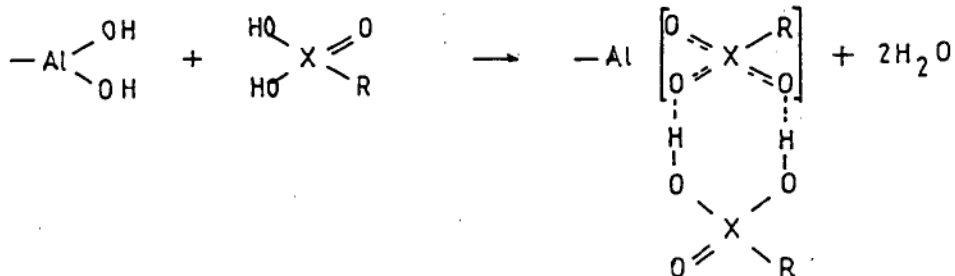
phosphonic acid chemisorbs on these minerals and puts forward the following chemisorption mechanisms from his study of phosphonate complexes and oxide model compounds.



Adsorption on cassiterite



Adsorption on hematite



Adsorption on aluminosilicate minerals

However these conclusions do not appear to be justified by the interpretation of the poor published spectra. The results published for the adsorption of phosphonic acids on cassiterite support the first mechanism but there is not sufficient detail in the spectra to support the other two mechanisms.

The chemisorption mechanism for adsorption of heptyl phosphonic acid and phenylethylene phosphonic acid (SPA) on pure tin oxide ( a model compound for natural cassiterite ) was verified using the radiotracer technique to quantitatively measure adsorption. Dietze showed that the measured adsorption isotherms could be fitted to the Langmuir and Freundlich models for chemisorption.

Dietze (1975) also investigated the adsorption of heptyl arsonic acid on cassiterite using infrared spectroscopy. He found that the bands at  $942$  and  $874\text{cm}^{-1}$  due to  $\nu_{\text{As=O}}$  vibrations,  $778\text{cm}^{-1}$  due to  $\nu_{\text{as,sAs-O}}$ ,  $\sim 2820\text{cm}^{-1}$  due to  $\nu_{\text{O-H}}$  and  $2345\text{cm}^{-1}$  due to  $\delta_{\text{O-H}}$  in the free acid are not present in the Sn(IV) complex. Instead there is a single band at  $840\text{cm}^{-1}$  due to the resonance stabilised arsonate ion. This band is also present in the adsorbate when cassiterite is treated with heptyl arsonic acid and the free acid bands are absent. From this Dietze concluded that the arsonic acid adsorbed by a chemisorption mechanism similar to that of the phosphonic acids.

Polkin et al.(1973) Used the KBr disc method to record the infrared spectra of p-tolyl arsonic acid adsorbed on hydrated tin oxide. They concluded from the increasing intensity of the arsonate band at  $843\text{cm}^{-1}$  that the quantity of chemisorbed arsonic acid increased with decreasing pH in the range 8-4 (Fig.15).

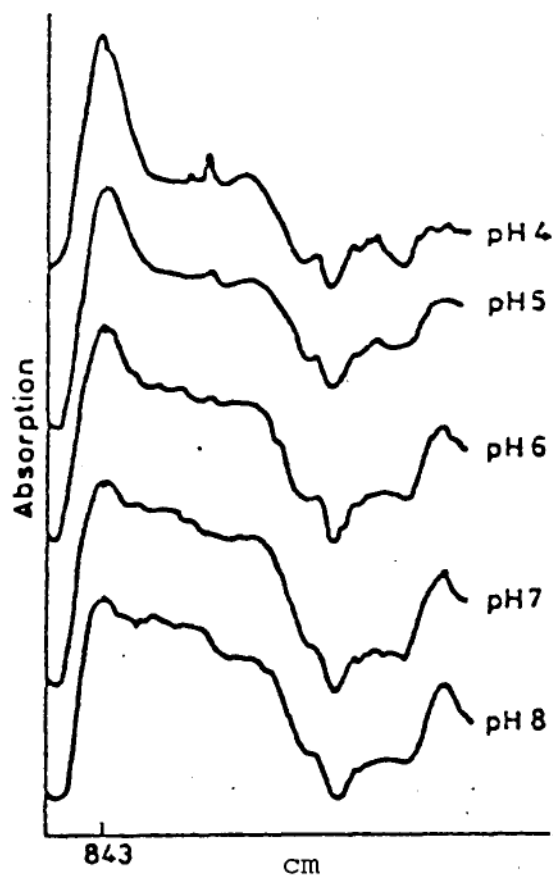


Fig.15 Infrared spectra of p-tolyl arsonic acid adsorbed on hydrated tin dioxide at various pH values. (From Polkin et al, 1973.)

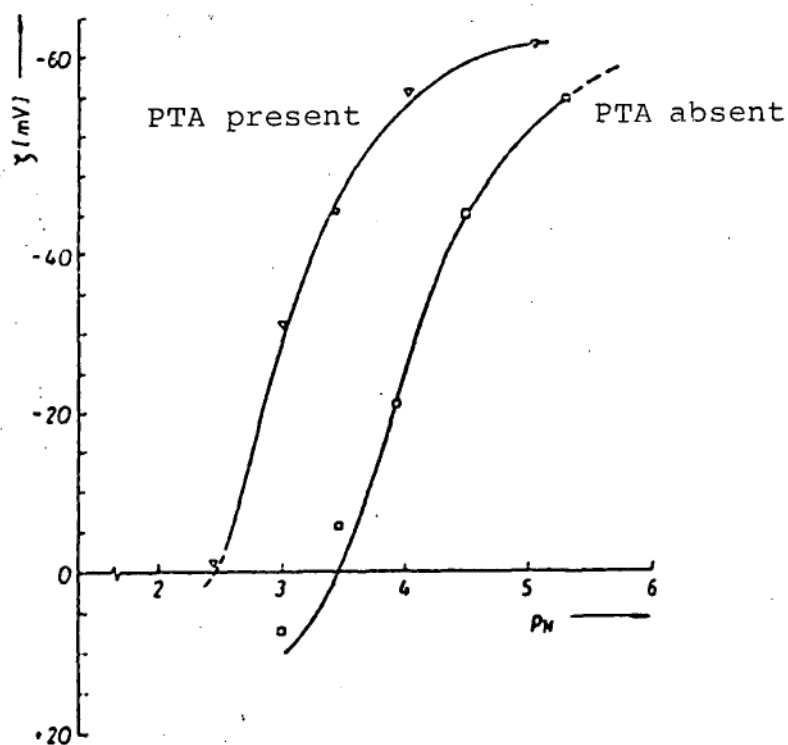


Fig.16 Zeta potential of cassiterite in the presence of  $1 \times 10^{-3}$  mol/l p tolyl arsonic acid. (From Raatz and Schubert, 1971,)

Pietzsch, Fritzsche, and Braun (1981) investigated the chemisorption mechanism for arsonic and phosphonic acids on cassiterite and attempted to determine if a correlation exists between the strength of the bond in the surface complex and the structure of the acid. These authors used Mossbauer spectroscopy to determine the binding states of tin (IV) arsonates and tin (IV) phosphonates. Their studies found that the values of the ionicity of the Sn-O bonds as well as the effective charge at the tin atom, for the tin arsonates and phosphonates, confirmed the acid-base reaction mechanism proposed for the formation of these complexes at the cassiterite surface.

Contrary to Dietze's contention that the heavy metal complexes of arsonic and phosphonic acids are compounds with mainly covalent bonds, strongly ionic bonds were found for all compounds investigated. However, from their investigations Pietzsch et al could not find any correlation between the ionicity of the Sn-O bond and the structure of the acid ligand. Hence there is little if any correlation between the Sn-O bond ionicity of the Sn(IV) complex and the flotation properties of the acid.

## 5.2 Sulphosuccinamates

The mechanism of action of sulphosuccinamate collectors was investigated by Salas, Ardaya and Navarro ( quoted in Senior and Poling, 1985 ). Salas *et al* recorded the infrared spectra of insoluble complexes of sulphosuccinamic acid. They found that the symmetric and assymetric stretching vibrations of the carboxylic acid groups in the Sn(II), Sn(IV), Fe(III) and Al(III) complexes showed changes in position and intensity, however no similar changes could be found in the sulphonate vibrations. From these observations Salas *et al* concluded that sulphosuccinamates adsorb by a chemisorption process involving the carboxylic acid groups.

Berger, Hoberg and Schneider (1980) investigated the adsorption of the sulphosuccinamate collector Aerosol 22 on cassiterite, tourmaline, hematite and quartz using infrared spectroscopy and thermogravimetric analysis. These authors used the KBr disc method to record the infrared spectra of Aerosol 22 adsorbed on cassiterite and hematite and compared these to the spectra of the tin and iron complexes of Aerosol 22.

The infrared spectra of Aerosol 22 in solution at pH 1, 4 and 7 are shown in Fig.17. The bands at  $2930\text{ cm}^{-1}$  and  $2860\text{ cm}^{-1}$  are due to the C-H vibrations and were used by Berger *et al* to quantitatively determine the adsorption of the collector from the band area. The

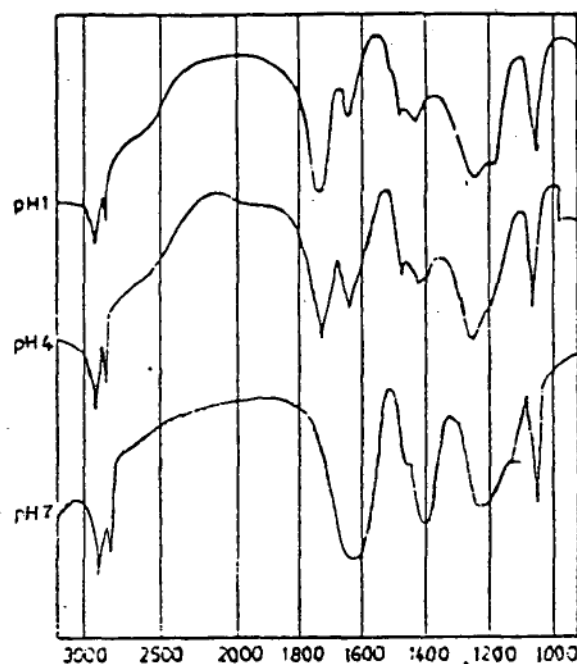


Fig.17 Infrared spectra of the sulphosuccinamate collector Aerosol 22 at pH 1,4 and 7.  
( From Berger, Hoberg and Schnieder, 1980 )

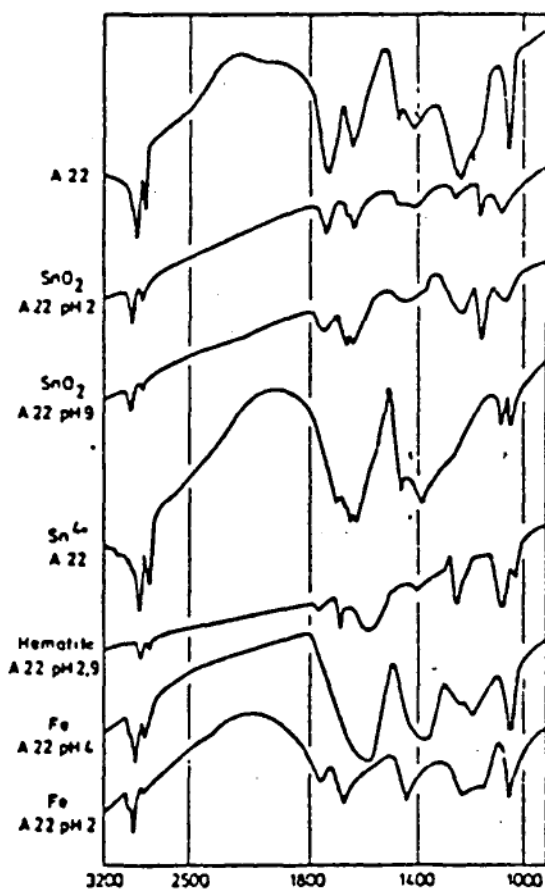


Fig.18 Infrared spectra of Aerosol 22, Aerosol 22 adsorbed on cassiterite and hematite, and the tin (IV) and iron (III) complexes with Aerosol 22.  
( From Berger, Hoberg and Schnieder, 1980 )

bands at  $1730\text{ cm}^{-1}$  and  $1630\text{ cm}^{-1}$  they attributed to the  $\nu$  C=O and  $\nu$  C-O vibrations of the carboxylate group while those at  $1250$  and  $1040\text{ cm}^{-1}$  they assigned to the sulphonate group. The infrared spectra of Aerosol 22, its Fe(III) and Sn(IV) complexes and Aerosol 22 adsorbed on hematite and cassiterite are shown in Fig 18. From these spectra Berger *et al* concluded that the sulphosuccinamate chemisorbed at the surface of both hematite and cassiterite with both the carboxylic acid and sulphonic acid groups taking part in complexation.

The adsorption density of sulphosuccinamate on the surface of cassiterite, hematite, tourmaline and quartz as a function of pH was determined from the peak area of the  $\delta$  C-H vibration at  $2930\text{ cm}^{-1}$ . The results of this investigation show that at pH 4 the collector adsorption on cassiterite and hematite is considerably greater than on quartz and tourmaline (Fig.19). At lower pH values the collector coverage on cassiterite and hematite decreases while that on tourmaline and quartz increases. At pH values greater than 4 the surface coverage of collector on all minerals decreases.

Gochin and Solari (1983) determined the electrophoretic mobility of cassiterite in various concentrations of the sulphosuccinamate collector AP 845 as a function of pH. For pH values at and below the isoelectric point, the electrophoretic mobility of cassiterite was found to decrease with increasing collector concentration and eventually reverse (Fig. 20).

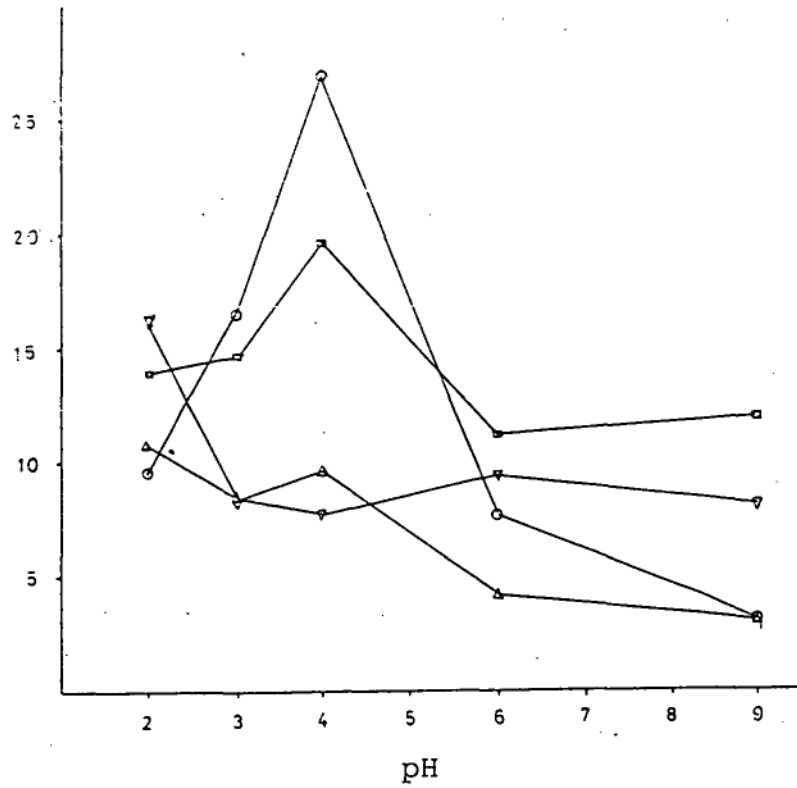


Fig.19 Adsorption of Aerosol 22 on cassiterite ( $\Delta$ ), hematite ( $\square$ ), tourmaline ( $\circ$ ) and quartz ( $\nabla$ ) as a function of pH.

(From Berger, Hoberg and Schnieder, 1980.)

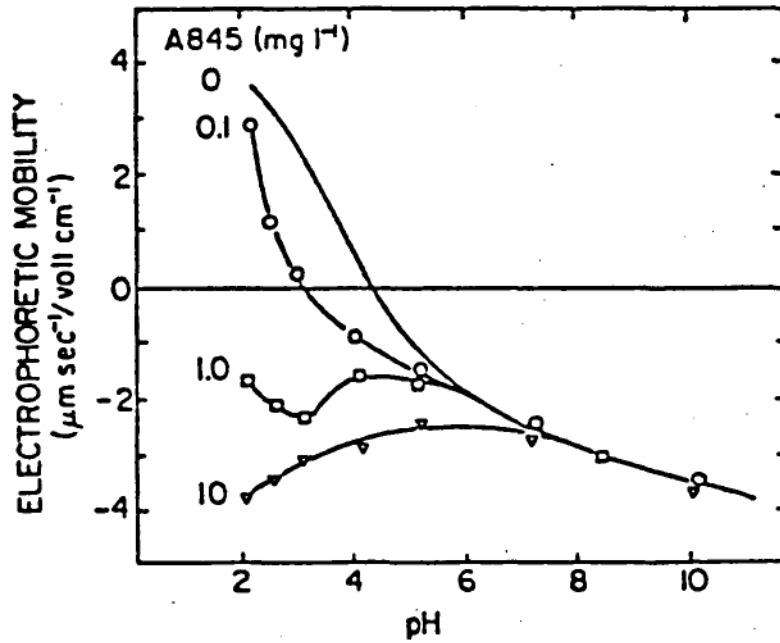


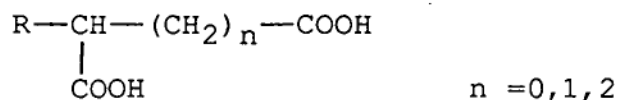
Fig.20 Electrophoretic mobility of cassiterite as a function of pH for various concentrations of the sulphosuccinamate collector AP 845.

(From Gochin and Solari, 1983.)

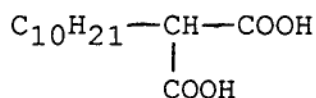
At higher collector concentrations the zeta potential becomes strongly negative. Gochin and Solari concluded from their study of electrophoretic mobilities that adsorption occurred mainly through an electrostatic attraction although a chemisorption component was thought to be involved given the change in electrophoretic mobility seen at the isoelectric point.

### 5.3 Carboxylic Acids

Following the early use of oleic acid as a cassiterite flotation collector, workers from the Freiberg Institute continued to pursue the use of carboxylic acids as cassiterite collectors. They concentrated on the use of alkane polycarboxylic acids. These reagents have been used to float cassiterite on a laboratory scale but have not been developed for use on an industrial scale because of their poorer selectivity compared to commercially available reagents. Recently the use of alkane dicarboxylic acids with the general structure,

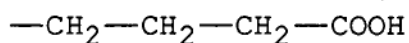


in conjunction with organic depressants has been proposed for the flotation of tin ores on an industrial scale. ( Singh, Baldauf and Schubert 1980, Baldauf, Schubert and Singh 1980, Baldauf, Schoenherr and Schubert 1985 ). The collector 1,1 undecane dicarboxylic acid,

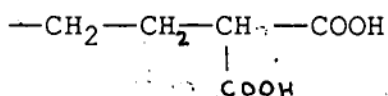


compares favourably with SPA as a cassiterite collector, however it also effectively recovers the gangue mineral topaz.

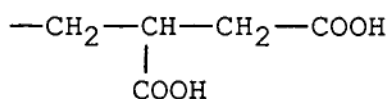
The adsorption of alkane polycarboxylic acids on cassiterite was studied by workers from the Freiberg Institute and the VEB Karl - Marx - Stadt ( Bochnia and Serrano, 1976 ). They studied a series of carboxylic acids of the following types.



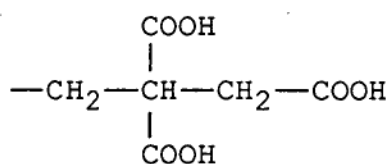
alkane carboxylic acids



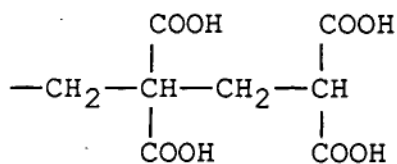
1,1 alkane dicarboxylic acids



1,x alkane dicarboxylic acids



1,x,x alkane tricarboxylic acids



1,1,x,x alkane tetracarboxylic acids

Bochnia and Serrano synthesised 18 of these acids and three acids in which one of the carboxylic acid groups was replaced by bromine. They determined the solubilities, dissociation constants and critical micelle concentrations. The effects of dimerisation, concentration, pH, temperature and metal ions ( Fe, Ca, Mg ) on the laboratory scale flotation of cassiterite and corundum ( $\text{Al}_2\text{O}_3$ ) were determined. The results indicated that 1,1 dicarboxylic acids were considerably better flotation collectors than monocarboxylic acids and the addition of more carboxylic acid groups to the alkyl chain did not necessarily improve the recovery. Hence research efforts were mainly concentrated on dicarboxylic acids as cassiterite collectors.

In order to determine the adsorption densities of the acids on cassiterite and corundum a radiotracer method using  $\text{C}^{14}$  labelled carboxylic acids were employed. Adsorption isotherms for the alkane monocarboxylic acids and 1,1 alkane dicarboxylic acids were determined at pH 6 and  $20^\circ\text{C}$  (Fig.21). From the isotherms the area of attachment of the acids on the cassiterite surface was determined to be 18.5 A for the alkane monocarboxylic acids and 32.5 A for the alkane 1,1 dicarboxylic acids. They proposed an adsorption mechanism where the carboxylic acids first chemisorbed on the cassiterite surface then physisorbed to form a bilayer (Fig.22).

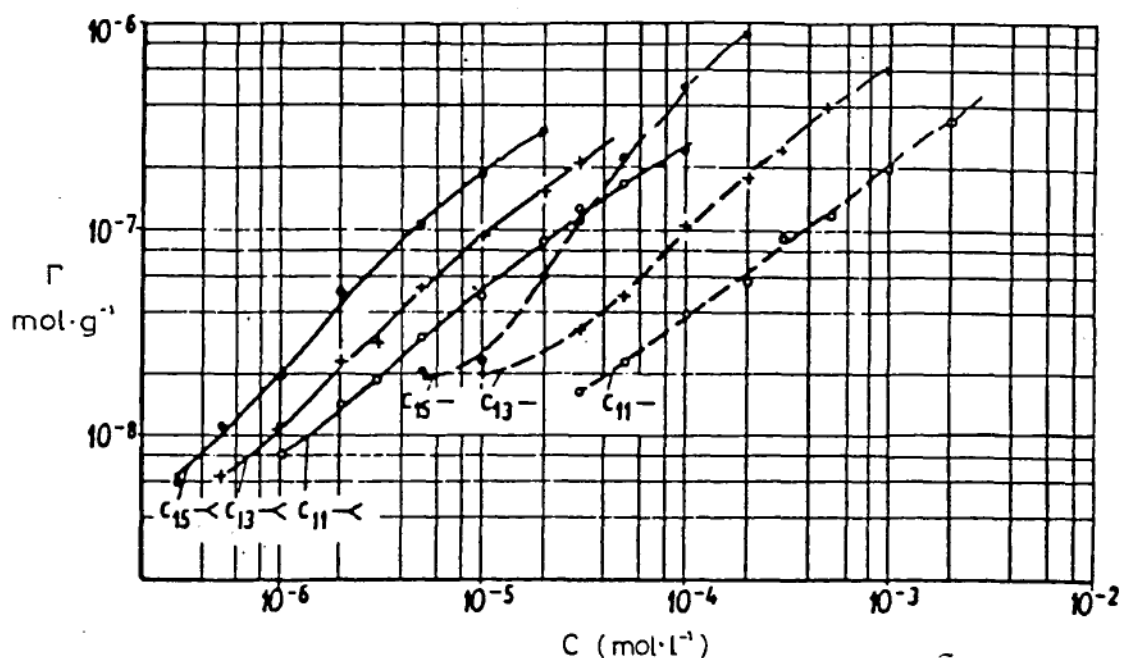


Fig.21 Adsorption isotherms for alkane carboxylic acids and 1,1 alkane dicarboxylic acids on cassiterite at pH 6 and 20°C. (From Bochnia and Serrano, 1976)

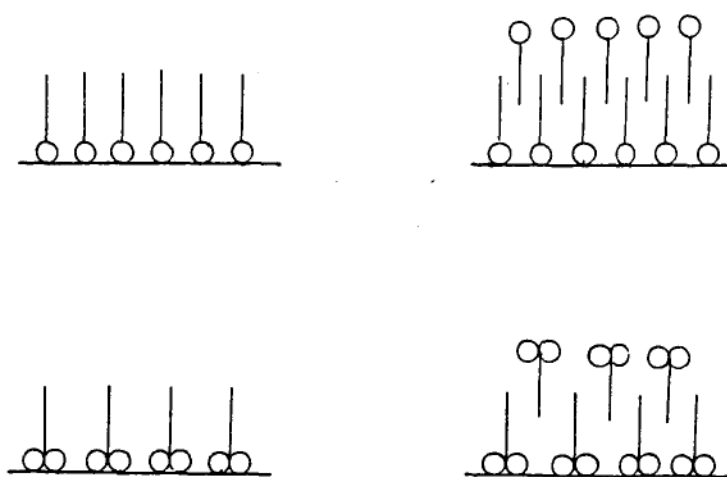


Fig.22 Diagrammatic representation of the chemisorption and physisorption of monocarboxylic and dicarboxylic acids on cassiterite. (From Bochnia and Serrano, 1976.)

To confirm their chemisorption theory for the carboxylic acids on cassiterite, Bochnia and Serrano carried out a study of the infrared spectra of the acids adsorbed on cassiterite using the KBr disc method. The free acids all show bands in their infrared spectra at  $\sim 1420\text{cm}^{-1}$  and  $1300 - 1200\text{cm}^{-1}$  due to the coupling of the  $\nu_{\text{as,s}}\text{C-O}$  vibrations and  $\rho\text{OH}$  vibrations of the dimer (Figs. 23, 24 to 26). There are also bands at  $\sim 3000 - 2500\text{cm}^{-1}$  and  $\sim 920\text{cm}^{-1}$  due to the  $\nu\text{O-H}$  and  $\omega\text{O-H}$  vibrations respectively. However in the  $\text{Sn(II)}$  complexes with these acids the bands due to  $\nu\text{O-H}$  and  $\omega\text{O-H}$  are absent and only two bands are present at  $\sim 1610 - 1450\text{cm}^{-1}$  and  $\sim 1400\text{cm}^{-1}$  due to the  $\nu_{\text{as}}\text{C-O}$  and  $\nu_{\text{s}}\text{C-O}$  vibrations of the carboxylate group. When the acids were adsorbed on cassiterite it was found that the bands due to the O-H vibrations were absent and a strong band was present at  $\sim 1630\text{cm}^{-1}$  due to the  $\nu_{\text{as}}\text{C-O}$  vibrations of the carboxylate group (Fig. 23). This confirmed that when the alkane carboxylic acids adsorbed on cassiterite a surface tin complex is formed.

		$\nu C = O$		$\nu C-O/\rho OH$		$\omega OH$	$\rho CH_2$
		$\left. \begin{array}{c} \diagup O \\ C \\ \diagdown O \end{array} \right\} \ominus$					
$C_{11}$ —	A	1710		1400	1200	960	740
	B		1570	1425			735
	C		1620	1410			740
	D		1625	1410			
$C_{11}$ —<	A	1730		1420 1270		945	720
	B		1590	1450 1330			720
	C		1640	1400 1320			720
	D		1625	1400			715
1,1 dicarboxylic (malonic)	A	1710		1435 1290	1235	940	730
	B		1580	1415 1320			730
	C		1610	1400 1330			730
	D		1615	1400			
$C_{12}$ —	A	1710		1435 1290	1230	950	730
	B		1585	1425 1310			730
	C		1610	1400 1320			730
	D		1615	1400			
1,2 dicarboxylic (succinic)	A	1710		1435 1290	1230	950	730
	B		1585	1425 1310			730
	C		1610	1400 1320			730
	D		1615	1400			
$C_{11}$ —/	A	1710		1435 1290	1230	950	730
	B		1585	1425 1310			730
	C		1610	1400 1320			730
	D		1615	1400			
1,3 dicarboxylic (glutaric)	A	1710		1435 1290	1230	950	730
	B		1585	1425 1310			730
	C		1610	1400 1320			730
	D		1615	1400			
$C_{14}$ —+	A	1710		1420	1210	925	725
	B		1580	1440 1370			725
	C		1605	1410 1380			725
	D		1615	1415			
1,2,2 tricarboxylic	A	1710		1410 1270		920	735
	B		1570	1420 1355			735
	C		1610	1400 1370			735
	D		1620	1400			
$C_{15}$ —/	A	1710		1410 1270		920	735
	B		1570	1420 1355			735
	C		1610	1400 1370			735
	D		1620	1400			
1,3,3 tricarboxylic	A	1710		1410 1270		920	735
	B		1570	1420 1355			735
	C		1610	1400 1370			735
	D		1620	1400			

Fig.23 Infrared spectral band assignments for alkane carboxylic acids (A), their sodium salts (B), their tin complexes (C), and adsorbates on cassiterite(D). In all spectra bands are present at 1470 cm ( $\delta CH_2$  and  $\delta_{as} CH_3$ ), 2860 cm ( $\nu_{as} CH_3$ ) and 2930 cm ( $\nu_{as} CH_2$ ).

(From Bochnia and Serrano, 1976).

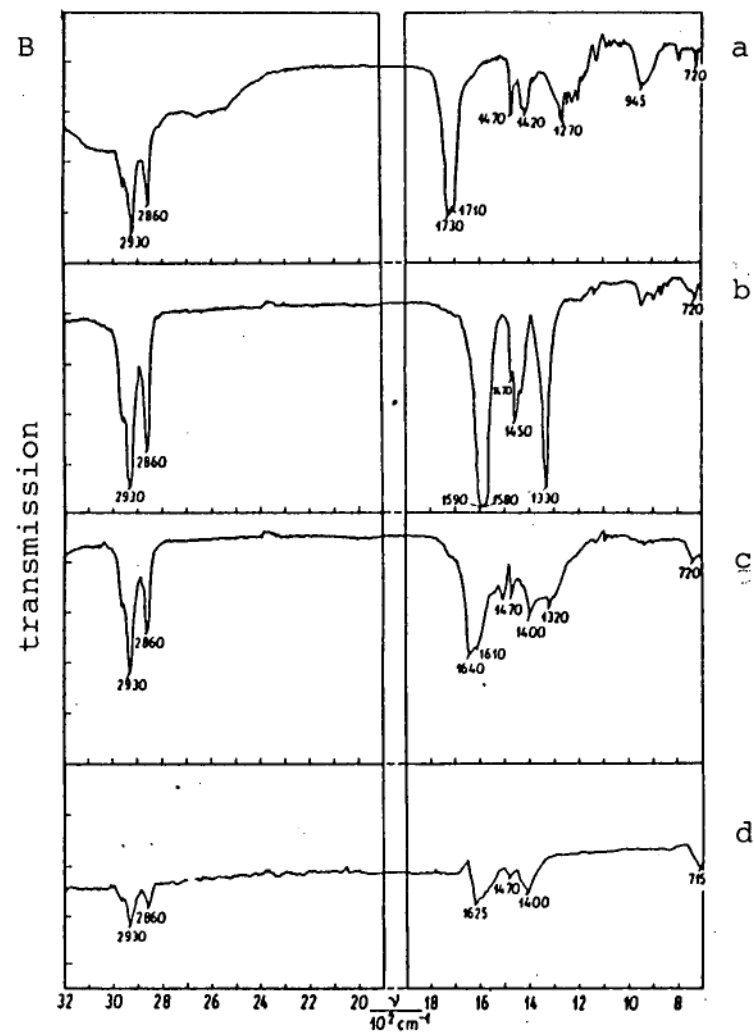
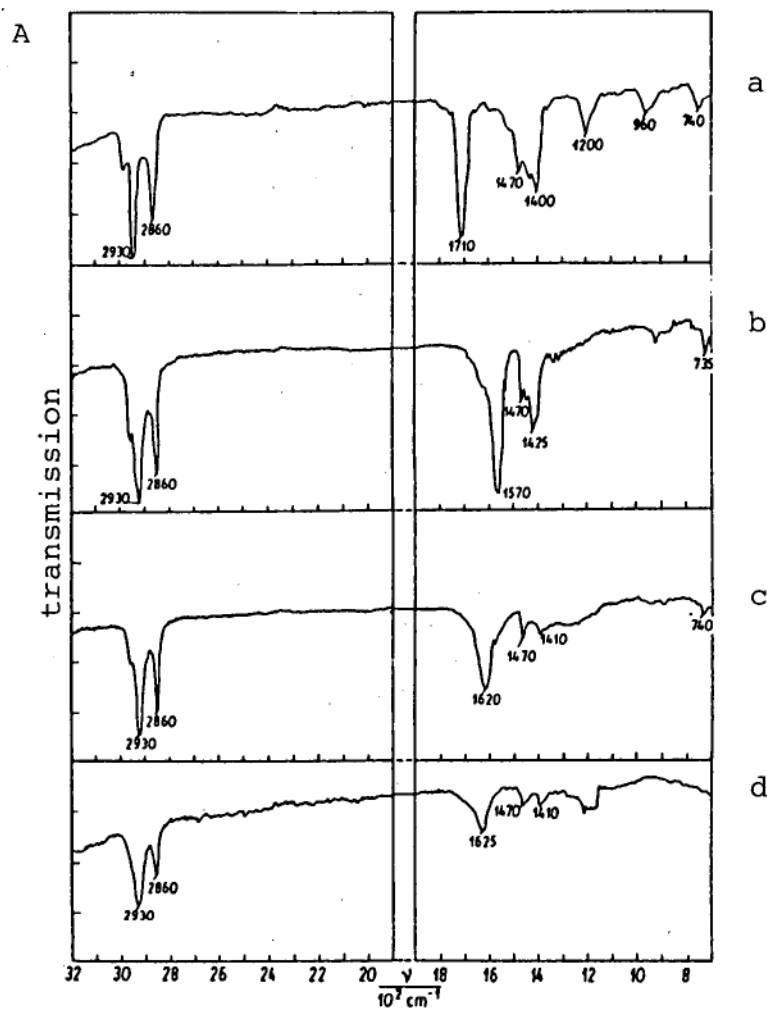


Fig.24 Infrared spectra of A-undecane carboxylic acid, B-1,1 undecane dicarboxylic acid  
 a - free acid, b - sodium salt, c - tin (IV) complex, d - adsorbate on cassiterite  
 (From Bochnia and Serrano, 1976 )

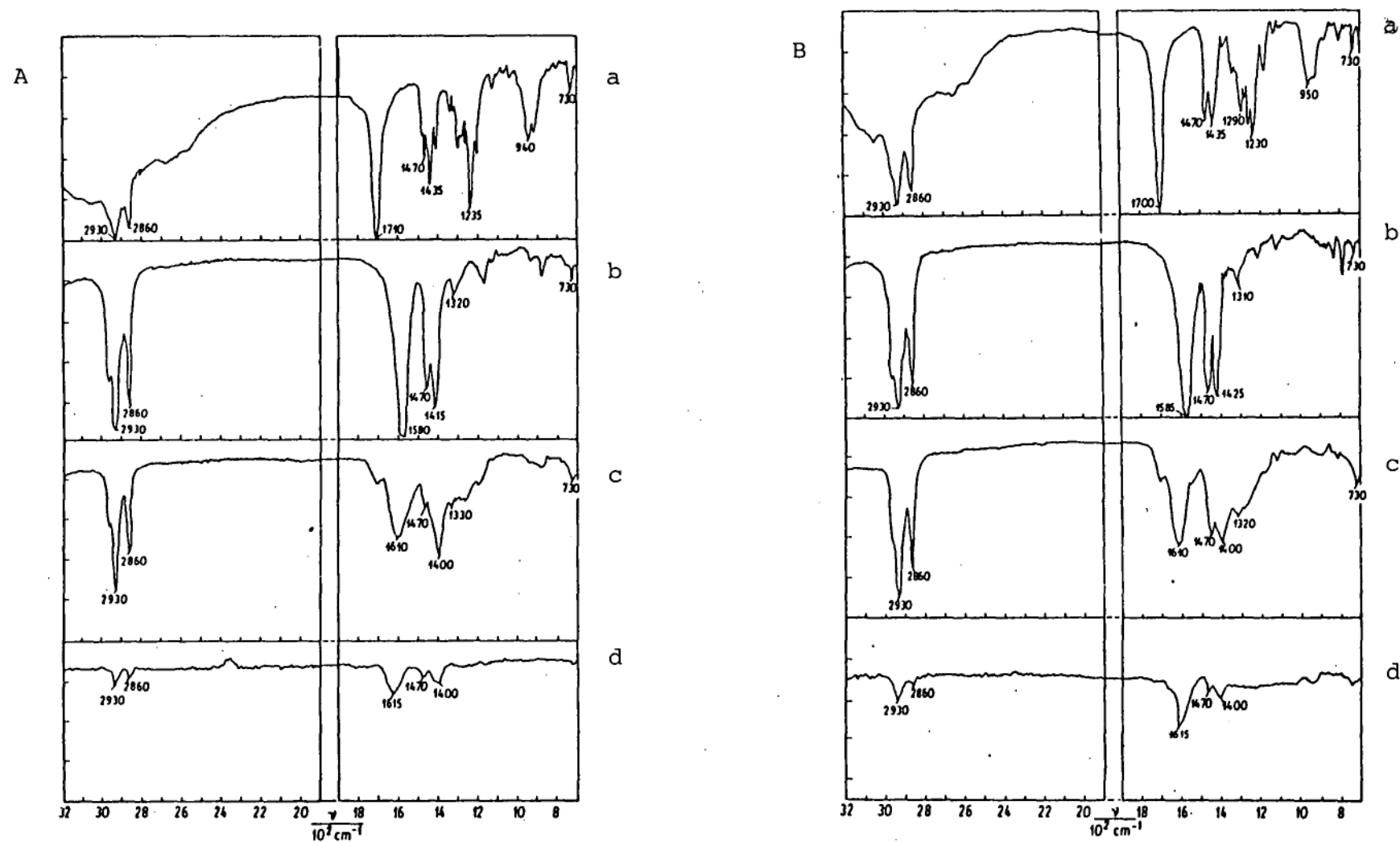


Fig.25 Infrared spectra of A - 1,2 dodecane dicarboxylic acid, B - 1,3 undecane dicarboxylic acid  
a - free acid, b - sodium salt, c - tin (IV) complex, d - adsorbate on cassiterite  
(From Bochnia and Serrano, 1976 )

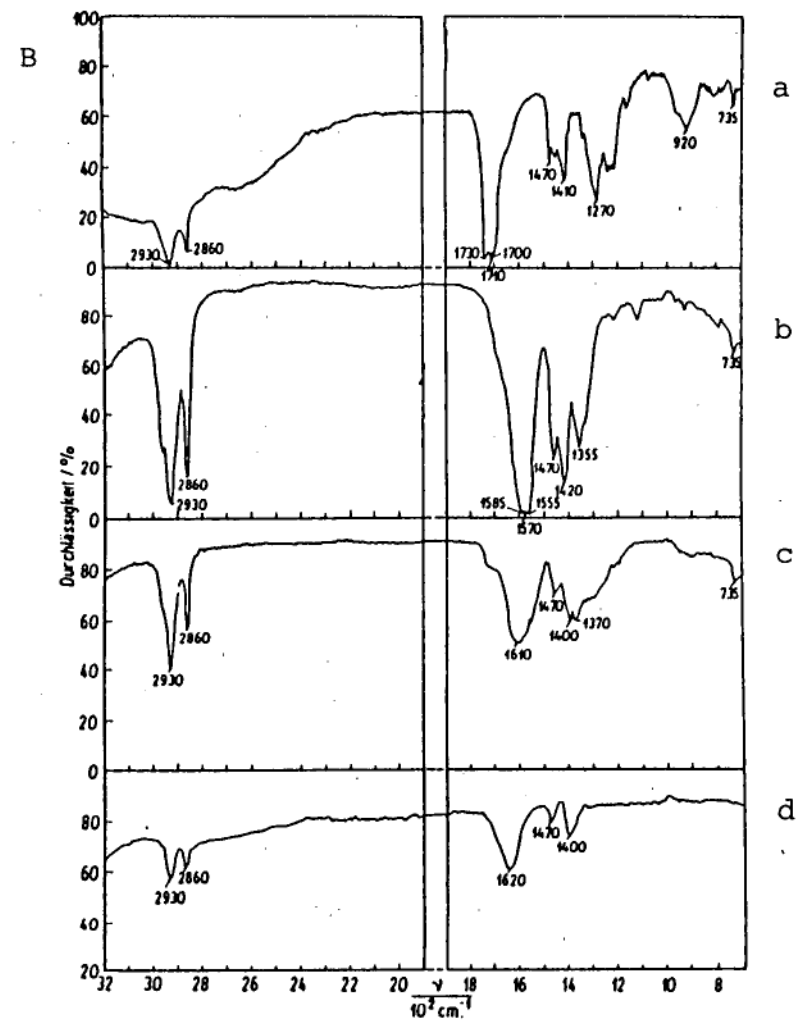
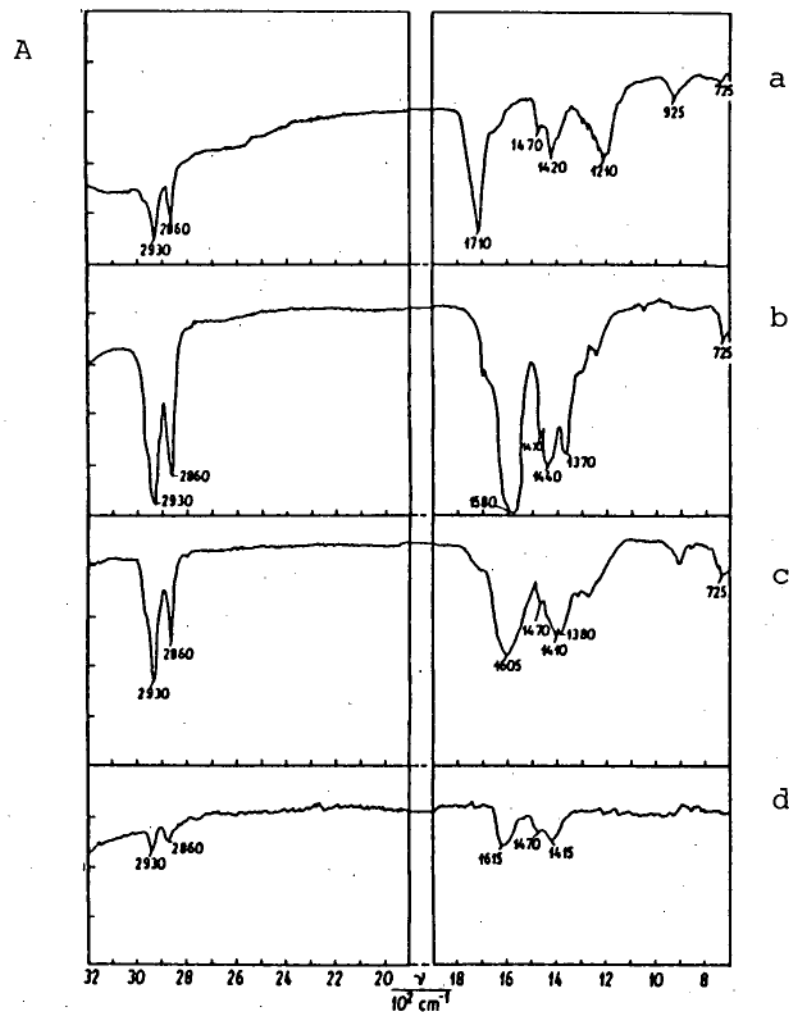


Fig.26 Infrared spectra of A 1,2,2 tetradecane tricarboxylic acid, B 1,3,3 pentadecane tricarboxylic acid a - free acid, b - sodium salt, c - tin (IV) complex d - adsorbate on cassiterite ( From Bochnia and Serrano, 1976 )

## 6. Spectroscopic Investigations of Collector Adsorption in Oxide Flotation Systems

### 6.1 Introduction

Spectroscopic methods have been used in the study of adsorption of flotation reagents on minerals since 1952. The application of spectroscopic techniques to the study of adsorption in flotation systems has been recently reviewed by Giesekke (1983), Barbary and Cecile (1979) and Stechemesser, Dietze and Wottgen (1976). As well as reviewing some of the more recent research in the application of spectroscopic techniques, these authors have looked at new techniques which, although potentially very useful, have not yet been applied to flotation systems.

Of the techniques previously used to study adsorption in flotation systems, infrared spectroscopy has been most frequently used. Infrared spectroscopic studies of adsorption behaviour at the solid-liquid interface have been reviewed by Little (1966) and Rochester (1980). Both absorption and reflection techniques have been used, however in most studies the solid and liquid phases have been separated before spectroscopic examination of the adsorbed species. This is due to the high absorption of radiation by the solvent. This problem has been partially overcome by the use of infrared adsorption cells with very short path lengths. However for aqueous solutions the

problem of solvent opacity is difficult to resolve hence infrared spectra of surface groups or adsorbed species on solids *in situ* in liquid water have only rarely been recorded.

Of the *ex situ* techniques available for studying adsorbates the simplest and most commonly used is the KBr disc method (Kirkland, 1955.). In the KBr disc method the solid and liquid phases are separated and the solid with attached adsorbate is dried and mixed with KBr and pressed into a disc which is mounted in the sample beam of the spectrometer.

In all forms of *ex situ* infrared studies of adsorption the removal of liquid from the solid surface may lead to changes in bonding of the adsorbate molecules to the surface or in the orientation of adsorbed species. For this reason *in situ* techniques are preferable in adsorption studies.

This section reviews the spectroscopic investigations which have been conducted on collector adsorption on oxide minerals. Studies of collector adsorption on minerals other than oxides are reviewed in Appendix 1.

## 6.2 Adsorption of Flotation Collectors on Oxide Minerals

Peck et al. (1966) studied the flotation of hematite ( $\text{Fe}_2\text{O}_3$ ) with oleic acid and sodium oleate using infrared spectroscopy. The KBr disc method was used to examine the infrared spectra of oleic acid and sodium oleate adsorbed on synthetic hematite, compact red hematite and specular hematite. The infrared spectra of oleic acid and sodium oleate are shown in Fig.27. The spectra of the adsorbates show a carbonyl band with maximum adsorbance between  $1520$  and  $1530\text{cm}^{-1}$  indicating chemisorbed oleate. A characteristic carbonyl band at  $1705\text{cm}^{-1}$  indicates the presence of physisorbed oleic acid on the mineral surface. The change in adsorption density of the adsorbed oleate with pH measured from the infrared spectra correlates well with the observed change in flotation properties with pH.

Paterson and Salman (1970) investigated the adsorption of oleate on cupric and ferric hydroxides using the KBr disc method. The infrared spectra indicate that when sodium oleate adsorbs onto precipitated cupric and ferric hydroxide both a chemisorbed monolayer and physically adsorbed, reversely oriented multilayers are present. By comparison of the spectra of the adsorbed species with the spectra of bulk cupric oleate and ferric oleate precipitated from solution they concluded that the surface compound was neither of these, but was probably a mono-oleate species for copper and a dioleate species for iron. They proposed several mechanisms for the formation

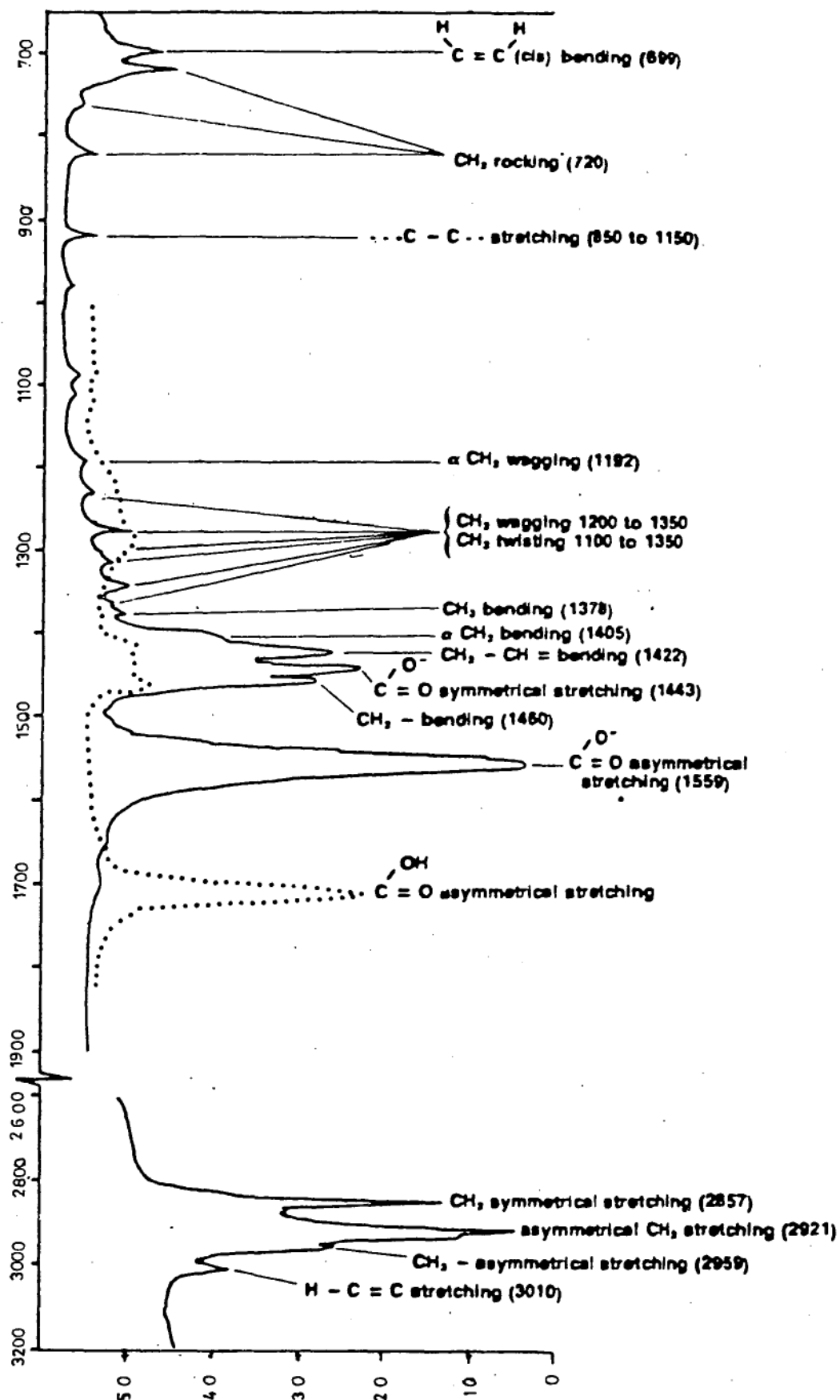
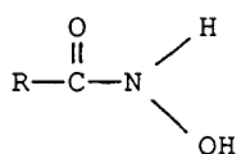


Fig.27 Infrared spectral band assignments for oleic acid and sodium oleate. (From Geisekke, 1983.)

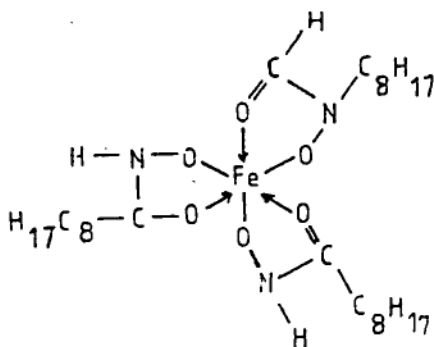
of the surface compounds which took into account the effect of pH.

Raghaven and Fuerstenau (1975) investigated the adsorption of chelating hydroxamate



R = alkyl

collectors on synthetic hematite. The infrared spectra of synthetic hematite exposed to potassium octyl hydroxamate was recorded using the KBr disc method and compared with that of the 1:3 iron hydroxamate chelate



The infrared spectrum of octyl hydroxamate has a broad band at  $1650\text{cm}^{-1}$  corresponding to the amide I band ( $\nu \text{ C=O}$ ). (Fig.28) Other prominent bands occur at  $3000\text{cm}^{-1}$  ( $\nu \text{ C-H}$ ),  $3250\text{cm}^{-1}$  ( $\nu \text{ N-H}$ ),  $1570\text{cm}^{-1}$  (amide II band),  $1000\text{cm}^{-1}$  ( $\omega \text{ C-H}$ ) and  $980\text{cm}^{-1}$  ( $\nu \text{ N-O}$ ). The spectrum of the

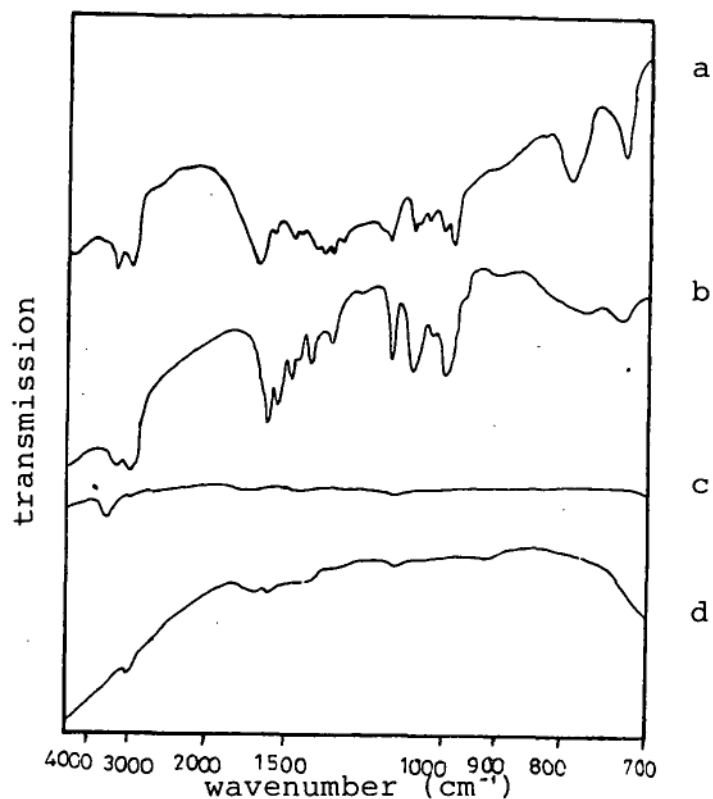


Fig.28 Infrared spectra of:

- a - potassium octyl hydroxamate
  - b - ferric octyl hydroxamate
  - c - hematite conditioned in water
  - d - hematite treated with octyl hydroxamate
- (From Raghaven and Fuerstenau, 1975.)

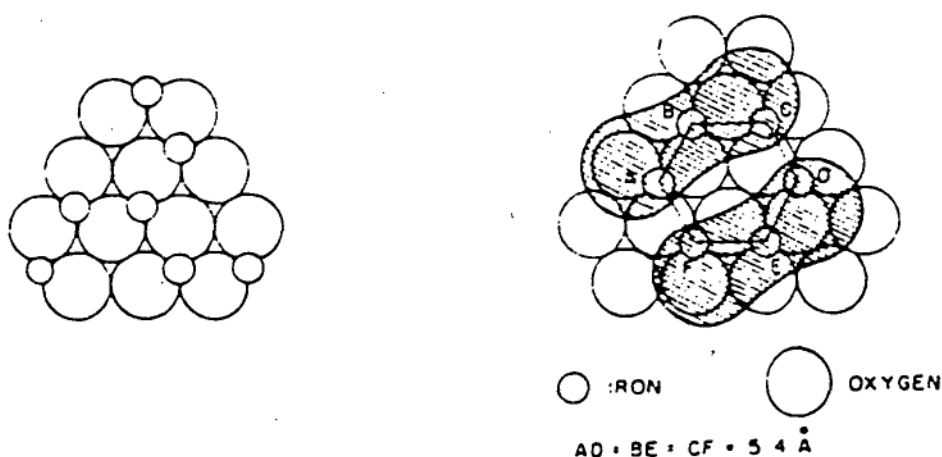
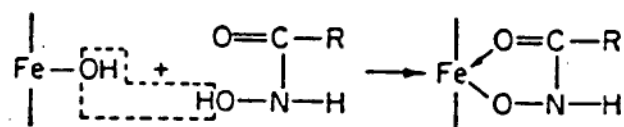


Fig.29 Proposed model of attachment of hydroxamate on the basal plane of hematite. The shaded dumb-bell shaped areas represent the polar head of the hydroxamate molecule.

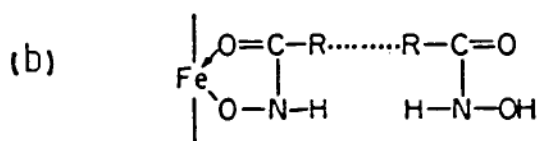
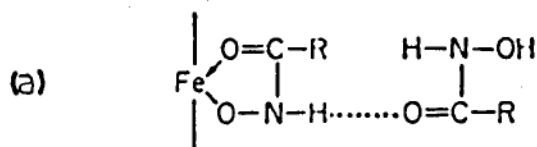
(From Raghaven and Fuerstenau, 1975.)

hydroxamate complex shows two characteristic bands, one at  $1600\text{cm}^{-1}$  ( $\nu \text{ C=O}$ ), the other at  $1650\text{cm}^{-1}$ . The increase in the stretching frequency of the  $\text{C=O}$  bond is due to the covalent bond formed by the carbonyl oxygen with the iron atom. The spectrum of ferric oxide conditioned with octyl hydroxamate shows two distinct peaks at  $1600\text{cm}^{-1}$  and  $1650\text{cm}^{-1}$ . The peak at  $1600\text{cm}^{-1}$  indicates the presence of the ferric hydroxamate chelate at the surface, whereas the peak at  $1650\text{cm}^{-1}$  is most likely due to physically adsorbed hydroxamate. From their infrared spectral study, Raghaven and Fuerstenau proposed the following adsorption mechanism.

1.



2.



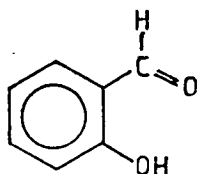
Hydroxamate chemisorbs onto hematite (1). Further hydroxamate molecules physisorb onto the first monolayer by hydrogen bonding (2a) or by association of the

hydroxamate (2b). The geometry of the adsorbed hydroxamate is shown in Fig.29.

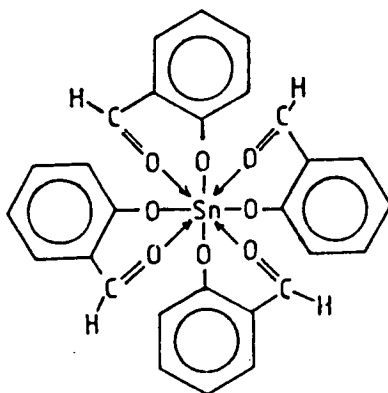
Palmer *et al.* (1975) attempted to investigate the adsorption of oleic acid on chromite ( $\text{FeO} \cdot \text{Cr}_2\text{O}_3$ ) using the KBr disc method but found the chromite too opaque to obtain spectra.

Guttierrez (1976) studied the adsorption of oleate on ilmenite ( $\text{FeTiO}_3$ ). He investigated the mechanism by which previous aeration in water or heating in air improved the flotation of ilmenite with oleic acid. Using the KBr disc method he found that in the spectrum of sodium oleate adsorbed on ilmenite there was a peak at  $1560\text{cm}^{-1}$  due to physisorbed sodium oleate and another at  $1538\text{cm}^{-1}$ . By comparison with the work of Peck *et al* (1966) he concluded that the peak at  $1538\text{cm}^{-1}$  was due to surface iron oleate ( for which the assymetric carbonyl vibrations occur between  $1520$  and  $1540\text{cm}^{-1}$  when oleate chemisorbs on hematite ). This differs from bulk ferric oleate for which the adsorption peak occurs at  $1590\text{cm}^{-1}$ . He concluded that the improvement in flotation after aeration or heating was due to the surface oxidation of the ilmenite. Oxidation of the surface iron atoms from the ferrous state to the ferric state results in an increase in the adsorption of oleic acid on the mineral due to the lower solubility of the  $\text{Fe(III)}$  surface compound compared with  $\text{Fe(II)}$  compound and a consequent increase in floatability.

Marabini (1978) studied the adsorption of the complexing collector salicaldehyde



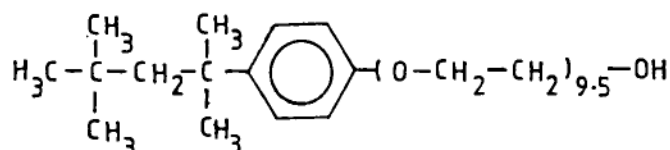
on cassiterite. Salicaldehyde was found to be able to float cassiterite in the pH range 1.5 - 7.5, but the high reagent consumption made the use of salicaldehyde as a cassiterite collector an uneconomic proposition. Marabini prepared the Sn(IV) complex with salicaldehyde



and claimed that the collector attaches to the cassiterite surface by a chelating mechanism. However he did not actually record the spectrum of the surface complex. He determined the amount of salicaldehyde removed from solution by measuring the  $2840\text{cm}^{-1}$  band of the salicaldehyde extracted into carbon tetrachloride. He concluded from this indirect method that multilayer

adsorption was required to render the cassiterite surface sufficiently hydrophobic for recovery by flotation.

Doren and Rouxhet (1982) studied the adsorption of a non-ionic surfactant, octyl phenyl polyoxyethylene glycol ether



(OPEG) on silica using infrared spectroscopy. This reagent has been successfully used in the flotation of quartz and cassiterite at low pH values. (Doren et al, 1975, Doren et al, 1981) Similar reagents are used as flotation frothers (eg: Dowfroth 200 = tripropylene glycol monomethyl ether, Dowfroth 250 = tetrapropylene glycol monomethyl ether, Aerofroth 65). It was thought that in the case of these surfactants in the formation of hydrogen bonds between the collector and the mineral surface could play an important role in flotation.

After adsorption of OPEG the porous silica was pressed into a wafer for infrared examination. The spectra of OPEG, pure silica and silica after OPEG adsorption are shown in Fig.30. The spectrum of pure silica has a sharp band at  $3745\text{cm}^{-1}$  due to free OH groups and broader components at lower wavenumbers due to bridged hydroxyls. As a result of adsorption of OPEG the intensity of the free OH band decreases and a broad band develops around  $3430\text{cm}^{-1}$ . As the amount of adsorbed OPEG increases the

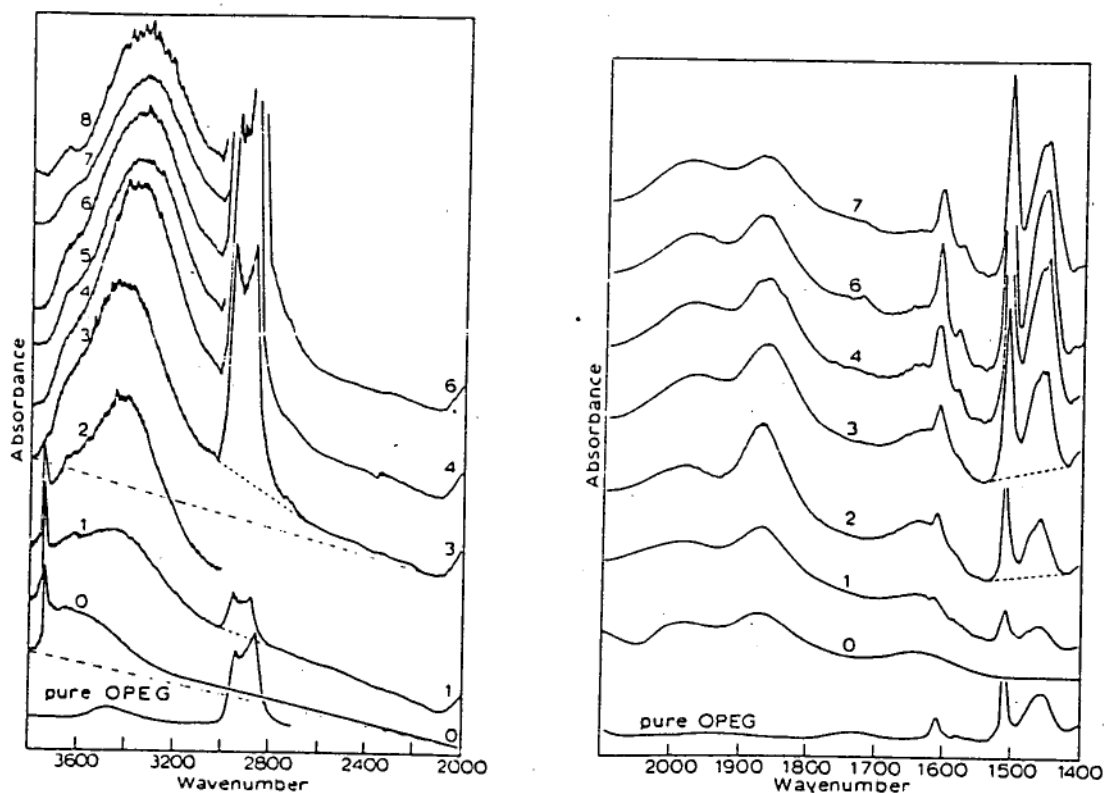


Fig.30. Infrared spectra of pure OPEG, silica and silica having adsorbed increasing amounts of OPEG corresponding to the numbered dots of Fig.31 . (From Doran and Rouxhet, 1982.)

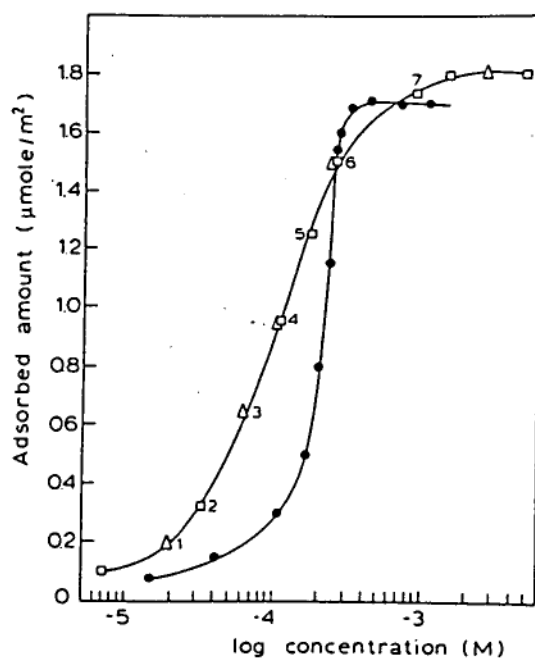
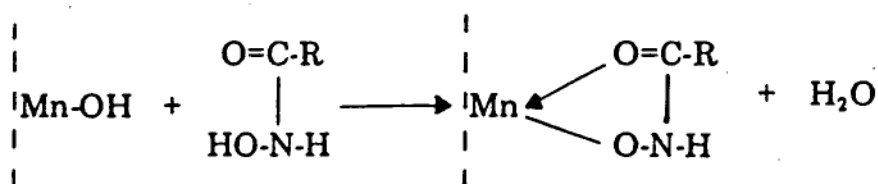


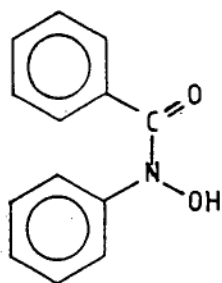
Fig.31 Adsorption isotherms for OPEG adsorption on quartz (•) and porous silica (◻, Δ: two independent sets of measurements). (From Doren and Rouxhet, 1982)

broad band shifts to lower wavenumbers. The small band at  $3648\text{cm}^{-1}$  is attributed to the hydroxyls of silica, it is already present in the untreated silica but appears more clearly after the removal of the sharp band due to the free hydroxyl. They concluded that the adsorption of OPEG involves OPEG involves hydrogen bonds between the surface hydroxyl groups and the ether groups of the polyoxyethylene chain. The frequency shift resulting from hydrogen bond formation ( $3745\text{cm}^{-1}$  to  $3430\text{--}3320\text{cm}^{-1}$ ) corresponds to that expected for an ether group.

Natarajan and Fuersteneau (1983) studied the adsorption of hydroxamate on synthetic  $\gamma$  manganese dioxide (nsutite) using the KBr disc method. They concluded that the surface species was manganous hydroxamate probably formed by the mechanism,



Marabini and Rinelli (1983) studied the adsorption of the complexing collector N-benzoyl-N-phenylhydroxylamine (N-BPHA)



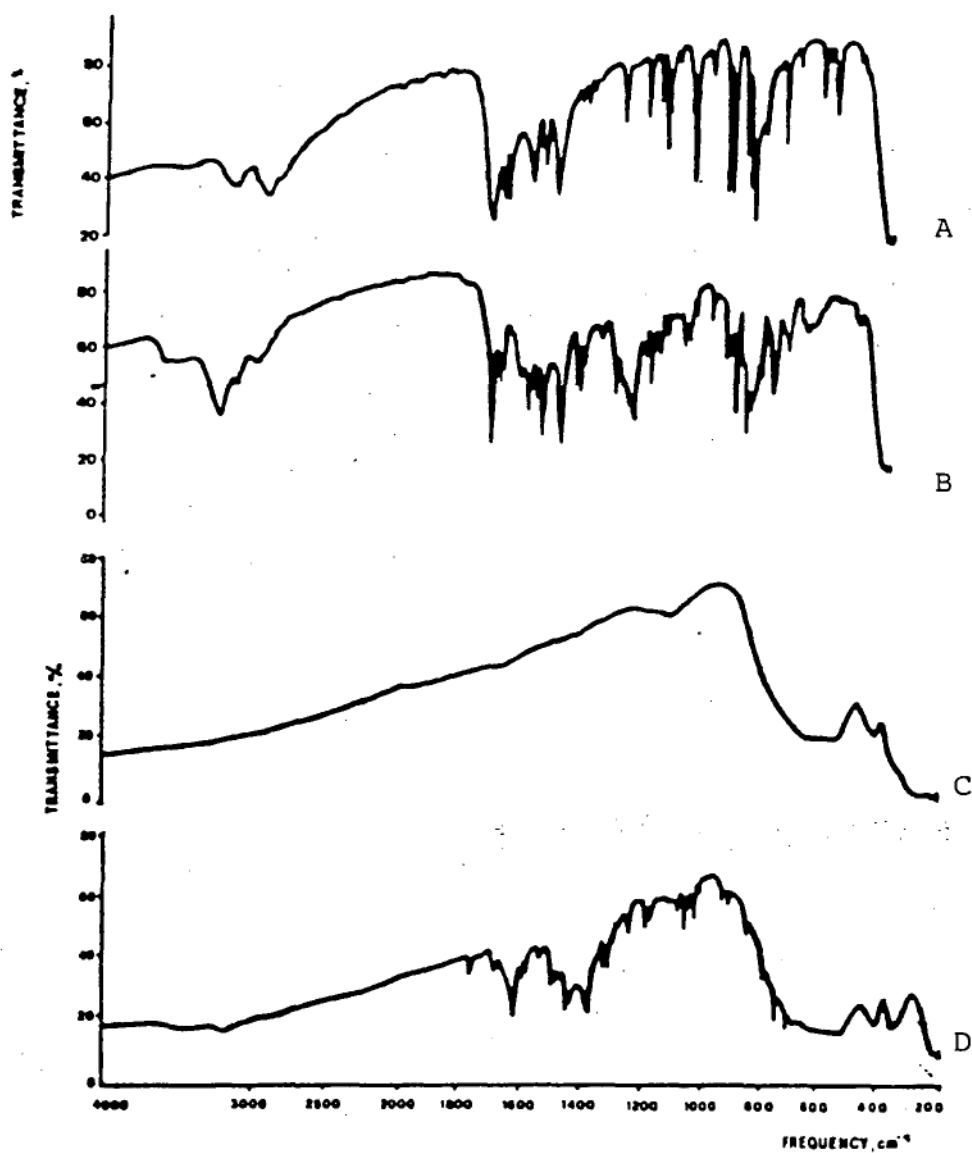


Fig. 32 Infrared spectra of:

A - N-BPHA

B - N-BPHA-titanium chelate

C - rutile

D - N-BPHA adsorbed on rutile

(From Marabini and Rinelli, 1983.)

on rutile using the KBR disc method. The spectra of rutile N-BPHA, the N-BPHA-titanium chelate and N-BPHA adsorbed on rutile are shown in Fig.32. They concluded from the spectra that adsorption occurred by a chemisorption mechanism similar to that proposed for hydroxamic acid adsorption.

### 6.3 Discussion

A review of spectroscopic investigations of adsorption in oxide flotation systems shows the wide range of information which can be obtained by the use of such methods. However most of the techniques used suffer from the problem that they can only be used to study the system *ex situ*. The only method which has been used to obtain *in situ* measurements in flotation systems is the attenuated total reflectance technique. For this reason this technique was chosen to study the adsorption of flotation collectors on cassiterite.

The ATR technique has recently been used in conjunction with Fourier transform infrared spectroscopy to record the adsorption of blood proteins onto polymers used to make artificial organs. (Gendreau and Jakobson 1978, Gendreau et al 1981, Gendreau 1982, Winters et al 1982) The combination of these two techniques was found to be capable of producing real time *in situ* spectra of adsorption from an aqueous solution. Hence these highly sensitive techniques was used in the present study.

## 7. Fourier Transform Infrared Attenuated Total Reflection Spectroscopy

### 7.1 Introduction

From a review of the spectroscopic methods which have been used in the investigation of flotation systems it can be seen that most previous studies have relied upon *ex situ* studies of adsorption behaviour. These methods all suffer from the disadvantage that removal of water from the solid surface may lead to changes in the bonding of the adsorbate molecules to the surface or in the orientation of the adsorbed species. Also there is often a long time lag between adsorption of the collector and the recording of the spectra of the adsorbate during which changes may occur on the surface.

The FTIR-ATR technique used in the present study was chosen because it could carry out real time, *in situ* studies of adsorption. The principles of operation of both the ATR technique and the FTIR technique are outlined here. These techniques will not be reviewed extensively but will only be discussed to the extent of their relevance to the present investigation viz. their operational principles, their advantages over other techniques used to record the spectra of absorbates on surfaces and their use in obtaining real time spectral measurements *in situ*.

## 7.2 Fourier Transform Infrared Spectroscopy

Fourier transform infrared (FTIR) spectroscopy was first commercially developed in the early 1960's. The operating principles of FTIR spectrometers and their use in adsorption studies are discussed extensively elsewhere [eg Ferraro and Basile (1978) and Bell and Hair (1980)].

A Fourier transform infrared spectrometer differs from a conventional grating infrared spectrometer in that it uses an interferometer in the optical system and is interfaced to a dedicated computer. The optical system of the Digilab FTS 20 FTIR spectrometer used in this study is shown in Fig.33. The light from an infrared source is sent to the beam splitter of a Michelson interferometer. The beam is split with half being transmitted to a moving mirror and half being reflected to the fixed mirror. Each component is reflected by the two mirrors and returns to the beam splitter undergoing interference. The reconstructed beam is then directed through the sample and focused onto the detector. For most mid-infrared work a triglycine sulphate (TGS) pyroelectric bolometer is used as the detector. For monochromatic incident radiation the detector will see a cosine signal, the amplitude of which will vary as a function of the path difference (retardation) of the two beams in the interferometer. In the case of polychromatic radiation entering the interferometer the signal received at the detector is a summation of all the interferences as each wavelength

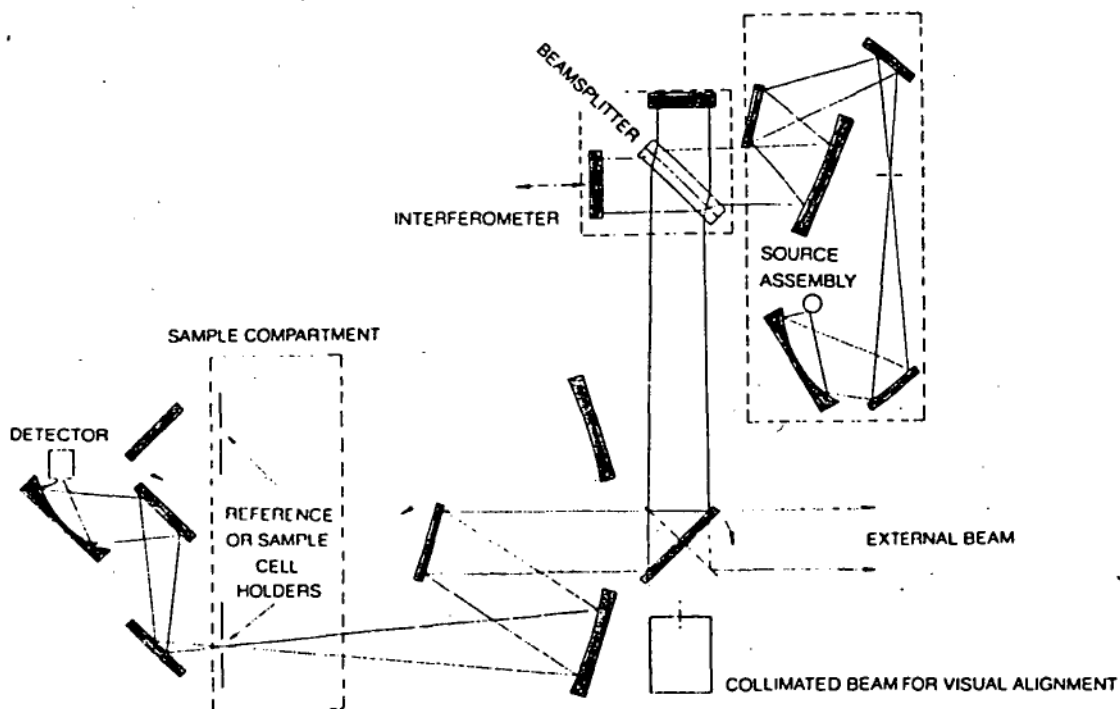


Fig.33 Optical arrangement of a Digilab Model FTS-20E FTIR spectrometer.

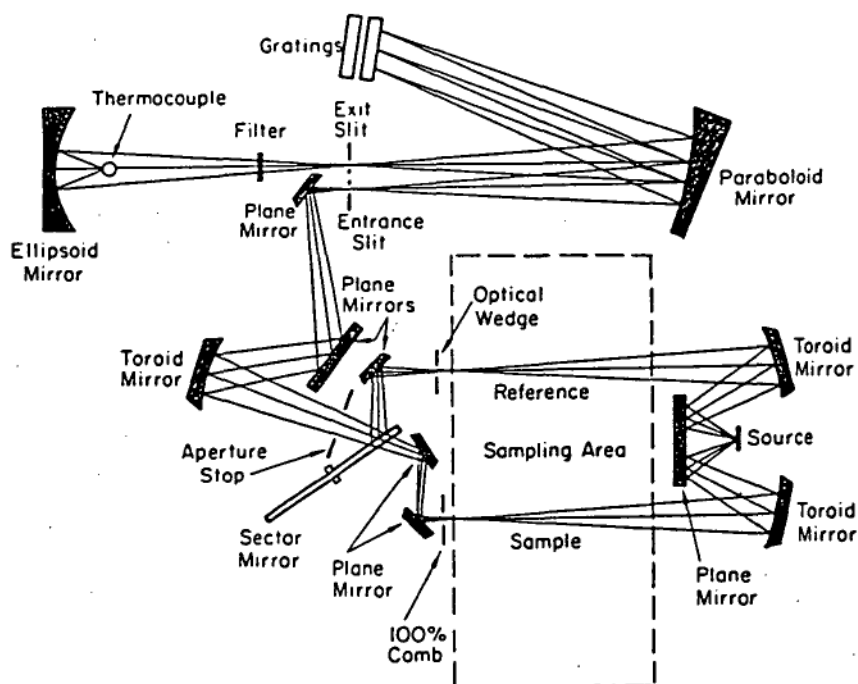


Fig.34 Optical arrangement of a Perkin Elmer Model 577 grating spectrometer.

component interacts constructively or destructively with every other component. The resulting signal is a complex pattern of light amplitude (energy) as a function of the retardation of the the two beams in the interferometer and is known as an interferogram. The interferogram is digitised by an analogue to digital converter and stored in the computer memory. The infrared spectrum [intensity as a function of frequency,  $I(\nu)$ ] can then be generated from the interferogram [intensity as a function of retardation  $I(x)$ ] by a cosine Fourier transform.

$$I(\nu) = \int_{-\infty}^{+\infty} I(x) \cos(2\pi\nu x) dx$$

Since all frequencies of light are measured simultaneously this spectrum gives an indication of the state of the chemical system being examined in real time.

Figure 34 shows the components of a double beam grating spectrometer (Perkin-Elmer 577) for comparison with the FTIR instrument. Light from the infrared source is divided into two beams. One passes through the sample while the other serves as a reference. A rotating sector mirror combines the two beams to form a single beam consisting of alternate pulses of radiation from the sample and reference beams. The combined beam enters the monochromator through a slit and is dispersed into different frequencies by a grating. Radiation of different frequencies corresponding to different orders of diffraction, emerge from the exit slit. An optical filter

is used to reject radiation from all but the desired order of diffraction. After filtering, radiation from the monochromator is focussed onto a thermocouple detector. The alternating signal at the detector is converted to the observed spectrum by electronic and mechanical means.

Fourier transform infrared spectroscopy offers considerable potential advantages over conventional dispersion infrared spectroscopy, viz

- 1) higher signal to noise ratios for spectra obtained under conditions of equal measurement time (and consequently the ability to obtain spectra of highly absorbing samples and samples at very low concentrations).
- 2) higher accuracy in frequency for spectra taken over a wide range of frequencies.

The higher signal to noise ratio is a consequence of the measurement of the detector signal at all frequencies of the spectrum simultaneously ( multiplex or Fellgett's advantage) and the higher optical throughput of the FTIR spectrometer (which has no slits) as compared to a dispersion instrument (throughput or Jacquinot's advantage).

The improvement in frequency accuracy of the FTIR spectrometer is a consequence of the use of a laser which references the measurements of the interferometer (laser reference or Conne's advantage).

Many applications of FTIR spectroscopy take advantage of the capacity of the instrument to produce spectra in energy limited situations. This makes the technique particularly useful in studies of adsorption at interfaces since generally very little adsorbant is present at the interface. The sample *per se* being small places very large demands on the instrumentation required to record spectra.

The throughput advantage of the FTIR spectrometer makes this instrument highly superior to a dispersion instrument in the observation of adsorption on surfaces in which the radiation coming from the sample is very low. This is since the radiation reaching the detector in the FTIR spectrometer is limited only by the absorbance of the sample whereas in the dispersion instrument much of the radiation is cut out by the slits.

The multiplex advantage of the FTIR spectrometer makes the instrument useful in the study of adsorption kinetics since the data acquisition time is limited. The FTIR spectrometer can produce a spectrum in a shorter time than a conventional grating instrument since all frequencies are scanned simultaneously in the FTIR spectrometer whereas in the conventional dispersion instrument they are scanned sequentially.

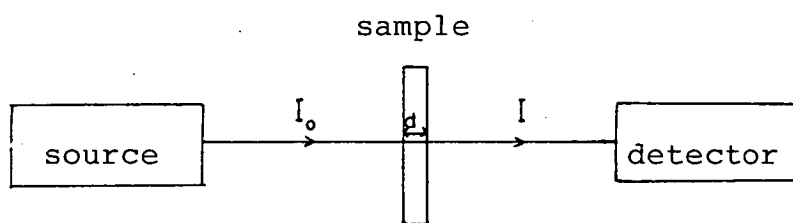
The laser reference advantage of the FTIR spectrometer makes it superior to the conventional dispersion spectrometer since frequency accuracy is greatly improved.

Another advantage of the FTIR spectrometer over conventional dispersion spectrometers is that manipulation of the digitised spectra is much easier than manipulation of analogue spectra. Manipulation of spectra can be carried out in the computer of the FTIR spectrometer so that baseline correction, scaling, change of output parameters, spectral addition, subtraction, integration and deconvolution are much easier to perform than in conventional dispersion spectroscopy. A great advantage of the FTIR spectrometer over conventional dispersion instruments is that referencing of spectra can be carried out by the comparing of single beam spectra in the computer memory rather than by using the instrument in the double beam mode. This is particularly useful in the present study in removing the effects of the highly absorbing solvent water.

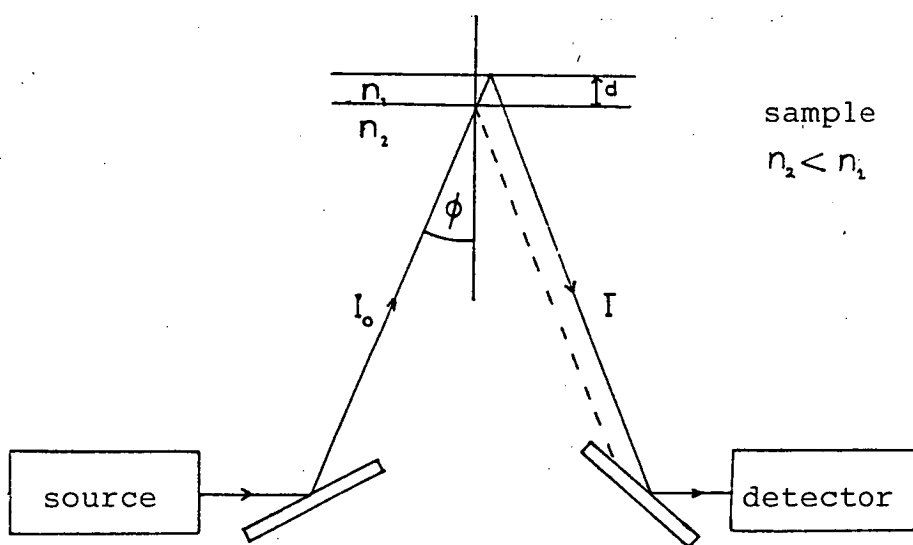
### 7.3 Attenuated Total Reflection Spectroscopy

Attenuated total reflection (ATR) spectroscopy, sometimes known as internal reflection spectroscopy (IRS), was developed independently by Harrick and Fahrenfort in 1960. The theory and practice of the technique is described extensively by Harrick (1967) and its use in studies of adsorption at the solid-liquid interface has been recently reviewed by Strojek et al (1983).

The main differences between conventional absorption spectroscopy and ATR spectroscopy are shown in Fig.35. In the absorption method radiation passes through the sample and the absorption of the radiation causes its intensity to drop from  $I_0$  to  $I$ . In the ATR method the radiation of intensity  $I_0$  strikes the interface of two media ( $n_1$ - $n_2$ ) from the side of a solid optically dense medium,  $n_1$  at an angle of incidence greater than the critical angle. The radiation is reflected with intensity  $I$ . The beam striking the interface  $n_1$ - $n_2$  penetrates the rarer medium  $n_2$  to some depth  $d_p$ . Hence the layer situated very close to the interface may be examined spectroscopically. If the rarer medium is an adsorbed layer the reflected beam will have an absorption spectrum characteristic of the coating. For this reason this technique is very useful for investigating the solid-liquid and solid gas interfaces.



Absorption spectroscopy



Attenuated total reflectance spectroscopy

Fig.35 Comparison of absorption and ATR spectroscopy.

One major difference between quantification of measurements from absorption and ATR spectra is the dependence of the intensity of the spectral bands on wavelength in ATR spectra. In adsorption spectra the intensity of the spectral bands follows the Beer-Lambert Law.

$$I = I_0 e^{-\epsilon c l}$$

$c$  = concentration  
 $\epsilon$  = extinction co-efficient  
 $l$  = pathlength

However in ATR spectroscopy it is found that for reflection from bulk materials the depth of penetration of the radiation beam increases with wavelength. There is a corresponding increase in intensity of bands at these wavelengths. The same effect also causes distortion on the longer wavelength side of absorption bands. However the study of thin films overcomes this problem in the depth of penetration.

If a thin film has a thickness much less than the depth of penetration of the beam then a considerable simplification in the interpretation of the ATR spectrum is possible. It can be shown that in this case the intensity is a function of the film thickness rather than the depth of penetration. Consequently the adsorption bands do not show the increased intensity at longer wavelengths found in ATR spectra of bulk materials nor does the absorption band become broadened on the long

wavelength side. In this case a Beer-Lambert type relationship can be applied to the variations of intensity with the concentration of species present.

At low absorbance values a similar relationship between band intensities can be found for both absorption spectroscopy and ATR spectroscopy. In absorption spectroscopy, for thin films a simplified version of the Beer-Lambert Law applies.

$$\frac{I}{I_0} = e^{-\alpha d} \quad \begin{array}{l} \alpha = \text{absorption coefficient} \\ d = \text{film thickness} \end{array}$$

For low absorbances, ie  $\alpha d \ll 1$ , this approximates to

$$\frac{I}{I_0} \approx 1 - \alpha d$$

As a result of this simplification the spectra of thin films closely resembles the analogous absorption spectra, allowing similar methods of quantitative interpretation. The simplification of ATR spectra for thin films makes the technique particularly suited to the study of absorbed molecules.

In order to increase the amount of sample scanned by the ATR method, and hence the intensity of the spectrum, Harrick developed a multi-reflection technique and designed many types of multiple internal reflection elements (MIRE). Typically these MIRE's are trapezoids of

a material which is transparent to the radiation being used and has a high refractive index [ quartz,  $n = 1.44$ , sapphire  $n = 1.75$  for UV-VIS spectroscopy, thallium bromoiodide (KRS5)  $n = 2.35$ , germanium  $n = 4.0$ , silicon  $n = 3.42$ , and zinc selenide  $n = 2.42$  for I.R. spectroscopy].

Using this kind of optical arrangement the thickness of sample studied is multiplied by the number of reflections giving an effectively greater sample thickness and hence greater absorption of the radiation. For  $N$  reflections in a MIRE with a thin film coating

$$\frac{I}{I_0} = (1 - \alpha d)^N$$

and for low absorbances  $\alpha d \ll 1$

$$\frac{I}{I_0} \cong 1 - N\alpha d$$

So for thin films and low absorbances, spectra from multiple internal reflection measurements can be quantitatively interpreted in a similar manner to absorption spectra.

The ATR technique presents a number of benefits over adsorption spectroscopy

1. It is possible to record the spectra of highly scattering substances (eg; powders).
2. It can be used to record the spectra of strongly

absorbing solids which for absorption spectroscopy would have to be prepared in impractically thin layers.

3. It can be used to record the spectra of substances in solution where the solvent strongly absorbs radiation (eg; water in the infrared).
4. It offers the potential to determine the molecular orientation by measuring the spectra as a function of beam polarisation.
5. It is one of the few spectroscopic techniques which make possible measurements of the adsorption of a substance at an interface *in situ*.

All of these advantages make the ATR method a very useful tool in investigations at the solid-liquid interface.

The possibility of using ATR spectroscopy to study adsorption phenomena at the liquid-solid interface was first investigated by Yang et al (1973). They used both conventional infrared spectroscopy and FTIR spectroscopy with the ATR method to study the adsorption of stearic acid dissolved in carbon tetrachloride on germanium ATR elements. They showed the utility of the method for obtaining information about kinetics of adsorption and desorption, adsorption isotherms, adsorbate-adsorbent perturbations, orientation and structure of the adsorbed layer and chemisorption. Low and Yang (1973) also demonstrated the capacity of the ATR method to measure the

spectra of aqueous solutions. Since then the ATR method has been frequently used to conduct *in situ* investigations of the solid-liquid interface.

## 8. Experimental Techniques

### 8.1 Reagents and Materials

Both commercially available cassiterite collectors and laboratory synthesised collectors were used in the adsorption experiments.

Styrene phosphonic acid (Mitsubishi) was purified by recrystallisation from acetone followed by precipitation from 4M sodium hydroxide solution with hydrochloric acid. The tin complexes with SPA were prepared by the methods of Dietze (1975). The tin (II) complex with SPA was prepared by precipitation from a solution of tin (II) chloride by the addition of an aqueous solution of SPA. The tin (IV) complex with SPA was prepared by the addition of aqueous SPA to an aqueous solution of tin (IV) chloride which has been complexed with tartaric acid. Precipitation of the complex was achieved by the addition of 4M aqueous ammonia

Since the commercially available sulphosuccinamate collectors Cyanamid AP845E and Allied Colloids CA540 are known to contain numerous impurities. This collector was synthesised and purified using the method of Laptev et al (1981). This reagent was recovered in the acid form as N-octadecyl (1,2- dicarboxyethyl) sulphosuccinamic acid. The tin (II) complex with this collector was prepared by a similar method to that used to prepare the tin (II) SPA complex.



presence of some iron, silicon, sulphur, and traces of manganese. Laboratory grade stannic oxide (BDH) was used without further purification as a model compound for cassiterite. Rutile type titanium dioxide was obtained from Tioxide Ltd., Burnie, Tasmania and used without further purification.

## 8.2 Apparatus and Experimental Procedure

A Digilab FTS 20 FTIR spectrometer was used to record all spectra throughout the investigation. The spectra of flotation collectors and their tin (II), tin (IV), titanium (III) and titanium (IV) complexes were recorded in KBr discs for comparison with the spectra of adsorbates recorded by the ATR method.

All ATR measurements were carried out using ATR elements of monocrystalline germanium with an angle of incidence of  $45^\circ$  and dimensions 50mm by 5mm by 2mm (Harrick). The germanium ATR elements used in this study are transparent in the range  $4000\text{ cm}^{-1}$  to approximately  $850\text{ cm}^{-1}$ . Hence it is possible to record the spectra of adsorbed phosphonic acids, sulphonic acids and carboxylic acids using germanium ATR elements. However since arsonic acids have adsorption bands in the range  $750\text{ cm}^{-1}$  to  $950\text{ cm}^{-1}$  (Fig.14) the apparatus used in this investigation cannot be used to record the spectra of adsorbed arsonic acids.

The germanium elements were coated with a thin film of tin (IV) oxide, natural cassiterite or titanium (IV) oxide using a vacuum evaporation method (Fig.36). The coating material was evaporated from a tungsten coil onto an unheated germanium optical element at a pressure of  $4-5 \times 10^{-5}$  torr in a JEOL JEE 48 vacuum operator. When using tin (IV) oxide or natural cassiterite as the coating material the coating formed at the temperatures used in the evaporation procedure (1800-1900°C) is tin (II) oxide. However this is rapidly oxidised to Sn(IV) oxide on exposure to air. Coatings with a thickness of about  $0.05 \mu\text{m}$  were obtained (as measured from interference fringes in visible light).

The reflection element with its tin oxide coating was placed in an ATR flow cell (Fig.37). This flow cell was constructed from Teflon in the Chemistry Department, University of Tasmania. The ATR flow cell was in turn placed in a Harrick 4ZV-550 ATR attachment (Fig.38) for the recording of the infrared spectra with the FTIR spectrometer. The cell was connected to a peristaltic pump which circulated the collector solution from a beaker through the flow cell then back to the beaker. The collector solution in the beaker could be kept agitated by means of a magnetic stirrer. The pH of the collector solution in the beaker was monitored throughout the experimental runs with a pH electrode placed in the beaker.

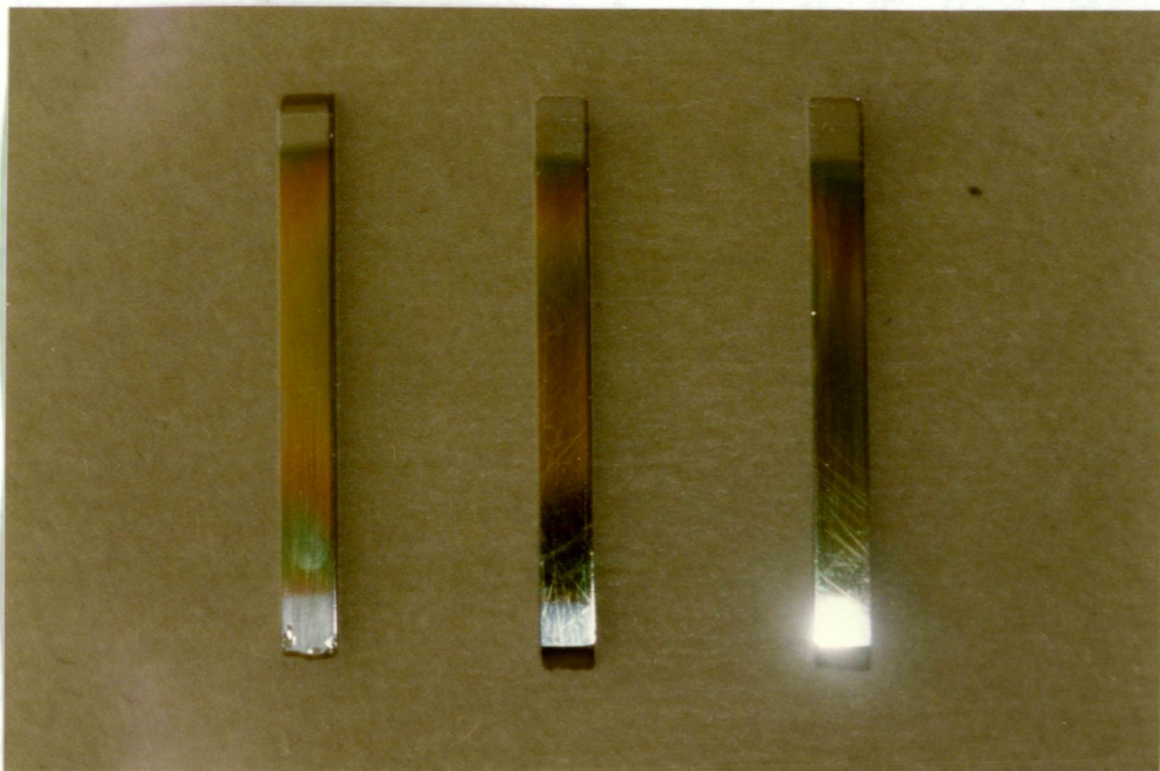


Fig.36 Germanium ATR elements after coating  
with tin (IV) oxide by vacuum evaporation.

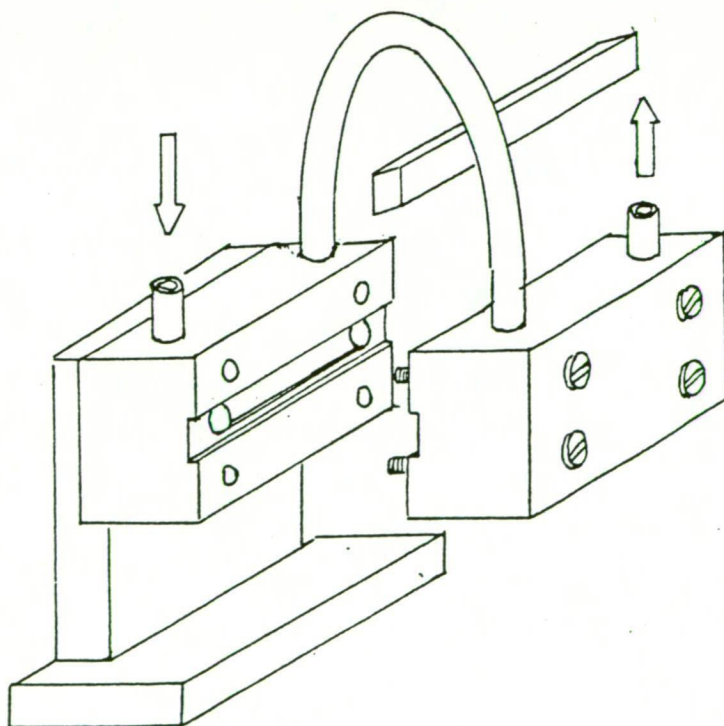
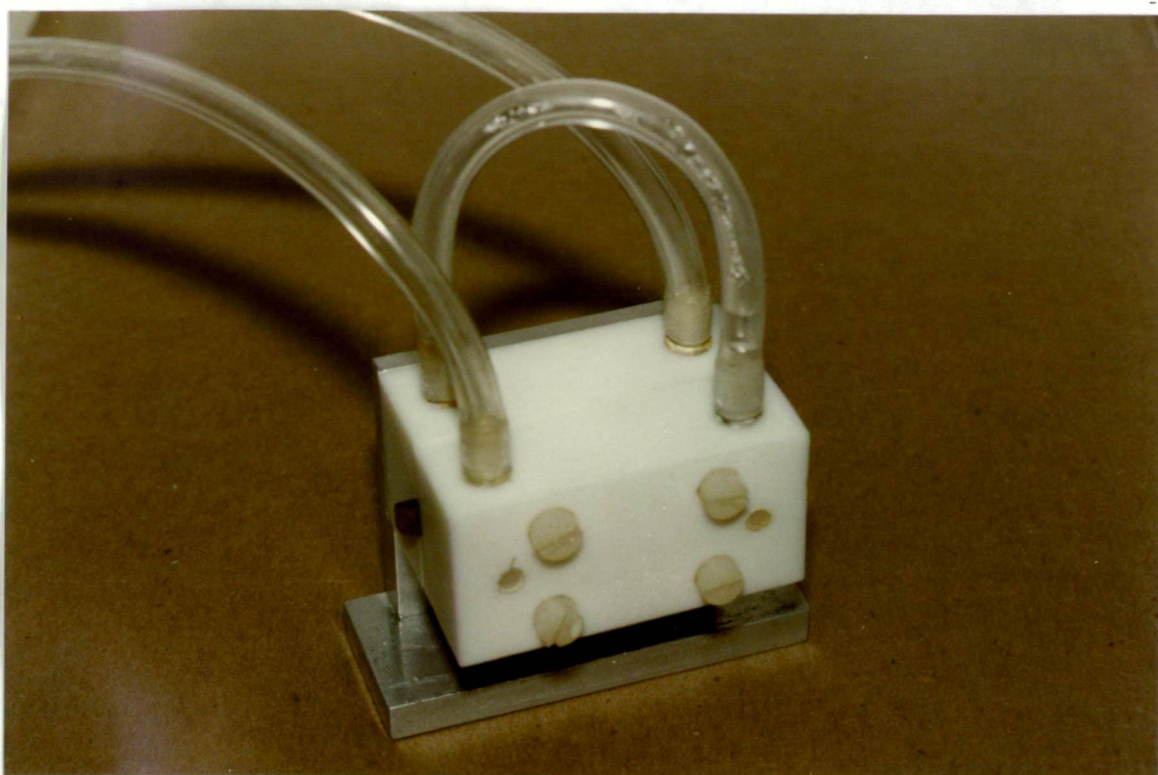


Fig. 37 The flow-through ATR cell.

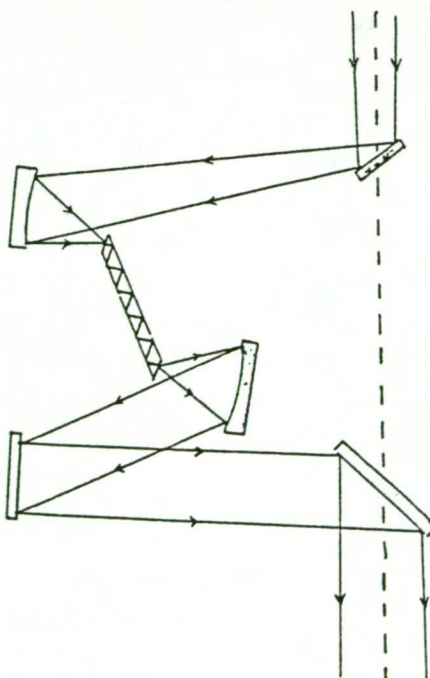
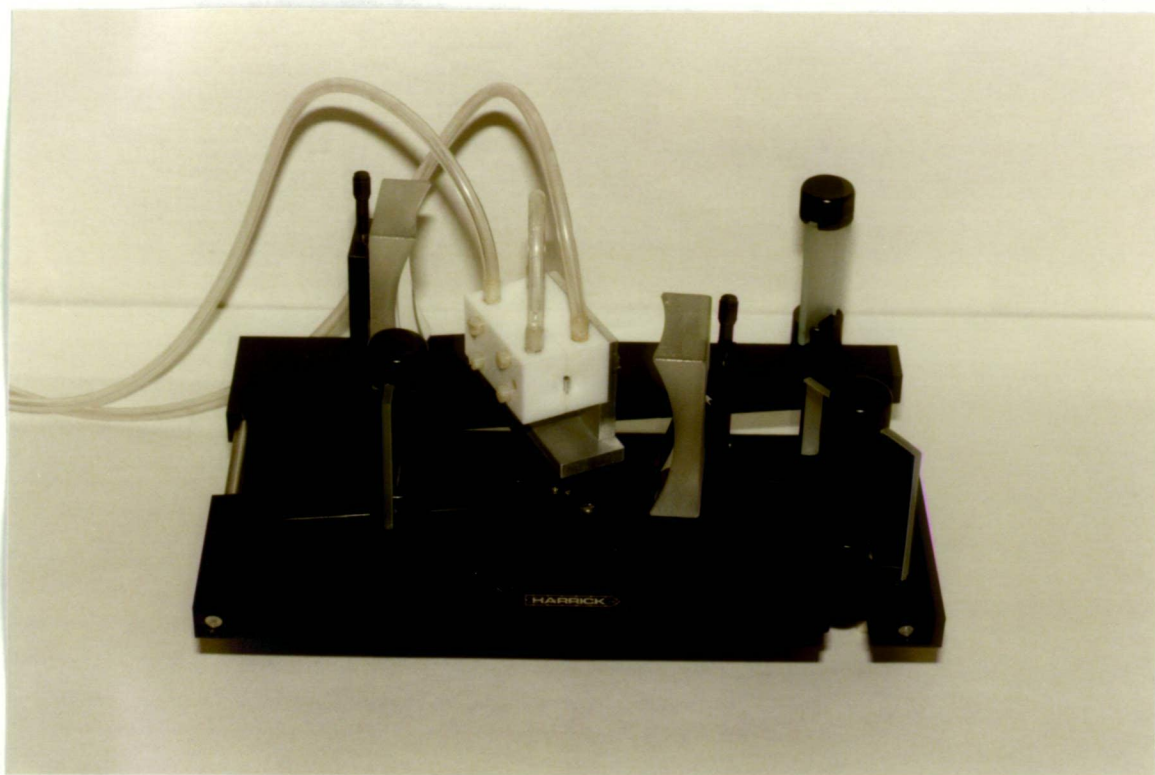


Fig. 38 The ATR optical attachment.

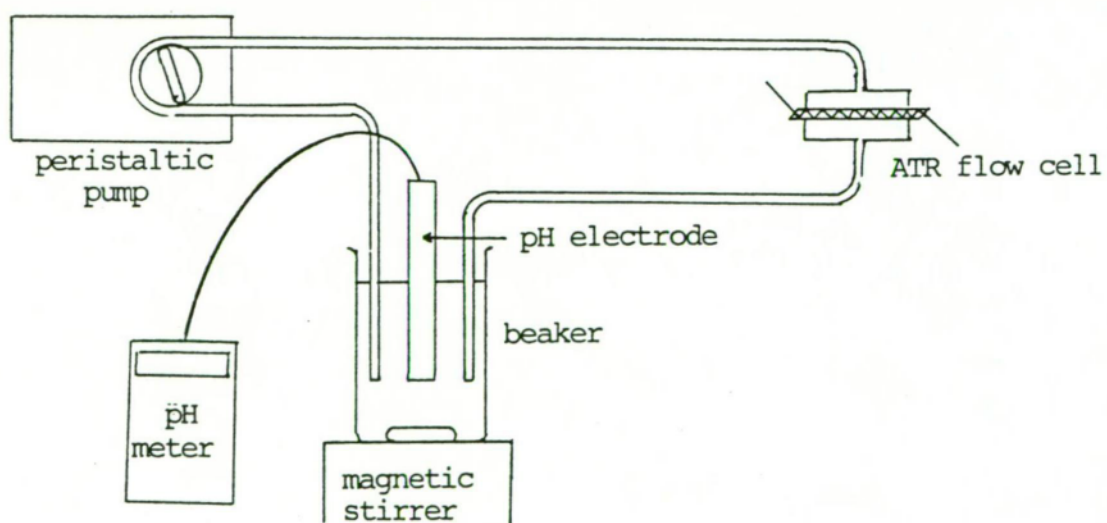
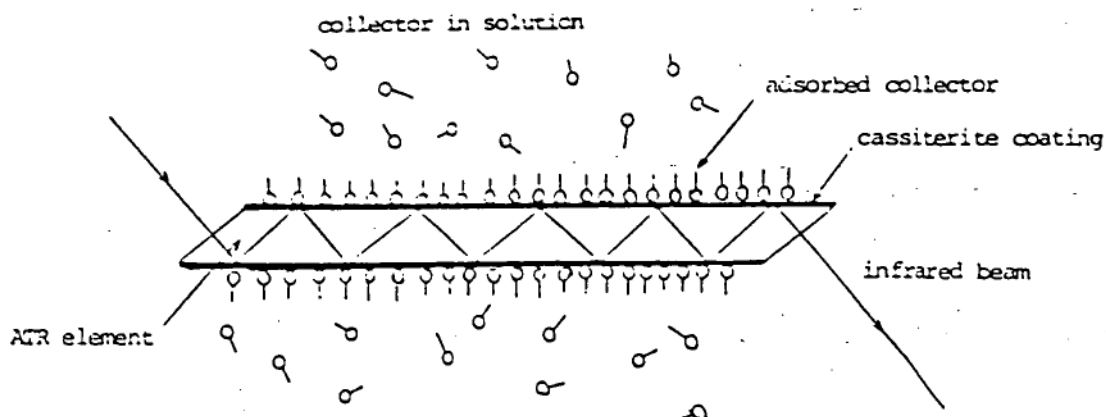


Fig. 39 Ancillary apparatus used in the FTIR-ATR study.

Initially distilled water with its pH adjusted to 4.5 (the pH used in cassiterite flotation practice at the Cleveland and Ardlethan mines) with hydrochloric acid was introduced into the ATR cell. The spectrum of the water on the tin oxide surface was taken as the reference spectrum for the adsorption experiments. After the water was pumped from the cell the collector solution was pumped in and acquisition of spectra commenced. Collector concentrations in the range 50-300 ppm were used in the experiments, this range being similar to that encountered in plant practice. Initially the pH of the collector solution was adjusted to 4.5 with hydrochloric acid or sodium hydroxide solution. Spectra were collected at intervals of approximately 90 seconds with each spectrum of 100 scans taking approximately 200 seconds. Collection of spectra was conducted for approximately two hours so sufficient spectra (~20) could be gathered to allow evaluation of the adsorption kinetics (in plant practice the cassiterite ore is conditioned with collector for approximately one hour before flotation and has a residence time of approximately 15 minutes in the flotation cell).

The infrared beam which has passed through the ATR element will have an adsorption spectrum characteristic of the collector adsorbed onto the mineral surface viz.



There is also a some contribution from collector in solution due to the infrared beam penetrating a short distance into the bulk solution. However an estimate of the distance which the beam penetrates the surrounding solution at various wavelengths shows that this contribution is negligible. At the concentrations of collector used in this investigation the greatest contribution to the spectrum will come from the water surrounding the ATR element. The contribution of the water to the spectrum can largely be overcome by the use of the spectrum of distilled water as the reference spectrum. However any uncompensated water was not corrected for by spectral addition or subtraction. Water vapour subtraction and spectral smoothing were carried out on the acquired spectra where necessary.

## 9. Adsorption of Styrene Phosphonic Acid on Cassiterite and Rutile

### 9.1 Introduction

Styrene phosphonic acid is probably the most commonly used cassiterite collector. Although not as selective as tolyl arsonic acid, styrene phosphonic acid is less expensive to produce and less toxic. Styrene phosphonic acid has no particular metallurgical advantages over other aryl phosphonic acids but is the least expensive to produce. The alkyl phosphonic acids have not been used industrially due to their poorer selectivity. Styrene phosphonic acid has also been used in the flotation of rutile, ilmenite and wolframite.

The phosphonic acids like the arsonic acids are weak dibasic acids. Chevane (1949, quoted in Senior and Poling, 1985) gives the first and second ionisation constants of styrene phosphonic acid as  $pK = 2.00$  and  $pK_2 = 7.10$  respectively. Hence in the pH range of cassiterite flotation (3.0 - 7.0) the singly dissociated species is the predominant species in solution.

### 9.2 Infrared Spectra of Styrene Phosphonic Acid and its Tin, Titanium and Iron Complexes

The interpretation of the infrared spectra of styrene phosphonic acid and its complexes is largely based on the

work of Dietze (1974a,b), Dietze (1975), and Wottgen and Dietze (1975).

The FTIR spectrum of styrene phosphonic acid in the region  $1900\text{--}850\text{ cm}^{-1}$  is shown in Fig.40. Bands due to the phosphorus-oxygen vibrations are prominent in this region of the spectrum. The band at  $1177\text{ cm}^{-1}$  is assigned to the  $\nu\text{ P=O}$  vibration while those at  $996\text{ cm}^{-1}$  and  $937\text{ cm}^{-1}$  are assigned to the  $\nu_{\text{as}}\text{P-O}$  and  $\nu_{\text{s}}\text{P-O}$  vibrations respectively. A broad band is present in the region  $3000\text{ cm}^{-1}$  to  $2800\text{ cm}^{-1}$  due to the  $\nu\text{ O-H}$  vibration and a weaker band is present at approximately  $2300\text{ cm}^{-1}$  due to the  $\delta\text{ O-H}$  vibration. of the phosphonic acid group

In the spectra of the tin (II) and tin (IV) complexes with SPA the bands due to  $\nu\text{P=O}$ ,  $\nu_{\text{as}}\text{P-O}$  and  $\nu_{\text{s}}\text{P-O}$  vibrations are absent and in the region  $1900$  to  $850\text{ cm}^{-1}$  only a single intense band is present (Figs.41,42). In the Sn(II) complex this band occurs at  $1053\text{ cm}^{-1}$  (Fig.41) while in the Sn(IV) complex it occurs at  $1050\text{ cm}^{-1}$  (Fig.42). This band is assigned to the vibrations of the  $\text{PO}_3$  group in which all three P-O bonds are equivalent. On complexation it is evident that the bands due to the  $\nu\text{ P=O}$ ,  $\nu_{\text{as}}\text{ P-O}$  and  $\nu_{\text{s}}\text{ P-O}$  vibrations of the phosphonic acid group are replaced by a single band due to the resonance stabilised phosphonate group. The bands due to the  $\nu\text{ O-H}$  and  $\delta\text{ O-H}$  vibrations are absent in the spectra of the tin complexes since the proton is lost on complexation.

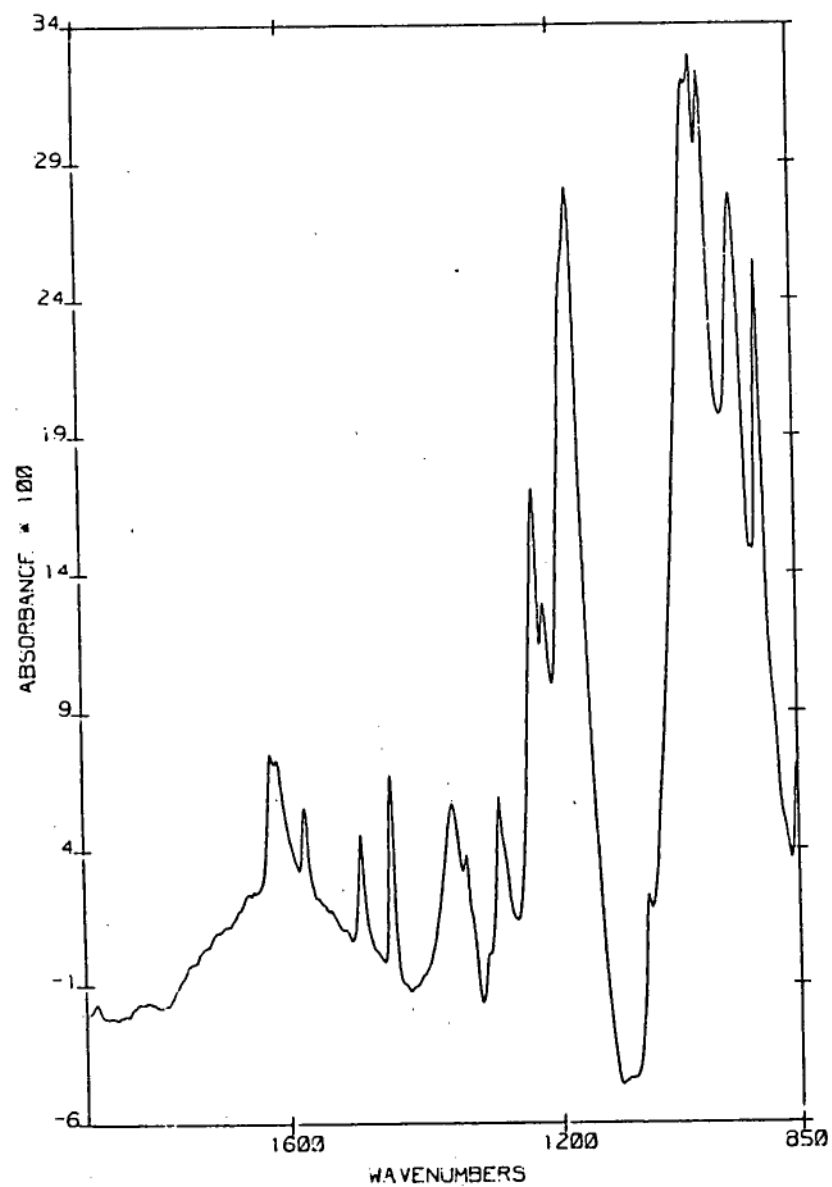


Fig.40 FTIR spectrum of styrene phosphonic acid.

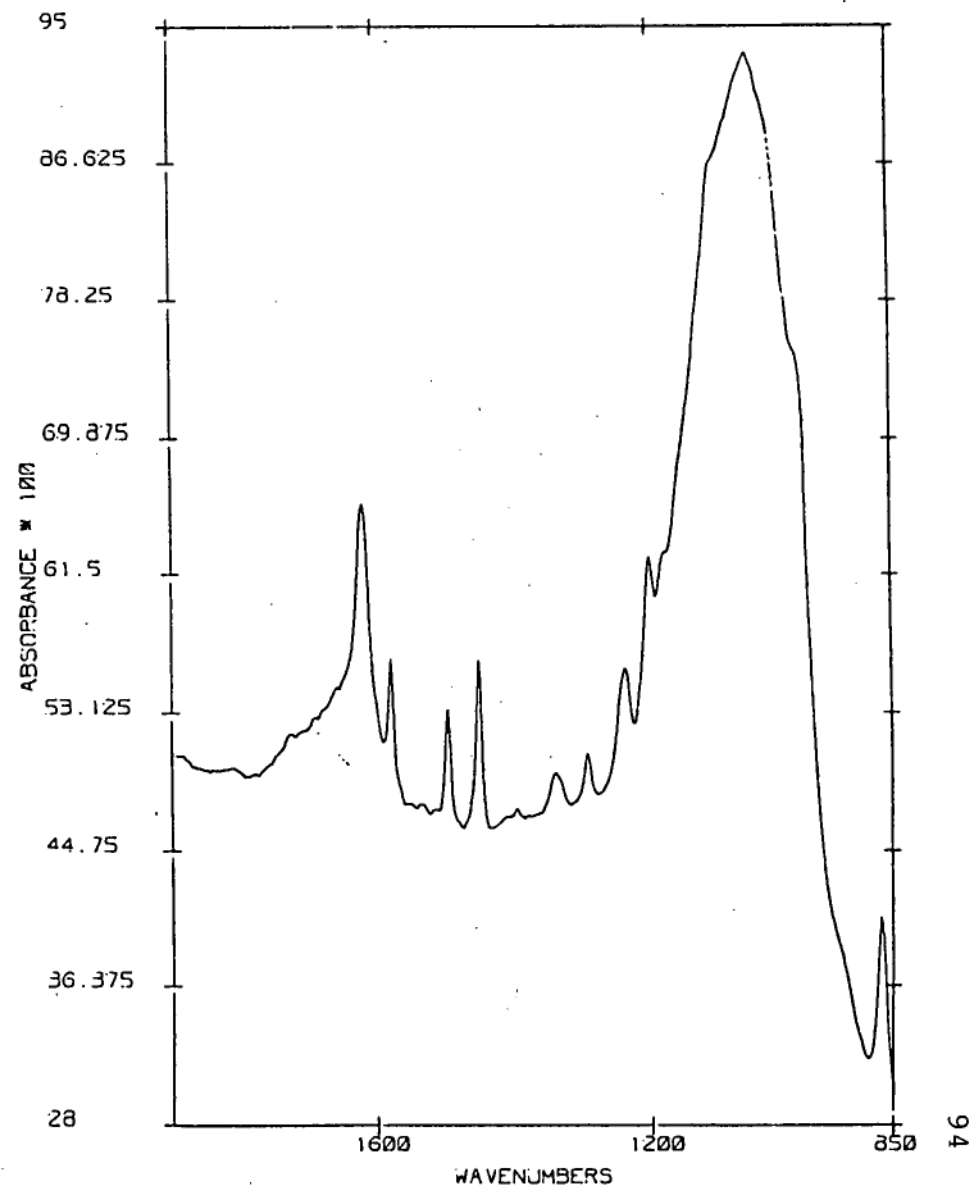


Fig.41 FTIR spectrum of the tin (II) complex with SPA.

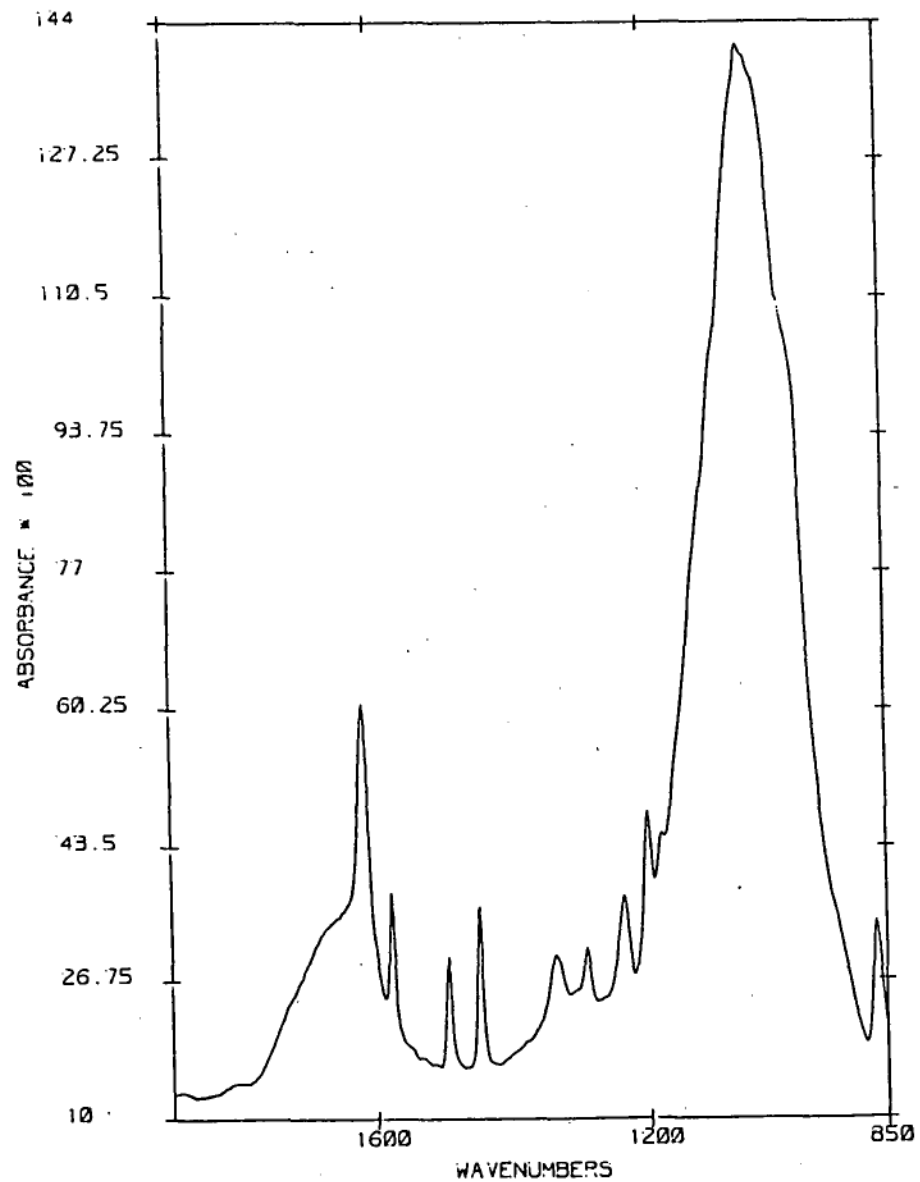


Fig.42 FTIR spectrum of the tin (IV) complex with SPA.

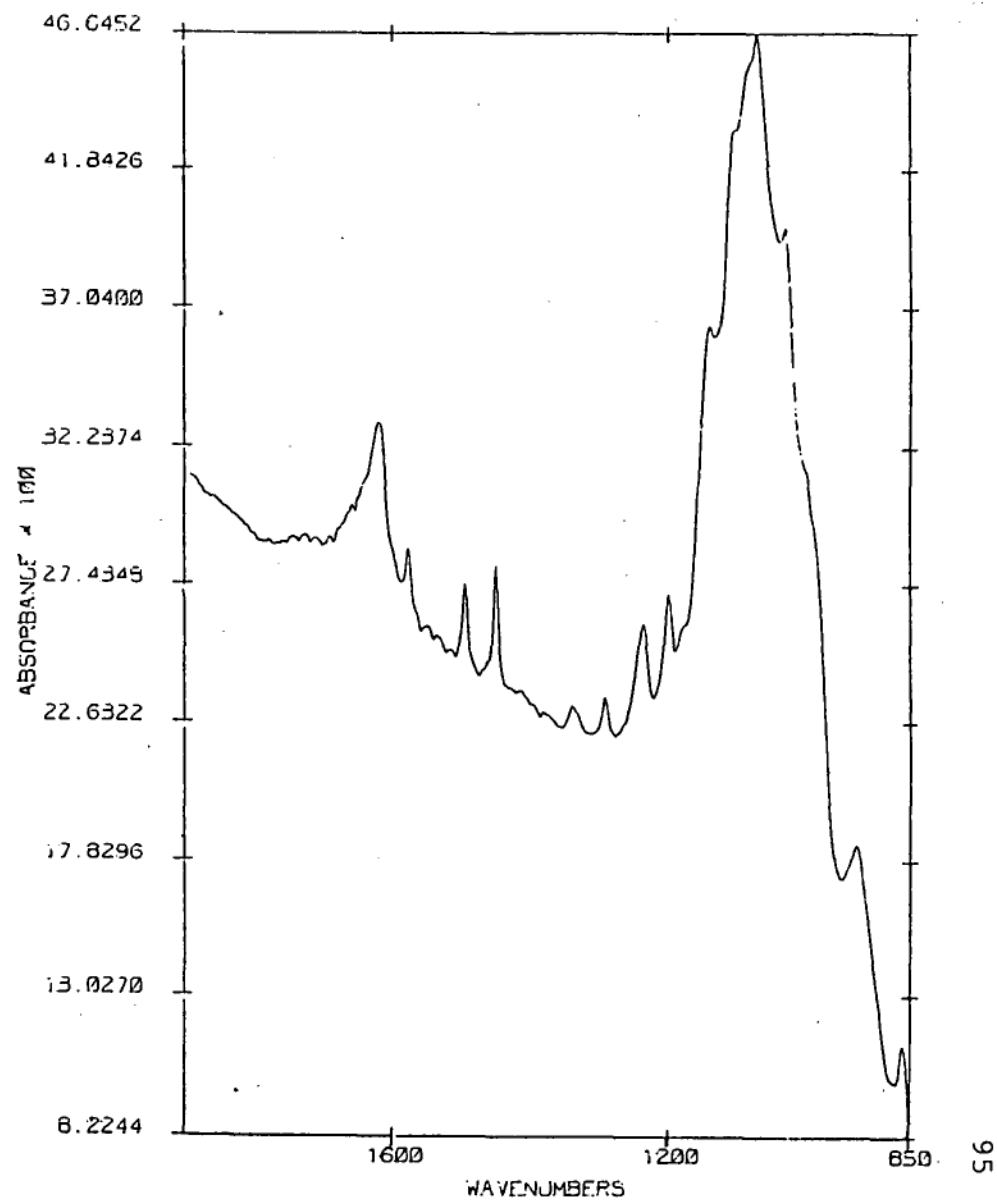


Fig.43 FTIR spectrum of the Fe (III) complex with SPA.

The FTIR spectra of the titanium (III) and titanium (IV) complexes with SPA show similar features to the tin complexes (Figs.44, 45). In the titanium (III) complex the peak due to the  $\text{PO}_3$  vibrations occurs at  $1028\text{ cm}^{-1}$  (Fig.44) while in the titanium (IV) complex it occurs at  $1034\text{ cm}^{-1}$  (Fig.45). Again the bands due to the  $\nu\text{O-H}$  and  $\delta\text{O-H}$  vibrations are absent.

In both the free acid and in the tin, titanium and iron complexes there are bands in the region  $1615\text{--}1440\text{ cm}^{-1}$  due to the styryl group. The position of these bands is consistent with the conjugation of the carbon-carbon double bond with the benzene ring.

The FTIR spectrum of the iron (III) complex with SPA was also recorded (Fig.43) since the sample of natural cassiterite used in the adsorption experiments is known to contain some iron. In the iron (III) complex the peak due to the phosphonate group occurs at  $1072\text{ cm}^{-1}$ . The bands due to the  $\nu\text{O-H}$  and  $\delta\text{O-H}$  vibrations are absent.

### 9.3 Infrared Spectra of Styrene Phosphonic Acid Adsorbed on Cassiterite

The FTIR spectrum of 50 ppm SPA adsorbed on a thin film of vacuum evaporated cassiterite is shown in Fig.46. This spectrum was obtained approximately an hour and a quarter after first contact of the tin oxide surface with the SPA solution at pH 4.5. A prominent band occurs at approximately  $1000\text{ cm}^{-1}$ . This band has similar

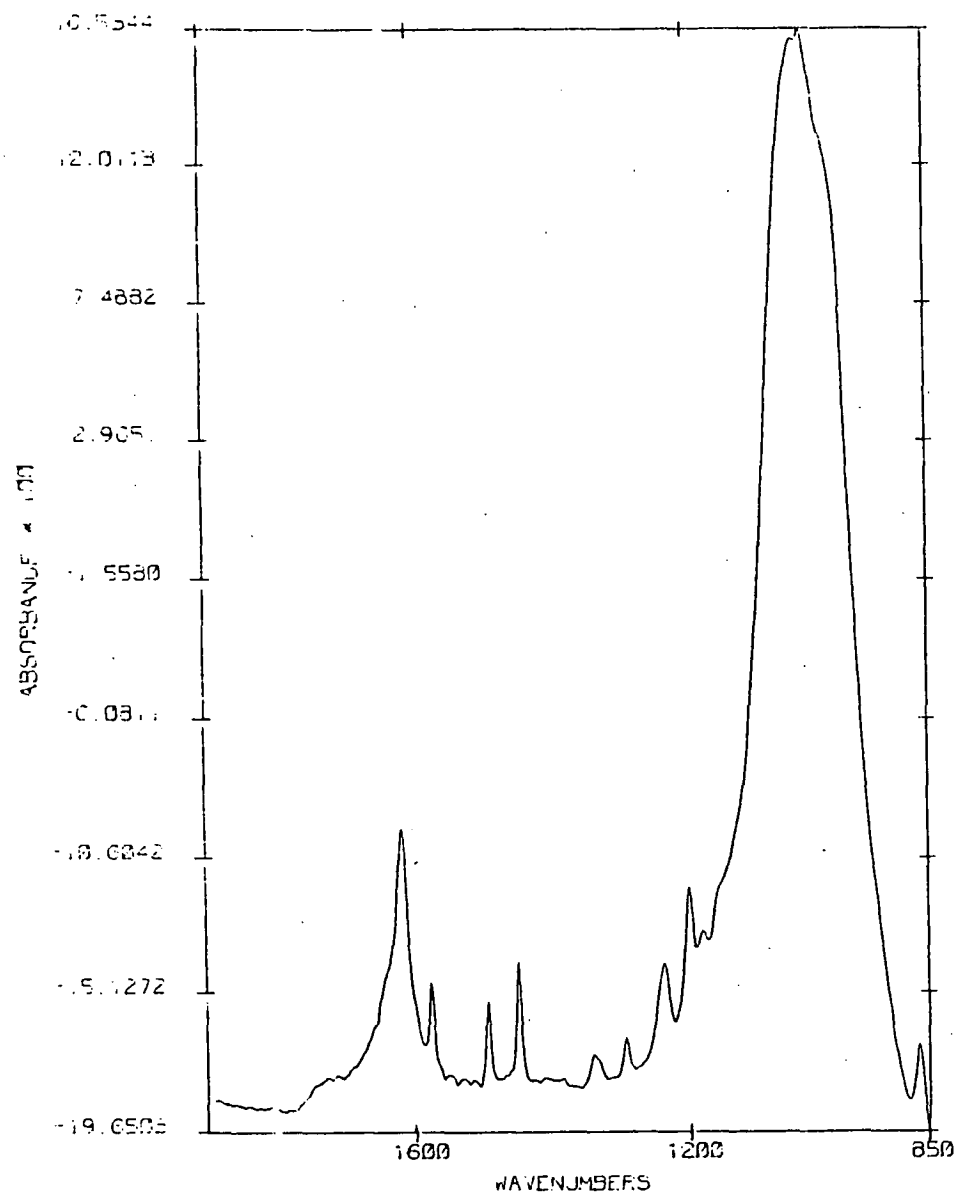


Fig.44 FTIR spectrum of the titanium (III) complex with SPA.

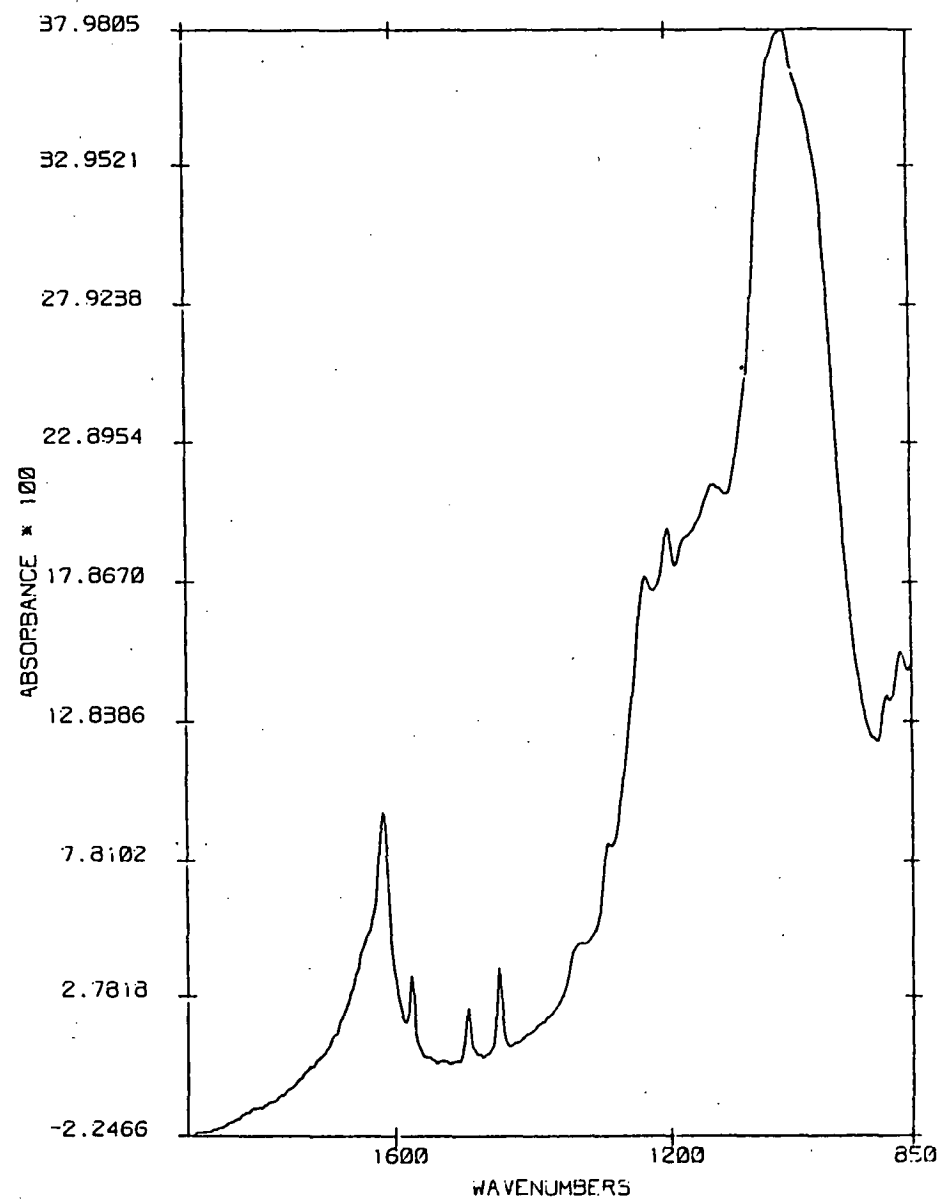


Fig.45 FTIR spectrum of the titanium (IV) complex with SPA.

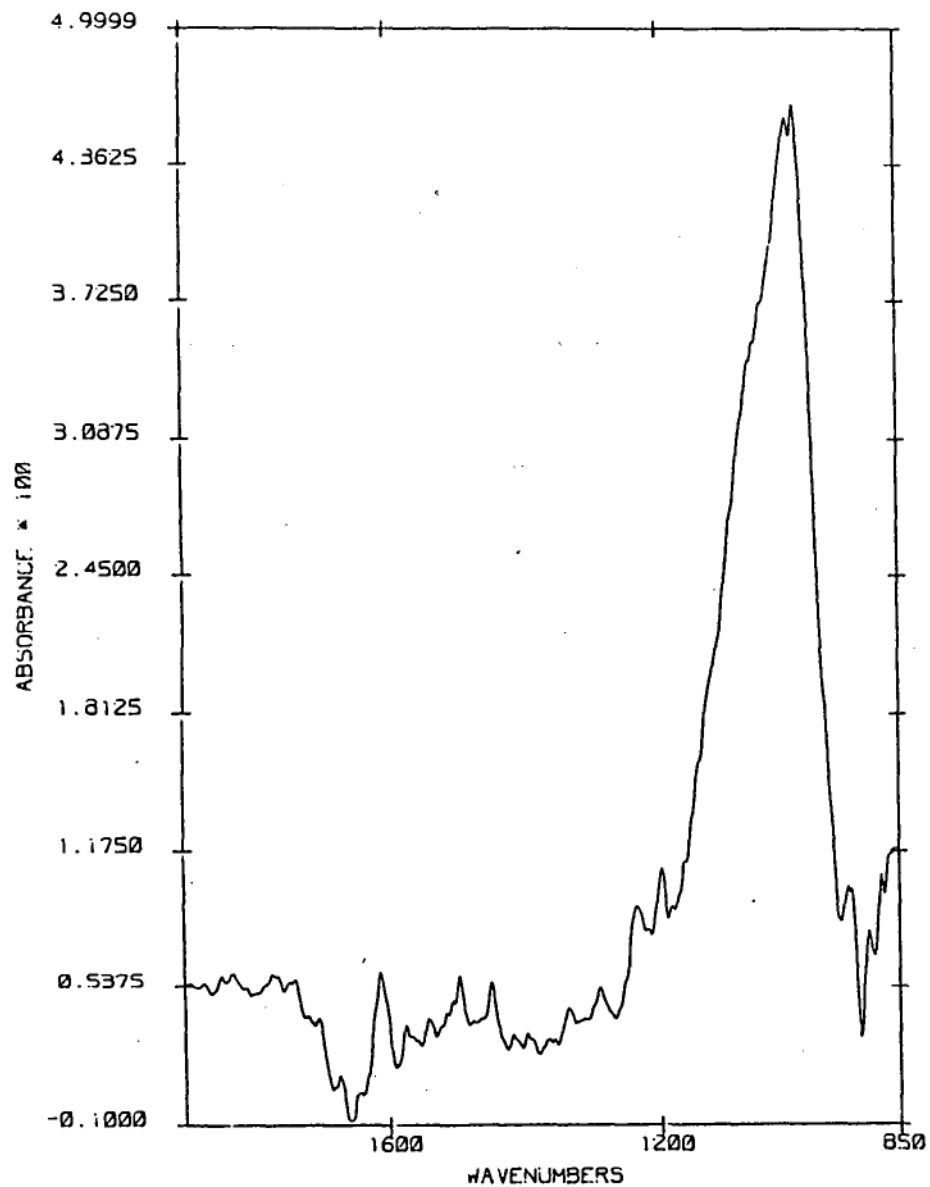


Fig.46 FTIR spectrum of 50 ppm SPA adsorbed on cassiterite at pH 4.5.

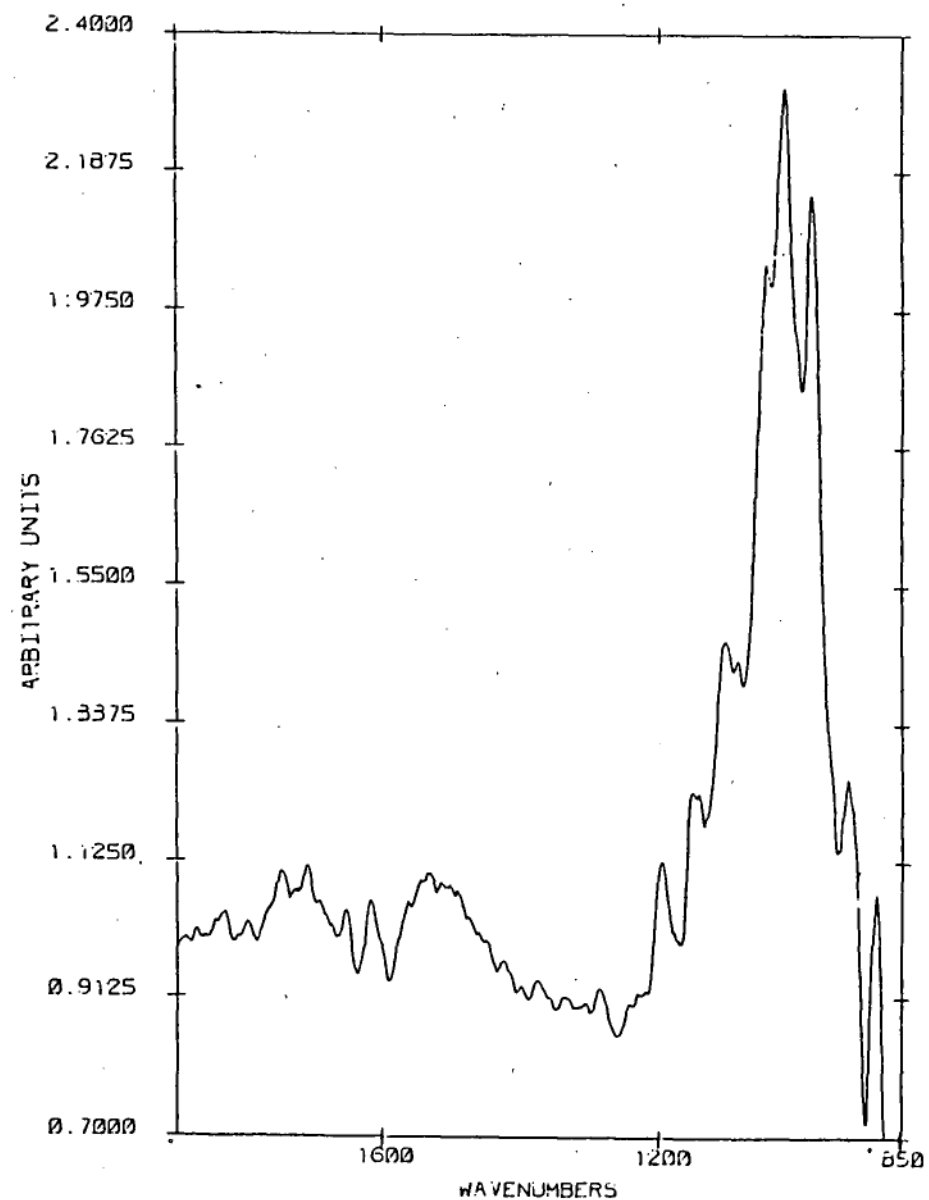


Fig.47 FTIR spectrum of 300 ppm SPA adsorbed on tin (IV) oxide at pH 4.5.

characteristics to the bands due to the phosphonate group in the tin complexes with SPA although it occurs at lower wavenumbers. The presence of a single peak similar to that in the tin complexes suggests that the collector adsorbs by forming a surface phosphonate complex with the tin sites of the tin (IV) oxide. This is also supported by the loss of the  $\delta$  O-H band although the presence or absence of the  $\nu$  O-H band could not be ascertained due to the obscuring of this part of the spectrum by the  $\nu$  O-H vibrations of uncompensated water.

The FTIR spectrum of 300 ppm SPA adsorbed on a vacuum evaporated thin film of pure tin (IV) oxide at pH 4.5 is shown in Fig.47. Again the spectrum shows only a single strong peak at approximately  $1022\text{ cm}^{-1}$ . However this peak shows considerably more fine structure than that of SPA adsorbed on cassiterite. The presence of only a single peak similar to those seen in the tin complexes again suggests that the styrene phosphonic acid adsorbs on cassiterite by a chemisorption mechanism. This is supported by the absence of the  $\delta$  O-H band.

It has been suggested that a valency change may occur on the tin oxide surface so that the surface complex is actually a tin (II) phosphonate complex rather than a tin (IV) phosphonate complex (T.W. Healy, *pers.comm.*). However the spectrum of the surface complex shows greater similarity to that of the tin (IV) phosphonate complex than to that of the tin (II) phosphonate complex suggesting a tin (IV) species is present at the surface.

#### 9.4 Effect of Iron on Adsorption of Styrene Phosphonic Acid on Cassiterite

Some authors have attributed the flotation properties of cassiterite to the presence of iron in the cassiterite crystal lattice or adsorbed on the cassiterite surface (Goold, 1973). It is also thought that iron in solution may catalyse the adsorption of SPA on the cassiterite surface (T.W.Healy, *pers.comm.*).

It is unlikely that the SPA is adsorbing on iron sites in the natural cassiterite as the phosphonate peak occurs at higher wavenumbers in the iron (III) SPA complex than in the tin (II) or tin (IV) SPA complexes. The absence of iron in the pure tin (IV) oxide film shows unequivocally that the presence of iron in the cassiterite lattice or adsorbed on the mineral surface is not necessary for adsorption of SPA.

Attempts were made to study the effect of iron on the adsorption of SPA on the pure tin (IV) oxide film by introducing 50 ppm  $\text{Fe}^{3+}$  into the collector solution and by immersing the thin film of tin (IV) oxide in a 100 ppm solution of iron (III) chloride in two separate experiments.

In the experiment with the SPA solution contaminated with  $\text{Fe}^{3+}$  it was found that the iron was removed from solution by the precipitation of the iron (III) SPA complex before the solution reached the tin oxide surface, hence no noticable effect on adsorption could be observed.

However this is almost certainly what would occur in industrial practice. Dissolved metal ions in the flotation pulp would remove the collector from solution by precipitation of metal-SPA complexes with the effect of increasing collector consumption.

In the experiment in which an attempt was made to produce a surface layer of adsorbed iron on the tin oxide surface the tin oxide coating was removed from the germanium ATR element and the germanium surface etched by immersion in a 100 ppm solution of iron (III) chloride. Hence no results could be obtained from this experiment.

#### 9.5 Effect of pH on Adsorption of Styrene Phosphonic Acid on Cassiterite

The effect of pH on the adsorption of SPA on thin tin (IV) oxide films was determined quantitatively by measuring the area under the phosphonate peak at different pH values. The SPA was initially adsorbed onto the tin oxide surface at a pH value of ~2 and the pH increased by adding small amounts of concentrated sodium hydroxide solution. The effect of pH on the intensity of the phosphonate peak for 300 ppm SPA adsorbed on a thin tin oxide film is shown in Fig.48. This shows that maximum adsorption of SPA occurs at approximately pH 5.5. This is somewhat higher than the pH of 4.5 used in industrial practice. It is also considerably higher than the pH of approximately 2 found for the maximum adsorption of

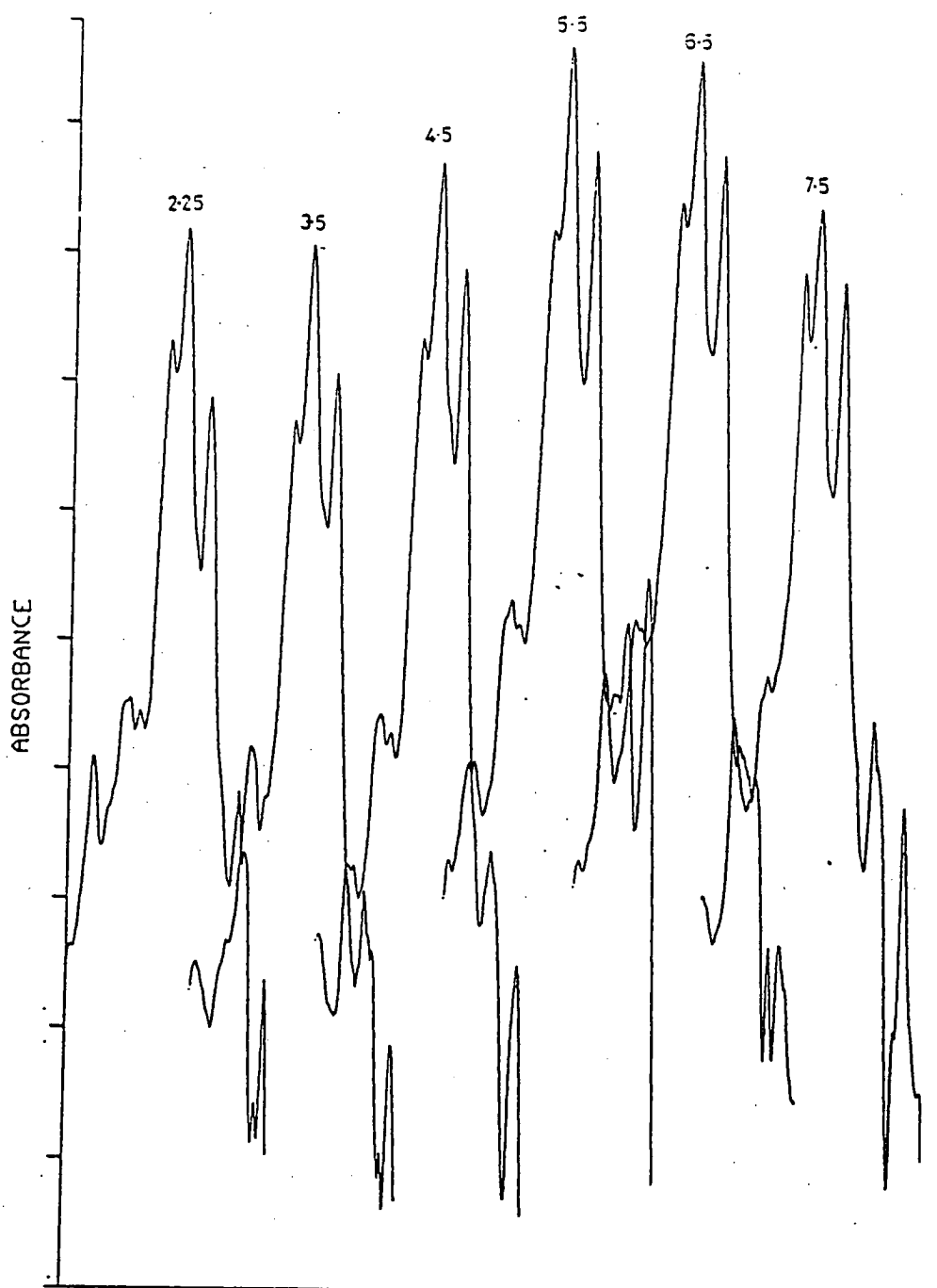


Fig.48 Change in the intensity of the phosphonate peak with pH for 300 ppm SPA adsorbed on tin oxide.

n-heptyl phosphonic acid on cassiterite by Wottgen (1975). This discrepancy may be due to the difference in techniques used. Wottgen (*op. cit.*) used a radiotracer method with  $^{32}\text{P}$  labelled phosphonic acids. This method would be incapable of distinguishing between chemisorbed phosphonic acid and phosphonic acid physically adhering to the surface.

#### 9.6 Kinetics of Adsorption of Styrene Phosphonic Acid on Cassiterite

The kinetics of the adsorption of SPA on cassiterite was studied by following the change in intensity of the phosphonate peak of the chemisorbed SPA with time. The change in intensity of the phosphonate peak with time for 300 ppm SPA adsorbed on a thin tin oxide film is shown in Fig.49. Information on the early stages of the adsorption process is unavailable or unreliable due to the poor quality of the spectra as there is so little SPA adsorbed on the surface initially. However it can be seen that the adsorption density has increased considerably after one hour (this is the time normally used for conditioning in industrial practice). Overnight kinetic runs show that an adsorption plateau has not been reached even after 24 hours. This is consistent with the findings of Farrow *et al.* (1986).

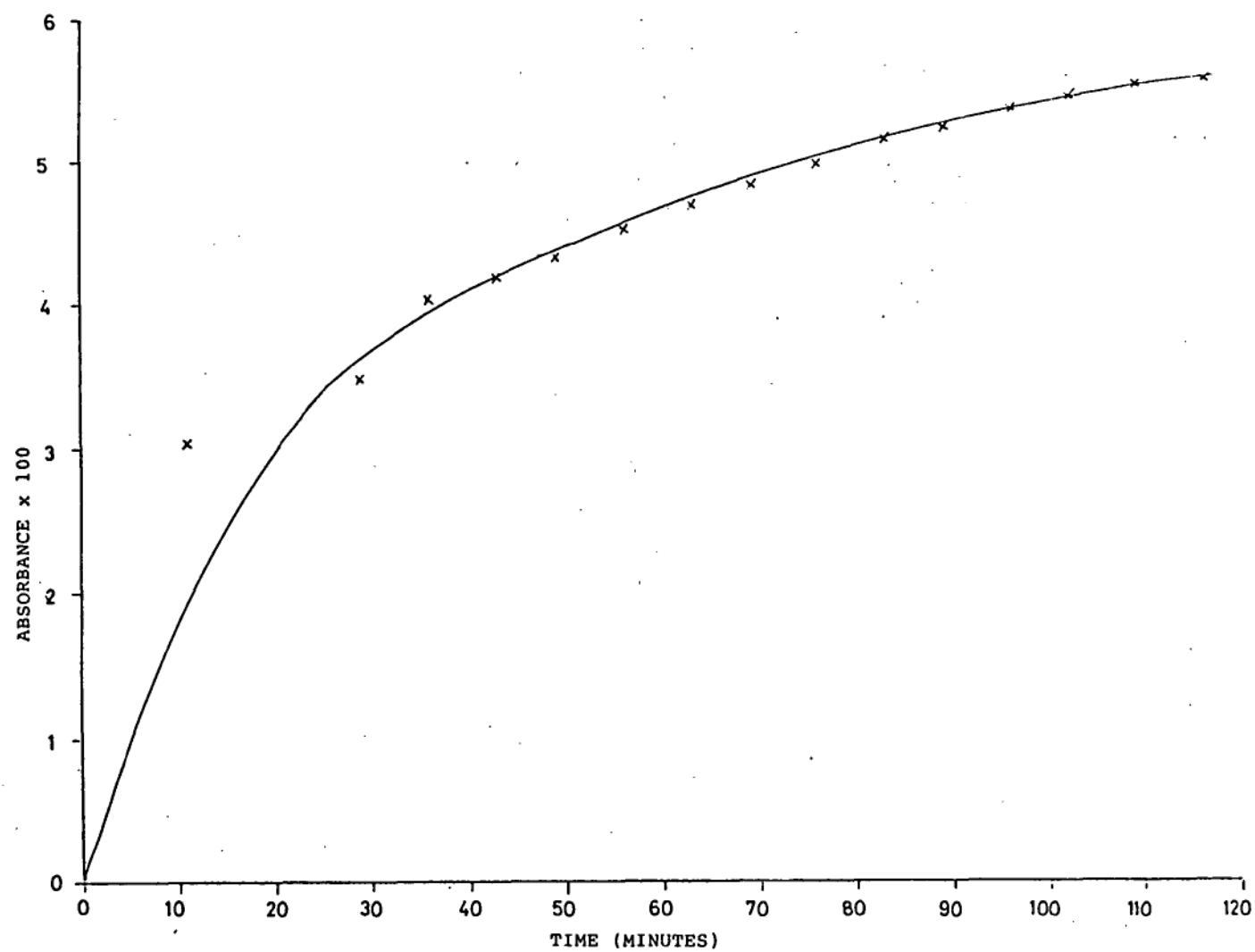


Fig. 49 Change in intensity of the phosphonate peak with time  
for 300 ppm SPA adsorbed on tin (IV) oxide at pH 4.5.

### 9.7 Infrared Spectra of Styrene Phosphonic Acid Adsorbed on Rutile

The infrared spectrum of SPA on a vacuum evaporated film of titanium (IV) oxide is shown in Fig.50. There is a single prominent band at  $1022\text{ cm}^{-1}$  similar to that in the titanium (III) and titanium (IV) complexes with SPA. The presence of a single band like that in the titanium complexes suggests that SPA adsorbs on rutile by a chemisorption mechanism similar to that proposed for the adsorption of SPA on cassiterite. This is further supported by the absence of the  $\delta\text{O-H}$  band in the spectrum of the adsorbate.

### 9.8 Discussion

The similarity between the spectra of SPA adsorbed on thin films of cassiterite, tin (IV) oxide and titanium (IV) oxide and the spectra of the tin and titanium complexes with SPA suggests that SPA adsorbs on cassiterite and rutile by a chemisorption mechanism in which a surface phosphonate complex is formed. This mechanism has been proposed previously by Dietze (1975). However his proposal was based on poor spectra recorded by an *ex situ* method. This study has largely confirmed Dietze's adsorption theory. However the mode of attachment of the phosphonate group is still uncertain.

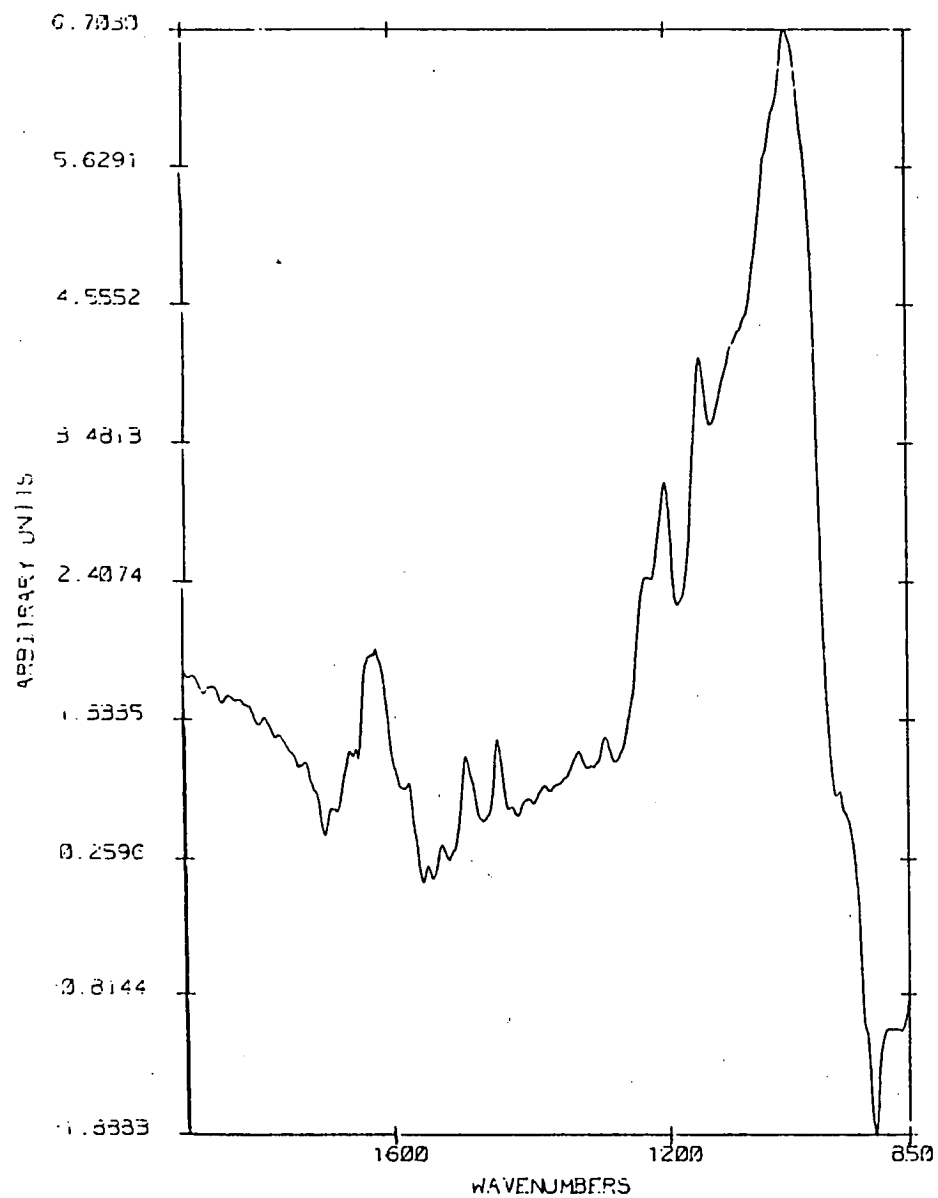
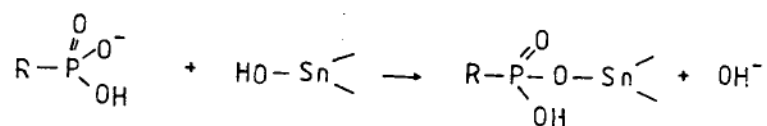
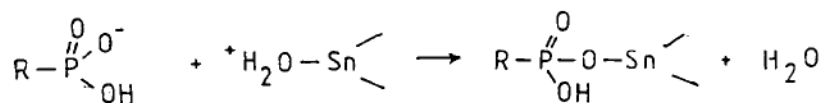


Fig.50 FTIR spectrum of SPA adsorbed  
on titanium (IV) oxide at pH  
4.5

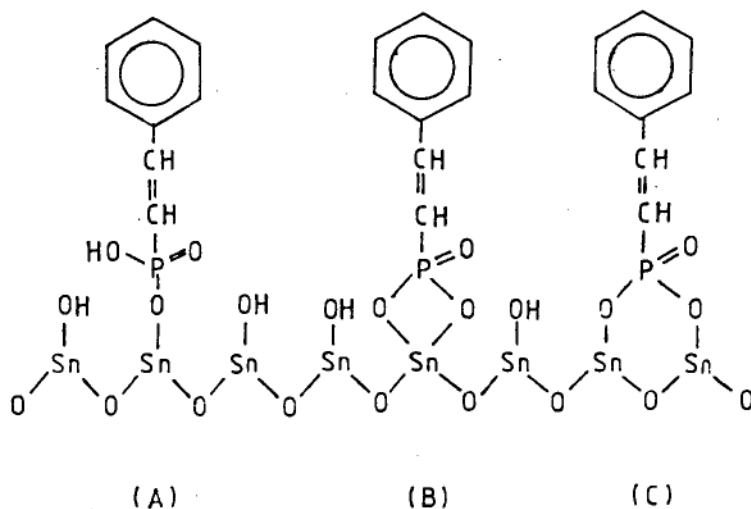
Farrow et al (1986) proposed that phosphonic acids adsorb on cassiterite by an exchange chemisorption reaction viz.



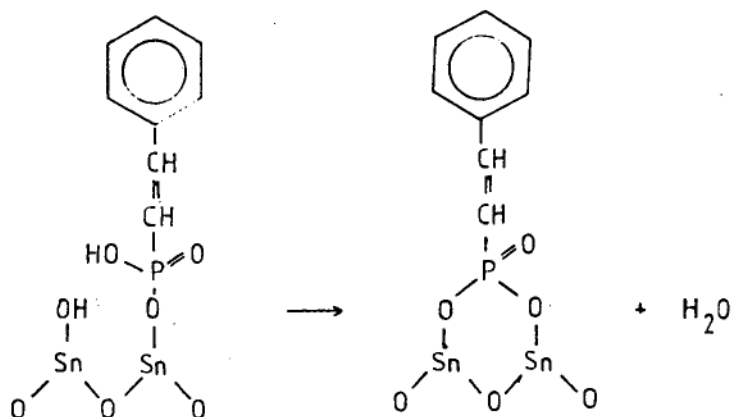
or



These reactions result in a monodentate surface complex (A).



This may then undergo ring closure to produce the binuclear complex (C) with the release of water.



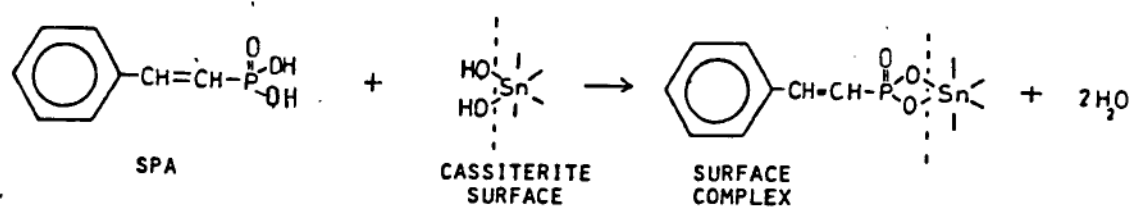
Information about the type of complexation of SPA to the cassiterite surface can be deduced from the fine structure of the phosphonate peak of the adsorbate. Atkinson et al (1974) and Parfitt et al (1976) carried out infrared spectral studies of phosphate adsorption on goethite. They compared the spectra of monodentate (1), bidentate (2), and binuclear (bridging) (3) phosphate complexes in order to deduce the structure of the surface complex.

band assignment	<div style="display: flex; justify-content: space-around; align-items: center;"> <div style="text-align: center;"> <math display="block">\begin{array}{c} \text{R} \\   \\ \text{O} \\   \\ \text{HO}-\text{P}=\text{O} \\   \\ \text{O} \\   \\ \text{M} \end{array}</math> </div> <div style="text-align: center;"> <math display="block">\begin{array}{c} \text{R} \\   \\ \text{O} \\   \\ \text{P}=\text{O} \\ / \quad \backslash \\ \text{O} \quad \text{O} \\ \backslash \quad / \\ \text{M} \end{array}</math> </div> <div style="text-align: center;"> <math display="block">\begin{array}{c} \text{R} \\   \\ \text{O} \\   \\ \text{P}=\text{O} \\ / \quad \backslash \\ \text{O} \quad \text{O} \\   \quad   \\ \text{M} \quad \text{M} \end{array}</math> </div> </div>		
	(1)	(2)	(3)
$A_1^*$	934-975 $\text{cm}^{-1}$	915 $\text{cm}^{-1}$	1110 $\text{cm}^{-1}$
E $B_1$	1035-1095 $\text{cm}^{-1}$	1085 $\text{cm}^{-1}$	1220 $\text{cm}^{-1}$
$B_2$		1050 $\text{cm}^{-1}$	1050 $\text{cm}^{-1}$
$A_1'$	755-980 $\text{cm}^{-1}$	900 $\text{cm}^{-1}$	815 $\text{cm}^{-1}$

\* infrared inactive

In the spectrum of SPA adsorbed on cassiterite there are bands at 1045, 1018 and 979  $\text{cm}^{-1}$ . The absence of bands due to P-OH vibrations excludes the possibility that the complex is monodentate. The band positions at 1043, 1018, and 979  $\text{cm}^{-1}$  correspond much better with those reported for bidentate complexes and the strong band at ~1200  $\text{cm}^{-1}$  characteristic of binuclear complexes is

absent. The band positions are somewhat displaced from those observed in the complexes but this may be due to hydrogen bonding with physically adsorbed water molecules. The present spectroscopic study would suggest that the SPA is present as a bidentate surface complex (B) and adsorption probably occurs by the following mechanism.



## 10. Adsorption of Sulphosuccinamate Flotation Collectors on Cassiterite

### 10.1 Introduction

Apart from SPA the most commonly used cassiterite collectors are the sulphosuccinamates, Cyanamid AP845E and Allied Colloids CA 540. CA540 is also used in the flotation of tantalite ores (Burt et al. 1982). The active constituent of these collectors is the tetrasodium salt of N-octadecyl (1,2 - dicarboxyethyl) sulphosuccinamic acid.

Sulphosuccinamate surfactants were first synthesised by the American Cyanamid Company and patented in 1947. They were found to be highly surface active with Miller and Dessert (1949, quoted in Senior and Poling, 1985) reporting a surface tension of 44 dynes per centimetre for a  $1 \text{ gL}^{-1}$  solution of sulphosuccinamate. The sulphosuccinamates have strong foaming characteristics, particularly at low pH, and are used in flotation without the addition of frothers.

Although less selective than arsonic and phosphonic acids sulphosuccinamates have a major advantage over these collectors as they are comparatively inexpensive. This is mainly due to their widespread use in applications other than that of cassiterite flotation. They are also less toxic than arsonic acids and have the advantage over phosphonic acids of being biodegradable.

Sulphosuccinamates contain four dissociable groups -

to pK values of 2.3 and 5.8 respectively (Senior, 1985 quoted in Senior and Poling, 1985). The pK of 2.3 corresponds to the dissociation of the highly acidic sulphonate group while the pK of 5.8 is typical of that for carboxylic acid groups. The three carboxylic acid groups probably dissociate over a very narrow pH range so that only one inflection point is observed in the potentiometric titration.

#### 10.2 Infrared Spectra of Sulphosuccinamates and their Tin Complexes

The FTIR spectrum of AP845E is shown in Fig.51. Strong bands can be seen at  $1597\text{ cm}^{-1}$  and  $1387\text{ cm}^{-1}$  due to  $\nu_{\text{as}}\text{C-O}$  and  $\nu_{\text{s}}\text{C-O}$  vibrations of the resonance stabilised carboxylate group. Strong bands are also present at  $1210\text{ cm}^{-1}$  and  $1040\text{ cm}^{-1}$  due to the  $\nu_{\text{as}}\text{S-O}$  and  $\nu_{\text{s}}\text{S-O}$  vibrations of the sulphonate group. Strong bands due to  $\nu\text{ C-H}$  vibrations of the long alkyl chain are also present in the regions  $2925 - 2915\text{ cm}^{-1}$  and  $2855 - 2850\text{ cm}^{-1}$ .

The FTIR spectrum of the N octadecyl sulphosuccinamic acid is shown in Fig.52. Bands due to the  $\nu\text{C=O}$ ,  $\nu\text{C-O}/\rho\text{ O-H}$  vibrations of the carboxylic acid group can be seen at  $1732\text{ cm}^{-1}$  and  $1470, 1443, 1402$  and  $1377\text{ cm}^{-1}$ . Bands due to the  $\nu_{\text{as}}\text{S-O}$  and  $\nu_{\text{s}}\text{S-O}$  vibrations of the sulphonic acid group can be seen at  $1213\text{ cm}^{-1}$  and  $1038\text{ cm}^{-1}$ . The sulphonic acid bands are displaced from their usual positions ( $\nu_{\text{as}}\text{S-O}$  at  $\sim 1350\text{ cm}^{-1}$  and  $\nu_{\text{s}}\text{S-O}$  at  $\sim 1160\text{ cm}^{-1}$ ) due to the

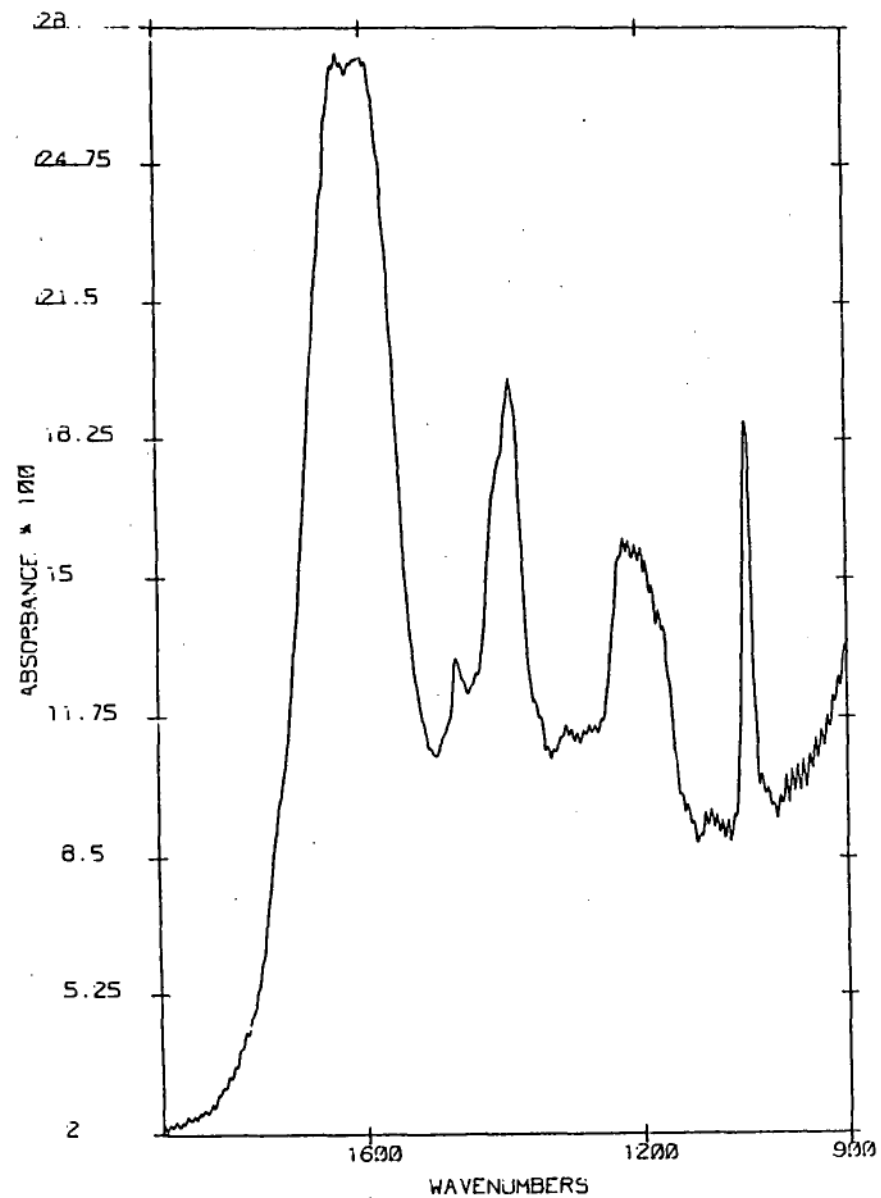


Fig.51 FTIR spectrum of Cyanamid AP845E.

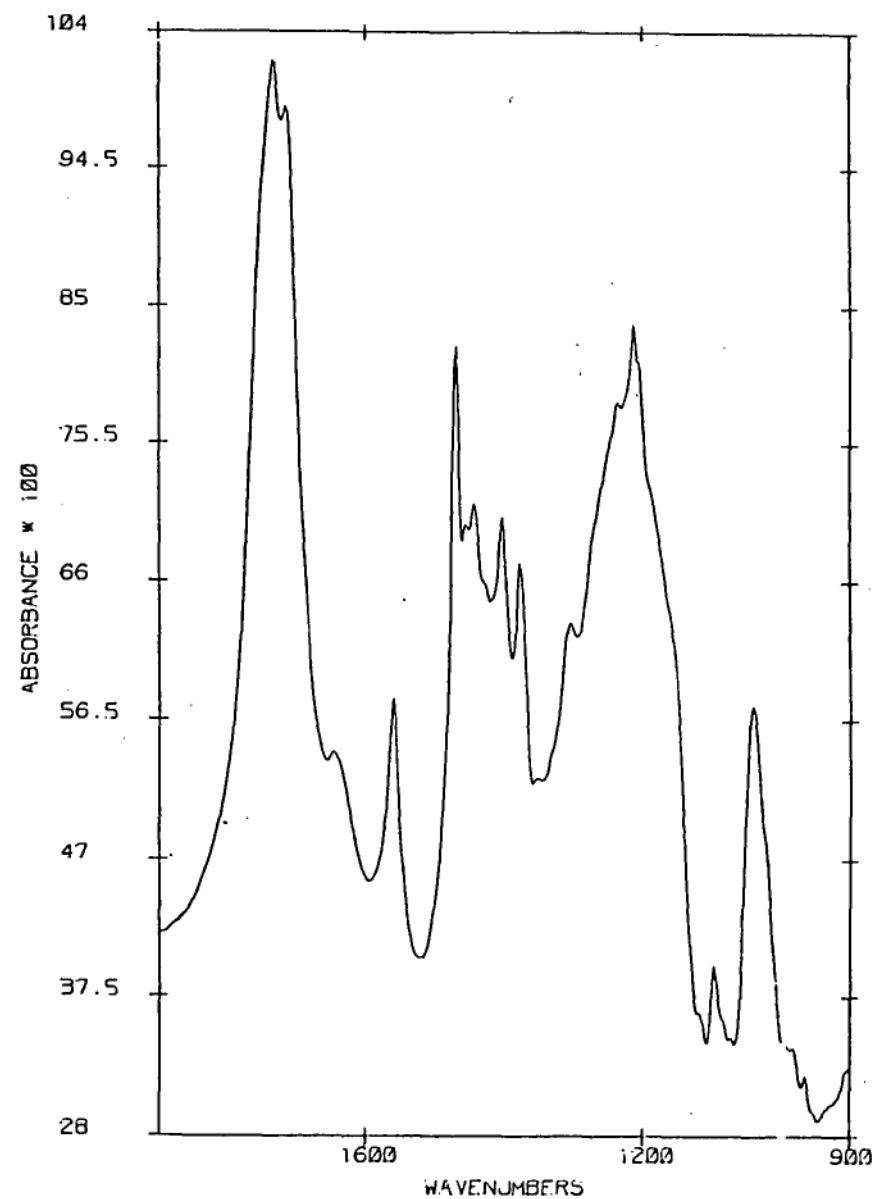


Fig.52 FTIR spectrum of N octadecyl sulphosuccinamic acid.

present at  $1603\text{cm}^{-1}$  and  $1387\text{cm}^{-1}$  due to the  $\nu_{\text{as}}\text{C-O}$  and  $\nu_{\text{s}}\text{C-O}$  vibrations of the carboxylate group and at  $1214\text{cm}^{-1}$  and  $1036\text{cm}^{-1}$  due to the  $\nu_{\text{as}}\text{S-O}$  and  $\nu_{\text{s}}\text{S-O}$  vibrations of the sulphonate group.

### 10.3 Infrared Spectra of Sulphosuccinamates Adsorbed on Cassiterite

The FTIR spectrum of 300 ppm N-octadecyl sulphosuccinamic acid adsorbed on a thin film of tin (IV) oxide is shown in Fig.54.

Bands can be seen corresponding to the  $\nu_{\text{s}}\text{C-O}$  and  $\nu_{\text{s}}\text{C=O}$  vibrations of surface carboxylate groups. A band can also be seen at  $\sim 1730\text{cm}^{-1}$  due to the  $\nu\text{ C=O}$  vibration of free carboxylic acid groups. Bands due to  $\nu_{\text{as}}\text{S-O}$  and  $\nu_{\text{s}}\text{S-O}$  vibrations are also present but because of the similarity of the band positions in the hydrated acid and the tin (II) complex it is not possible to assign these bands to free sulphonic acid groups or surface sulphonate groups. However there is considerable difference in the fine structure of the S-O stretching vibrations of the adsorbed sulphosuccinamate from that of the tin (II) complex and the free acid. Especially prominent is the broadening of the  $\nu_{\text{s}}\text{S-O}$  band.

Since the sulphosuccinamic acid molecule contains three carboxylic acid groups it is possible that some of the carboxylic acid groups are chemisorbing at the tin oxide surface while some remain protonated. Alternatively

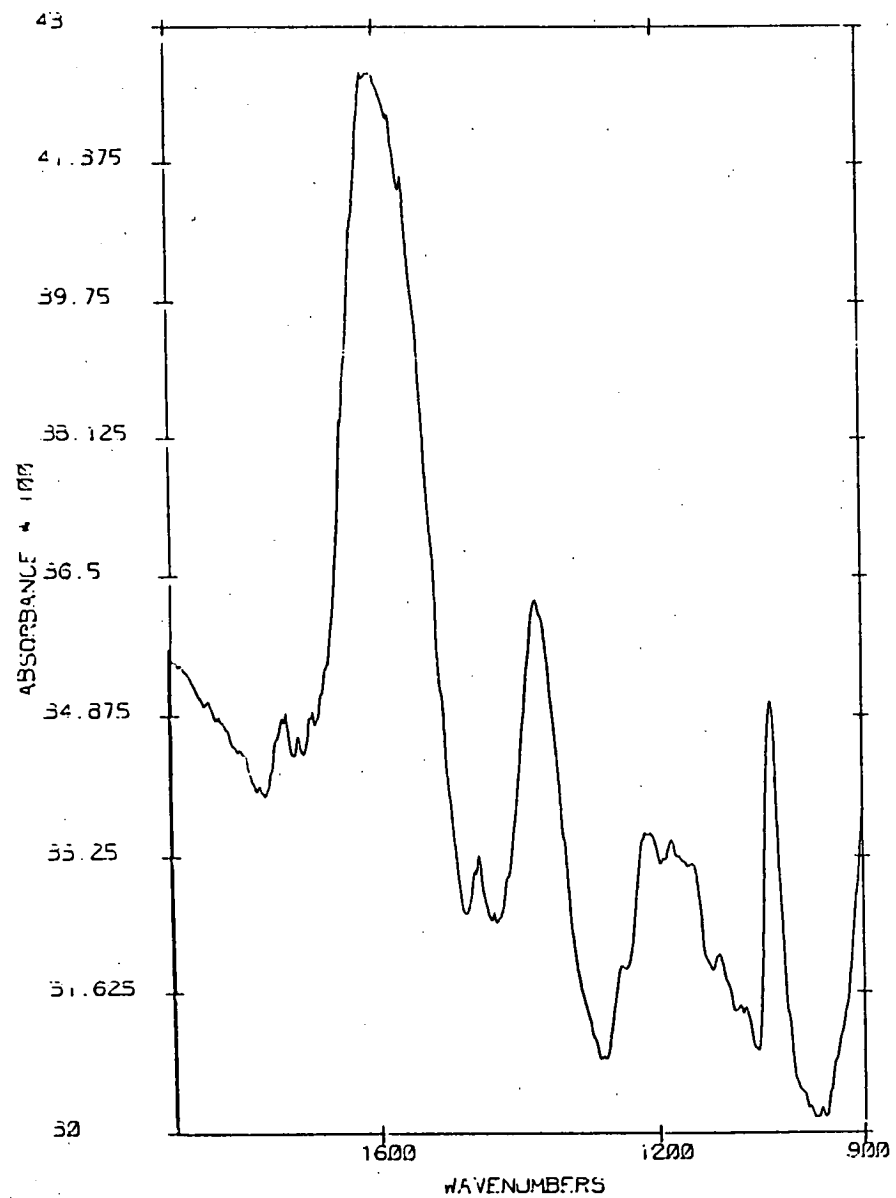


Fig. 53 FTIR spectrum of the tin (II) sulphosuccinamate complex.

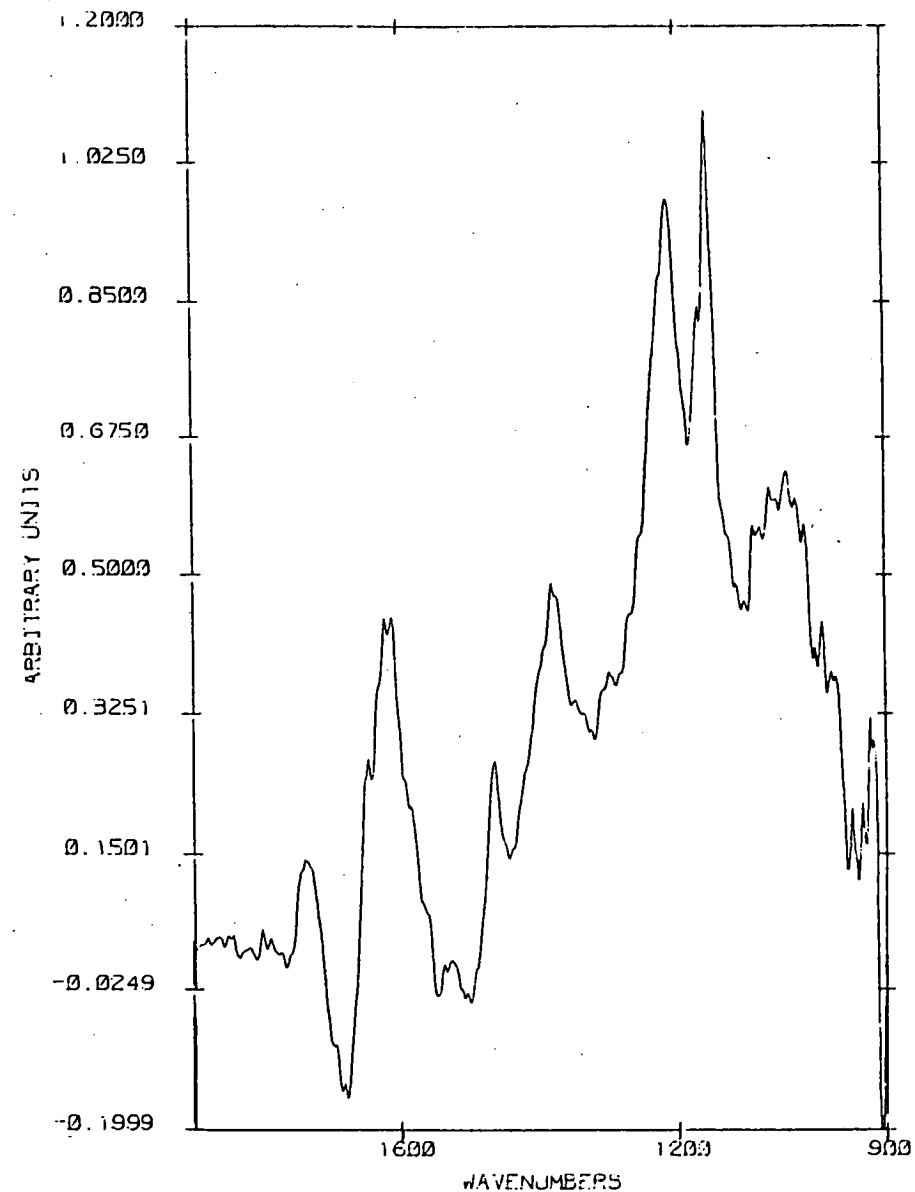


Fig. 54 FTIR spectrum of 300 ppm sulphosuccinamate adsorbed on tin (IV) oxide at pH 4.5.

there may be some physisorbed sulphosuccinamic acid molecules, with the carboxylic acid groups all protonated, adsorbed at the tin oxide surface. It is not possible to determine if the sulphonic acid group is chemisorbing at the tin oxide surface from the spectrum.

#### 10.4 Discussion

Although it was not possible to determine if the sulphonic acid chemisorbed on the tin oxide surface at least some of the carboxylic acid groups attach to the surface by chemisorption. Berger, Hoberg and Schneider (1980) determined that the carboxylic acid groups of the sulphosuccinamate chemisorbed on the cassiterite surface although some free carboxylic acid groups were present at the surface. These investigators felt that the sulphonate group also chemisorbed on the cassiterite surface. However the shifts they observed in the infrared spectra of the S-O stretching vibrations of the sulphosuccinamate adsorbed on cassiterite could not be found in the tin (IV) sulphosuccinamate complex. Measurements of the adsorption behaviour of sodium dodecyl sulphonate on cassiterite carried out by Yap (1975, quoted in Ball, Cox and Yap, 1979) could not be correlated with electrokinetic measurements however these measurements suggest that the adsorption of sulphonates on cassiterite is not solely the result of electrostatic interactions.

## 11. Adsorption of Polycarboxylic Acid Collectors on Cassiterite and Rutile

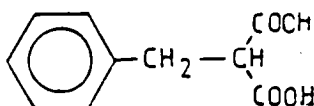
### 11.1 Introduction

The East German workers, Bochnia and Serrano (1976), Baldauf, Singh and Schubert (1980), Singh, Baldauf and Schubert (1980), Baldauf, Shoenherr and Schubert (1985) have proposed the use of alkyl polycarboxylic acids as cassiterite collectors. These have proved successful in laboratory tests but have not been put into industrial use due to their poor selectivity. Recently numerous new flotation collectors for cassiterite have been synthesised by Mr Greg Lane. These collectors are polycarboxylic acids or compounds containing both carboxylic acid and phosphonic acid groups. However instead of using a long chain alkyl group as the hydrophobic group substituted aromatic groups were used based on their effectiveness in p tolyl arsonic acid and styrene phosphonic acid. Although numerous such collectors have been synthesised and tested for their flotation properties only selected collectors have been used in adsorption studies due to their particular structural type, their superior collecting properties and their analogy with collectors which produce good flotation responses.

Absorption measurements were carried out on three collectors which are dicarboxylic acids with the acid group in different positions. These aryl substituted

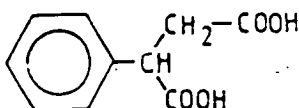
malonic, succinic and glutaric acids were chosen for investigation since Bochnia and Serrano (1976) had carried out adsorption measurements on similar acids which incorporated long alkyl chains as the hydrophobic group. These collectors were designated GL29 (benzylmalonic acid) GL24 (phenylsuccinic acid) and GL 5,6,7 (methyl phenyl glutaric acid). The structures of these collectors are shown below.

GL29



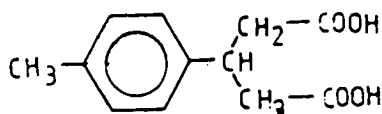
benzylmalonic acid

GL24



phenylsuccinic acid

GL5, 6, 7



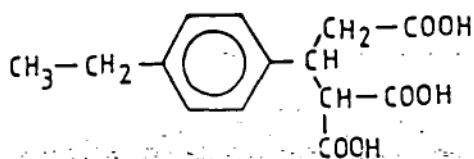
p-methylphenylglutaric acid

GL29, GL24 and GL5,6,7 are all good collectors for

cassiterite flotation.

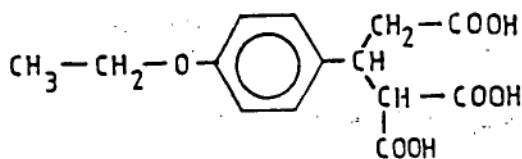
The adsorption behavior of three polycarboxylic acids which are 2-carboxy glutaric acids with the hydrophobic substituent in the 3 position were also investigated as this structural type was found to be a highly effective cassiterite collector. These collectors were designated GL33 [ 2-carboxy-3-(4-ethylphenyl) glutaric acid ] and GL12 [ 2-carboxy-3-(4-ethoxyphenyl) glutaric acid ]. The structure of these collectors is shown below.

GL33



2-carboxy-3-(4-ethylphenyl) glutaric acid

GL12

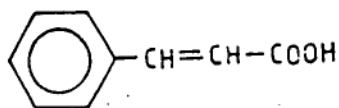


2-carboxy-3-(4-ethoxyphenyl) glutaric acid

The relationship between this class of collectors and those based on glutaric acid can be seen by comparison of these structures with that of GL 5,6,7.

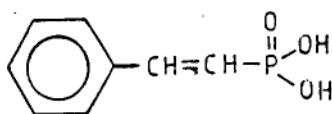
The flotation collector GL 28 (cinnamic acid) was also used in adsorption experiments because of its analogous structure with SPA as can be seen from the structures below.

GL28



cinnamic acid

SPA

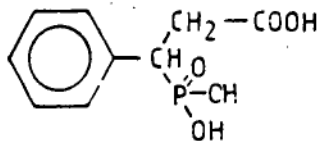


styrene phosphonic acid

Flotation tests, however, showed that cinnamic acid is a very poor collector for cassiterite.

A highly effective cassiterite flotation collector was found in GL40 which contains both a carboxylic acid group and a phosphonic acid group. Its structure is shown below.

GL40

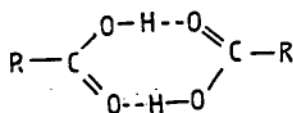


3-(4-methylphenyl)-3-phosphonopropanoic acid

It is analogous to GL24 as can be seen by comparison of their structures. This collector was used in adsorption studies to investigate the effect of using different acid groups in the same collector.

### 11.2 Infrared Spectra of Carboxylic Acids and their Tin Complexes.

The interpretation of the infrared spectra of the polycarboxylic acids is based largely on the work of Bochnia and Serrano, 1976. There are five characteristic bands in the infrared spectra of carboxylic acids. The most prominent bands in the spectra is due to the  $\nu_{C=O}$  vibration of the acid dimer at  $\sim 1716 \text{ cm}^{-1}$ . The strong bands at  $\sim 1420$ ,  $1300$ , and  $1250 \text{ cm}^{-1}$  are due to the  $\nu_{C-O}$  vibrations coupled with  $\delta_{O-H}$  vibrations of the acid dimer viz .



The broad band at  $3000-2500 \text{ cm}^{-1}$  is due to  $\nu_{O-H}$  vibrations. The band at  $920 \text{ cm}^{-1}$  is due to  $\omega_{O-H}$  vibrations.

The FTIR spectra of the dicarboxylic acids GL29, GL24 and GL5,6 and 7 from  $1900 \text{ cm}^{-1}$  to  $900 \text{ cm}^{-1}$  are shown in Figs. 55,58, and 60. The spectra of the tricarboxylic acids GL33 and GL12 are shown in Figs.63 and 67 and the

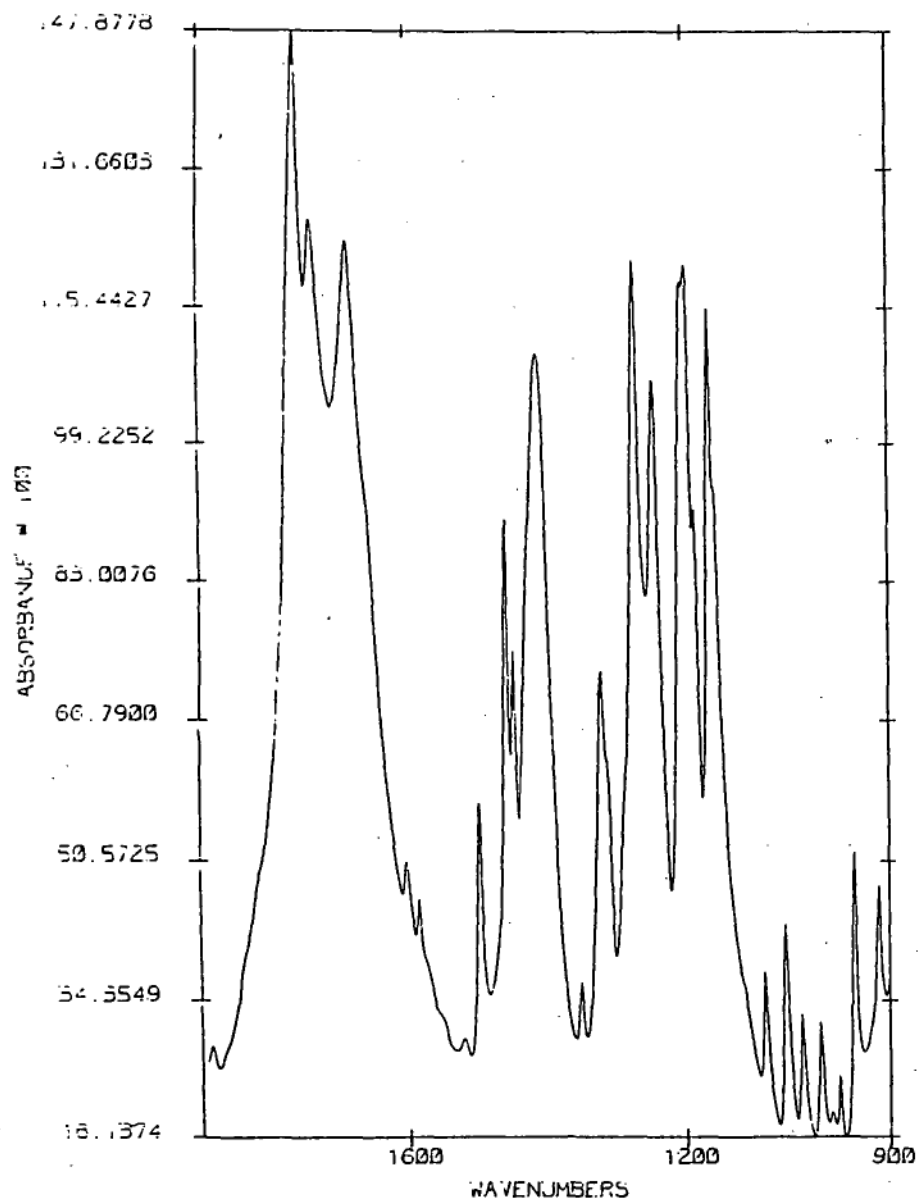


Fig.55 FTIR spectrum of GL29

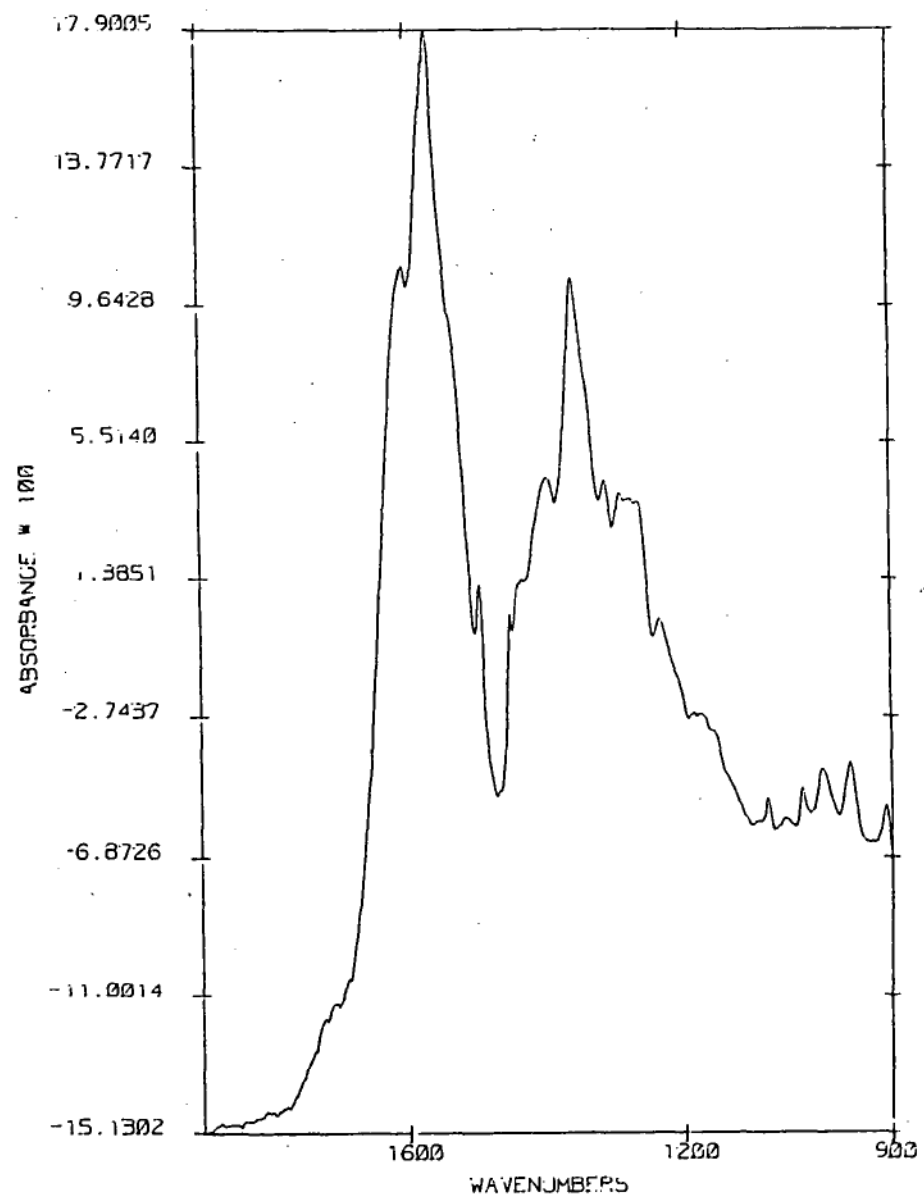


Fig.56 FTIR spectrum of the tin (II) complex with GL29

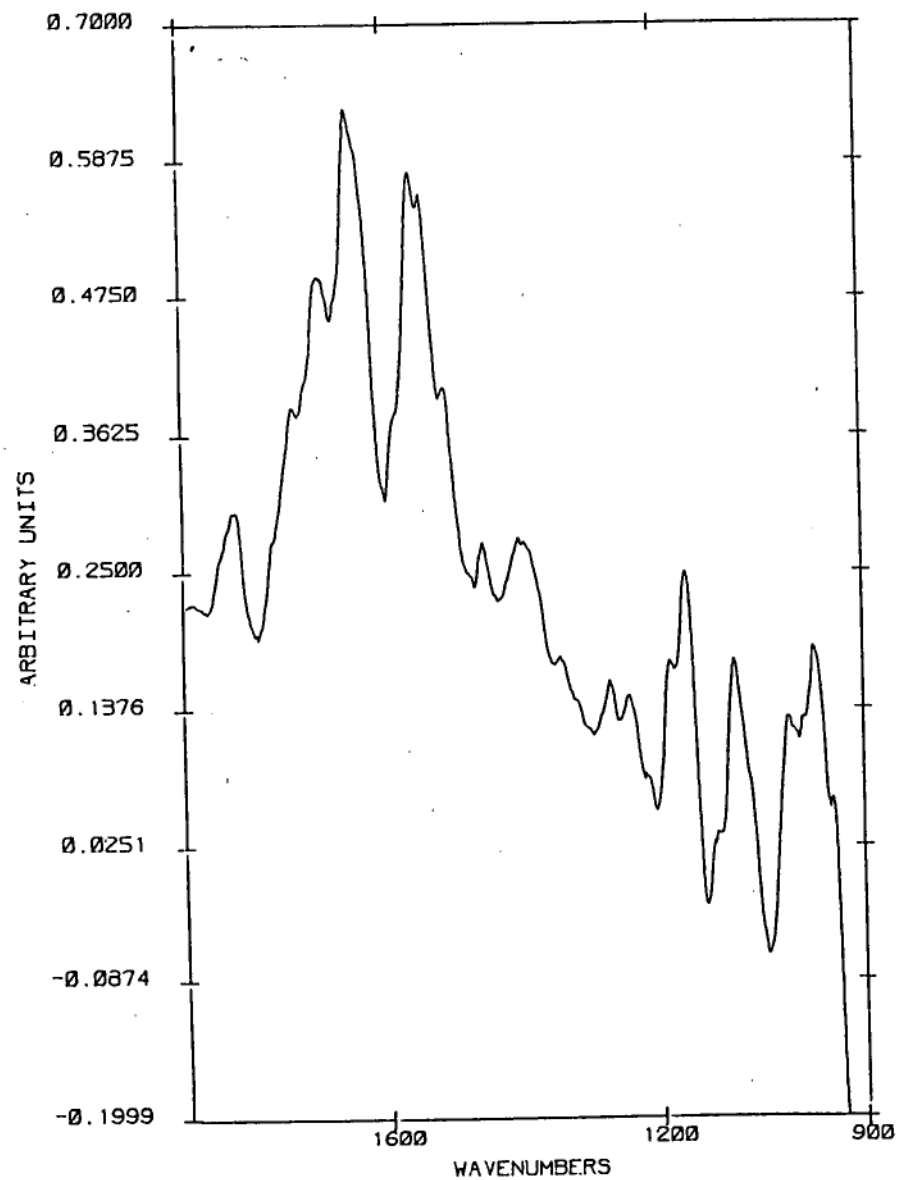


Fig.57 FTIR spectrum of 300 ppm  
GL29 adsorbed on tin (IV) oxide at pH 4.5

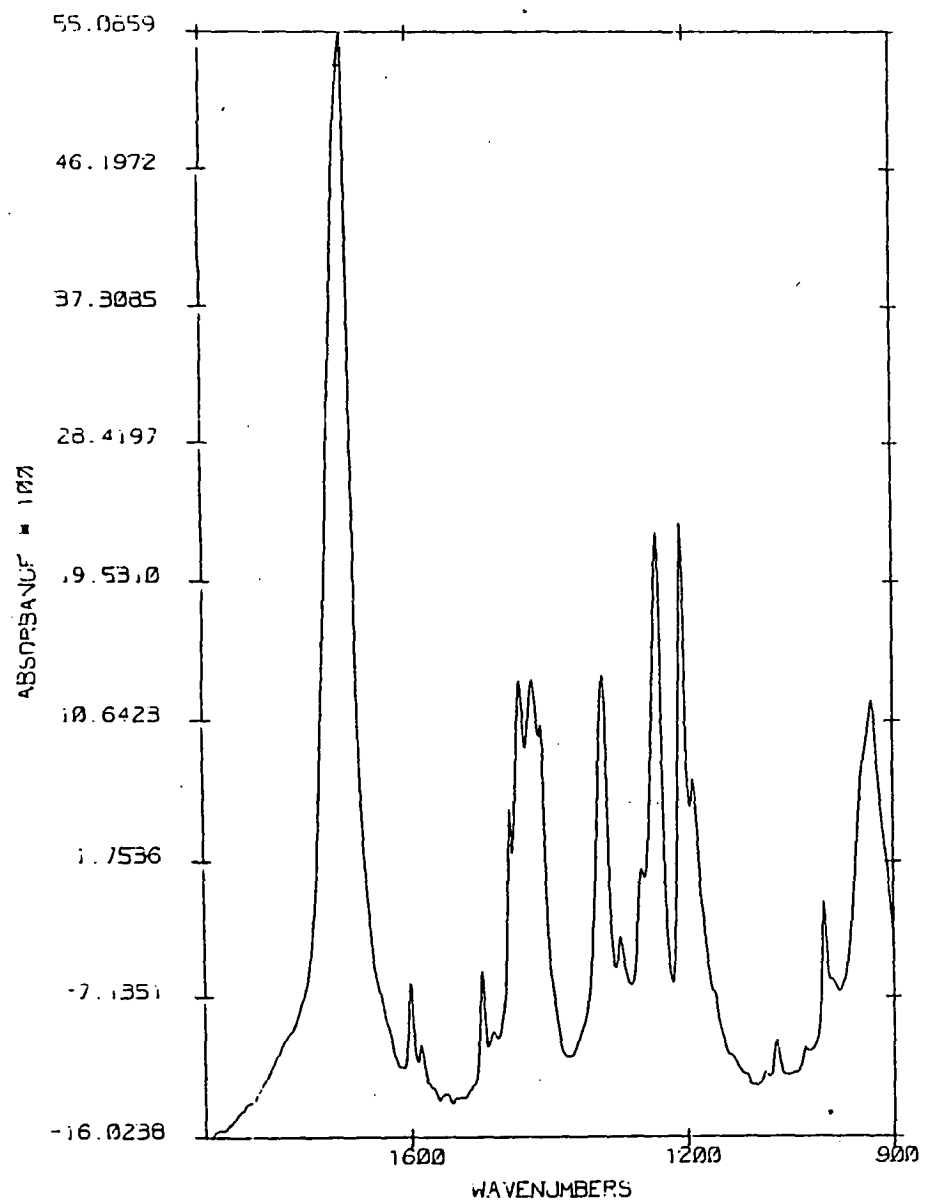


Fig.58 FTIR spectrum of GL24

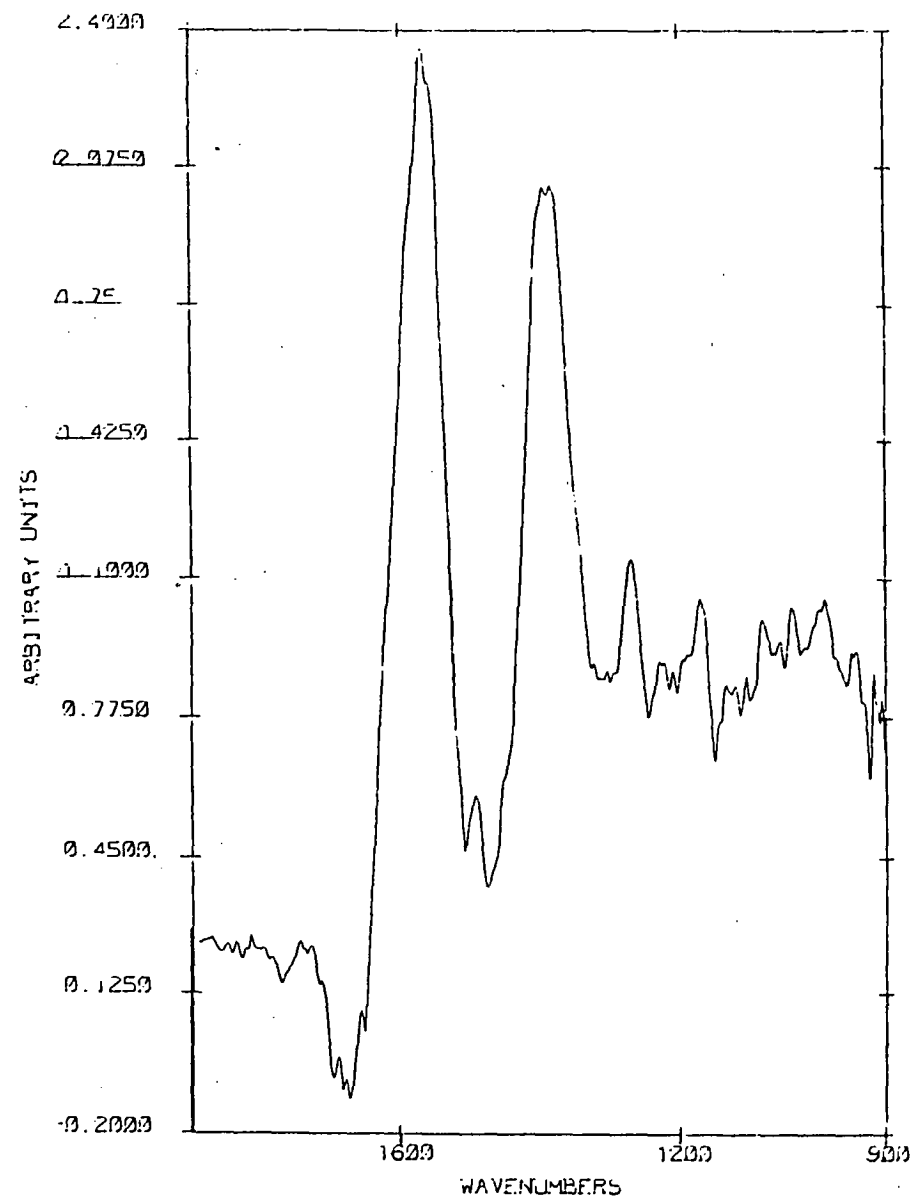


Fig.59 FTIR spectrum of 300ppm GL-24  
adsorbed on tin (IV) oxide at  
pH=4.5

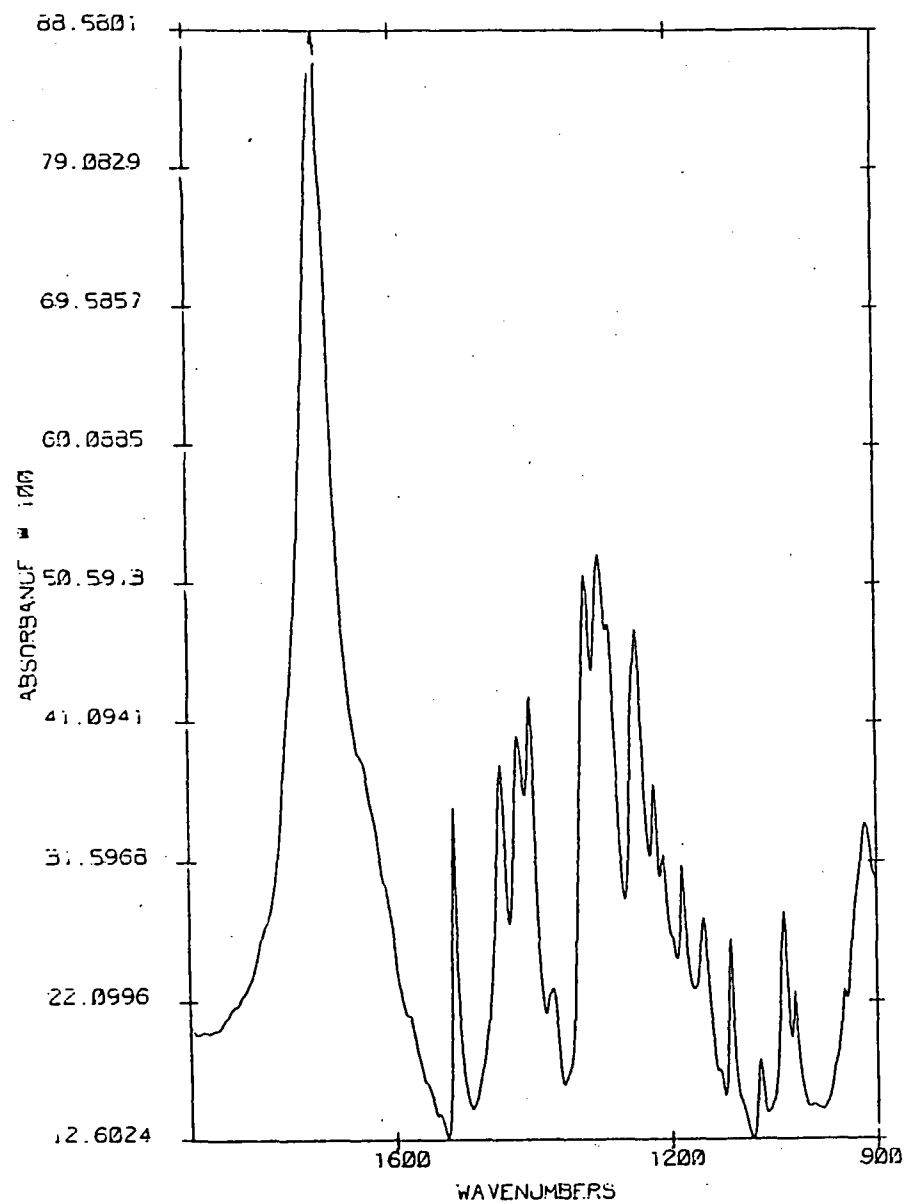


Fig. 60 FTIR spectrum of GL5,6,7

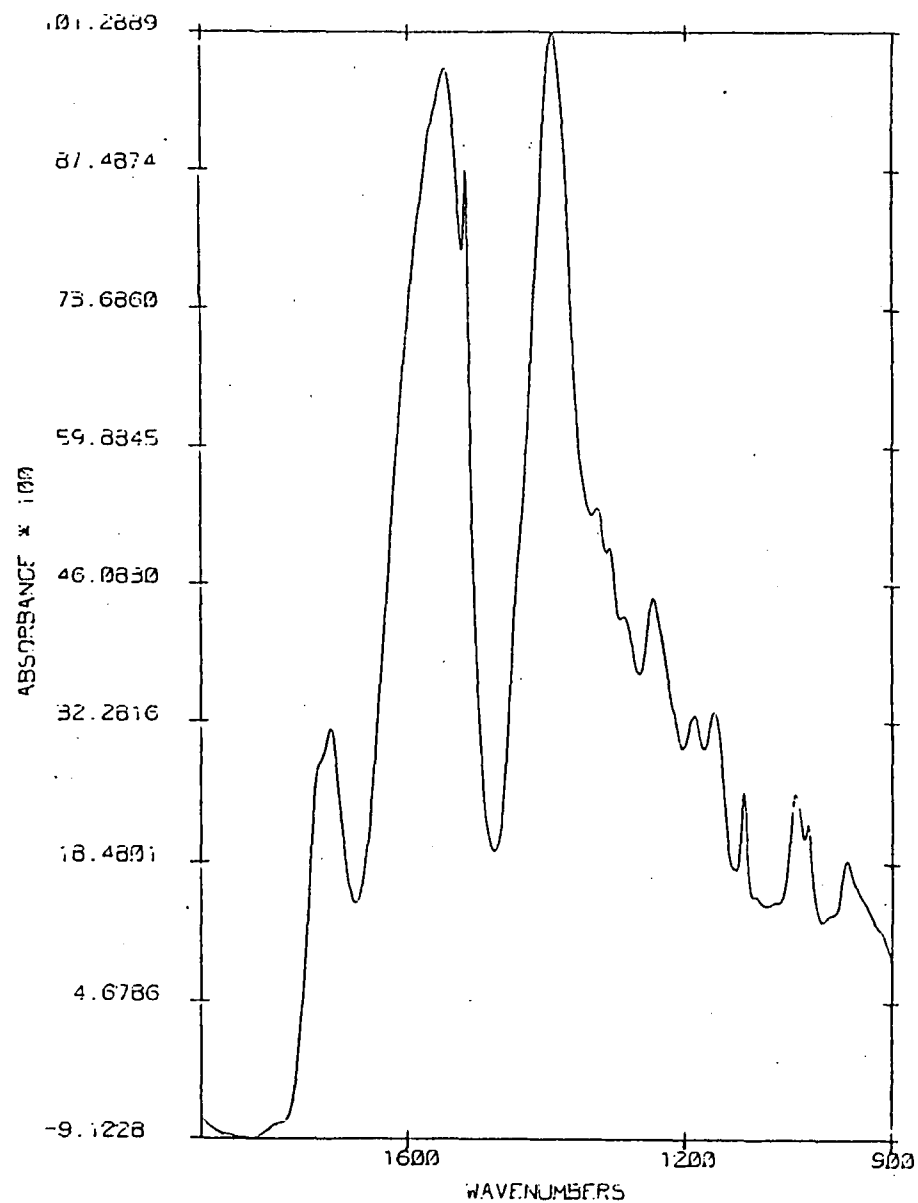
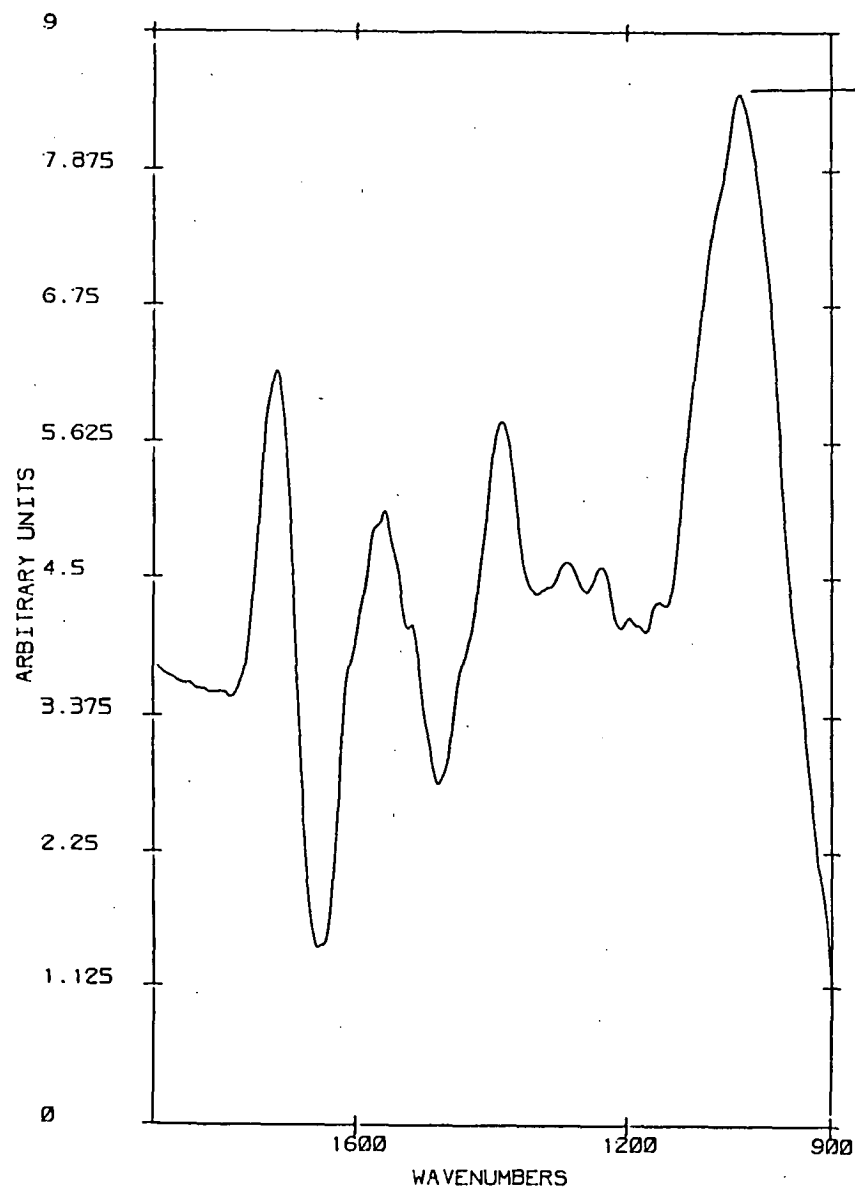


Fig. 61 FTIR spectrum of tin (II)  
complex with GL5,6,7



The origin of this peak is unknown but may possibly be due to surface Sn-O-H vibrations seen as a consequence of the pH of the water used to obtain the reference spectrum being incorrectly adjusted.

Fig.62 FTIR spectrum of 300 ppm GL5,6,7 on tin (IV) oxide at pH 4.5.

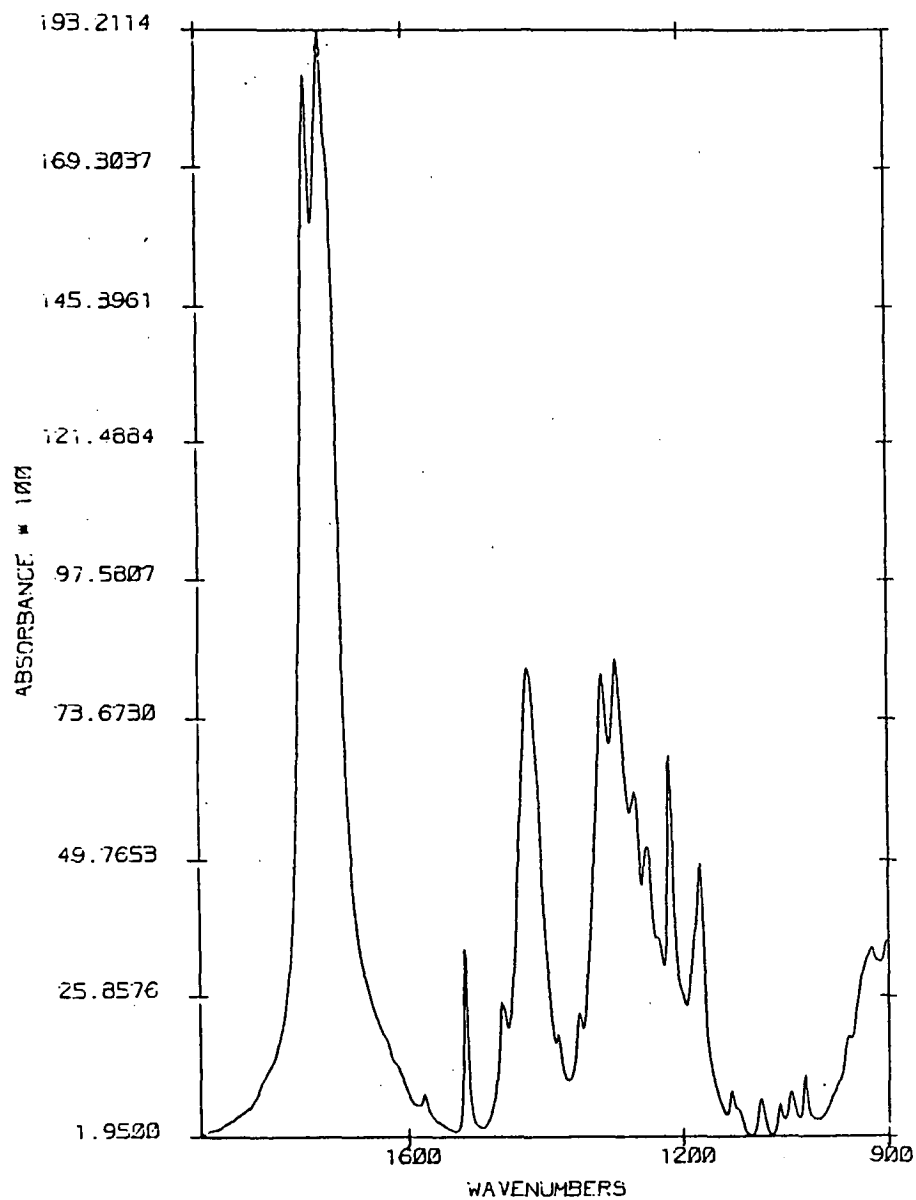


Fig.63 FTIR spectrum of GL33

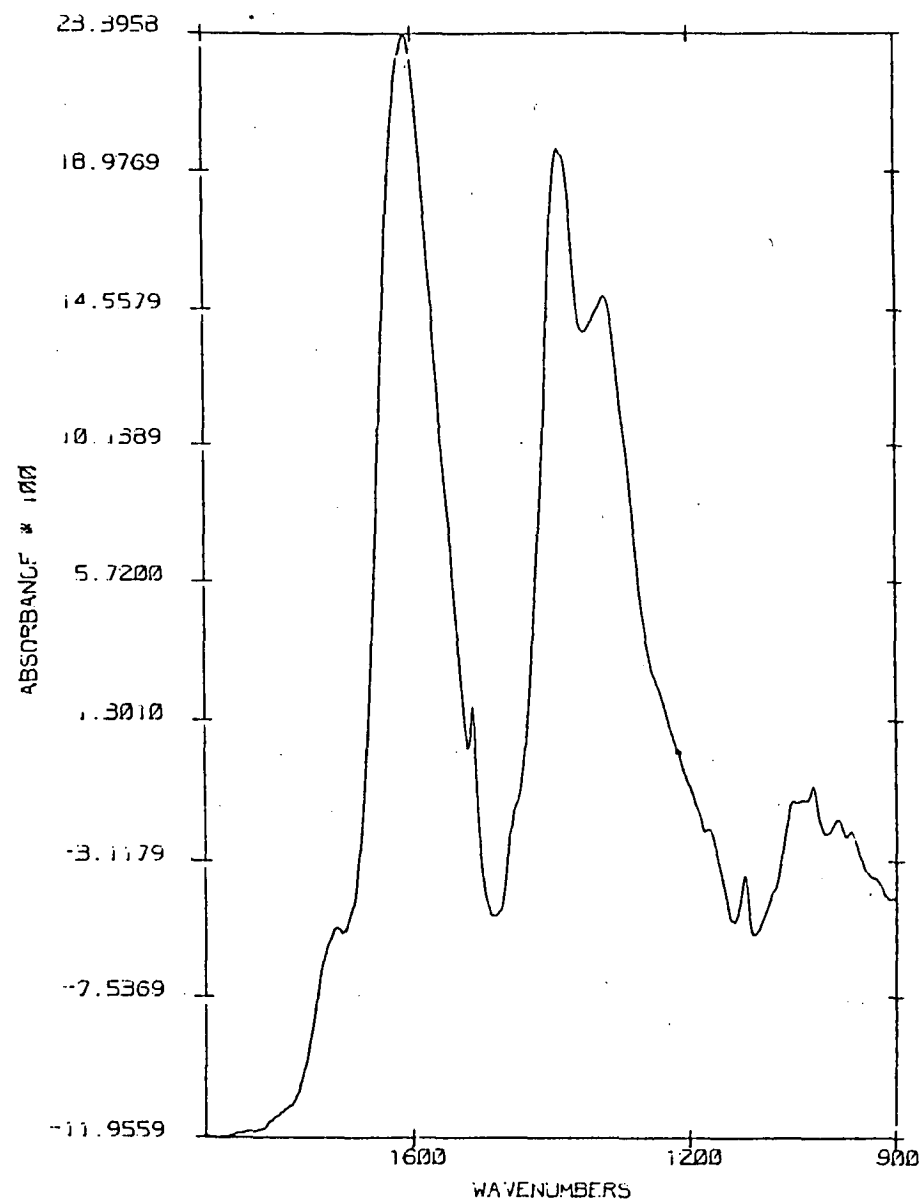
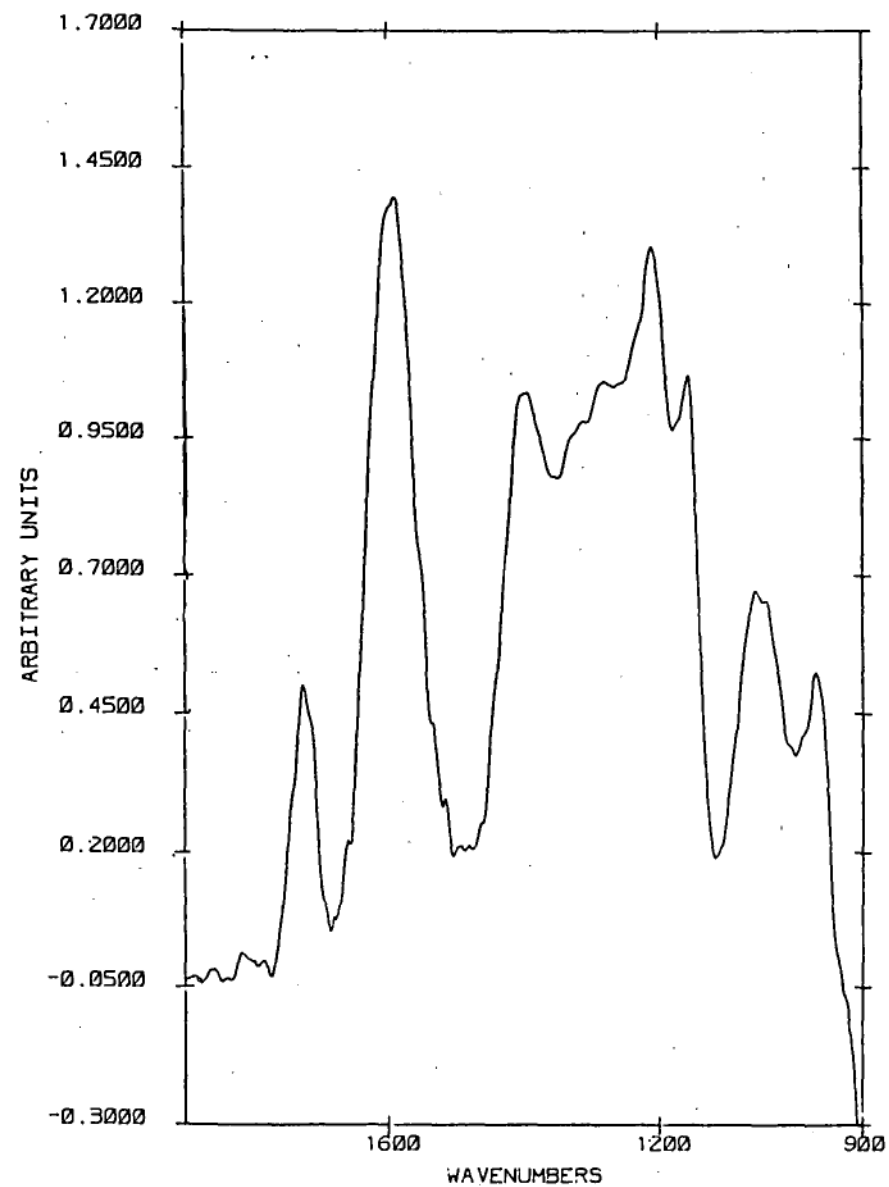
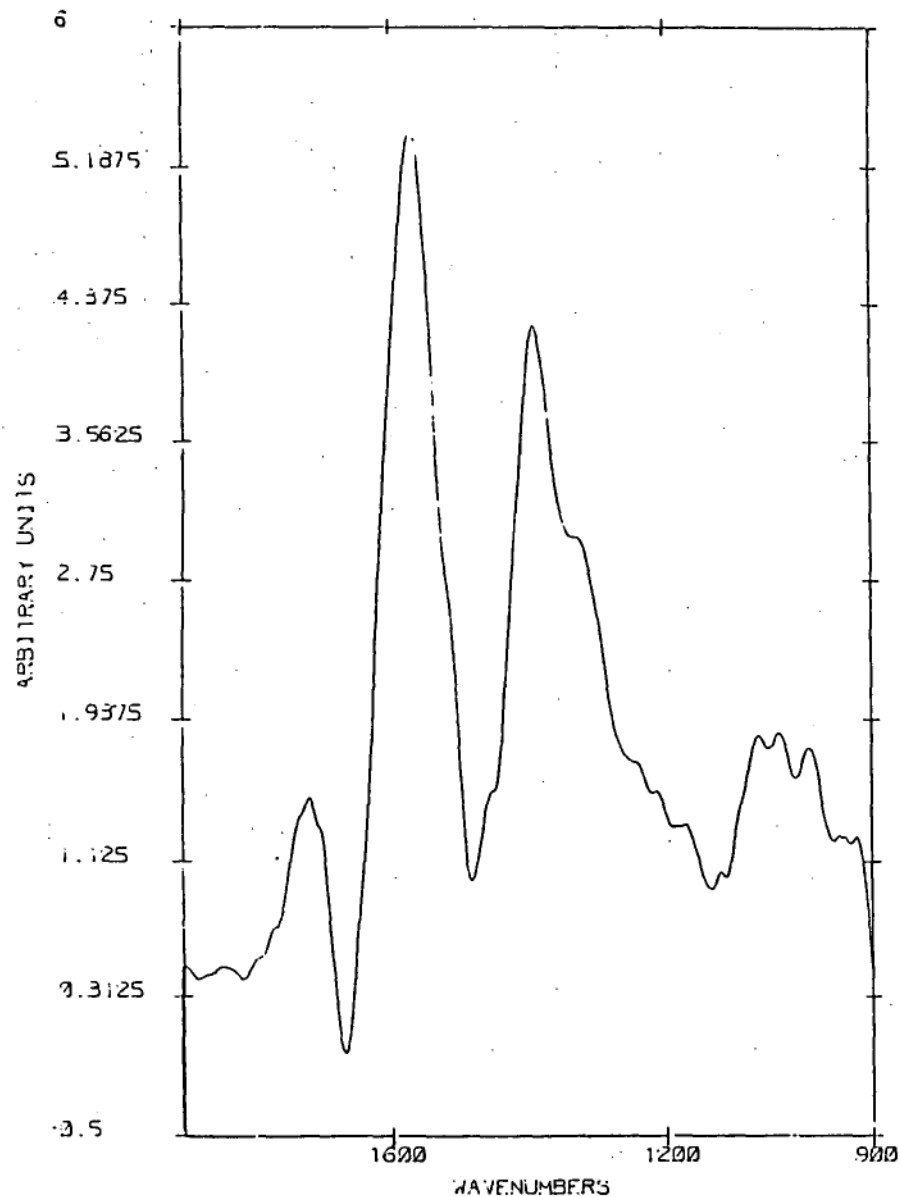


Fig. 64 FTIR spectrum of tin (II)  
complex with GL33.



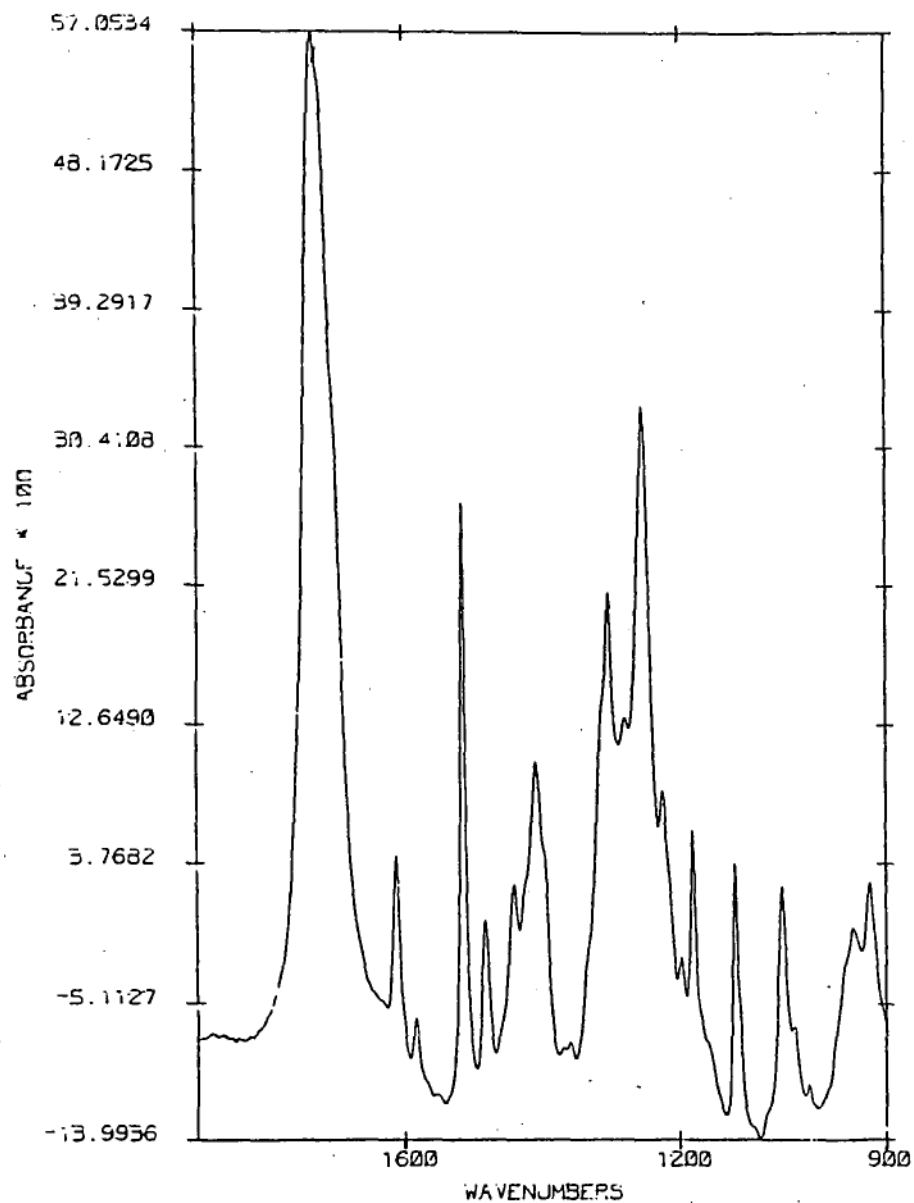


Fig.67 FTIR spectrum of GL12

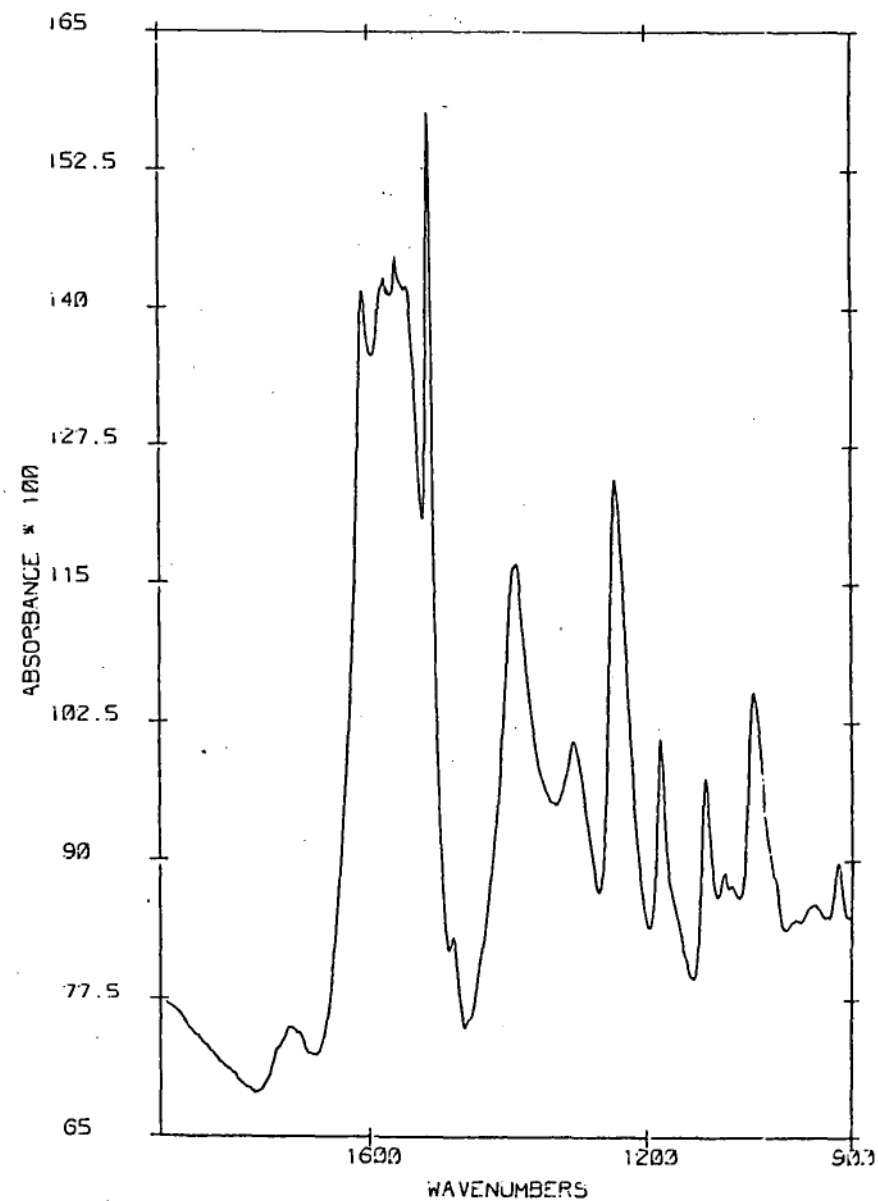


Fig.68 FTIR spectrum of tin (II)  
complex with GL12

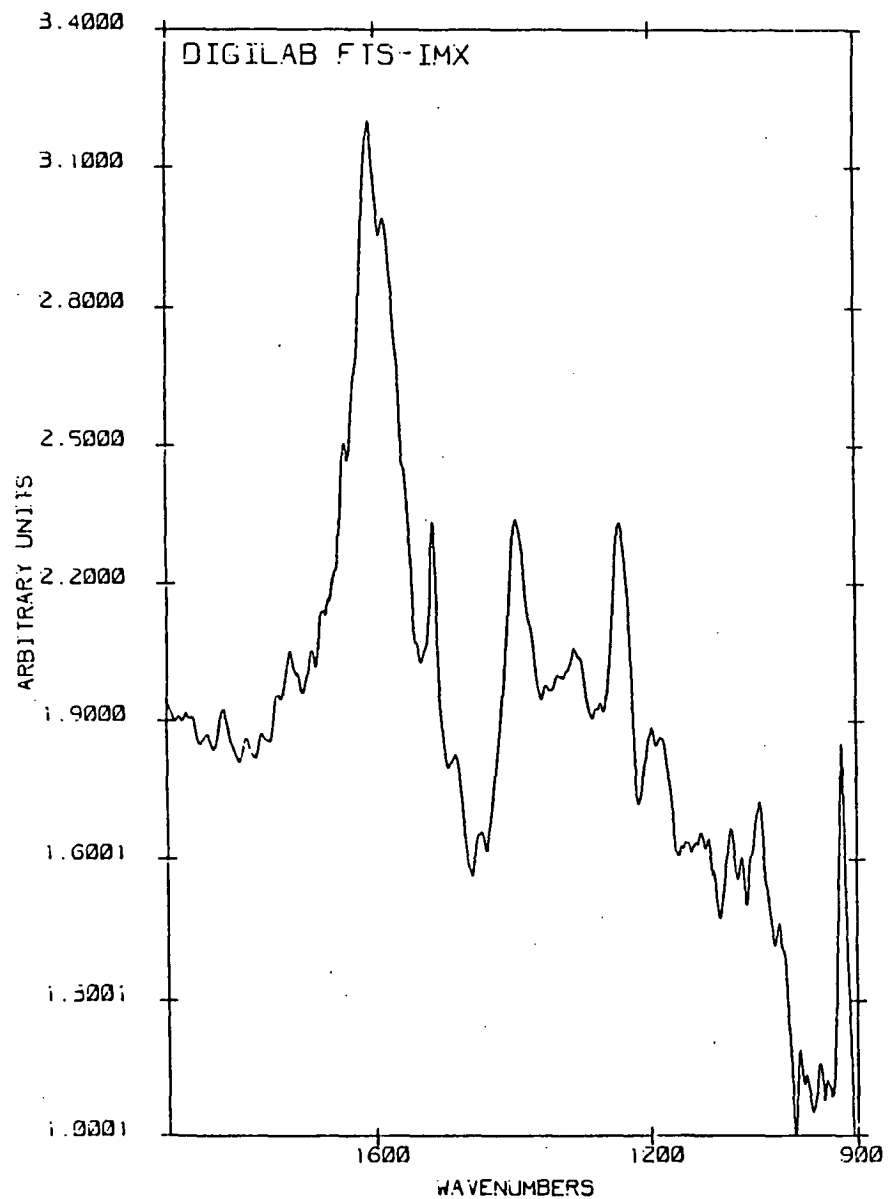


Fig.69 FTIR spectrum of 50 ppm GL12  
on cassiterite at pH 4.5

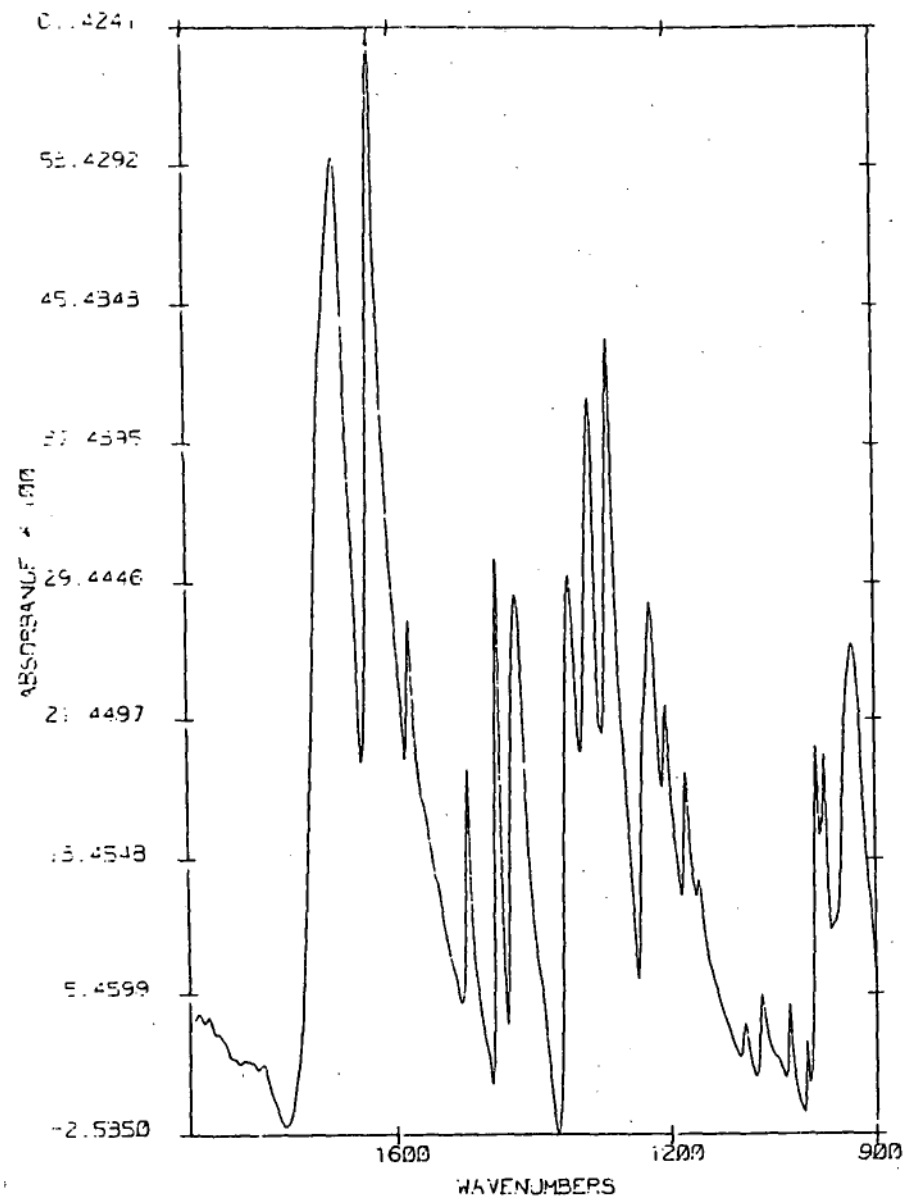


Fig.70 FTIR spectrum of cinnamic acid

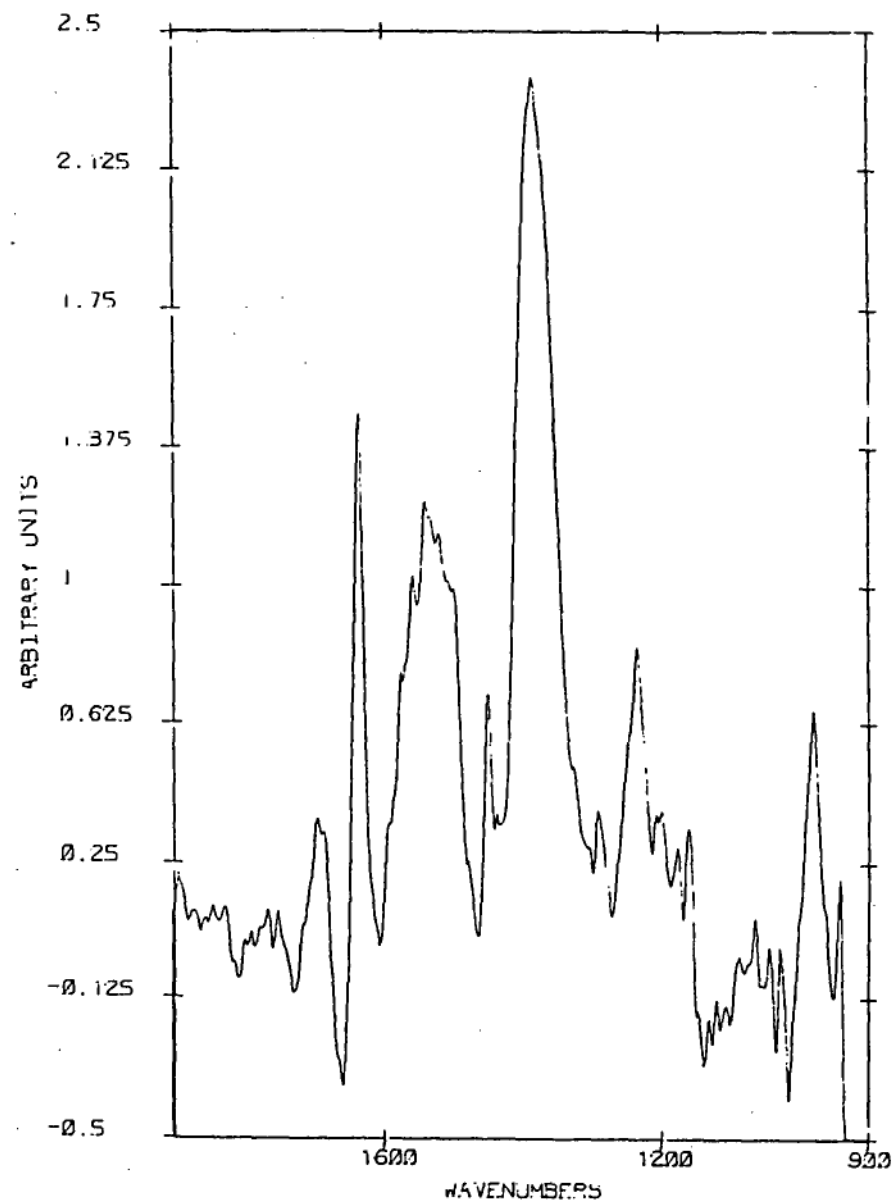


Fig.71 FTIR spectrum of cinnamic acid on tin (IV) oxide at pH 3.3

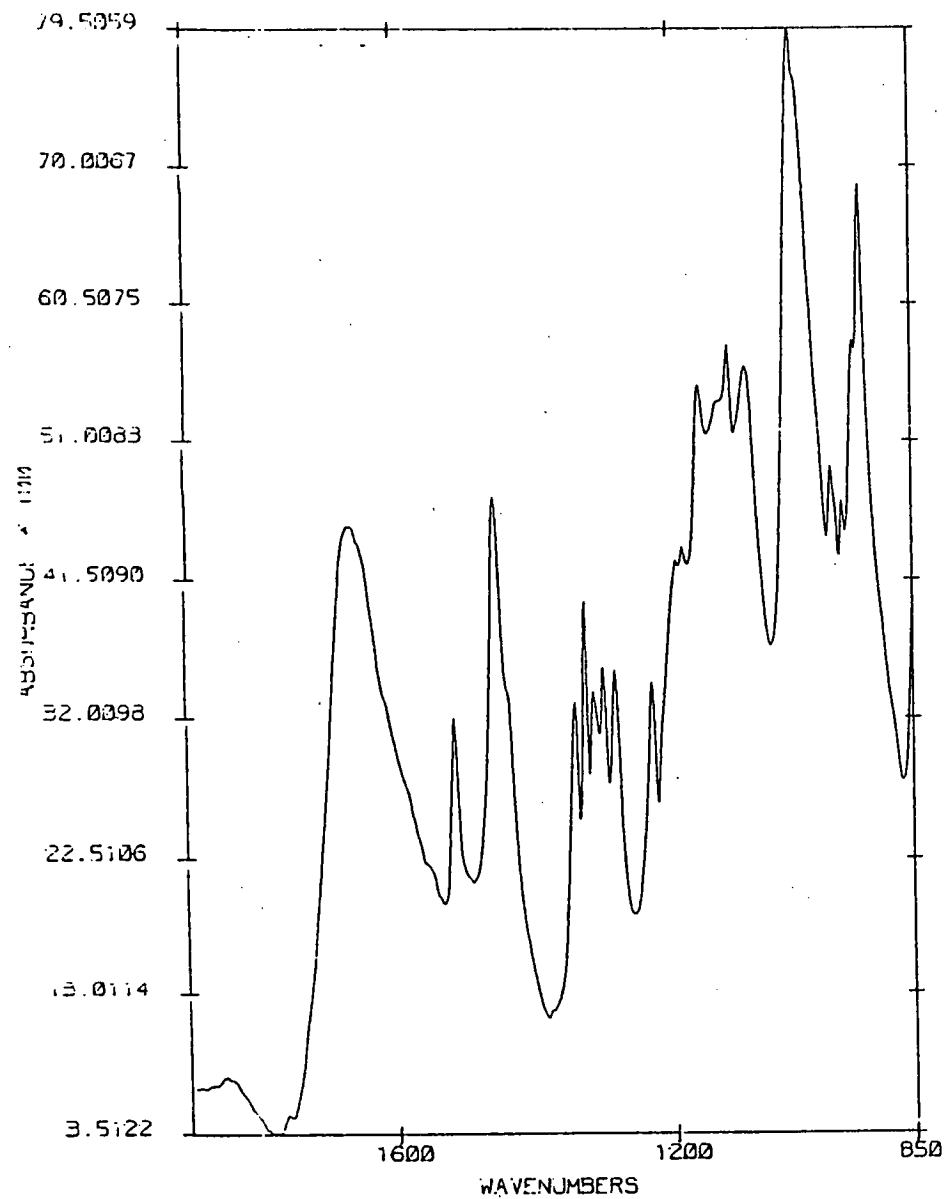


Fig.72 FTIR spectrum of GL40

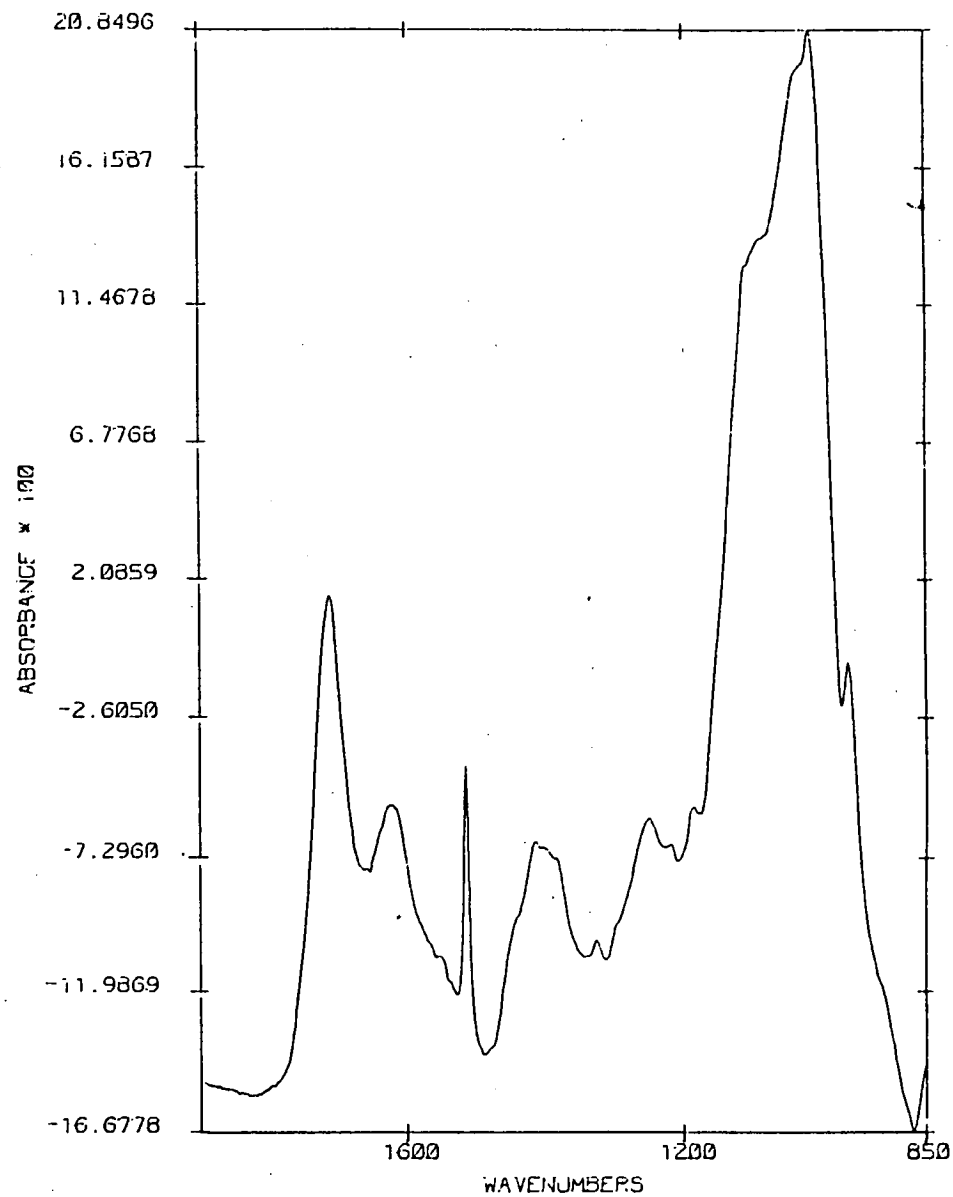
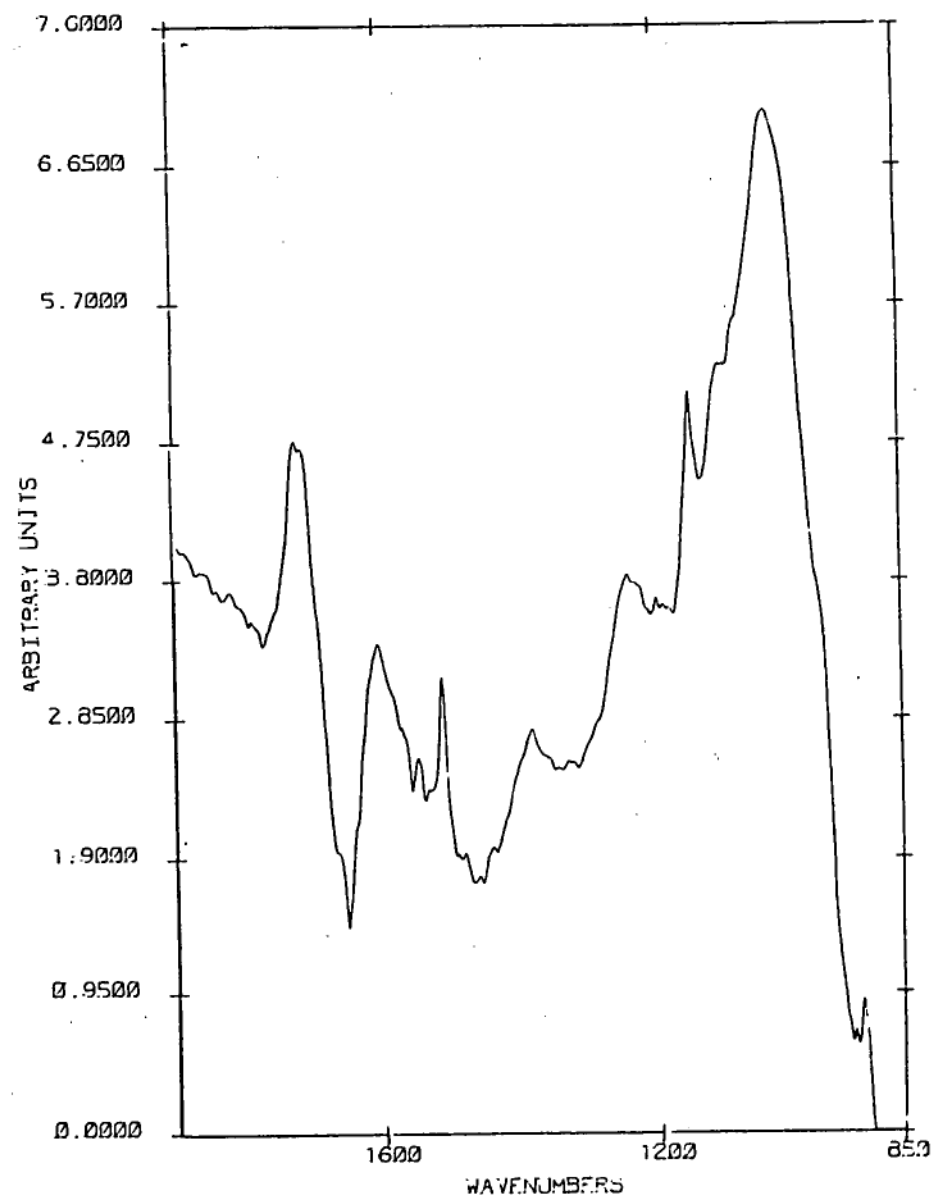
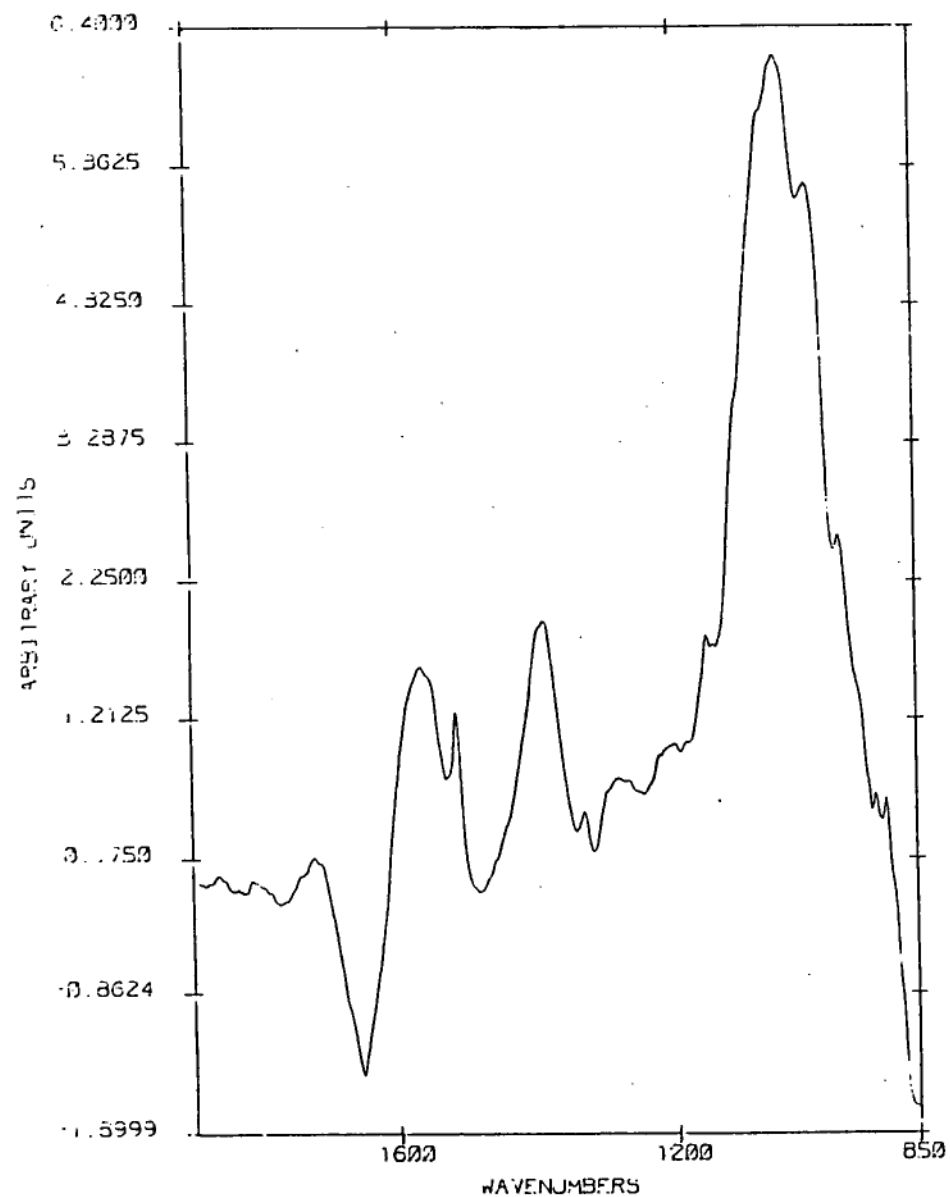


Fig.73 FTIR spectrum of tin (II)  
complex with GL40



spectrum of the SPA analogue GL28-cinnamic acid is shown in Fig.70. The C=O stretching frequency is prominent in each spectrum at  $\sim 1710\text{cm}^{-1}$ . Two groups of bands due to the  $\nu\text{C-O}/\delta\text{OH}$  vibrations can be seen at  $1520\text{--}1350\text{cm}^{-1}$  and  $1350\text{ to }1080\text{cm}^{-1}$ . These correspond to the  $\nu_{\text{as}}\text{C-O}$  and  $\nu_{\text{s}}\text{C-O}$  vibrations respectively. At  $980\text{--}900\text{cm}^{-1}$  a band can be seen due to  $\omega\text{OH}$  vibrations.

There are only two characteristic bands in the infrared spectra of the tin complexes due to  $\nu_{\text{s}}\text{C-O}$  and  $\nu_{\text{as}}\text{C-O}$  vibrations. The  $\nu_{\text{as}}\text{C-O}$  vibrations occur in the region  $\sim 1610\text{--}1450\text{cm}^{-1}$  and the  $\nu_{\text{s}}\text{C-O}$  vibrations at  $\sim 1400\text{cm}^{-1}$ .

The FTIR spectra of the tin (II) complexes with GL29, GL5,6,7, GL33 and GL12 are shown in Figs.56,61,64 and 68. The spectra show two prominent bands or groups of bands at  $1700\text{--}1460\text{cm}^{-1}$  peaking at  $\sim 1510\text{--}1590\text{cm}^{-1}$  and  $1460\text{--}1180\text{cm}^{-1}$ . These correspond to the  $\nu_{\text{as}}\text{C-O}$  and  $\nu_{\text{s}}\text{C-O}$  vibrations of the carboxylate group.

The FTIR spectrum of GL40 is shown in Fig.72. This collector contains both a carboxylic acid group and a phosphonic acid group. Bands due to the  $\nu\text{C-O}/\rho\text{OH}$  vibrations of the carboxylic acid group are present at  $1660\text{cm}^{-1}$  and  $1520\text{--}1240\text{cm}^{-1}$ . The two groups of bands at  $1520\text{--}1380$  and  $1380\text{--}1240\text{cm}^{-1}$  correspond to the  $\nu_{\text{as}}\text{C-O}$  and  $\nu_{\text{s}}\text{C-O}$  vibrations of the carboxylic acid group. The bands at  $1200\text{--}1060\text{cm}^{-1}$ ,  $1060\text{--}970$  and  $950\text{--}870\text{cm}^{-1}$  correspond to the  $\nu\text{P=O}$ ,  $\nu_{\text{as}}\text{P-O}$  and  $\nu_{\text{s}}\text{P-O}$  vibrations of the phosphonic acid group.

In the tin (II) complex with GL40 (Fig.73.) there are bands at  $\sim 1620\text{cm}^{-1}$  and  $1480\text{--}1290\text{cm}^{-1}$  due to the  $\nu_{\text{as}}\text{C-O}$  and  $\nu_{\text{s}}\text{C-O}$  vibrations of the carboxylate group. There is also an intense band at  $1016\text{cm}^{-1}$  due to the P-O stretching vibrations of the resonance stabilised phosphonate group.

### 11.3 Infrared Spectra of Carboxylic Acids Adsorbed on Cassiterite and Rutile

The infrared spectra of GL29, GL24, GL5,6,7, GL33, GL12, and cinnamic acid (GL28) adsorbed on thin films of tin (IV) oxide are shown in Figs. 57,59,62,65,69 and 71.

All spectra show bands due to the  $\nu_{\text{as}}\text{C-O}$  and  $\nu_{\text{s}}\text{C-O}$  vibrations of a chemisorbed carboxylate group. The infrared spectra of the adsorbates of GL29, GL5,6,7 and GL33 on cassiterite and rutile also have bands due to the  $\nu\text{C=O}$  vibrations of free carboxylic acid groups. This suggests that either some of the carboxylic acid groups are still protonated when the collector attaches to the mineral surface or some free acid is physisorbed on the surface. Which of these processes is occurring cannot be determined from the spectral evidence.

Experiments were carried out on the effect of pH on the adsorption of GL33 on the tin oxide surface. At pH 2.2 bands due to both the  $\nu\text{C-O}$  bands are considerably stronger than the  $\nu\text{C=O}$  band indicating that most of the acid is present as a chemisorbed surface complex, although some protonated carboxylic acid groups are present. As

the pH is increased to 4.5 the intensity of the  $\nu$  C=O band decreases indicating that further acid groups have complexed to the surface or possibly physically adsorbed acid is ionised with increasing pH. At pH 6.6 the  $\nu$  C=O band is absent indicating that the free carboxylic acid groups are absent at this pH. With an increase in pH the intensities of all absorbance bands decrease suggesting that there is a greater surface coverage at low pH values.

The infrared spectrum of GL33 adsorbed on a thin film of titanium dioxide is shown in Fig.66. As in the spectrum of GL33 adsorbed on tin (IV) oxide there are bands due to both  $\nu$  C=O and  $\nu$  C-O vibrations indicating the presence of both chemisorbed carboxylate groups and free carboxylic acid groups. Hence a chemisorption mechanism similar to that by which GL33 adsorbs on cassiterite must be responsible for the adsorption of this collector on rutile.

From the infrared spectra the monocarboxylic acid cinnamic acid would appear to adsorb by the same chemisorption mechanism as the dicarboxylic acids GL29, GL24 and GL5,6,7 and the tricarboxylic acids GL33 and GL12. However cinnamic acid is a very poor cassiterite collector while the other collectors are better than the industrially used collector styrene phosphonic acid. Cinnamic acid is the carboxylic acid analogue of SPA. The failure of cinnamic acid to produce flotation response may be due to the surface coverage being too low to induce sufficient hydrophobicity with the monocarboxylic acid or

the need for attachment of the collector in such a way that the hydrophobic group has a specific orientation. All the other collectors studied can attach to the tin oxide surface by at least two bonds which would determine the orientation of the hydrophobic group. However cinnamic acid can only attach to the surface by one bond so that the orientation of the hydrophobic group is not fixed.

The adsorption of GL40 on both cassiterite and rutile was studied by the FTIR-ATR technique. GL40 contains both a carboxylic acid group and a phosphonic acid group and is analogous with the dicarboxylic acid GL24.

The FTIR spectrum of GL40 adsorbed on a thin film of tin (IV) oxide is shown in Fig.74. Bands are present at  $\sim 1570\text{cm}^{-1}$ ,  $1394\text{cm}^{-1}$  and  $1050\text{cm}^{-1}$ . The bands at  $1570\text{cm}^{-1}$  and  $1394\text{cm}^{-1}$  correspond to the  $\nu_{\text{as}}\text{C-O}$  and  $\nu_{\text{s}}\text{C-O}$  vibrations of chemisorbed carboxylate groups while the band at  $1050\text{cm}^{-1}$  corresponds to the  $\nu\text{PO}_3$  vibrations of a chemisorbed phosphonate group. This indicates that both the carboxylic acid group and phosphonic acid group take part in attachment of the collector to the cassiterite surface by the formation of a surface complex.

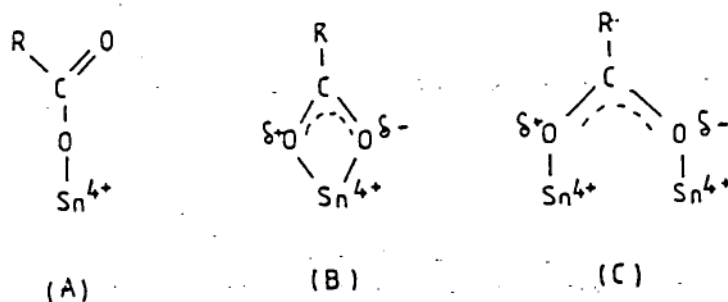
The FTIR spectrum of GL40 adsorbed on a thin film of titanium dioxide is shown in Fig.75. There bands are present at  $1740\text{cm}^{-1}$ ,  $1616\text{cm}^{-1}$ ,  $1394\text{cm}^{-1}$ ,  $1200\text{cm}^{-1}$  and  $1040\text{cm}^{-1}$ . The bands at  $1616\text{cm}^{-1}$  and  $1394\text{cm}^{-1}$  correspond to the  $\nu_{\text{as}}\text{C-O}$  and  $\nu_{\text{s}}\text{C-O}$  vibrations of a chemisorbed carboxylate group while the band at  $1040\text{cm}^{-1}$  corresponds

to the  $\nu\text{PO}_3$  vibrations of a chemisorbed phosphonate group. The band at  $1740\text{cm}^{-1}$  corresponds to the  $\nu\text{C}=\text{O}$  vibrations of free carboxylic acid groups while that at  $1200\text{cm}^{-1}$  is due to  $\nu\text{P}=\text{O}$  vibrations of free phosphonic acid groups. The presence of both chemisorbed collector and free acid groups suggests that at the pH of the experiment (2.4) not all acid groups are attached to the cassiterite surface or that there is physisorbed acid present at the surface.

#### 11.4 Discussion

The infrared spectra of mono, di and tri carboxylic acid collectors suggest that these collectors adsorb onto cassiterite by a chemisorption mechanism involving the formation of a carboxylate surface complex. This is in agreement with the findings of Bochnia and Serrano (1976) who proposed a chemisorption mechanism for the attachment of alkyl dicarboxylic acids to cassiterite.

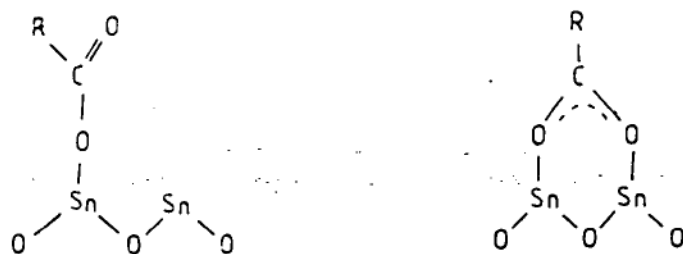
Previous authors have used the separations,  $\Delta\nu_{\text{CO}}$ , of the positions of the bands assigned to the asymmetric and symmetric stretching vibrations of the surface carboxylate group to determine the type of carboxylate co-ordination (Griffiths and Rochester 1977, Buckland et al, 1980, Deacon and Phillips, 1980). Carboxylate groups with unidentate co-ordination (A) are generally associated with values of  $\Delta\nu_{\text{CO}}$  ranging from  $150\text{cm}^{-1}$  to  $300\text{cm}^{-1}$ .



Carboxylate groups with chelating bidentate co-ordination (B) are usually associated with values in the range  $50\text{cm}^{-1}$  to  $150\text{cm}^{-1}$  while bridging bidentate carboxylate groups (C) generally have values of  $\Delta\nu_{\text{CO}}$  in the range  $120\text{--}170\text{cm}^{-1}$ .

For GL28 (cinnamic acid) a  $\Delta\nu_{\text{CO}}$  value of  $155\text{cm}^{-1}$  was found for the adsorbate on tin (IV) oxide. For the dicarboxylic acids adsorbed on tin oxide values of  $\Delta\nu_{\text{CO}}$  are  $211\text{cm}^{-1}$  for GL29,  $189\text{cm}^{-1}$  for GL24 and  $166\text{cm}^{-1}$  for GL5,6,7. For the tricarboxylic acids adsorbed on tin oxide values of  $\Delta\nu_{\text{CO}}$  are  $177\text{cm}^{-1}$  for GL33 and  $211\text{cm}^{-1}$  for GL12. The value of  $\Delta\nu_{\text{CO}}$  for cinnamic acid is in the range associated with all of unidentate, chelating bidentate and bridging bidentate co-ordination. The values for the di- and tricarboxylic acids are in the range generally associated with unidentate co-ordination but it is unreliable to extend the correlation between  $\Delta\nu_{\text{CO}}$  and co-ordination type to these acids as these correlations are essentially empirical and only based on data for monocarboxylic acids.

Both unidentate and bridging bidentate co-ordination have been proposed for the adsorption of monocarboxylic acids on tin oxide surfaces (Harrison and Maunders, 1984) viz.



Information from infrared bands in adsorbed carboxylates has been used by previous authors to give information on their orientation at the solid-liquid interface (Hasegawa and Low, 1969 a,b). In long alkyl chain compounds methylene groups interact with each other so that they vibrate with various phase differences if they are arranged in a coplanar *trans* zigzag configuration. The position of the coupled wagging vibrations of the methylene groups is dependent on the arrangement of the chains and the positioning of the polar end groups. Band shifts in the methylene wagging vibrations give an indication of the orientation of alkyl carboxylic acids at the surface.

Such information cannot be gained from the acids used in this experiment since they incorporate aromatic rings as the hydrophobic group. However information on orientation may be gained from measurement of polarised infrared spectra (Yang et al, 1973.). The ratio of the intensities of a band measured with radiation polarised parallel to the incident beam which forms a  $45^\circ$  angle with

the interface to the intensity measured with a perpendicular polarised beam is dependent on the orientation of the adsorbate at the interface. High values of  $A_{\perp}/A_{\parallel}$  indicate that the molecule is close to normal to the interface. Low values indicate that the adsorbate molecules lie flat on the surface. Intermediate values indicate a more random orientation.

An attempt was made to determine adsorbate molecule orientations using polarised infrared radiation, however this was unsuccessful as the polariser, which was designed for a dispersion instrument, was found to be incompatible with the FTIR spectrometer.

## 12. Conclusion

Comparison of the infrared spectra of phosphonic, sulphonic and carboxylic acids used as cassiterite flotation collectors, their tin (II) and tin (IV) complexes, and their adsorbates on cassiterite show that these reagents adsorb on the mineral surface by forming a tin - collector complex. A similar mechanism was also found for the adsorption of these reagents on rutile. The type of surface complexation was deduced from the fine structure of the spectra of the adsorbates. Phosphonic acids probably form a bidentate surface complex while carboxylic acids probably form a monodentate surface complex. On both cassiterite and rutile some collector molecules may also be physically adsorbed at the surface. The adsorption density and chemical form of the adsorbed collectors were found to be dependant on pH. The adsorption kinetics are such that considerable reagent adsorption occurs within the time used for conditioning in industrial practice. The presence of iron in the cassiterite lattice or adsorbed on the cassiterite surface was found not to be necessary for collector adsorption to occur. The presence of dissolved iron in the flotation pulp also did not effect the adsorption characteristics of the collector. The ability of the FTIR-ATR technique to produce direct, real time, *in situ* information about interactions at the solid - liquid interface makes this method a powerful tool for investigations of the

adsorption of flotation reagents at the mineral - aqueous interface.

### 13. Suggestions for Further Work

As well as phosphonic acids and the sulphosuccinamates, arsonic acids have also found wide scale application in the industrial flotation of cassiterite. The adsorption of arsonic acids on cassiterite was not covered in this investigation as the infrared spectral bands due to the  $\nu_{\text{As=O}}$ ,  $\nu_{\text{asAs-O}}$  and  $\nu_{\text{sAs-O}}$  vibrations occurring in the region 600 to 1000  $\text{cm}^{-1}$  (Fig.76) which is partially outside the region of transparency of the germanium ATR element. Information on the adsorption of these collectors on cassiterite could be obtained by the use of an alternative material which is transparent in this region of the spectrum, such as zinc selenide, for the construction of the ATR element. An FTIR-ATR study of the adsorption of arsonic acids on cassiterite would be a useful complement to the present investigations.

The use of the flotation collectors studied in this investigation is not confined to the flotation of cassiterite. Sulphosuccinamates, phosphonic acids and arsonic acids have been used industrially in the flotation of wolframite,  $(\text{Fe,Mn})\text{WO}_4$  (Maranakis and Kelsall, 1985). Phosphonic acids have also been used in the laboratory flotation of ilmenite,  $\text{FeTiO}_3$  and tantalite,  $(\text{Fe,Mn})\text{Ta}_2\text{O}_6$ , (Burt et al, 1980) and sulphosuccinamates have been used industrially to float tantalite (Burt et al. *op.cit.*). There is also the possibility that the novel carboxylic acid collectors developed by Greg Lane may also be

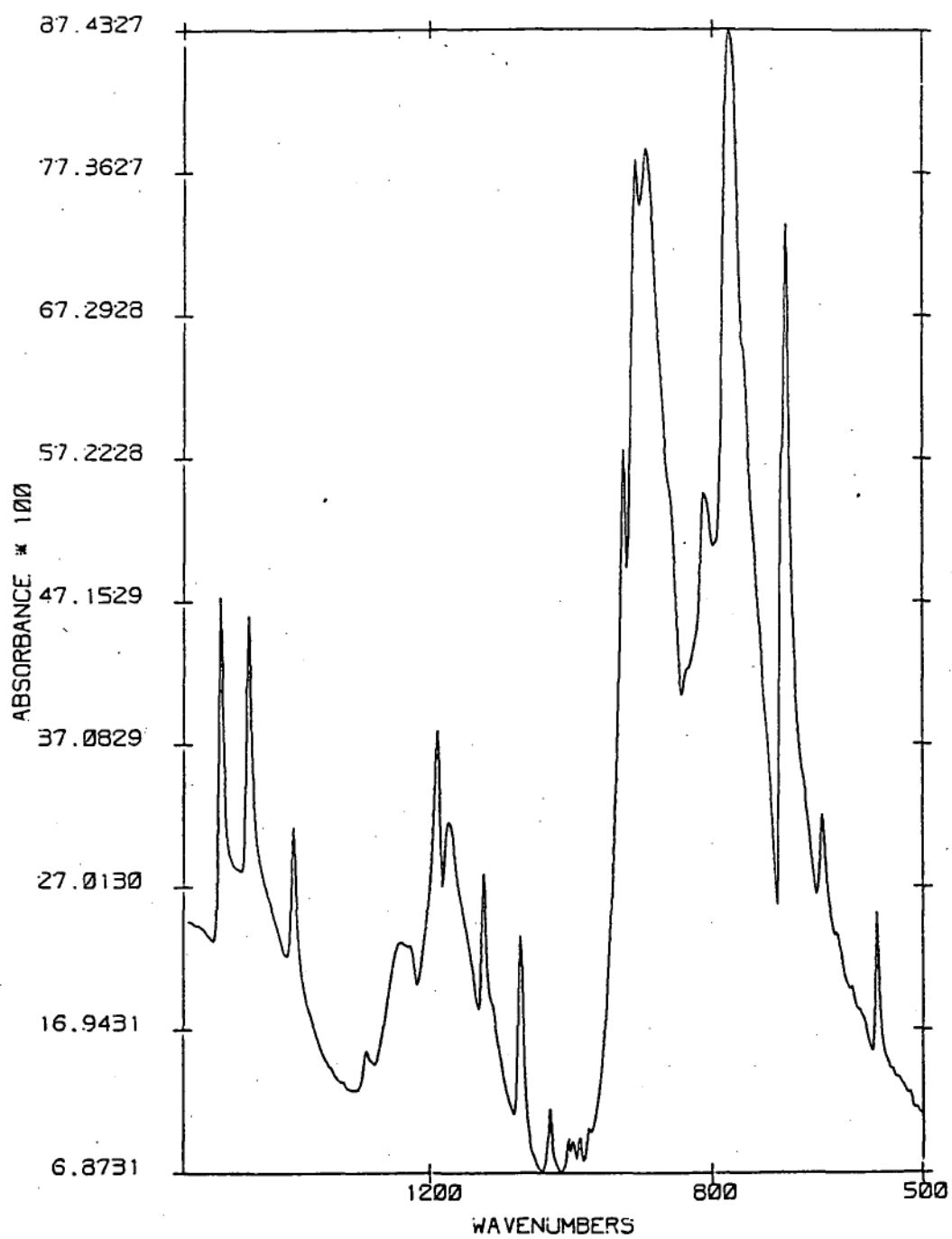


Fig.76 FTIR spectrum of benzyl arsonic acid

suitable for use as collectors for ilmenite, wolframite and the columbite - tantalite series of minerals  $[(\text{Fe},\text{Mn})\text{Nb}_2\text{O}_6 - (\text{Fe},\text{Mn})\text{Ta}_2\text{O}_6]$ . The adsorption of these reagents on wolframite, ilmenite and the columbite - tantalite series could also be investigated by the FTIR-ATR technique. Such an FTIR-ATR study of the adsorption of flotation reagents on oxide minerals other than cassiterite and rutile would produce a greater understanding of the flotation of these minerals and could lead to advances in the development of new reagents for their flotation.

### References

**Atkinson R.J, Parfitt R.L and Smart R.St.C.**

Infrared study of phosphate adsorption on goethite.

*JCS Faraday* 1. 70 1472-1479, 1975.

**Baldauf H., Schoenherr J. and Schubert H.** Alkane dicarboxylic acids and aminonaphthol sulphonic acids - a new reagent regime for cassiterite flotation. *Int. J. Mineral Processing*. 15 117-133, 1985.

**Baldauf H., Serrano A., Schubert H. and Bochnia D.**

Über die Eignung von Dikarbonsäuren als

Flotationssammler. *Neue Bergbautechnik*. 4 532-538, 1974.

**Baldauf H., Singh D.V. und Schubert H.** Zur

Flotation von Zinnerzen mit Dikarbonsäuren. *Neue*

*Bergbautechnik*. 10 692-698, 1980.

**Ball B., Cox C.H. and Yap S.H.** Effect of inorganic

ions on the sulphonate flotation of cassiterite.

*Trans.AIME*. 266 2022-2026, 1979.

**Barbery G. and Cecile J.L.** Methodes nouvelles de

l'élude des mécanismes d'adsorption en flottation.

*Industrie Minerale - Mineralurgie*. Sept. 109-121, 1979.

**Bell A.T. and Hair M.L.** Vibrational Spectroscopies

for Adsorbed Species. *American Chemical Society*.

Washington, 1980.

**Berger F., Hoberg H. and Schneider F.U.** Neue

Untersuchungen und Entwicklungstendenzen in der

Oxidflotation. *Erzmetall*. 33 314-319, 1980.

**Bochnia D. and Serrano A.** Untersuchungen an substituierten Alkankarbonsäuren im Hinblick auf ihre Sammlereigenschaften. *Freiberger Forschungshefte Reihe A.* 565 1-102, 1976

**Buckland A.D., Rochester C.H. and Topham S.A.**  
Infrared study of the adsorption of carboxylic acids on haematite and goethite immersed in carbon tetrachloride. *JCS Faraday* 1. 76 302-313, 1980.

**Burt R.O., Flemming J., Mills C. and Hamonic F.**  
The Flotation of tantalum minerals. *Paper presented at the 14th International Mineral Processing Congress, Toronto, October, 1982.*

**Collins D.N., Wright R. and Watson D.** Use of alkyl-imino-bis-methylene phosphonic acids as collectors for oxide and salt-type minerals. *Reagents Miner. Ind. Pap.* 1-12, 1984.

**Deacon G.B and Phillips R.J.** 1980. Relationships between the carbon-oxygen stretching frequencies of carboxylato complexes and the type of carboxylate co-ordination. *Coord. Chem. Rev.* 33 227-250, 1980.

**Detoni S. and Hadzi D.** 1957. Infrared spectra of some organic sulphur compounds. *Spectrochimica Acta.* 11 601-608, 1957.

**Dietze U.** Zur Kenntnis der Infrarotspektren einiger Arbonsäuren. *Journal für praktische Chemie.* 313 889-898, 1971.

**Dietze U.** Infrarotspektren von Phosphonsäuren I Alkanphosphonsäuren. *Journal für praktische Chemie.* 316 293-298, 1974a.

**Dietze U.** Infrarotspektren von Phosphonsauren. II. Arylphosphonsauren. *Journal fur praktische Chemie.* 316 485-490, 1974b.

**Dietze U.** Infrarotspektroskopische Untersuchungen zum Anlagerungsmechanismus von Phosphon- und Arsonsauren an Kassiterit bei dessen Flotation. *Freiberger Forschungshefte Reihe A.* 551 7-38, 1975.

**Doren A. and Rouxhet P.G.** Infrared study of the adsorption on silica of a collector with an oxyethylene chain. *Int. J. Mineral Processing.* 9 343-351, 1982.

**Doren A., van Lierde A., de Cuyper J.A.** Influence of non-ionic surfactants on the flotation of cassiterite. In *Developments in Mineral Processing* (J. Laskowski. Ed.) Vol 2. Part A. 86-109, Elsevier, New York, 1981.

**Doren A., Vargas D. and Goldfarb J.** Non-ionic surfactants as flotation collectors. *Trans. Inst. Mining and Metallurgy.* 84 C34-37, 1975.

**Farrow J.B., Houchin M.R. and Warren L.J.** Mechanism of adsorption of organic acids on stannic oxide. Preprint of paper to be delivered at the 5<sup>th</sup> Australian Conference on Colloids and Surfaces, Brisbane, February, 1986.

**Ferraro J.R. and Basile L.J.** Fourier Transform Infrared Spectroscopy - Applications to Chemical Systems. Academic Press. New York, 1978.

**Foo K.A. and Enraght-Moony J.N.R.** 1982. The loss of fines in tin beneficiation - an economic challenge. Paper presented at a technical meeting on *The Recovery of Fine Particles.* AMIRA, Melbourne, 1982.

**Geisekke E.W.** A review of spectroscopic techniques in the study of interactions between minerals and reagents in flotation systems. *Int. J. Mineral Processing* 2 19-56, 1983.

**Gendreau R.M.** Breaking the one second barrier: fast kinetics of protein adsorption by FTIR. *Applied Spectroscopy*. 36 47-49, 1982.

**Gendreau R.M and Jakobsen R.J.** 1978. FTIR techniques for studying complex biological materials. *Applied Spectroscopy*. 32 326, 1978.

**Gendreau R.M., Winters S., Leininger R.I., Fink D., Hassler C.R. and Jakobsen R.J.** 1981. Fourier transform infrared spectroscopy of protein adsorption from whole blood: *Ex vivo* dog studies. *Applied Spectroscopy*. 35 353-357, 1981.

**Griffiths D.M. and Rochester C.H.** Infrared study of the adsorption of [ $^2\text{H}_4$ ] acetic acid on rutile. *J.C.S. Faraday 1*. 73 1988-1997, 1977.

**Gochin R.J. and Solari J.A.** Dissolved air flotation of fine cassiterite. *Trans. Inst. Mining and Metallurgy*. 92 C52-58, 1983.

**Goold L.A.** Preliminary investigations into the flotation of tin dioxide, cassiterite and some related gangue minerals. *National Institute for Metallurgy of South Africa. Report. No. 1589.* 1973.

**Gutierrez C.** Influence of previous aeration in water or heating in air on the flotation of ilmenite with oleic acid. *Int. J. Mineral Processing*. 3 247-256, 1973.

**Harrick N.J.** Internal Reflection Spectroscopy.  
Interscience Publishers. New York, 1967.

**Harrison P.G. and Maunders B.M.** Tin oxide surfaces -  
11 Infrared study of the chemisorption of ketones on tin  
(IV) oxide. *J.C.S. Faraday 1.* 80 1329-1340, 1984.

**Hasegawa M. and Low M.J.D.** Infrared study of  
adsorption *in situ* at the liquid-solid interface - II  
adsorption of stearic acid on zinc oxide. *J. Colloid  
Interface Sci.* 29, 593-600, 1969.

**Hasegawa M. and Low M.J.D.** Infrared study of  
adsorption *in situ* at the liquid-solid interface - III  
Adsorption of stearic acid on silica and on alumina and  
decanoic acid on magnesia. *J. Colloid Interface Sci.* 30,  
378 - 386, 1969.

**Houchin M.R. and Warren L.J.** Surface titrations and  
electrokinetic measurements on stannic oxide suspensions.  
*J. Colloid Interface Sci.* 100. 278-286, 1984.

**Kirchberg H. und Wottgen E.** Untersuchungen zur  
Flotation von Zinnstein mit Phosphon-, Arson und  
Stibonsauren. *4th International Congress on Surface  
Active Substances.* Brussels, 1984.

**Kirkland J.J.** 1955. Quantitative application of the  
potassium bromide disc technique in infrared spectroscopy.  
*Anal. Chem.* 27 1537-1541, 1955.

**Laptev S.F., Ignatenko L.P., Ushakov D.M., Malii  
V.A., Gnatyuk P.P.** Production and use of the  
flotation reagent Asparal F. *Soviet Chemical Industry.* 13  
187-191, 1981.

**Little L.H.** Infrared Spectra of Adsorbed Species. Academic Press. London, 1966.

**Low M.J.D. and Yang R.T.** The measurement of infrared spectra of aqueous solutions using Fourier Transform Spectroscopy. *Spectrochimica Acta*. 29 A 1761-1772, 1973.

**Marabini A.M.** Study of adsorption of salicylaldehyde on cassiterite. *Trans. Inst. Mining Metallurgy*. 87 76-78, 1978.

**Marabini A.M. and Rinelli G.** Development of a specific reagent for rutile flotation. *Trans. AIME*. 274 1822-1827, 1983.

**Marinakos K.I. and Kelsall G.H.** 1985. Adsorption of Dodecyl Sulphate and Decyl Phosphonate on Wolframite ( $\text{Fe,Mn})\text{WO}_4$  and their use in the two-liquid flotation of fine wolframite particles. *J. Colloid. Interface Sci.* 106 517-531, 1985.

**Natarajan R. and Fuerstenau D.W.** Adsorption and flotation behaviour of manganese dioxide in the presence of octyl hydroxamate. *Int. J. Mineral Processing*. 11 139-153, 1983.

**O'Connor D.J. and Buchanan A.S.** Electrokinetic properties of cassiterite. *Aus. J. Chem.* 6 278-293, 1953.

**Palmer B.R, Gutierrez B.G, Fuerstenau M.C and Aplan F.F.** Mechanisms involved in the flotation of oxides and silicates with anionic collectors. *Trans. AIME*. 258 257-263, 1975.

**Parfitt R.L, Russell J.D and Farmer V.C.**

Confirmation of the surface structures of goethite and phosphated goethite by infrared spectroscopy.

*JCS Faraday* 1. 72 1082-1087, 1976.

**Paterson J.G, and Salman T.** Adsorption of sodium

oleate on cupric and ferric hydroxides. *Trans. Inst.*

*Mining Metallurgy.* 79 C91-C102, 1970.

**Peck A.S, Raby L.H, Wadsworth M.E.** An infrared study

of the flotation of hematite with oleic acid and sodium oleate. *Trans AIME.* 238 301-307, 1966.

**Pietzsch C, Fritzsche E. and Braun H.** The binding

state of tin (IV) arsonates and tin (IV) phosphonates

studied by mossbauer spectroscopy. *Radiochem. Radioanal. Letters.* 47 243-250, 1981.

**Polkin S.I, Laplev S.F, Adamov E.V, Krasnukhina**

**A.V. and Purvinskii O.F.** Theory and practice in the

flotation of cassiterite fines. *Proceedings Tenth*

*International Mineral Processing Congress.* London,

Jones M.J. Ed. IMM, London 593-614, 1973.

**Raghaven S. and Fuerstenau D.W.** The adsorption of

aqueous octylhydroxamate on ferric oxide. *J. Colloid*

*Interface Science* 50 319-329, 1975.

**Rochester C.H.** Infrared spectroscopic studies of

adsorption behaviour at the solid-liquid interface.

*Advances in Colloid and Interface Science.* 12 43-82,

1980.

**Senior G.D and Poling G.W.** 1986. The Chemistry of

Cassiterite Flotation. Preprint of paper to be presented

at the Gaudin Symposium, February 1986.

**Serrano A, Baldauf H, Schubert H, Bochnia D.**

Untersuchungen substituierter Karbonsauren im Hinblick auf ihre Sammlerwirkung. *Freiberger Forschungshelfte Reihe A* 544, 111-121, 1975.

**Singh D.V, Baldauf H. und Schubert H.** Flotation von Kassiterit-Erzen mit Alkandicarbonsauren und organischen Drukern. *Aufbereit-Tech.* 21 566-578, 1980.

**Stechemester H, Dietze U, und Wottgen E.** Über die derzeitigen Möglichkeiten zur Strukturuntersuchung von Adsorptionsschichten auf Festkörperoberflächen in der Flotationforschung. *Neue Bergbautechnik* 6 689-704, 1976.

**Strojek J.W, Mielczarski J. and Nowak P.**

Spectroscopic investigations of the solid-liquid interface by the ATR technique. *Advances in Colloid and Interface Science.* 19 309-327, 1983.

**Winters S, Gendreau R.M, Leininger R.I. and**

**Jakobsen R.J.** Fourier transform infrared spectroscopy of protein adsorption from whole blood:II. *Ex vivo* sheep studies. *Applied Spectroscopy.* 36 404-409, 1982.

**Wottgen E.** Adsorption of phosphonic acids on cassiterite. *Trans. Inst. Mining Metallurgy.* 78 C91-97, 1969.

**Wottgen E.** Steigerung der Effektivität der Zinnsteinflotation durch Weibrentwicklung der Reagenzienführung und Anwendung einer Erzvorbe-handlung. *Freiberger Forshungshefte Reihe A* 621 1-80, 1980.

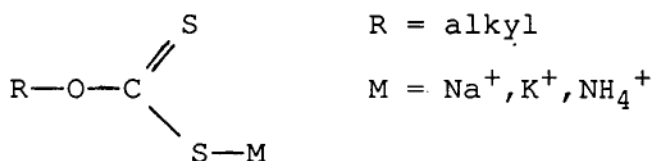
**Wottgen E. und Dietze U.** Über die Anlagerung von Phosphonsauren an Kassiterit bei der Flotation. *Zeitschrift für anorganische und allgemeine Chemie.* 369 64-72, 1969.

**Yang R.T, Low M.J.D, Haller G.L and Fenn J.** Infrared study of adsorption *in situ* at the solid-liquid interface IV the utility of internal reflection techniques. *J. Colloid Interface Science.* 44 249-258, 1973.

Appendix 1. Spectroscopic Investigations of Collector  
Adsorption in Flotation Systems other than  
those used to recover Oxides

1.1 Adsorption of Flotation Collectors on Sulphide  
Minerals

Flotation of sulphide minerals is most commonly carried out using xanthate collectors.



The earliest spectroscopic studies of adsorption in mineral flotation systems were concerned with the adsorption of xanthate collectors on flotation minerals. Hagihara (1952) investigated the adsorption of sodium and potassium alkyl xanthates on galena (lead sulphide) by electron diffraction spectrometry. He placed cleaved samples of galena in aqueous xanthate solutions which were then removed and their electron diffraction patterns recorded. His studies indicated that under mildly oxidising conditions a monolayer of xanthate is attached to the surface by strong bonds between surface lead ions and the sulphur of the xanthate group, each surface lead ion being attached to only one xanthate (Fig.1). On more highly oxidised samples bulk lead xanthate was formed.

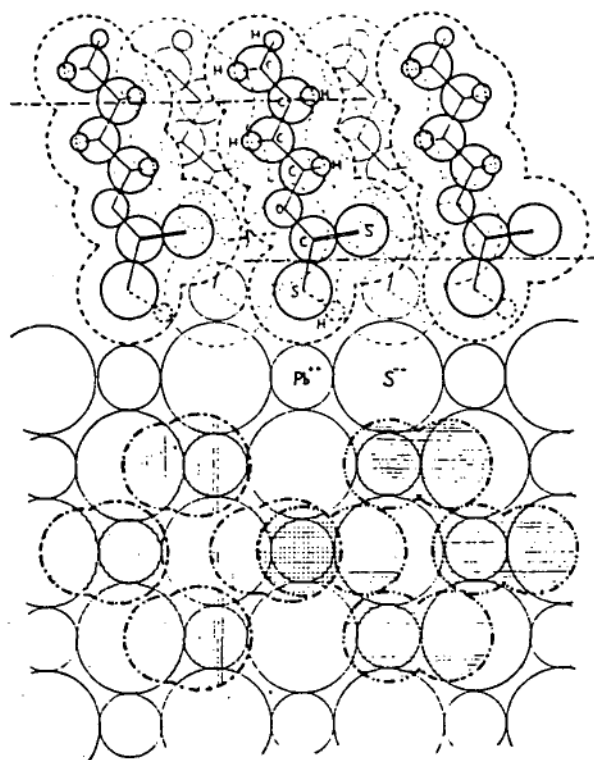


Fig. 1 Model of proposed xanthic acid collector film on galena. (From Hagihara, 1952.)

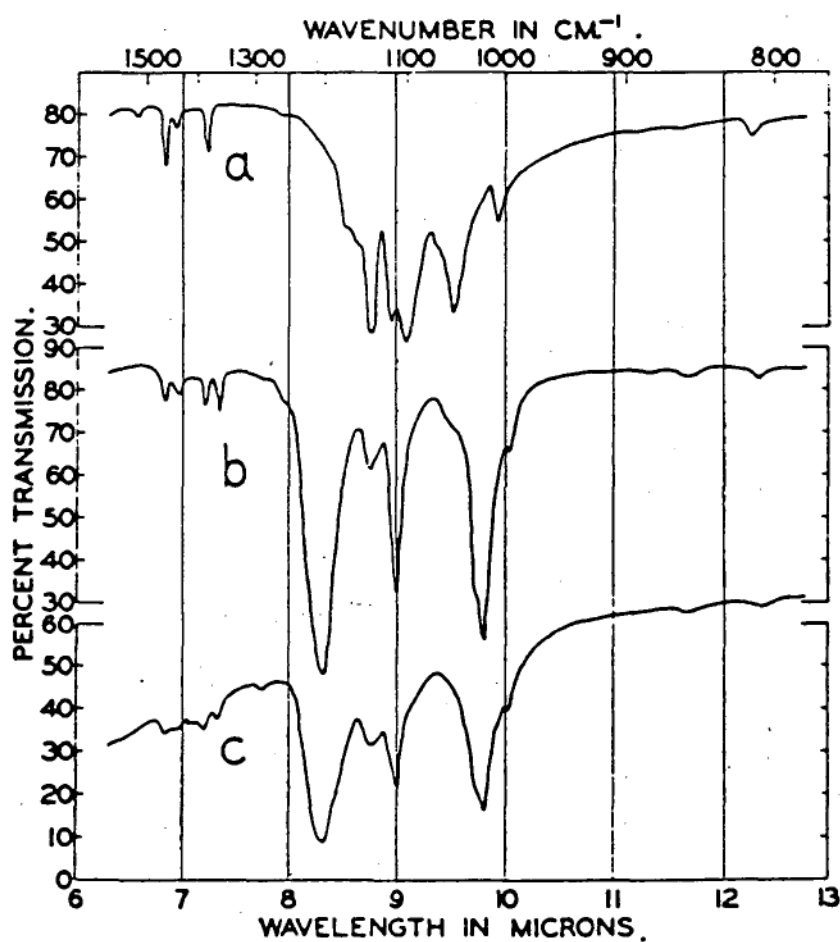
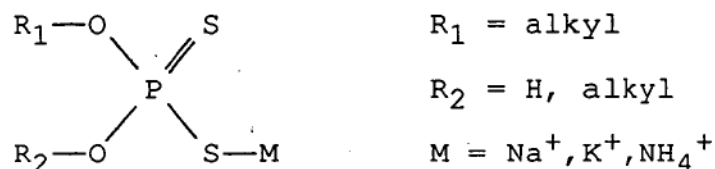


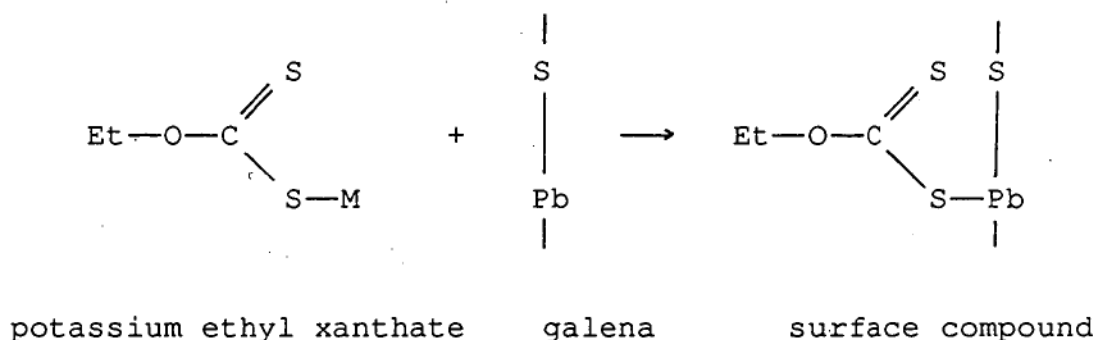
Fig. 2 Infrared spectra of potassium ethyl xanthate, lead ethyl xanthate and galena after treatment in KEX solution. (From Greenler, 1962.)

Hagihara and Uchikoshi (1954) extended this work to cover the adsorption of dithiophosphates

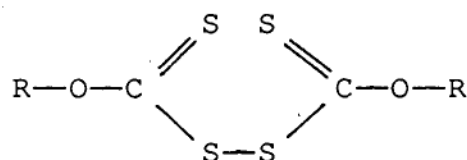


on galena finding a similar adsorption mechanism.

The first attempts to study the adsorption of xanthates on sulphides by infrared spectroscopy were made by Greenler (1962). Greenler precipitated lead sulphide from solution under homogenous conditions. He treated the precipitates with aqueous potassium ethyl xanthate and recorded the spectrum of the adsorbed xanthate using the KBr disc method. He compared the spectrum of the adsorbed xanthate with that of potassium ethyl xanthate and lead ethyl xanthate (Fig.2). Greenler concluded that the xanthate adsorbed by forming a surface compound of lead xanthate consistent with the earlier findings of Hagihara (1952) and Hagihara and Uchikoshi (1954) viz.



Leja, Little and Poling (1963,a,b) and Poling and Leja (1963) used infrared spectroscopy to study xanthate adsorption on vacuum deposited films of copper and lead sulphide. Their work was aimed at determining the mechanism of adsorption of the xanthate collector and the role of oxidation in sulphide flotation. At the time xanthate was thought to adsorb by either of two methods - an ion exchange mechanism involving replacement of previously adsorbed inorganic anions by xanthate anions or a hydrolytic or free acid mechanism involving hydrolysis of the xanthate anions to xanthic acid which can then adsorb as neutral molecular species. It had also been found that if oxygen is excluded from the flotation system xanthate collectors were incapable of rendering the sulphide surface hydrophobic. Hence a preliminary alteration of the adsorbant surface to an oxidation product was thought to be necessary for xanthate adsorption. It was also thought that xanthate oxidation may play an important part in the adsorption mechanism. Xanthate ions may be oxidised to the neutral molecule dioxanthogen



which then acts as the adsorbing species.

Previous work ( Little, Poling and Leja, 1961 ) in which they made infrared spectral band assignments for xanthates and dixanthogens allowed them to distinguish between adsorbates of this different species. In xanthates they assigned the  $1020$  to  $1050\text{cm}^{-1}$  band to the C=S stretching mode and the  $1100$  to  $1120\text{cm}^{-1}$  and  $1150$  to  $1265\text{cm}^{-1}$  bands to the C-O-C stretching vibrations (Fig.3). In dixanthogen a characteristic C-O stretching band occurs at  $1240$  to  $1265\text{cm}^{-1}$  whereas in the heavy metal xanthates it occurs at  $1150$  to  $1210\text{cm}^{-1}$ .

The studies of Leja, Little and Poling and Poling and Leja (1963) were conducted by either transmitting the infrared beams through an evaporated film or by subjecting it to multiple reflection from the sample using the apparatus shown in Figs.4 and 5. When oxidised or sulphidised copper films were treated with an aqueous solution of pure ( dixanthogen free ) potassium ethyl xanthate the spectra indicated that cuprous xanthate is the adsorbed species (Fig.6). However if treated with dixanthogen it was found that the dixanthogen dissociated on adsorption to form a layer of cuprous xanthate which physically co-adsorbed any excess of undissociated dixanthogen. The co-adsorbed dixanthogen imparted a greater hydrophobicity to the surface.

In the case of adsorption of xanthates on thin lead sulphide films it was found that before the xanthate was adsorbed onto the evaporated lead sulphide film, the spectrum showed intense adsorption bands in the region

	$\nu_{C=S}$	$\nu_{C-O-C}$	$\nu_{S-S}$
potassium ethyl xanthate	1015 1055	1107 1122 1145	
sodium ethyl xanthate	1010 1040	1115 1153 1170	
zinc (II) ethyl xanthate	1035	1130 1120	
copper (I) ethyl xanthate	1015 1040 1053	1127 1200	
diethyl dixanthogen	1020	1110 1153 1245	850

Fig. 3 Infrared spectral band assignments for xanthates and dixanthogen. (From Little, Poling, and Leja, 1961.)

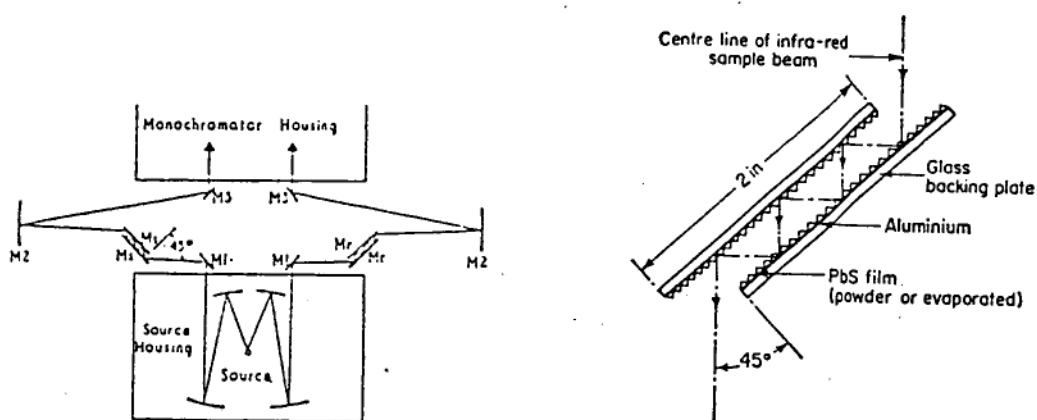


Fig. 4 Optical arrangement for multiple reflection spectral studies of adsorption of xanthates on PbS films. (From Leja, Little and Poling, 1963)

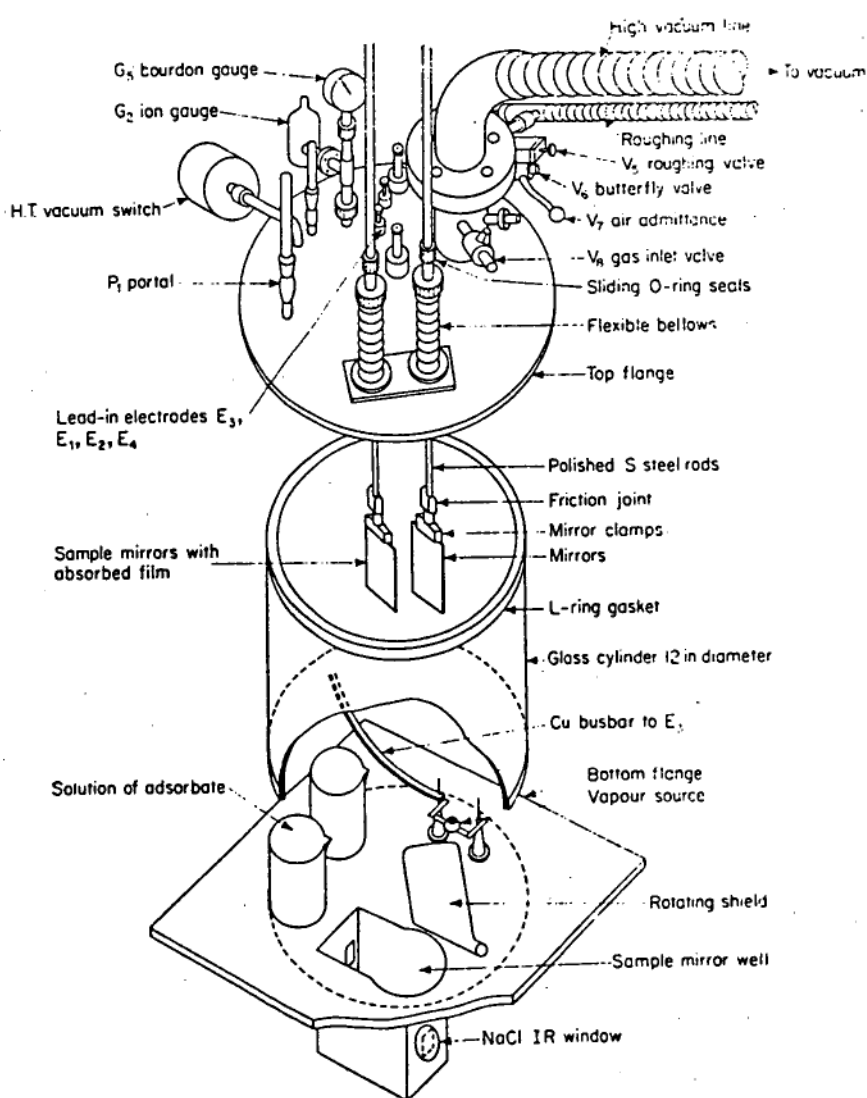


Fig. 5 Infrared vacuum cell for studying the adsorption of xanthates on PbS films. (From Poling and Leja, 1963)

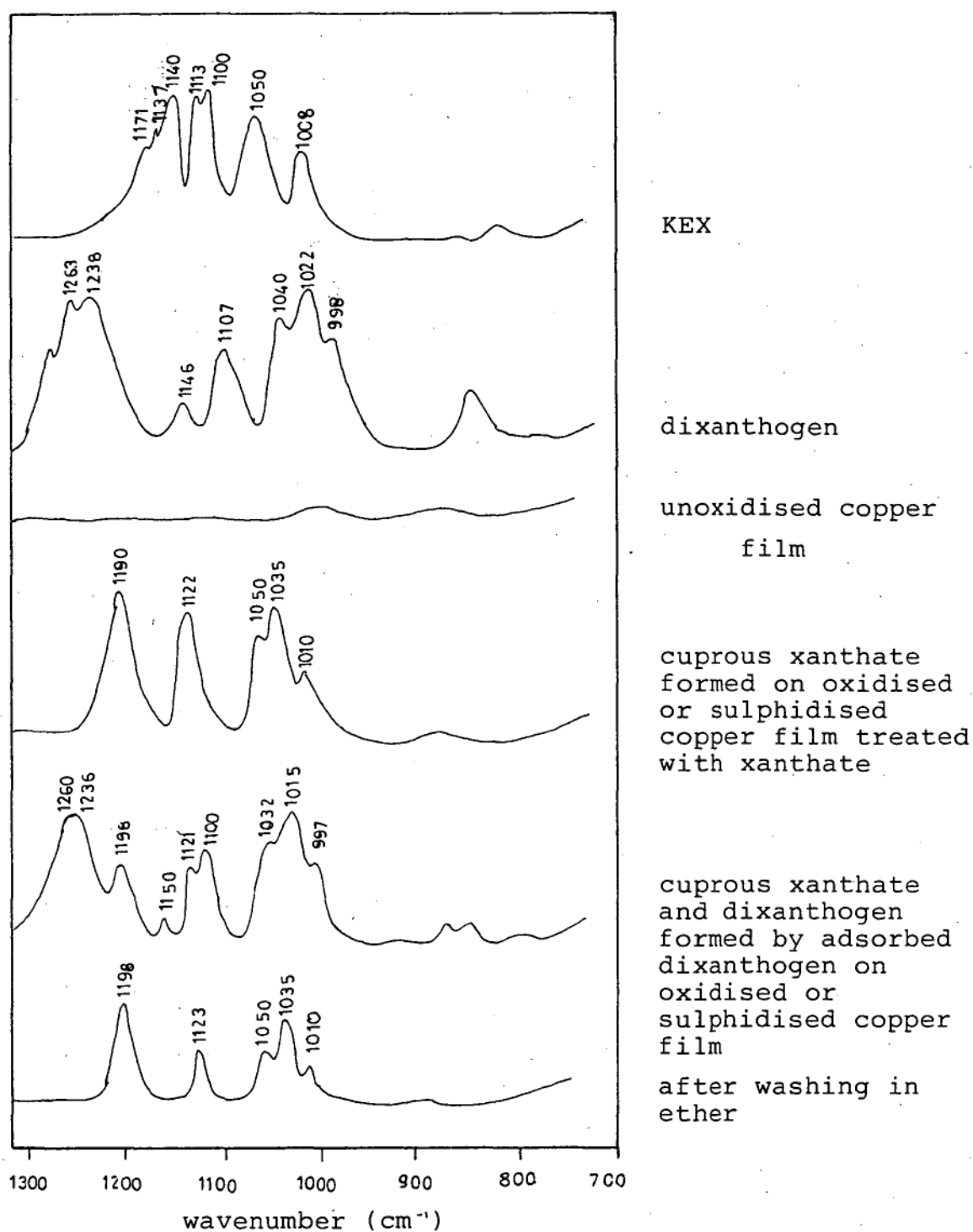


Fig. 6 Infrared spectra of xanthate species adsorbed on oxidised and sulphidised copper substrates.  
(From Leja, Little and Poling, 1963.)

1200-900 $\text{cm}^{-1}$ . These bands were shown to be due to atmospheric oxidation of the sulphide surface. From the spectra shown in Fig.7 the oxidation product on the surface can be shown to be lead thiosulphate,  $\text{PbS}_2\text{O}_3$ . The immersion of the lead sulphide in an aqueous solution of alkali metal xanthate resulted in the replacement of the lead thiosulphate surface film by a layer of lead xanthate. Prolonged washing of the lead xanthate layer with ether resulted in the partial restoration of the lead thiosulphate. Lead thiosulphate was probably formed by the atmospheric oxidation of the lead sulphide when the protective lead xanthate layer was removed. Pyridine completely removed the lead xanthate from the surface. The lead xanthate layers were also found to co-adsorb dixanthogen rendering the surface more hydrophobic as was the case for the copper films.

In the case where freshly deposited lead sulphide films were exposed to xanthate solutions in deoxygenated conditions no reaction took place confirming the importance of oxidation.

When dixanthogen was adsorbed onto the oxidised lead sulphide films a layer of lead xanthate was found to be formed followed by co-adsorbed dixanthogen (Fig.8). If fresh lead sulphide films were used under anoxic conditions the same lead xanthate layer was found to be formed followed by co-adsorbed dixanthogen.

From their work, Leja, Little and Poling concluded that the mechanism of adsorption of xanthates depends on

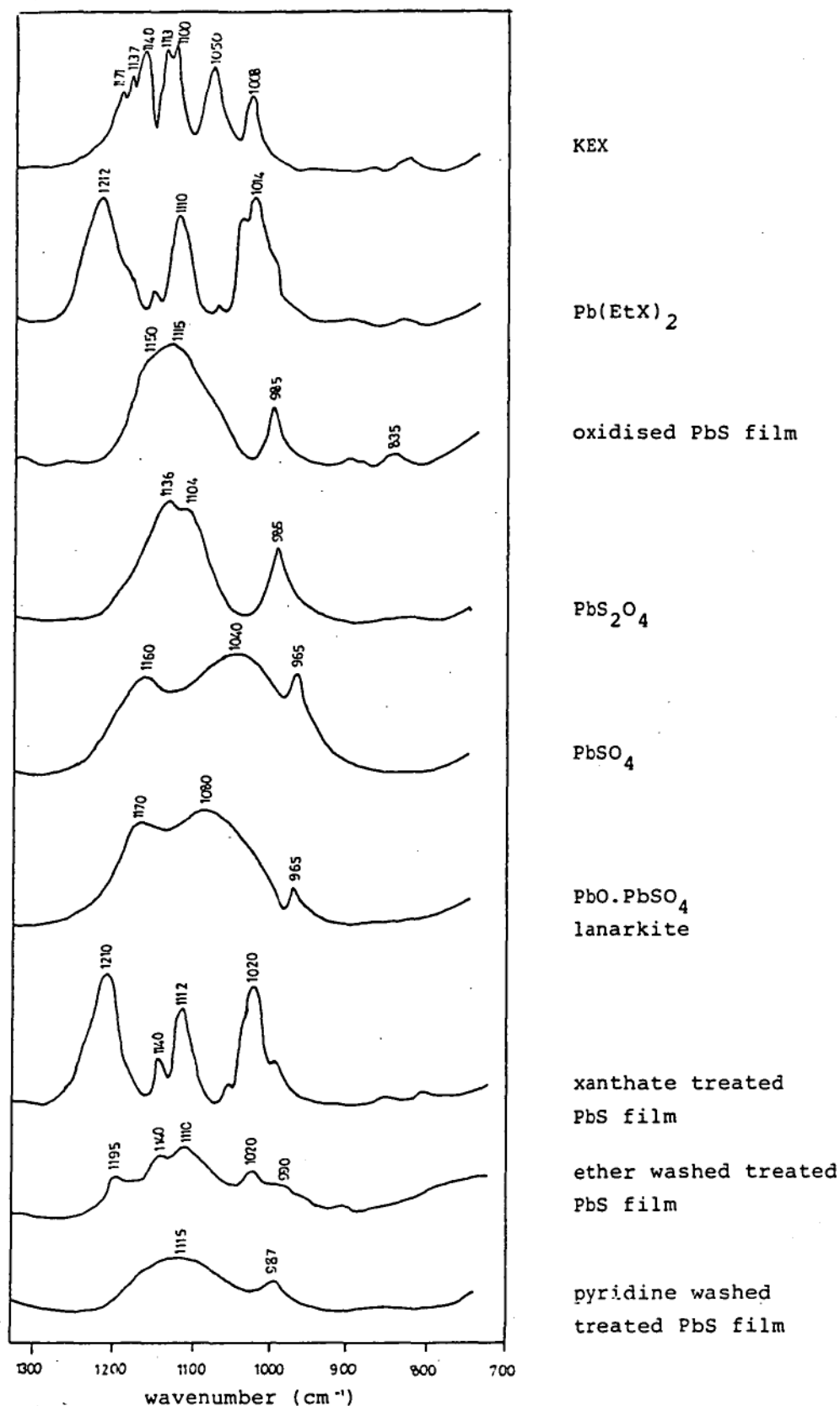


Fig. 7 . Infrared spectra of oxidised PbS films, bulk oxidation products, and products formed by the adsorption of ethyl xanthate on oxidised PbS films. (From Leja, Little and Poling, 1963.)

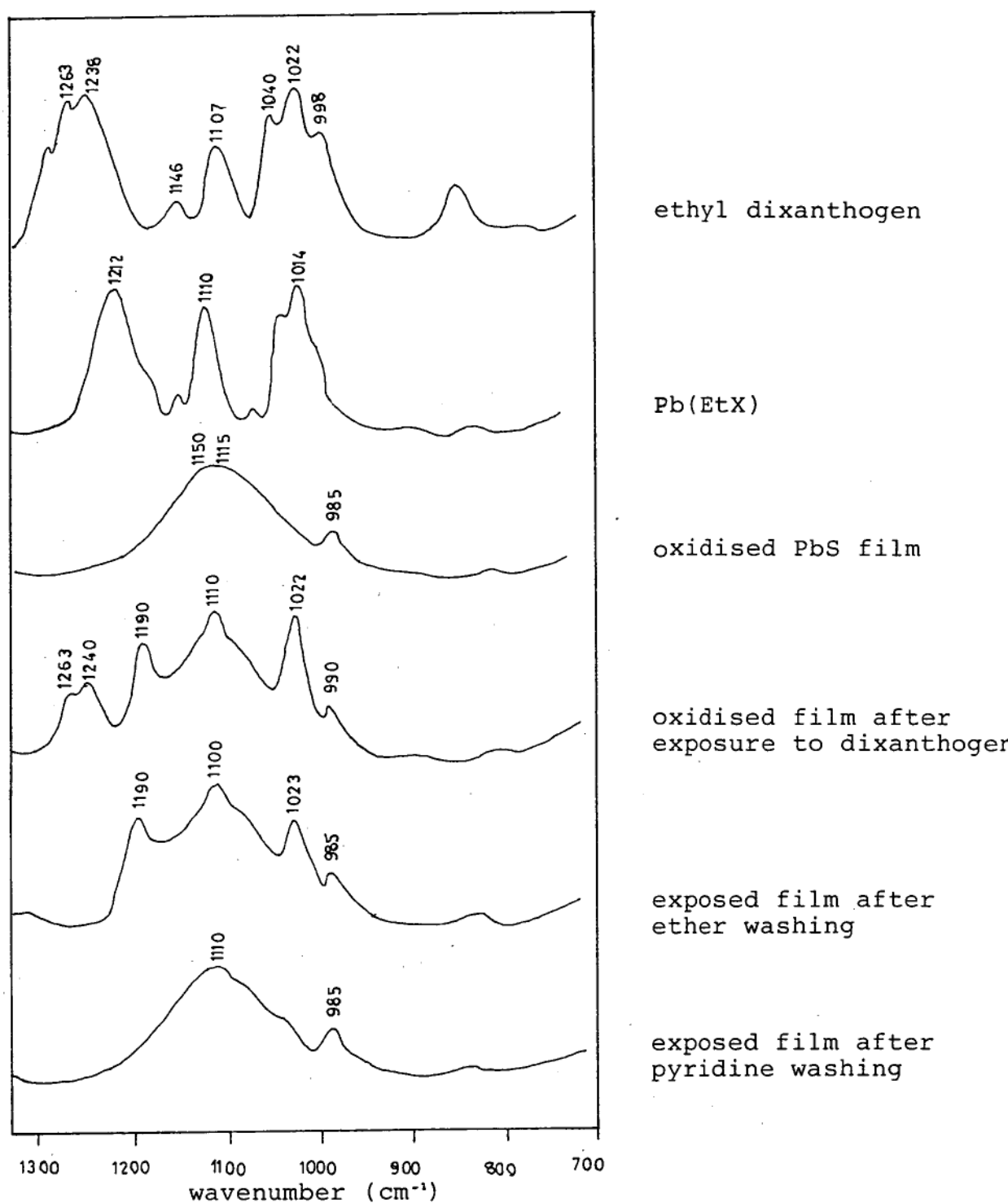


Fig. 8 Infrared spectra of products formed by adsorption of ethyl dixanthogen on oxidised PbS films. (From Leja, Little and Poling, 1963.)

the formation of dixanthogen and requires the presence of oxygen. They envisaged that :

- 1) xanthate was oxidised to dixanthogen in solution
- 2) dixanthogen is physically adsorbed on galena
- 3) adsorbed dixanthogen dissociates and reacts with lead xanthate to form lead xanthate
- 4) some dixanthogen becomes or remains physically co-adsorbed with the lead xanthate

They interpreted the shift in the C-O-C band observed in the spectra of xanthates adsorbed in near monolayer thicknesses as indicating a 1:1 co-ordination between the surface divalent metal (Pb or Cu) and the xanthate. In the overlying multilayers of adsorbed xanthate the 1:2 co-ordination is retained. They also interpreted the close similarity between the spectra of the first monolayer and the covalently bonded metal xanthate complexes as indicating that the chemisorption bonding is also covalent.

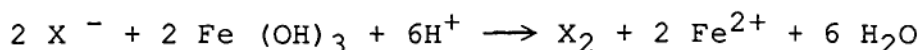
Yamasaki and Usui (1965) studied the adsorption of xanthate on sphalerite (zinc sulphide). Powdered sphalerite was surface oxidised by hydrogen peroxide before being treated with dodecyl xanthate. The treated sphalerite was examined using the KBr disc method. The spectra gave strong evidence for the presence of zinc xanthate but no trace of dixanthogen on the sphalerite surface.

Coleman and Powell (1966) carried out the first practical attempt to use the attenuated total reflectance technique to investigate the adsorption of xanthate on galena. They used a flat-sided polished galena sample which, after exposure to xanthate and drying, was pressed against an ATR element of thallium bromoiodide. However they met with little success, possibly because of the poor contact between the sample and the ATR plate.

Coleman, Powell and Cochran (1966) successfully used the ATR method to investigate the adsorption of ethyl xanthate on sphalerite activated copper sulphate. After treating the sphalerite with very concentrated solutions of copper sulphate and xanthate, drying and contacting the sample with the thallium bromoiodide ATR element they found peaks due to cuprous ethyl xanthate and ethyl dixanthogen.

Majima and Takeda (1968) studied the adsorption of xanthate and dixanthogen on pyrite (iron sulphide). They found that when using either collector, dixanthogen was present at the pyrite surface. They proposed an adsorption mechanism involving the catalytic oxidation of xanthate by oxygen at the pyrite surface to form dixanthogen.

Fuerstenau, Kuhn and Elgillani (1968) also detected the formation of dixanthogen at the surface of pyrite treated with xanthate which was examined in nujol mulls. They proposed a mechanism involving oxidation by surface ferric hydroxide followed by physical adsorption viz



Banerji (1968) examined the adsorption of xanthate on chalcopyrite ( $\text{CuFeS}_2$ ). He used a solvent extraction method to examine the infrared spectra of adsorption products formed when a chalcopyrite surface which had been oxidised with hydrogen peroxide was exposed to a solution of sodium ethyl xanthate. After exposure the adsorption product was extracted from the chalcopyrite surface with carbon disulphide and this solution allowed to evaporate on a sodium chloride disc. The spectrum of the evaporated extract showed the presence of both cuprous xanthate and dixanthogen. He proposed a three step mechanism to explain the presence of both xanthate and dixanthogen viz.

- 1)  $\text{CuS} + 2\text{O}_2 \longrightarrow \text{CuSO}_4$
- 2)  $\text{CuSO}_4 + 2 \text{NaEtX} \longrightarrow \text{Cu}(\text{EtX})_2 + \text{Na}_2\text{SO}_4$
- 3)  $2 \text{Cu}(\text{EtX})_2 \longrightarrow \text{Cu}_2(\text{EtX})_2 + (\text{EtX})_2$

Tipman and Leja (1969) used an ATR method to investigate the adsorption of potassium ethyl xanthate on thin copper films. Vacuum evaporated copper films were exposed to xanthate solutions, dried then pressed against a thallium bromoiodide ATR element. They found that with their ATR apparatus and grating spectrometer they would need an increase in surface area of 50 to 500 times or an increase in instrument sensitivity of 20 - 100 times in

order to measure coverages less than a monolayer ( in the region of adsorption where the majority of sulphide flotations were carried out ). Fuerstenau, Clifford and Kuhn (1974) examined the adsorption of xanthate on sphalerite. They used the KBr disc method to record the infrared spectra of sphalerite which had been contacted with hexyl xanthate at pH values of 5.5 and 10. At pH 5.5 the adsorbate showed adsorption bands indicating the formation of zinc xanthate on the surface. At pH 10 the infrared spectra showed bands indicating the formation of both zinc xanthate and dixanthogen.

Mielczarski, Nowak and Strojek (1980,a,b) have studied the adsorption of potassium ethyl xanthate on galena, powdered lead sulphide films by the ATR technique. Their studies were carried out in both oxidising (1980 a) and reducing (1980 b) conditions. In the studies involving galena and powdered lead sulphide the wet sample, after exposure to xanthate, was pressed against a germanium ATR element. The experiment with the chemically deposited lead sulphide films was carried out *in situ* using the flow cell used in Fig.9. In oxidising conditions ( exposure to air ) all samples showed surface oxidation and on contact with xanthate showed the formation of adsorbed layers of lead xanthate but no dixanthogen. In reducing conditions ( sample treated with sodium sulphite or ammonium acetate ) the lead xanthate layer formed was less than a monolayer in thickness, indicating that surface xanthate is necessary for xanthate

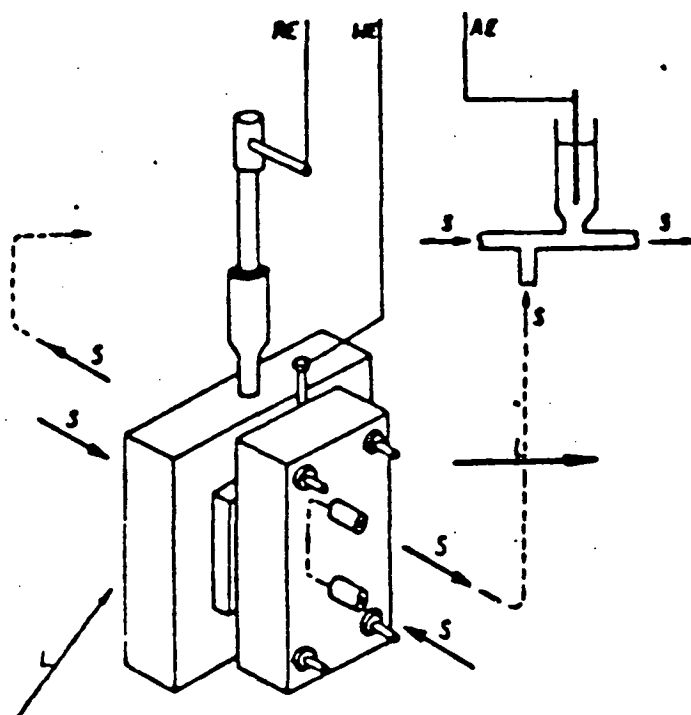


Fig. 9 Schematic view of an ATR cell for combined spectrophotometric and electrochemical measurements.  
 RE - reference electrode (saturated calomel electrode)  
 WE - working electrode (ATR element with a deposited lead sulphide film)  
 AE - auxiliary electrode (platinum wire)  
 S - solution  
 L - infrared beam  
 (From Mielczarski et al, 1981.)

adsorption.

Mielczarski, Nowak, Strojek and Pomianowski (1981) investigated the adsorption of xanthates and dixanthogens on galena, chalcocite ( $\text{Cu}_2\text{S}$ ) and sphalerite and synthetic  $\text{PbS}$ ,  $\text{Cu}_2\text{S}$  and  $\text{ZnS}$  using the ATR technique. Adsorption of xanthate on oxidised chalcocite and galena lead to the formation of copper (I) and lead (II) xanthates on the surface (Figs.10B,11A). The adsorption of xanthate on sphalerite occurs only if the sample has been previously activated by copper (II) salts. The xanthate adsorption product, in this case, is copper (I) ethyl xanthate (Fig.11B). At higher concentrations of the activating solution some dixanthogen was formed. Dixanthogen was also formed in some cases where xanthate was adsorbed on chalcocite. When dixanthogen was adsorbed on chalcocite both adsorbed copper (I) xanthate and dixanthogen were observed. From their studies they concluded surface oxidation or activation was necessary for xanthate adsorption but it was not possible to suggest a uniform mechanism of adsorption for all sulphide minerals.

Recently Fourier transform infrared diffuse reflectance spectroscopy has been used to study the adsorption of potassium n amyl xanthate on galena (Kongolo et al. 1984). Kongolo et al. (op cit.) found that  $-15\mu\text{m}$  galena which had been exposed to air showed reflectance bands due to surface lead sulphate, lead thiosulphate and lead carbonate (Fig.12). After flotation with  $10^{-2}$

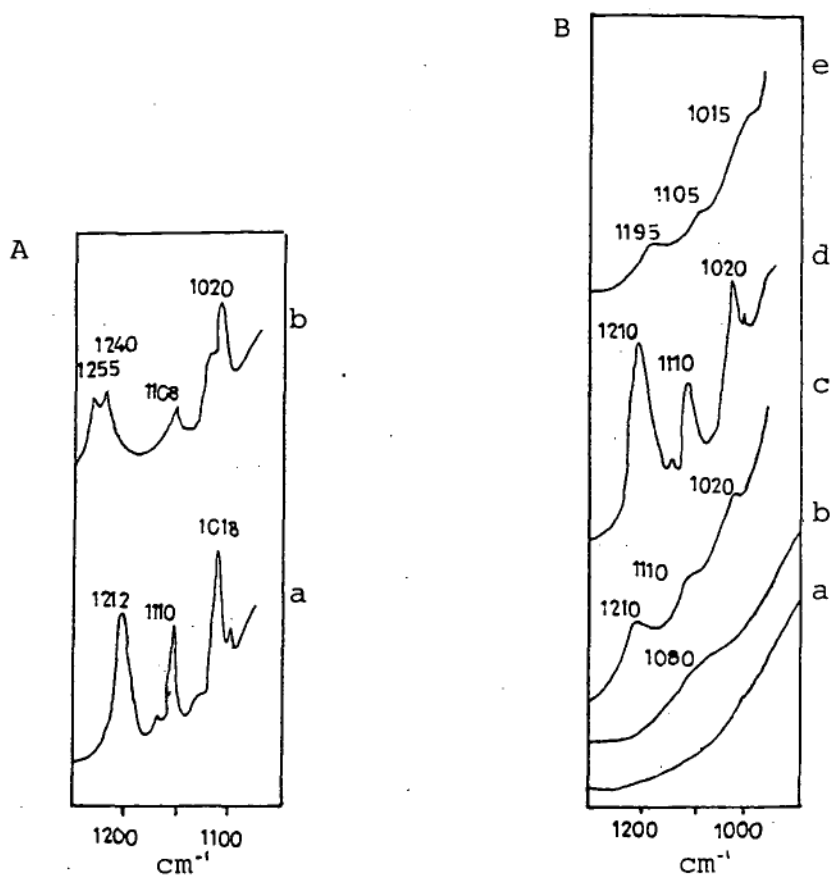


Fig.10 A. ATR spectra of:

- a - lead ethyl xanthate
- b - ethyl dixanthogen

B. ATR spectra of galena samples:

- a - immediately after grinding
- b - one month after grinding
- c - freshly ground sample after treatment with xanthate solution
- d - sample exposed to air for a month after treatment with xanthate solution
- e - sample exposed to air for a month, washed with ammonium acetate, then treated with xanthate solution

(From Mielczarski et al, 1981.)

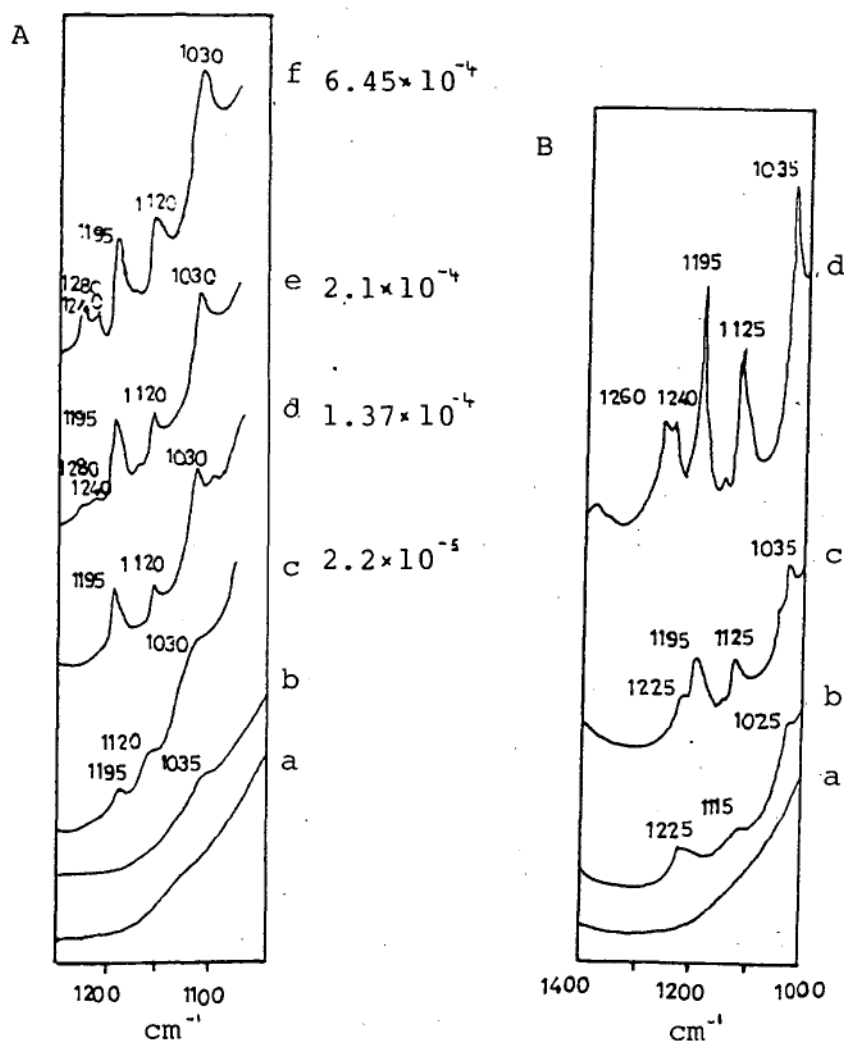


Fig. 11A. ATR spectra of chalcocite samples:

- a - immediately after grinding,
- b - one month after grinding,
- c, d, e, f - after treatment with xanthate solutions of various concentrations.

B. ATR spectra of synthetic ZnS samples treated with xanthate solution:

- a - unactivated sample,
- b - sample activated with acidic  $\text{CuSO}_4$  solution,
- c - sample activated by prolonged contact with acidic  $\text{CuSO}_4$  solution,
- d - sample activated with concentrated basic  $\text{CuSO}_4$  solution.

(From Mielczarski et al, 1981.)

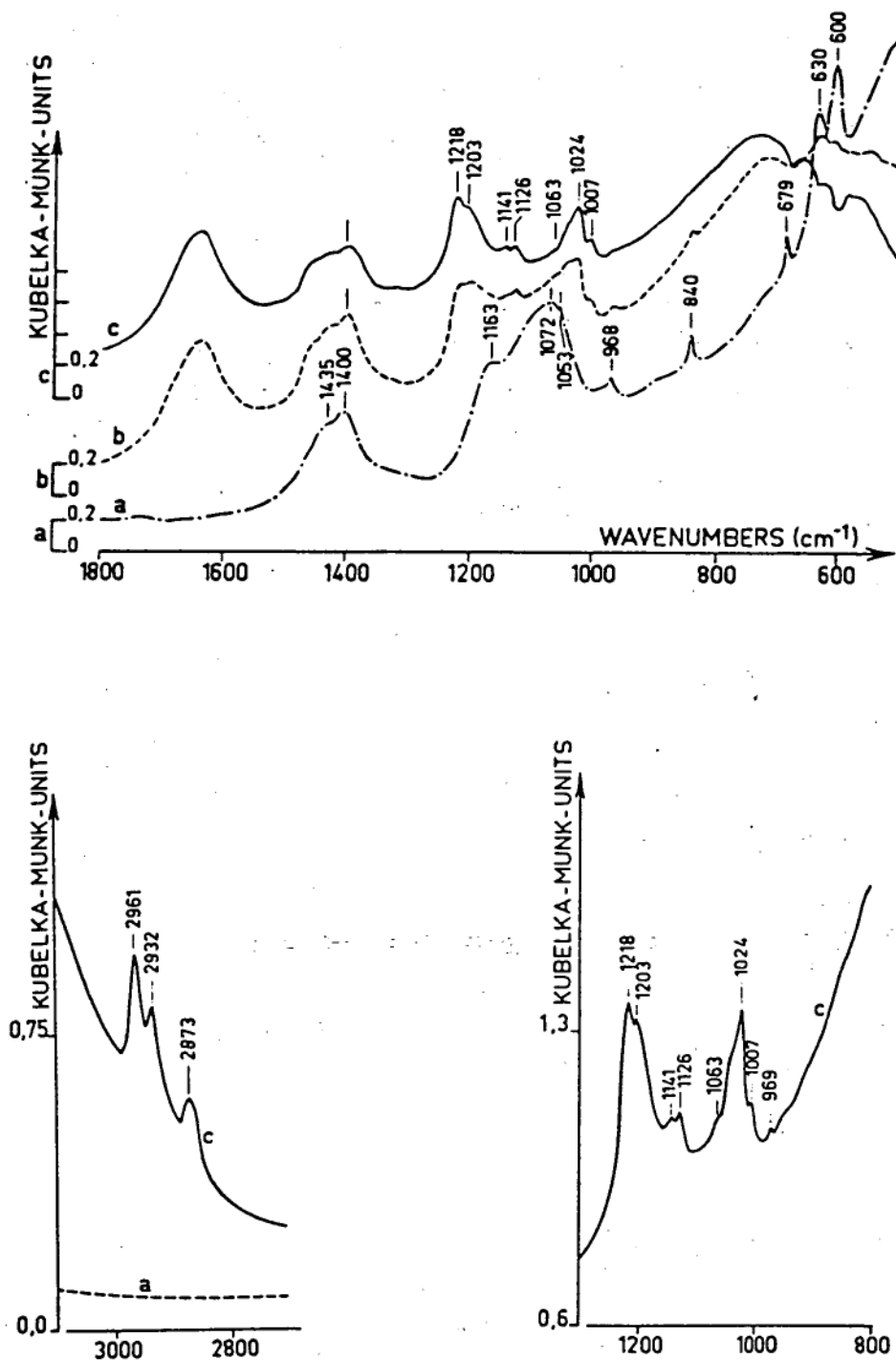


Fig. 12 FTIR diffuse reflectance spectra of -15μm galena

- a - before conditioning
- b - after flotation with  $10^{-2}$  mol l<sup>-1</sup> potassium n-amyl xanthate
- c - difference spectrum

mole<sup>-1</sup> potassium n amyl xanthate bands due to adsorbed xanthate are present. The difference spectrum (Fig.12) shows bands at 1218 cm<sup>-1</sup> and 1024 cm<sup>-1</sup> which they attributed to surface -PbAX.

X-ray photoelectron spectroscopy (XPS), also known as Electron Spectroscopy for Chemical Analysis (ESCA) has recently been applied to the study of flotation reagents adsorbed on minerals

Manocha and Park (1977) used XPS to study galena surfaces after exposure to air and to aqueous environments. Their results showed that the major oxidation process is PbSO<sub>4</sub>, however small quantities of elemental sulphur were detected during the early stages of oxidation.

Predali, Brion, Hayer and Pelletier (1979) used XPS to investigate the surface alteration of the components of a pyritic copper-lead-zinc ore during flotation in order to establish a mechanism for pyrite depression. They concluded that pyrite depression occurred through the formation of an iron oxide-hydroxide or hydroxide on the pyrite surface when treated with the depressants NaCN, CaO, CuSO<sub>4</sub> and ZnSO<sub>4</sub>.

Brion (1980) studied the changes on the surfaces of pyrite, chalcopyrite, sphalerite and galena on exposure to air and water. In air the rate of oxidation decreased in the order FeS<sub>2</sub> > CuFeS<sub>2</sub> > PbS > ZnS, whereas on exposure to water only CuFeS<sub>2</sub> showed any sign of surface oxidation with the formation of iron oxide-hydroxide or hydroxide

within the first few layers.

Ranta et al studied the adsorption of xanthate on copper sulphide using XPS. The XPS spectrum of copper sulphide before and after treatment with xanthate is shown in Fig.13. The S(2p), emission from the copper sulphide shows very little shift after xanthate adsorption. The C(1s) emission for the KEX treated sample shows, in addition to a contamination line at 285.0 eV another line at 1.6 eV higher binding energy. This is due to the carbon atoms of the xanthate ion. Theoretically the binding energies of the three carbon atoms in ethyl xanthate are all different ( $C^I H_3 C^{II} H_2 O C^{III} S_2$ ). Ranta et al contend that the  $C^I$  emission coincides with the contamination line and that the  $C^{II}$  emission occurs at ~ 286.5 eV and the  $C^{III}$  emission at 286.2 eV, too close to be resolved. The O(1s) emission lines for the copper sulphide prior to xanthate adsorption consist of two badly resolved components at 530.4 eV and 531.4 eV assigned to  $Cu_2O$  and adsorbed oxygen from the atmosphere. Upon xanthate adsorption a new peak at a binding energy of 532.9 eV is present due to the C-O-C group and the peak due to atmospheric contamination is absent.

XPS has been recently used to study the oxidation of sulphide minerals which occur in flotation systems ( Buckley and Woods 1983, 1984a,b,1985 ). These studies were initiated to determine the source of the natural hydrophobicity of most sulphides which allows the minerals to adhere to rising gas bubbles in the flotation process

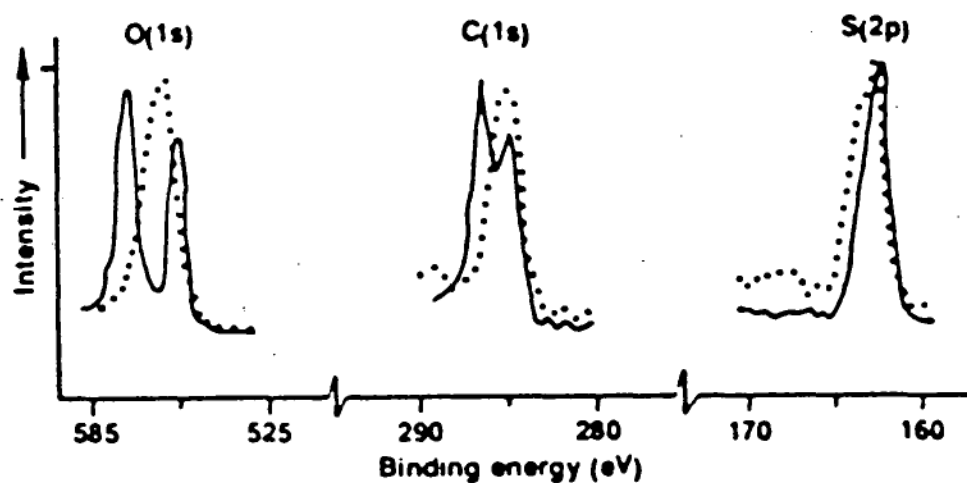


Fig.13 XPS spectrum of copper sulphide before (...) and after (—) treatment with potassium ethyl xanthate. (From Ranta et al, 1981.)

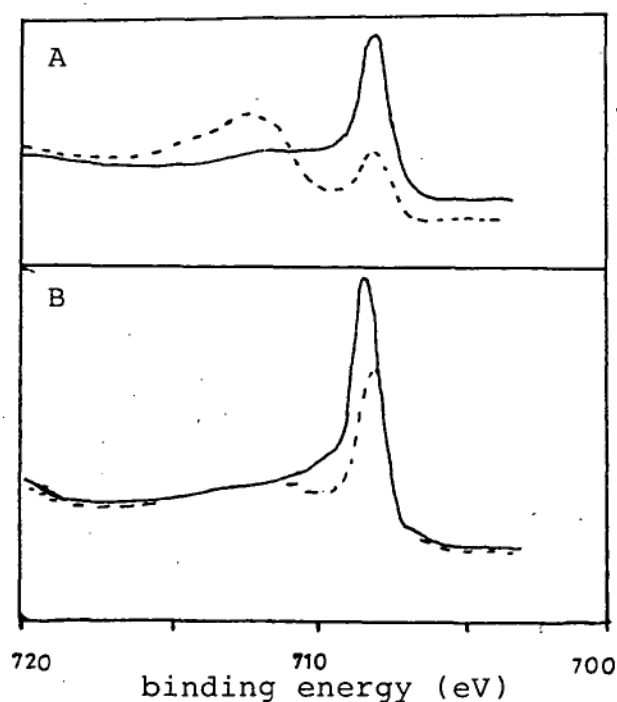


Fig.14 Fe<sub>2</sub>p<sub>3/2</sub> XPS spectra of pyrite samples before (--) and after (—) treatment with potassium ethyl xanthate:

A - with O<sub>2</sub> bubbling

B - with N<sub>2</sub> bubbling

(From Pillai et al, 1985.)

without the addition of surfactants ("collectorless flotation"). It is generally agreed that oxidising conditions are necessary for sulphide minerals to be naturally floatable but the nature of the surface species imparting hydrophobicity remains a topic of debate (although it is most commonly thought to elemental sulphur).

Buckley and Woods (1983, 1984 a,b, 1985) examined the fracture surfaces of galena, chalcopyrite, bornite ( $\text{Cu}_5\text{FeS}_4$ ) and pyrrhotite ( $\text{Fe}_{1-x}\text{S}$ ) by XPS and found no evidence of the formation of elemental sulphur other than at very high oxidation potentials. Initial oxidation of the sulphides involves migration of metal atoms from the surface layers leaving a sulphide lattice essentially unaltered from that in the original material. The metal atoms which have migrated form a hydroxyoxide covering the metal-deficient sulphide. While a metal-deficient sulphide would be expected to be hydrophobic, collectorless flotation does not occur in basic solutions when metal oxides are also formed at the surface. If these metal oxides remained as an overlayer the surface would be expected to be hydrophilic, however it is possible that the oxides are removed from the surface in the turbulent environment of the flotation cell.

Pillai, Young and Bockris (1985) have recently investigated the adsorption of xanthate on pyrite using XPS. (Fig.14) They found that in oxygenated solution the pyrite surface was extensively oxidised to hydrated  $\text{FeOOH}$

, and adsorbed  $\text{SO}_2$  and  $\text{SO}_3$  were found on the surface. XPS shows that adsorbed xanthate and  $\text{Fe(III)}$ -xanthate complexes are only minor forms of xanthate on the surface. Dixanthogen could not be observed by this technique since the melting point of ethyl dixanthogen is so low ( $28-32^\circ\text{C}$ ) that it is pumped away by the vacuum system of the spectrometer.

Pillai, Young and Bockris have also used XPS to study the adsorption of xanthate on galena but their results have not yet been published.

## 1.2 Adsorption of Flotation Collectors on Silicate Minerals

Peck and Wadsworth (1967 a) studied the adsorption of oleic acid on phenacite ( $\text{Be}_2\text{SiO}_4$ ). Examinations of the phenacite after contact with oleic acid by the KBr disc method shows the presence of chemisorbed oleate by the band at  $1623\text{cm}^{-1}$  due to the asymmetric C=O stretch. Physisorbed oleic acid was found to be present from the  $\nu$  C=O band at  $1708\text{cm}^{-1}$ . Again change in flotation behaviour with pH directly correlated with change in quantity of adsorbed oleate.

Peck and Wadsworth (1967 b) also investigated the adsorption of oleic acid on beryl ( $\text{Be}_3\text{Al}_2\text{Si}_6\text{O}_{16}$ ) which had been activated with hydrofluoric acid. In this case they found that only free oleic acid was found on the surface of the beryl and not chemisorbed oleate. Physisorbed oleic acid was detected from the  $\nu$  C=O peak at  $1708\text{cm}^{-1}$ . They concluded that hydrofluoric acid activates the beryl surface for oleic acid attachment via hydrogen bonds.

Dixit and Biswas (1973) used infrared spectroscopy to investigate the flotation of zircon ( $\text{ZrSiO}_4$ ) with sodium oleate. The adsorption of oleate on the zircon surface was examined using the KBr disc method. They found a peak at  $1700\text{cm}^{-1}$  in the spectra of the adsorbate corresponding to physically adsorbed oleic acid dimers but no evidence of chemisorbed oleate. They concluded that adsorption was due to van der Waal's interactions between the collector

and mineral surface.

Palmer et al (1975) studied the adsorption of hydroxamate collectors on chrysocolla ( $\text{CuSiO}_4$ ) and rhodonite ( $\text{MnSiO}_4$ ). They used the KBr disc method to record the infrared spectra of hydroxamate species adsorbed on powdered mineral samples which had been in contact with solutions of potassium octyl hydroxamate. The spectra of rhodonite and chrysocolla after contact with the hydroxamate solution are shown in Figs.15 and 16 along with the spectra of manganous octyl hydroxamate and cupric octyl hydroxamate. They concluded that the collector attached to the mineral surface by a chemisorption process. However flotation was only possible in the pH range where the metals could hydrolyse from  $\text{Mn}^{2+}$  to  $\text{MnOH}^+$  and  $\text{Cu}^{2+}$  to  $\text{CuOH}^+$ . Hence mineral dissolution and metal ion hydrolysis are intimately involved in the adsorption process (Fig.17).

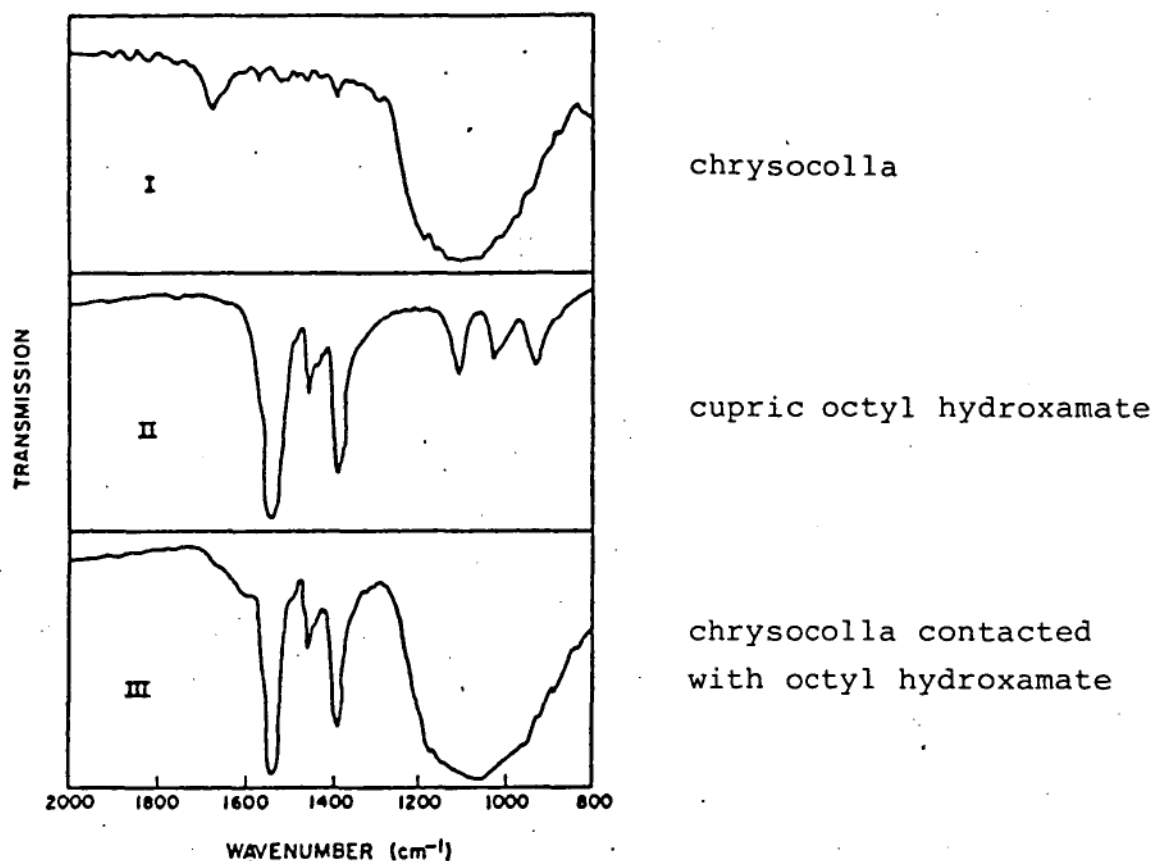


Fig. 15 Infrared spectra of chrysocolla, cupric octyl hydroxamate and chrysocolla contacted with octyl hydroxamate. (From Paterson et al, 1975)

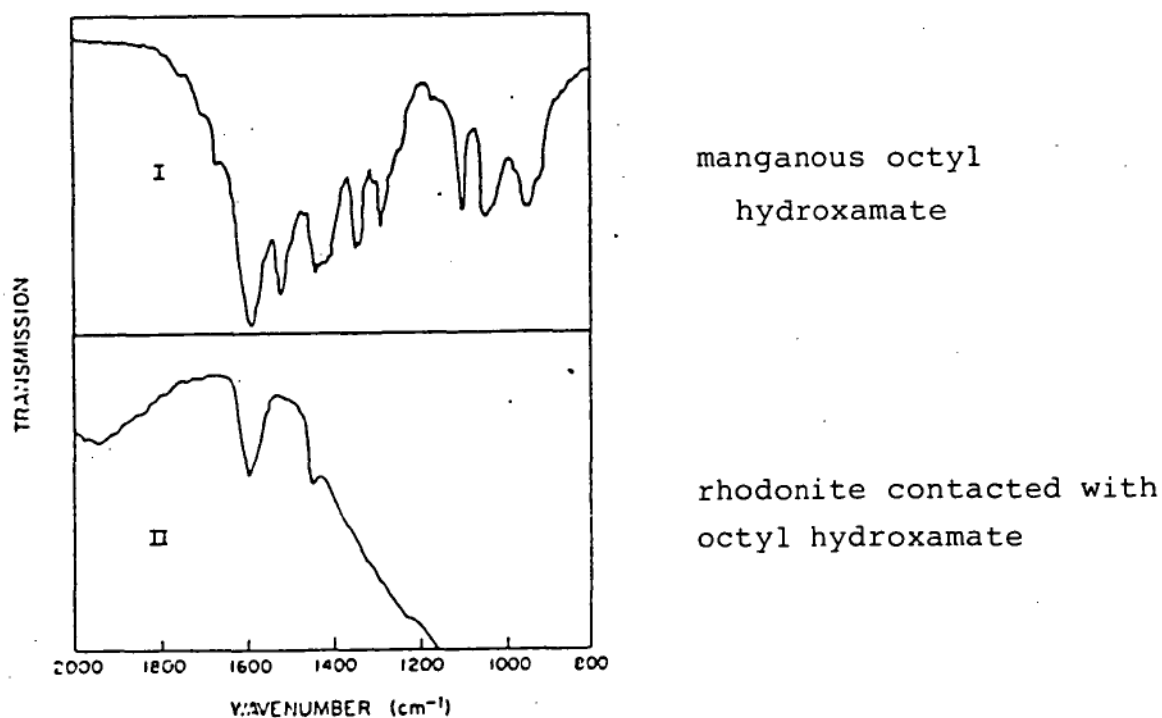
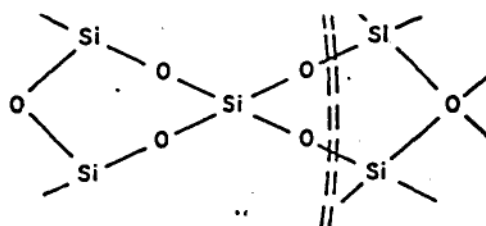
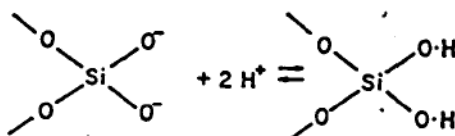


Fig. 16 Infrared spectra of manganous octyl hydroxamate and rhodonite contacted with octyl hydroxamate. (From Paterson et al, 1975)

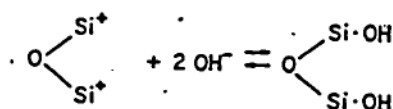


Plane of Fracture

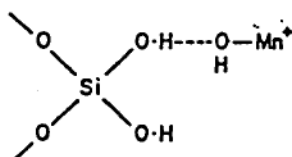
Hydrogen ion can adsorb on oxide sites:



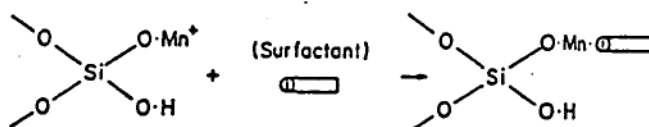
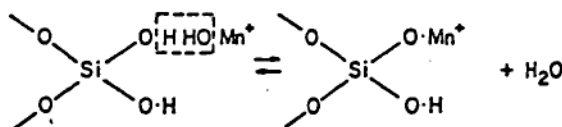
and hydroxyl ion on silicon sites:



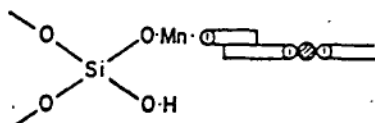
Hydrogen bonding could occur between adsorbed hydrogen ion and the complex:



or adsorption of  $\text{MnOH}^+$  could occur by splitting out water:



Precipitated metal-surfactant could adsorb via hydrocarbon chain association:



where

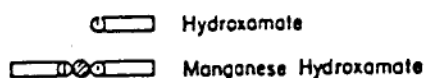


Fig.17 Mechanism of hydroxamate adsorption on rhodonite. (From Palmer et al, 1975.)

### 1.3 Adsorption of Flotation Collectors on Semi-soluble Salt Minerals

The first application of infrared spectroscopy to the study of adsorption of flotation minerals was carried out in 1954 when French, Wadsworth, Cook and Cutler (1954) investigated the adsorption of sodium oleate solution on fluorite. After washing and drying the fluorite was examined by the KBr disc method. Carboxylate groups were present in the spectrum of the treated fluorite and were presumed to be adsorbed mainly as calcium oleate. In addition some undissociated oleic acid was detected. This could be removed by washing with acetone, so was believed to be physically adsorbed. After the acetone washing the adsorbed layer due to calcium oleate remained.

Peck (1963, quoted in Giesecke, 1983) studied the adsorption of oleic acid and sodium oleate on fluorite, calcite and barite. He found in all cases that both chemisorbed and physisorbed oleate were present at the mineral surfaces.

Shergold (1972) studied the adsorption of sodium dodecyl sulphate on fluorite using a KBr disc technique to record the spectra of surface products. He compared the spectrum of the dodecyl sulphate species adsorbed on precipitated calcium fluoride and natural fluorite with that of sodium dodecyl sulphate, calcium dodecyl sulphate, and dodecyl sulphuric acid and mixtures of SDS and CDS. His studies showed that the surface compound was

not the same as any of the reference samples. His findings suggested that the adsorption of dodecyl sulphate is predominantly a chemisorption process, resulting in the formation of calcium dodecyl sulphate on the surface although the exact nature of this surface compound could not be determined.

Lovell, Goold and Finkelstein (1974) investigated the adsorption of sodium oleate and oleic acid on fluorite. Again the KBr disc method was used. Figure.18 shows the infrared spectra of sodium oleate and calcium oleate, while Figure.19 shows the spectra of sodium oleate adsorbed on fluorite. The spectra of sodium oleate adsorbed on fluorite shows peaks at  $1613\text{cm}^{-1}$  and  $1562\text{cm}^{-1}$ . The peak at  $1613\text{cm}^{-1}$  corresponds to a chemisorbed surface calcium oleate and the peak at  $1562\text{cm}^{-1}$  to both surface calcium oleate and physically adsorbed sodium oleate. They concluded that there was strong evidence for both physically and chemically adsorbed oleate on the fluorite surface.

Plitt and Kim (1974) studied the adsorption of oleate on barite by the KBr disc method. They used the bands at  $1710\text{cm}^{-1}$  and  $1560\text{cm}^{-1}$  for the quantitative determination of free oleic acid and sodium oleate respectively. The asymmetrical peak at  $2920\text{cm}^{-1}$  corresponding to the  $\text{CH}_2$  stretching frequency was used to determine the total oleate adsorbed. At pH values higher than 10 only sodium oleate was observed at the surface. Both sodium oleate and oleic acid are present in the pH range 6-10. The

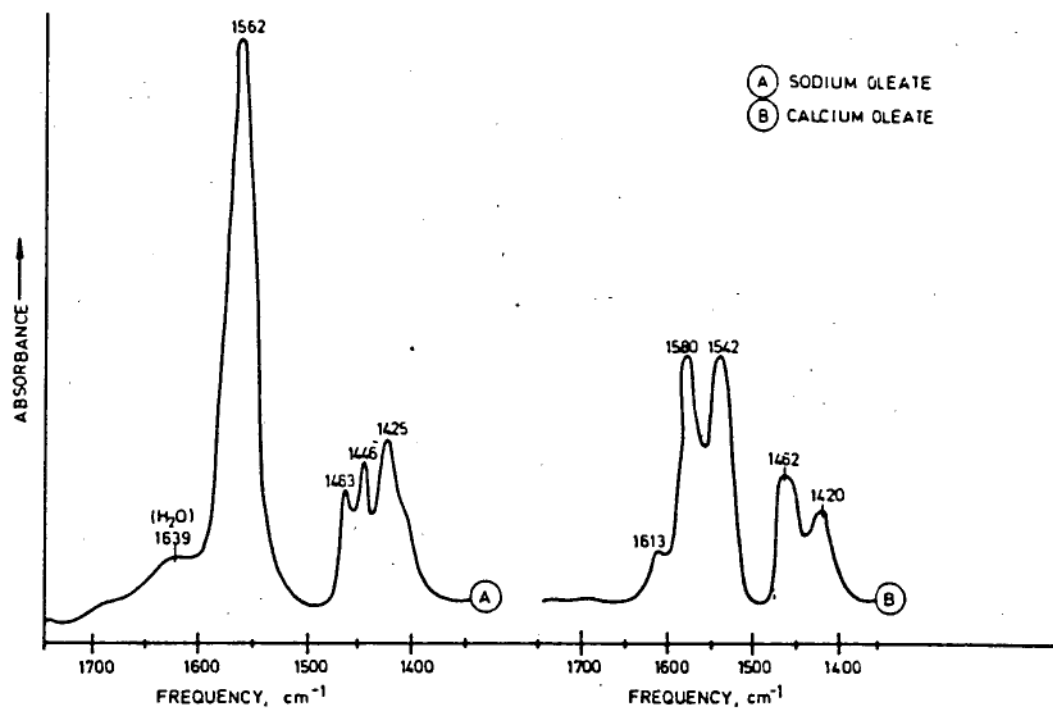


Fig.18 Infrared spectra of sodium oleate and calcium oleate.  
(From Lovell et al, 1974)

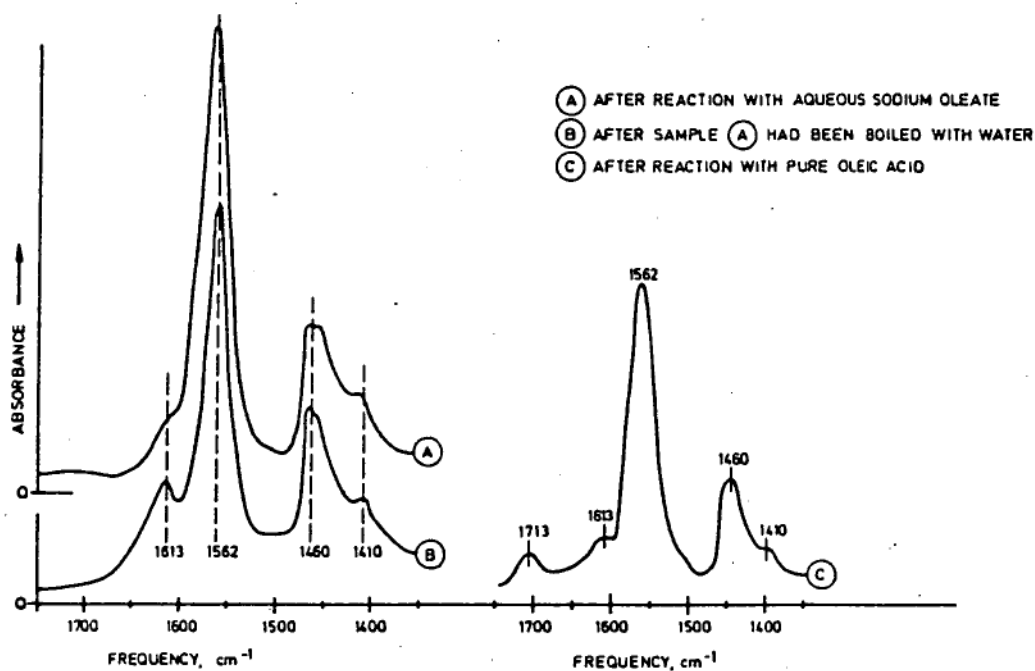


Fig.19 Infrared spectra of calcium fluoride after treatment  
with oleate. (From Lovell et al, 1974)

bands of barium oleate were not observed throughout the experiment.

A major problem with the study of oleate adsorption is the relatively small differences in positions of the carboxylate adsorption bands for sodium (physisorbed and chemisorbed), calcium, barium and other oleates. This makes definitive recognition of the surface compound difficult.

Iskra and Kielkowska (1980) studied the adsorption of oleate on fluorite in the presence of depressant quebracho (a polyphenol extracted from the tannin of a South American tree). The adsorption of oleate and quebracho on fluorite was followed using an *in situ* ATR technique in which a thin film of fluorite was vacuum evaporated onto a germanium ATR element. The infrared spectra of the adsorbate confirmed their contention that the di- and trihydric phenol groups of the quebracho interact with the mineral surface. Their studies suggest that the mechanism for the depression of fluorite by quebracho is by competitive adsorption of the depressant and the collector at the mineral surface.

Mielczarski, Nowak and Strojek (1983) used an *in situ* ATR method to study the adsorption of sodium dodecyl sulphate on fluorite. Again the fluorite was deposited as a vacuum evaporated film on a germanium ATR element. On exposure to sodium dodecyl sulphate they found that the spectra of the adsorbed product differed from the spectra of both sodium dodecyl sulphate and calcium dodecyl

sulphate (Figs.20A and B). They concluded that the adsorption product consisted of two layers - a chemisorbed layer of dodecyl sulphate and a physisorbed layer of calcium dodecyl sulphate. They suggest that the concentration of  $\text{Ca}^{2+}$  ions from the fluorite in solution and the presence of other ions which form sparingly precipitates with dodecyl sulphate ions (eg  $\text{Ba}^{2+}$ ) play an important role in the fluorite - sodium dodecyl sulphate system.

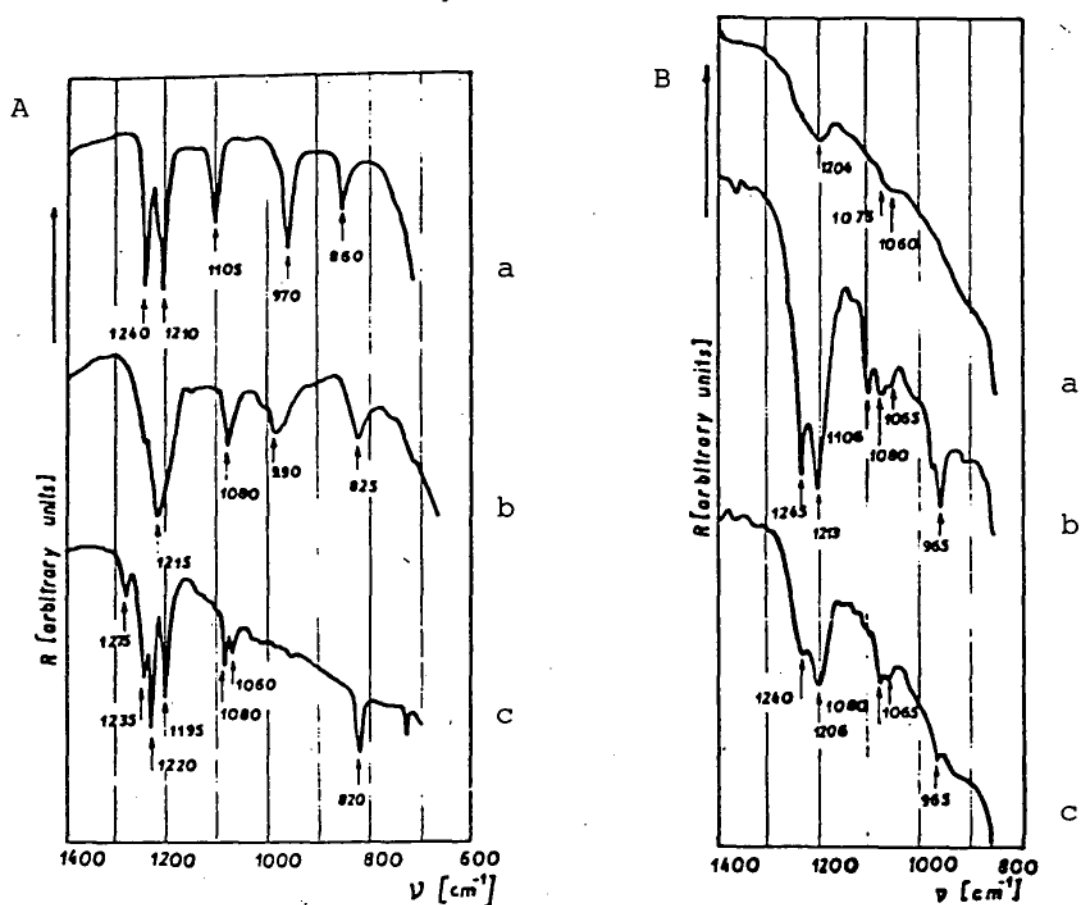


Fig.20 A. ATR spectra of:

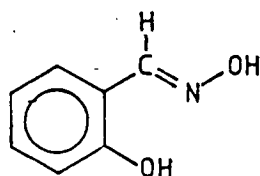
- a - calcium dodecyl sulphate
- b - sodium dodecyl sulphate
- c - barium dodecyl sulphate

B. ATR spectra of the products of sodium dodecyl sulphate adsorption on the surface of thin films of calcium fluoride:

- a - after 30 minutes of adsorption in  $5 \times 10^{-4} \text{ mol l}^{-1}$  sodium dodecyl sulphate solution
  - b - after 30 minutes of adsorption in  $8 \times 10^{-4} \text{ mol l}^{-1}$  sodium dodecyl sulphate solution
  - c - sample treated in b after washing in water
- (From Mielczarski et al, 1983.)

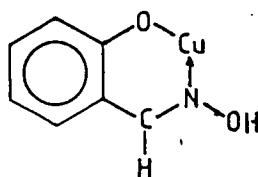
#### 1.4 Adsorption of Flotation Collectors on Carbonate Minerals

Cecile et al (1981) investigated the adsorption of the complexing collector salicylaldoxime

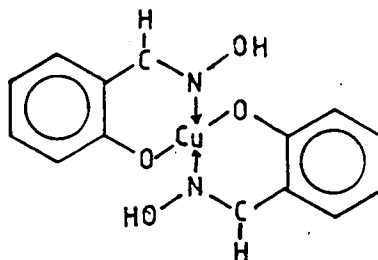


on malachite (  $\text{Cu}(\text{OH})\cdot\text{CuCO}_3$  ).

Salicylaldoxime is used as a collector for the selective flotation of oxidised copper ores. They used the KBr disc method to record the spectrum of malachite treated with salicylaldoxime which is shown in Fig.21 along with the spectra of the two copper complexes :



mono-salicylaldoximato copper (II)



bis-salicylaldoximato copper (II)

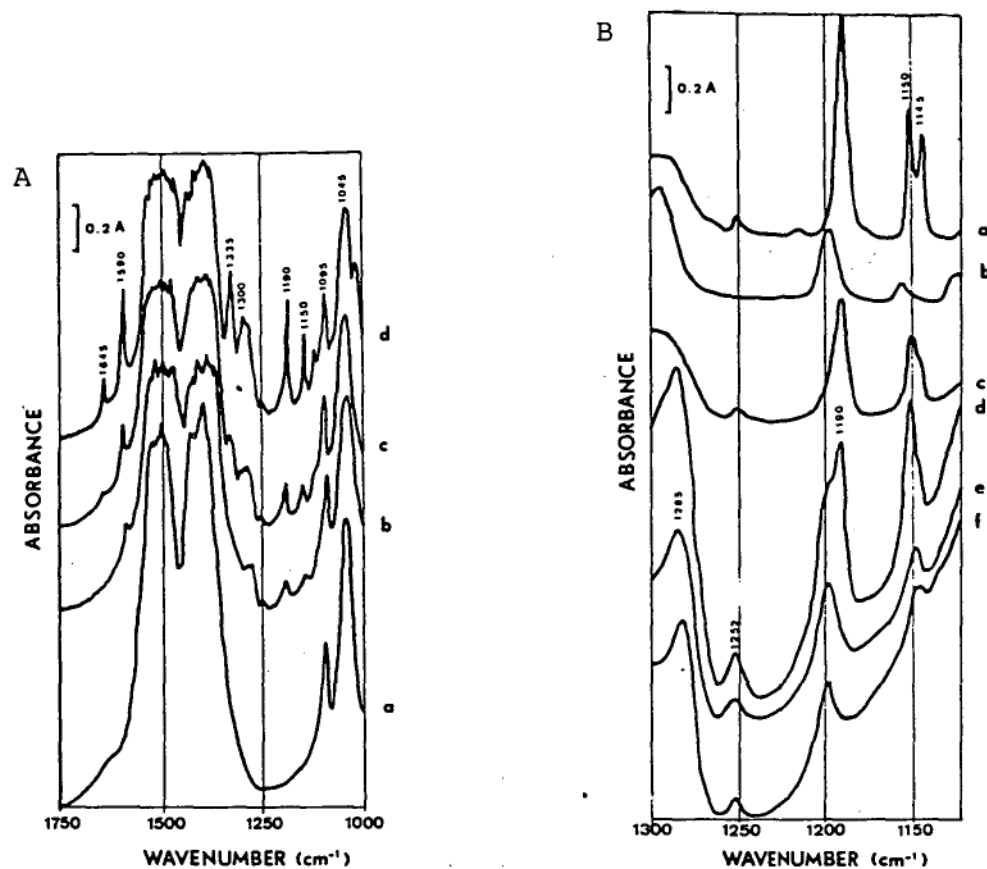


Fig.21 A. Infrared spectra of:

a - malachite

b,c,d - malachite with different amounts of adsorbed salicylaldoxime

b - 5.5  $\text{mMg}^{-1}$

c - 14.1  $\text{mMg}^{-1}$

d - 29.0  $\text{mMg}^{-1}$

B. Infrared spectra of:

a - bis-salicylaldoximate copper (II)

b - mono- salicylaldoximate copper (II)

c-f - malachite with different amounts of adsorbed salicylaldoxime

c - 29.0  $\text{mMg}^{-1}$

d - 15.5  $\text{mMg}^{-1}$

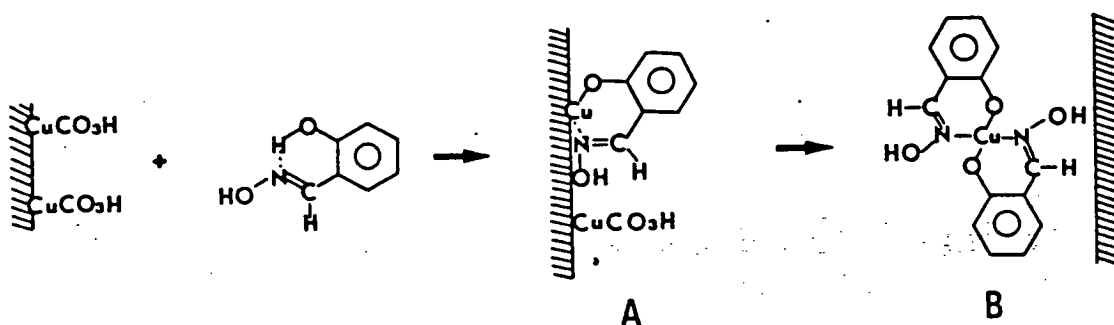
e - 10.4  $\text{mMg}^{-1}$

f - 5.5  $\text{mMg}^{-1}$

(From Cecile et al, 1975.)

The infrared band assignments for the copper (II) complexes are shown in Fig.22. The strong N-O stretching frequency occurs at  $1200\text{cm}^{-1}$  for the mono complex and at  $1190\text{cm}^{-1}$  for the bis complex. From the infrared spectra of the adsorbate it was concluded that at high collector concentrations the bis complex is present at the surface whereas the mono complex is favoured at lower concentrations.

The authors proposed the following mechanism for the adsorption of salicylaldoxime on malachite.



Initially at low concentrations, an exchange of a  $\text{CO}_3\text{H}$  group by the oximate group produces a mono-salicylaldoximate copper (II) surface complex (A) (spectra e and f). Further addition of oxime transforms the compound into the bis-salicylaldoximate copper (II) complex (B) (spectra c and d).

Malachite	Salicyl- aldoxime	Bis-salicyl- aldoximate- copper II	Monosalicyl- aldoximate- copper II (basic salt)	Possible assignments
	3610 V.W.	3600 m		
3400	3420 m	3400 V.W.	3400	
3320	3380 V.S.	3300	3160	
	3200	3050	3130 m	OH stretch. vibr.
		3010	3090 m	
			3015 V.S.	
			2960	
			2930	CH stretch. vibr.
			2830	
	1630 V.S.	1600 V.S.	1645 S	OH deform. vibr.
	1620 S	1600 V.S.	1600 V.S.	C=N stretch. coupled with C=C stretch.
	1580 S	1545 V.S.	1545 V.S.	
1500				C-O deform. vibr.
1400				
	1495 V.S.	1475 V.S.	1510 S	
	1475 m	1440 V.S.	1470 V.S.	Ortho disubstituted benzene ring vibr.
	1415 S		1445 V.S.	
	1400 S	1355	1405	
	1310		1335 V.S.	CH vibr. in plane
	1300	1325 S	1310 S	
	1290	1295 V.S.	1295 S.W.	
	1255 V.S.		1255 m	OH deform. vibr.
	1235		1220	C-C deform. vibr. in disub. benzene ring
	1210			
	1196 S	1200 S	1190 V.S.	N-O stretch. vibr.
	1155 S	1155 m	1150 S	C-C deform. vibr. in disub. benzene ring
	1115	1125 m	1125 m	
1095				C-O deform. vibr.
	1040	1040 S	1055 m	Benzene ring breathing
	990 V.S.	1030 V.S.	1025 S	C-O stretch. vibr.
1045				OH deform. vibr. out of plane
875				
	980	940 m	965 S	Benzene ring Ortho disub. vibr.
	960 S	920 V.S.	915 S	N-O stretch. vibr.
	940			
	905			
	860		860 m	
	790	845 m	805 S	CH out of plane
	765	820 m	750 V.S.	
	740	745 S	740 V.S.	
820				C-O deform. vibr.
	725	730 S		
	706	665 V.S.	665 S.W.	
		620 m	645 S	
			615 S	
		600 S	600 S	
750				
710				C-O deform. vibr.

<sup>a</sup> S, strong; V.S., very strong; m, medium; W, broad.

Fig. 22 Infrared spectral bands and their assignments for salicylaldoxime and its copper complexes. (From Cecile et al, 1975.)

### References

- Banerji B.K.** Effect of aeration in the xanthate flotation of pyrite. *AMDEL Bulletin*. 5 65-75, 1978.
- Brion D.** Etude par spectroscopy de photoelectrons de la degradation superficielle de  $\text{FeS}_2$ ,  $\text{ZnS}$  et  $\text{PbS}$  a l'air et dans l'eau. *Appl. Surface Sci.* 5 133-152, 1980.
- Buckley A.N. and Woods R.** An X-ray photoelectron spectroscopic investigation of the tarnishing of bornite. *Aus. J. Chem.* 36 1793-804, 1983a.
- Buckley A.N and Woods R.** An X-ray photoelectron spectroscopic study of the oxidation of chalcopyrite. *Aus. J. Chem.* 37 2403-2413, 1983b.
- Buckley A.N and Woods R.** An X-ray photoelectron spectroscopic study of the oxidation of galena. *Appl. Surface Sci.* 17 401-414, 1984.
- Buckley A.N and Woods R.** X-ray photoelectron spectroscopy of oxidised pyrrhotite surfaces 1 Exposure to air. *Appl. Surface Sci.* 22 280-287, 1985.
- Cecile J.L., Cruz M.I., Barbery G. and Fripiat J.J.** Infrared spectral study of species formed on the malachite surface by adsorption from aqueous salicylaldoxime solution. *J. Colloid and Interface Science.* 80 589-597, 1981.
- Coleman R.E. and Powell H.B.** Infrared spectroscopic studies of the xanthate-galena system. *Rep Inv. US. Bur. Mines.* 6816 24p, 1966.

**Coleman R.E., Powell H.B. and Cochran A.A.**

Infrared studies of products of reaction between activated zinc sulphide and potassium ethyl xanthate. *Trans AIME*. 238 408-412 1966.

**Dixit S.G. and Biswas A.K.** Studies on the

zircon-sodium oleate flotation system. *Trans. Inst. Mining and Metallurgy*. 82 C140-C144, 1973.

**French R.O., Wadsworth M.E., Cook M.A. and Cutler**

**I.B.** Infrared spectroscopy in studies of surface chemistry. *J. Phys. Chem.* 58 805-811, 1954.

**Fuerstenau M.C., Clifford K.L. and Kuhn M.C.** The

role of zinc xanthate in sphalerite flotation. *Int. J. Mineral Processing*. 1 307-318, 1974.

**Fuerstenau M.C., Kuhn M.C. and Elgillani D.A.**

The role of dixanthogen in the flotation of pyrite. *Trans. AIME* 241 148-156, 1968.

**Greenler R.G.** Infrared Investigation of xanthate

adsorption by lead sulphide. *J. Phys. Chem.* 66 879-883, 1962.

**Hagihara H.** Mono and Multilayer Adsorption of Aqueous

Xanthate on Galena Surfaces. *J. Phys. Chem.* 56. 616-621, 1952.

**Hagihara H. and Uchikoshi H.** Adsorption of alkyl

xanthate and dithiophosphate on a cleavage face of galena as revealed by electron diffraction. *Nature*. 174 80-81, 1954.

**Iskra J. and Kielkowska M.** Application of the ATR

technique to fluorite-oleate-quebracho systems. *Trans. Inst. Mining Metallurgy*. 89 C87-C90, 1980.

**Kongolo M., Cases J.M., Burneau A. and Predali J.J.**

Spectroscopic study of potassium amyl xanthate adsorption on finely ground galena: relations with flotation.

*Reagents Miner. Ind. Pap.* 79-87, 1984.

**Little L.H., Poling G.W., and Leja J.** Infrared

spectra of xanthate compounds. II Assignment of vibrational frequencies. *Canadian J. Chem.* 39 745-754, 1961.

**Lovell V.M., Goold L.A. and Finklestein N.P.**

Infrared studies on the adsorption of oleate species on calcium fluoride. *Int. J. Mineral Processing.* 1 183-192, 1974.

**Majima H. and Takeda M.** Electrochemical studies on

the system xanthate - dixanthogen on pyrite. *Trans AIME* 241 431-436, 1968.

**Manocha A.S and Park R.L.** Flotation related ESCA

studies on lead (II) sulphide surfaces. *Appl. Surface Sci.* 1 129-141, 1977.

**Mielczarski J, Nowak P. and Strojek, J.W.**

Spectrophotometric investigation of products of potassium ethyl xanthate sorption on lead sulphide and galena surfaces. Part 1. oxidised samples. *Polish Journal of Chemistry* 54 279-291, 1980.

**Mielczarski J, Nowak P, Strojek J.W. and**

**Pomianowski A.** Investigations of the products of ethyl xanthate sorption on sulphides by IR-ATR spectroscopy. In *Developments in Mineral Processing.* (J.Laskowski. Ed.) Vol 2. Part A. 110-132, Elsevier, New York, 1981.

**Mielczarski J, Nowak P. and Strojek J.W.**

Correlation between the adsorption of sodium dodecyl sulphate on calcium fluoride (fluorite) and its floatability - an infrared internal reflection study. *Int. J. Mineral Processing.* 11 303-317, 1983.

**Nowak P, Mielczarski J. and Strojek J.W.**

Spectrophotometric investigations on products of potassium ethyl xanthate sorption on lead sulphide and galena surfaces. Part 2. samples washed with solutions of sodium sulphide and ammonium acetate. *Polish Journal of Chemistry.* 54 517-527, 1980.

**Palmer B.R, Gutierrez B.G, Fuerstenau M.C and Aplan**

**F.F.** Mechanisms involved in the flotation of oxides and silicates with anionic collectors. *Trans. AIME.* 258 257-263, 1975.

**Peck A.S. and Wadsworth M.E.** Infrared study of the activation and flotation of beryl with hydrofluoric and oleic acid. *Trans. AIME* 235 301-307, 1967.

**Peck A.S. and Wadsworth M.E.** An infrared study of the flotation of phenacite with oleic acid. *Trans AIME.* 238 245-248, 1967.

**Pillai K.C, Young V.Y. and Bockris J.O.M.** X-ray photoelectron spectroscopy studies of xanthate adsorption on pyrite surfaces. *J. Colloid. Interface Sci.* 103 145-153, 1985.

**Plitt L.R. and Kim M.K.** Adsorption mechanism of fatty acid collectors on barite. *Trans. AIME.* 256 188-193, 1974.

**Pradip and Fuerstenau D.W.** The adsorption of hydroxamate on semi-soluble minerals, Part 1. Barite, calcite and bastnaesite. *Colloids and Surfaces*. 8 103-119, 1983.

**Predali J.J, Brion D, Hayer J. and Pelletier B.** Characteristics by ESCA spectroscopy of surface compounds on the fine sulphide minerals in flotation. In *Advances in Mineral Processing* (J. Laskowski. Ed.) Vol 2. Part A. 134-156, Elsevier, New York, 1981.

**Ranta L, Minni E, Suoninen E, Meimala S, Hintikka V, Saari M and Rastas J.** XPS studies of adsorption of xanthate on sulphide surfaces. *Appl. Surface Sci.* 7 393-401, 1981.

**Shergold H.L.** Infrared study of adsorption of sodium dodecyl sulphate by calcium fluoride (fluorite) *Trans. Inst. Mining Metallurgy*. 81 C148-C156. 1972.

**Somasundaran P, Ananthapadmanabhan K.P. and Ivanov I.B.** Dimerisation of Oleate in Aqueous Solutions. *J. Colloid Interface Science*. 99 128-135, 1984.

**Yamasaki T. and Usui S.** I.R. Spectroscopic studies on xanthate adsorbed on ZnS. *Trans AIME*. 232 36-45, 1965.

Depth of Penetration calculated from equation in N.J. Harrick p.30  
"Internal Reflection Spectroscopy" (Interscience 1967)  
 and optical constants for H<sub>2</sub>O in Optika Spektroskopija 27 430-2 (1969),  
V.M. Zolotarev et al.

$\lambda(\mu\text{m})$	$n_{\text{H}_2\text{O}}$	$d_p(\mu\text{m})$
2.5	1.240	0.157
3.0	1.400	0.193
3.5	1.400	0.227
4.0	1.347	0.256
4.5	1.331	0.287
5.0	1.329	0.319
5.5	1.300	0.349
6.0	1.276	0.378
6.5	1.330	0.415
7.0	1.313	0.445
7.5	1.302	0.476
8.0	1.288	0.506
8.5	1.272	0.532
9.0	1.252	0.565
9.5	1.229	0.594
10.0	1.208	0.622
10.5	-	-
11.0	1.149	0.678
11.5	-	-
12.0	1.114	0.735

#### Symbols

$d_p$	=	depth of penetration of radiation in water
$n_2$	=	$n_2/n_1$
$n_2$	=	$n_{\text{H}_2\text{O}}$ = refractive index of water
$\lambda(\text{lambda})$	=	wavelength of radiation
$n_1$	=	refractive index of Ge (= 4 at all wavelengths)
$\theta$	=	angle of incidence = 45°

Equation:-

$$d_p = \frac{\lambda}{n_1 (2\pi(\sin^2 \theta - n_2^2))^{1/2}}$$

Experimental test of equation using Ge ATR and benzene

1959 cm<sup>-1</sup> band of benzene i.e. 5.2  $\mu\text{m}$

Theoretically

$$d_p = \frac{5.2}{4 (2\pi(\sin^2 45 - (\frac{1.48}{4})^2))^{1/2}}$$

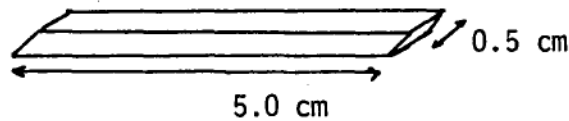
$$= 0.34 \mu\text{m}$$

Experimentally  $d_p = 0.32 \mu\text{m}$  (4/5/84)

N.K. Roberts  
 Physikalisch Chemisches Institut  
 der Universität München  
 West Germany

Comparison of the Concentration of  
the Adsorbate on the Surface and  
in the Adjacent Solution

Consider a germanium prism of the following dimensions



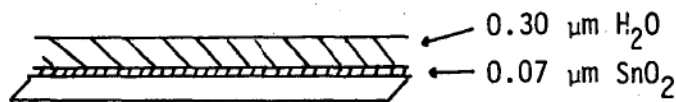
In Solution

According to Harrick's equation

$$d_p \text{ (at } \lambda = 6 \text{ } \mu\text{m}) = 0.38 \text{ } \mu\text{m of H}_2\text{O}$$

From interference measurements the prism is coated with  $\text{SnO}_2$  with a thickness of  $\sim 0.07 \text{ } \mu\text{m}$ .

$$\text{Hence } d_p \sim 0.30 \text{ } \mu\text{m of H}_2\text{O}$$



Hence the volume of water penetrated

$$\begin{aligned} &= 5 \times 0.05 \times 0.30 \times 10^{-4} \text{ cm}^3 \\ &= 0.75 \times 10^{-4} \text{ cm}^3 \end{aligned}$$

For both sides of the prism, volume

$$= 2 \times 0.75 \times 10^{-4} \text{ cm}^3 = 1.5 \times 10^{-4} \text{ cm}^3$$

Now for a solution of 50 ppm styrene phosphonic acid

$$\sim 0.25 \times 10^{-3} \text{ M l}^{-1}$$

$$\sim 0.25 \times 10^{-6} \text{ M cm}^{-3}$$

Hence the number of moles of SPA in  $1.5 \times 10^{-4} \text{ cm}^3$

$$= 1.5 \times 10^{-4} \times 0.25 \times 10^{-6} \text{ moles}$$

$$= 4.0 \times 10^{-11} \text{ Moles}$$

ie for 50 ppm there is approximately  $4.0 \times 10^{-11}$  moles of SPA in the solution adjacent to the Ge prism.

On the Surface

Now if the area of the SPA molecule on the surface is assumed to be  $50 \text{ \AA}^2$

$$\begin{aligned} &= 50 \times 10^{-16} \text{ cm}^2 \\ &= 5 \times 10^{-15} \text{ cm}^2 \end{aligned}$$

And the area of both sides

$$= 2 \times 5.0 \times 0.5 \text{ cm}^2 = 5 \text{ cm}^2$$

Hence the number of molecules on the surface if a monolayer is formed

$$= 5/5 \times 10^{-15} = 10^{15} \text{ molecules}$$

Hence the number of moles on the surface

$$= 10^{15} / \text{Avagadro's number}$$

$$= 10^{15} / 6 \times 10^{23} \text{ moles}$$

$$= 1.7 \times 10^{-9} \text{ moles}$$

ie if a monolayer is formed there is a  $1.7 \times 10^{-9}$  moles of SPA present on the surface.

Hence the contribution from the species in solution at monolayer coverage is negligible.